

PORTABLE FALLING WEIGHT
DEFLECTOMETER STUDY

Byran C. Steinert, Dana N. Humphrey,
and Maureen A. Kestler

March 11, 2005

NETCR52

NETC Project No. 00-4

Prepared for
New England Transportation Consortium

Prepared by:
Department of Civil and Environmental Engineering
University of Maine
Orono, Maine

with assistance from:
USDA Forest Service

This report, prepared in cooperation with the New England Transportation Consortium, does not constitute a standard, specification or regulation. The contents of this report reflect the views of the authors who are responsible for the facts and the accuracy of the data presented herein. The contents do not necessarily reflect the views of the New England Transportation Consortium or the Federal Highway Administration.

Technical Report Documentation Page

1. Report No. NETCR52		2. Government Accession No. N/A		3. Recipient's Catalog No. N/A	
4. Title and Subtitle Portable Falling Weight Deflectometer Study				5. Report Date March 11, 2005	
				6. Performing Organization Code N/A	
7. Author(s) Bryan C. Steinert, Dana N. Humphrey, & Maureen A. Kestler				8. Performing Organization Report No. N/A	
9. Performing Organization Name and Address Department of Civil and Environmental Engineering University of Maine 5711 Boardman Hall Orono, ME 04469-5711				10. Work Unit No. (TRAIS) N/A	
				11. Contract or Grant No. N/A	
12. Sponsoring Agency Name and Address New England Transportation Consortium 179 Middle Turnpike Unit 5202 University of Connecticut Storrs, CT 06269-5202				13. Type of Report and Period Covered FINAL	
				14. Sponsoring Agency Code N/A	
15. Supplementary Notes N/A					
16. Abstract: This research investigated the effectiveness of the Portable Falling Weight Deflectometer (PFWD) for evaluating the support capacity of pavements during the spring thaw and evaluating the adequacy of subgrade and base compaction during construction. The performance of ten asphalt and gravel surfaced low volume roads were evaluated through spring thaw and recovery. Comparisons were made to the traditional FWD as well as other portable measuring devices. It was shown that the PFWD was able to follow seasonal stiffness variations and compared well with FWD derived moduli on both asphalt and gravel surfaces. Recommendations were made for using a PFWD to determine when to place and remove load restrictions. Field and laboratory tests were conducted to develop correlations between composite modulus, percent compaction, and water content for a range of aggregate types typical of New England. Comparisons were made between multiple PFWDs. A tentative technique was recommended for using a PFWD for compaction quality control for aggregate base and subbase courses. This is based on a rough equivalency between the PFWD composite modulus and percent compaction for aggregate at optimum water content. Factors are provided to correct the modulus at the field water content to the equivalent value at optimum.					
17. Key Words falling weight deflectometer, thaw weakening, load restrictions, low-volume roads, spring thaw, compaction, quality control, modulus, aggregate base course			18. Distribution Statement No restrictions. This document is available to the public through the National Technical Information Service Springfield, Virginia 22161		
19. Security Classif. (of this report) Unclassified		20. Security Classif. (of this page) Unclassified		21. No. of Pages 299	22. Price N/A

PORTABLE FALLING WEIGHT DEFLECTOMETER STUDY
NETC Project No. 00-4

EXECUTIVE SUMMARY

By: Bryan C. Steinert, Dana N. Humphrey, and Maureen A. Kestler
Department of Civil & Environmental Engineering, University of Maine, Orono, Maine

Portable falling weight deflectometers (PFWD) were investigated as a tool to aid in determining when to impose weight restrictions on low-volume roads during the spring thaw, and for compaction quality control for aggregate base courses and other soils. PFWDs operate on the same principle as conventional falling weight deflectometers (FWD), wherein a falling weight applies a force to a plate and the resulting deflection is measured using one or more deflection sensors. An advantage of a PFWD over a FWD is the former's significantly lower purchase and operation costs. Comparing a PFWD to a nuclear moisture density meter (NDM) for compaction quality control, the latter has burdensome licensing and operational requirements due to the nuclear source. Moreover, PFWDs directly measure stiffness of pavement systems and compacted layers which is needed for mechanistic pavement design.

There are several previous studies that compared composite modulus values for paved road determined by PFWDs, FWDs and Benkelman Beams. In general, the comparisons showed marginal correlation coefficients (r^2) less than 0.5, however one study obtained an r^2 of 0.86 for a correlation between moduli determined by the FWD and PFWD. The PFWD generally produced higher modulus values than the FWD, possibly due to the smaller depth of influence of the PFWD resulting in the stiff pavement having a greater influence on the resulting modulus. Some investigators imply that the PFWD is better suited to roads with thin pavements. Limited studies have been conducted to evaluate the PFWD as a tool for tracking seasonal stiffness variations. For this application, correlation coefficients relating the PFWD and the Benkelman Beam were generally high. For thin pavement sections, the PFWD adequately followed seasonal stiffness variations. Work done in Washington State has suggested that using deflection data to aid in load restriction placement and removal can be done and recommends that during the spring thaw, restrictions should be placed once the stiffness drops below 40 to 50% of their fully recovered values and then removed when the stiffness recovers to above these values.

A Prima 100 PFWD was selected as the primary instrument for this research because it can be used with three different drop weights, three plate diameters, adjustable fall heights, and up to three deflection sensors. Other PFWDs did not have this level of flexibility. Results from the Prima 100 PFWD were compared to other similar devices.

Spring Thaw Monitoring

The performance of seven paved and three gravel surfaced roads were monitored during the spring of 2004. Test sites were located in Maine, New Hampshire, and Vermont. One of the gravel surfaced sites located in New Hampshire was also monitored during the spring of 2003. Two additional sites in Northern Maine were used for testing

on one day as part of an ongoing MaineDOT research project. Thermocouples, thermistors, and frost tubes were used at selected sites to monitor the advance and retreat of freezing conditions during late winter and spring months. Vibrating wire and standpipe piezometers were installed at selected sites to monitor pore water pressures in the subbase and subgrade layers. Time Domain Reflectometry (TDR) probes were used to monitor water content through the spring thaw and recovery periods at some sites. Instrumentation was used to examine the extent to which the road had thawed and provided the context for interpretation of PFWD and FWD results.

Prima 100 PFWD and traditional FWD measurements were taken at a minimum of eight locations at each test site. Measurements were taken approximately weekly during the spring thaw period. In addition, Loadman PFWD measurements were taken at spring thaw test sites in Rumney, New Hampshire. Clegg Impact Hammer and Humboldt Soil Stiffness Gauge measurements were taken at the United States Forest Service (USFS) Parking Lot during the spring of 2003 and 2004. With the Prima 100 PFWD, six measurements were taken at each of three different drop heights, at each test location. The first reading was neglected and the average of the remaining five was used for analysis and comparison. In addition, five Loadman PFWD, four Clegg Impact Hammer, and one Soil Stiffness Gauge measurement was taken at each test location. Moduli were backcalculated from FWD data using either DARWin or Evercalc.

Subsurface temperatures measurements taken at asphalt surfaced test sites indicated freezing temperatures penetrated to their maximum depths between February 17 and March 24, 2004. Maximum depths ranged from 866 mm (34 in.) to 1930 mm (76 in.). Complete thaw occurred at all test sites between mid-March and mid-April. Measurements taken at gravel surfaced test sites indicated freezing temperatures penetrated to their maximum depths between March 1 and April 21, 2004. Maximum depths ranged from 1128 mm (44 in.) to 2134 mm (84 in.). Complete thaw had occurred at all sites between early April and mid May. At most sites higher porewater pressures in the subgrade and subbase soils were associated with the thawing period. This is a factor that could contribute to reduction of pavement stiffness during the spring thaw.

For each test site, Prima 100 PFWD composite modulus, and where it is available, FWD asphalt, subbase, subgrade, and composite modulus and Loadman PFWD composite modulus values were plotted versus date. In general, for asphalt surfaced test sites, the moduli were high when the pavement section is frozen and during the early part of the thaw period when section is partially thawed. At some field sites there were significant differences in moduli from nearby test locations and from one week to the next. This variability is more apparent in gravel surfaced test sites compared to asphalt surfaced test sites. For both asphalt and gravel surfaced test sites, composite moduli generally decreased as thawing progressed. It was anticipated that a distinct minimum would occur before increasing through the recovery period. However, this was only evident at the Buffalo Road (NH), USFS Parking Lot (NH), Knapp Airport Parking Lot (VT), Crosstown Road (VT), and to a lesser extent Stinson Lake Road (NH). At the remaining sites, the composite modulus that was reached during the spring thaw was about the same as, or in some, cases greater than the values measured during the summer. FWD derived layer moduli confirm these observations. In general, portable and traditional FWD moduli follow similar trends for both asphalt and gravel surfaced test

sites through the monitoring period. Thus, the PFWD and FWD would be equally as effective in monitoring stiffness change during the spring thaw.

The degree of correlation between composite moduli backcalculated using FWD and Prima 100 PFWD results were investigated. This was done for five sites in Maine where the composite moduli from the FWD were available. Regression analyses yielded correlation coefficients ranging from 0.336 to 0.950. In general, correlation coefficients tended to increase as pavement thickness decreased. The data from three test sites with asphalt thicknesses less than or equal to 127 mm (5 in.) were combined and produced the best correlation with $r^2 = 0.873$. Two test sites with an asphalt thickness of 152 mm (6 in.) followed with $r^2 = 0.559$. However, when excluding unreasonably high moduli greater than 4000 MPa, the correlation improves to $r^2 = 0.802$. Route 1A (ME) was the single test site with a 180 mm (7 in.) asphalt thickness and produced the poorest correlation with $r^2 = 0.336$. A regression analysis combining all asphalt surfaced test sites produced a correlation coefficient of 0.531. Again, when moduli greater than 4000 MPa are excluded, the correlation improved with $r^2 = 0.809$. These results suggest that the PFWD could be used as an alternative to conventional FWDs for estimation of composite moduli of pavement sections for some pavement thicknesses.

Loadman and Prima 100 PFWD composite moduli were compared to FWD derived subbase moduli for two asphalt surfaced test sites in Rumney, New Hampshire. The Loadman PFWD provides a composite modulus that is less than that provided by the Prima 100. The Prima 100 PFWD correlates better to FWD derived subbase moduli ($r^2 = 0.552$) than composite moduli obtained from the Loadman PFWD ($r^2 = 0.245$).

The effect of Prima 100 PFWD drop weight (10, 15, and 20 kg (22, 33, and 44 lb)), plate diameters (100, 200, and 300 mm (4, 8, and 12 in.)), and drop height (850, 630, and 420 mm (33.5, 24.8, and 16.5 in.)) were investigated. In general, composite modulus increased with decreasing drop weight but was independent of plate diameter for the larger two drop weights. At the 10 kg (22 lb) drop weight the moduli decreased with increasing loading plate diameter. A possible explanation for this behavior is that a small plate diameter and drop weight influence only the upper portions of the pavement section and thus the deflection responses are dominated by the stiffer pavement layer, producing a larger composite modulus. In general, reduced drop heights produce moduli that are slightly less than moduli derived from using the full (850 mm) drop height. For most applications the largest drop weight, largest plate diameter, and largest drop height should be used for testing.

Up to three deflection sensors can be used with the Prima 100 PFWD. However, when backcalculating moduli current software makes use of only one sensor's results at a time. Moduli derived from measurements from the outer two geophones are significantly greater than the composite moduli determined from the center geophone. Until software is developed to incorporate the deflections from all three geophones simultaneously into a backcalculation routine, the additional geophones provide little useful additional information.

Six Prima 100 PFWD measurements were taken at each of three different drop heights, at each test location. For the majority of points tested at the field sites; the first measurement was less than subsequent measurements. This was consistent with

observations made by other researchers. On the average, first drop was less than the average of the remaining five drops by nearly 10%. However, the second drop was only 1% less than the average of the remaining four drops. This shows that the results of the first drop should always be neglected. It is recommended that the results from drops two through six be averaged to obtain results that are representative of a test location.

Field testing techniques for monitoring seasonal stiffness variation in paved and unpaved low volume roads using the Prima 100 PFWD were developed. The core of the recommendations is that load restrictions are placed once the composite moduli measured with the PFWD drops below 80% of the fully recovered baseline value measured during the summer and early fall. The load restriction is then removed when the moduli recover to 80% of the baseline value. The selection of 80% is arbitrary since the amount of damage that would occur at the reduced modulus depends on individual pavement sections, allowable vehicle weight, and traffic levels. Assessment of these factors was beyond the scope of this study. Baseline and spring thaw measurements should be made at the same locations. During the early portion of thawing period, it may be necessary to take daily readings to monitor the sometimes rapid decrease in composite modulus.

Compaction Control

Five field test sites in Maine, New Hampshire, and Connecticut were used to evaluate the effectiveness of the PFWD as a tool to monitor compaction. Tests were performed at a minimum of 12 locations, utilizing both the Prima 100 PFWD and Nuclear Moisture Density Meter (NDM). Samples were taken at each site for sieve analysis, maximum dry density, and optimum water content determination. The field component included tests on two subgrades, one construction sand, two base aggregates, and one reclaimed stabilized base product.

The primary purpose of the laboratory component of this project was to determine a relationship between PFWD results and percent compaction under controlled conditions. Tests were performed on five soil types representative of New England base and subbase aggregates. These materials included: one crushed material, one construction sand, and three base/subbase aggregates. The tests were conducted in a 1.8 m x 1.8 m x 0.9 m (6 ft x 6 ft x 3 ft) deep test container. Material was added to the container in approximately 152 mm (6 in.) lifts. Each lift was compacted using a hand tamper and electric jackhammer with a modified flat plate attachment. Each aggregate was compacted in the container to approximately 90, 95, and 100% of the maximum dry density (AASHTO T 180). The effect of water content was determined at 95% of the maximum dry density. Measurements were taken at optimum water content as well as $\pm 3\%$ of the optimum water content. Once all the material was compacted in the test container, the following portable testing devices were used: Prima 100 PFWD, Clegg Impact Hammer, NDM, and Dynamic Cone Penetrometer (DCP). Prima 100 PFWD and Clegg Impact Hammer measurements were taken in the same manner as was done for the spring thaw portion of the research. In addition, one sand cone test was completed, and two water content samples were taken for each trial for comparison to NDM measurements. NDM measurements were used as the prime basis for comparison.

For the laboratory tests, the composite moduli generally increased as percent compaction increased. This was true for all samples with the exception of the New

Hampshire Gravel which exhibited the opposite trend. With the exception of the New Hampshire Sand, the correlation coefficients were less than 0.5 indicating poor correlation. Combining all the results yielded a correlation coefficient of 0.045, indicating no correlation. However, including only the results for Connecticut crushed gravel, New Hampshire sand, and Wardwell gravel resulted in a higher correlation coefficient of 0.35, but still indicating a poor correlation. Results from the field test sites also indicate that as the degree of compaction increases, composite modulus increases. In general, correlation coefficients were greater for field test results compared to laboratory test results. Combining the results for the three base materials tested in the field, resulted in a correlation coefficient of 0.818, which is a relatively strong correlation. However, the significance of this correlation is diminished by the fact the water content at all the field sites was dry of optimum.

Laboratory results also show that there is a general trend that the composite moduli tends to decrease as water content increases. Correlation coefficients ranged from 0.003 (Connecticut Crushed Gravel) to 0.814 (Wardwell Gravel). The low correlation coefficients for several of the samples are due in part to the role that percent compaction plays in the composite modulus, which is not accounted for when only water content is considered. Combining at the laboratory results yielded a correlation coefficient of 0.285 which indicates poor correlation. For measurements taken at field sites the correlation coefficient ranged from 0.008 (Route 25 Gravel) to 0.521 (Route 25 Sand). However, water contents measured at field sites were generally drier than -3% of the OWC and in some instances were as low as -9%, which are significantly different from water contents obtained during laboratory tests.

Multivariable linear regression analyses were used to determine the best fit line for composite modulus as a function of percent compaction and water content. The coefficient of multiple determination (R^2) for the laboratory materials ranged from 0.141 (Connecticut crushed gravel) to 0.867 (Wardwell gravel). Combining all laboratory samples produced an R^2 of 0.326. However, including only laboratory results for Connecticut crushed gravel, New Hampshire sand, and Wardwell gravel increased the R^2 to 0.624. This indicates that 62% of the variation in composite modulus is explained by the percent compaction and water content relative to optimum. The R^2 for the field materials ranged from 0.001 (Route 25 gravel) to 0.679 (I-84 crushed gravel). Combining the three field sites where granular base was tested yielded an R^2 of 0.823, which indicates a reasonably strong correlation of composite modulus with percent compaction and water content, independent of the type of material tested. However, the water contents for the field sites were all dry of optimum which may limit the significance of this result. The multi-variable linear regressions based on the three laboratory samples indicated above and field results yielded predicted composite modulus at 95% percent compaction that agreed within 20% which is reasonable agreement. Overall, the analysis shows that both percent compaction and water content relative to optimum have an important influence on composite modulus.

Based on the results of this research the tentative procedure given below is recommended for using the Prima 100 PFWD to monitor compaction of granular base courses. The procedure is based on the observation that there is a rough equivalency between percent compaction and composite modulus for granular base at optimum water

content. Correction factors are recommended to correct the composite modulus measured at the field water content to the equivalent value at optimum water content. The regression equation for the combined laboratory results for Connecticut crushed gravel, New Hampshire sand, and Wardwell gravel was used to derive the recommendations. This equation was used since it had a higher correlation coefficient than the regression that included all five laboratory samples combined and it had a larger range of water contents than the field samples.

The target composite modulus at optimum water content should be chosen based on Table 1 that gives a rough equivalency with percent compaction based on AASTHO T-180. Composite moduli measured in the field should be corrected to the equivalent composite modulus at optimum water content by adding the factors given in Table 2. Thus, it is necessary to determine the field water content relative to OWC to apply this procedure. Possibilities for measuring the water content include oven drying, pan drying, Speedy Moisture Meter©, time domain reflectometry, or nuclear density meter in backscatter mode. The researchers caution that the values given in Tables 1 and 2 are based on a limited dataset. It is recommended that these equivalences be confirmed for additional materials used by individual state DOTs.

Table 1 Tentative equivalences between percent compaction and composite modulus at optimum water content for base and subbase course aggregate.

Percent Compaction based on AASTHO T-180 (%)	Equivalent Prima 100 PFWD Composite Modulus (MPa) at Optimum Water Content
90	92
95	115
98	130
100	139

Table 2 Factor to correct composite modulus measured at field water content to equivalent value at optimum water content.

Water Content Relative to Optimum		Correction Factor to be Added to Composite Modulus (MPa) Measured at Field Water Content
Dry of OWC	-4%	-31
	-3%	-23
	-2%	-15
	-1%	-8
At OWC		0
Wet of OWC	+1%	8
	+2%	15
	+3%	23
	+4%	31

PORTABLE FALLING WEIGHT DEFLECTOMETER STUDY

Byran C. Steinert, Dana N. Humphrey, and Maureen A. Kestler

Prepared for
New England Transportation Consortium

March 11, 2005

NETCR52

NETC Project No. 00-4

Prepared by:
Department of Civil and Environmental Engineering
University of Maine
Orono, Maine

with assistance from:
USDA Forest Service

This report, prepared in cooperation with the New England Transportation Consortium, does not constitute a standard, specification or regulation. The contents of this report reflect the views of the authors who are responsible for the facts and the accuracy of the data presented herein. The contents do not necessarily reflect the views of the New England Transportation Consortium or the Federal Highway Administration.

ACKNOWLEDGEMENTS

The researchers acknowledge the New England Transportation Consortium for providing funding for this research project. We especially thank Bill Real, Steve Colson, Chris Benda, Don Larsen, Matt Turo, and James Walls who served on the New England Transportation Consortium Technical Committee assigned to this project. Additional thanks go to Charlie Smith from the Cold Regions Research & Engineering Laboratory and to Jim Raymond of the Vermont Agency of Transportation.

TABLE OF CONTENTS

EXECUTIVE SUMMARY	iii
ACKNOWLEDGEMENTS	x
TABLE OF CONTENTS	xi
LIST OF TABLES	xiv
LIST OF FIGURES	xviii
1. INTRODUCTION.....	1
1.1 BACKGROUND	1
1.2 SCOPE OF STUDY.....	3
1.3 ORGANIZATION OF THE REPORT	3
2. LITERATURE REVIEW	5
2.1 INTRODUCTION	5
2.2 PFWD AS ALTERNATIVE FOR COMPACTION CONTROL	5
2.2.1 Current Compaction Control Methods.....	5
2.2.2 PFWD Equipment.....	10
2.2.3 Past Test Programs, Results, and Recommendations	18
2.3 PFWD AS TOOL TO EVALUATE THAW WEAKENING OF ROADS	40
2.3.1 Current Methods to Evaluate Thaw Weakening of Roads.....	42
2.3.2 Past Test Programs, Results, and Recommendations	50
2.4 PFWD QUESTIONNAIRE	51
2.4.1 2003 Results.....	52
2.4.2 2004 Results.....	52
2.5 SUMMARY	52
3. FIELD & LABORATORY TEST PROTOCOL	55
3.1 INTRODUCTION	55
3.2 FIELD TEST SITE LOCATIONS	55
3.2.1 Seasonally Posted Low Volume Roads	55
3.2.2 Compaction Control Field Test Sites.....	76
3.3 INSTRUMENTATION	83
3.3.1 Frost Penetration Measurement	83
3.3.2 Pore Water Pressure Measurement	90
3.4 FIELD TESTING PROCEDURES	95
3.4.1 Spring Thaw Monitoring.....	95

3.4.2 Subgrades and Construction Materials	104
3.5 LABORATORY TESTING PROCEDURES	107
3.5.1 Spring Thaw Monitoring.....	107
3.5.2 Subgrades and Construction Materials	107
3.6 SUMMARY	111
4. SPRING THAW MONITORING	113
4.1 INTRODUCTION	113
4.2 FROST PENETRATION	114
4.3 PORE WATER PRESSURE	116
4.4 SEASONAL STIFFNESS VARIATIONS.....	122
4.4.1 Backcalculation of Layer Moduli	122
4.4.2 Asphalt Surfaced Roads.....	127
4.4.3 Gravel Surfaced Roads	136
4.5 COMPARISON OF PFWD AND FWD MODULI	142
4.5.1 Route 11 & Route 167 Field Test Sites	142
4.5.2 Composite Modulus.....	147
4.5.3 Subbase Modulus.....	154
4.6 COMPARISON TO OTHER PORTABLE DEVICES.....	169
4.7 EVALUATION OF FIELD TESTING TECHNIQUES	171
4.7.1 Loading Plate Diameter and Drop Weight.....	171
4.7.2 Drop Height	173
4.7.3 Moduli Derived from Additional Geophones	176
4.7.4 Multiple Measurements at Each Test Location	179
4.8 RECOMMENDATIONS.....	181
4.8.1 Factors that Affect Need for Seasonal Load Restrictions	182
4.8.2 Field Testing Techniques.....	182
4.8.3 Application of Procedure to Field Sites.....	185
4.9 SUMMARY	189
5. COMPACTION CONTROL	193
5.1 INTRODUCTION	193
5.2 IN-PLACE WATER CONTENT AND DRY DENSITY	194
5.3 FACTORS AFFECTING COMPOSITE MODULUS.....	199
5.3.1 Effect of Percent Compaction on Composite Modulus	200
5.3.2 Effect of Water Content on Composite Modulus.....	217
5.3.3 Multivariate Linear Regression.....	226
5.3.4 Additional Factors Influencing Composite Modulus.....	231
5.4 COMPARISON OF PORTABLE DEVICES.....	232
5.4.1 Prima 100 PFWD Comparison	234

5.4.2 Clegg Impact Hammer	238
5.4.3 Effect of Operator Technique	241
5.5 RECOMMENDATIONS	242
5.6 SUMMARY	246
6. SUMMARY, CONCLUSIONS, AND RECOMMENDATIONS	251
6.1 SUMMARY	251
6.1.1 Literature Review	253
6.1.2 Field & Laboratory Test Protocol	255
6.1.3 Spring Thaw Monitoring	258
6.1.4 Compaction Control	265
6.2 CONCLUSIONS	269
6.2.1 Spring Thaw Monitoring	270
6.2.2 Field Testing Techniques	270
6.2.3 Compaction Control	271
6.3 RECOMMENDATIONS FOR FURTHER RESEARCH	272
REFERENCES	273
APPENDIX A - GRAIN SIZE DISTRIBUTION CURVES	279
APPENDIX B - MOISTURE DENSITY CURVES	289
APPENDIX C - COMPACTION CONTROL RAW LABORATORY DATA	295

LIST OF TABLES

Table 2.1	Correlation coefficients of 20 test points on two TMS structures (SHT, 1998).	23
Table 2.2	Summary of correlations between the FWD and GDP, TFT, and Prima 100 PFWF at Mountsorrel and Bardon test sites (Fleming, et al., 2000).	33
Table 2.3	Summary of correlations between the Prima 100 PFWF and GDP and TFT at Mountsorrel and Bardon test sites (Fleming, et al., 2000).	34
Table 2.4	Description of foundations applied to theoretical model (Thom and Fleming, 2002).	35
Table 2.5	Predicted surface moduli from different dynamic plate test devices (Thom and Fleming, 2002).	35
Table 2.6	Road user feedback to DOTs and USFS on spring thaw load (Kestler, et al., 2000).	44
Table 2.7	Benefits from seasonal load restrictions (FHWA, 1990).	45
Table 2.8	Summary of recommendations made by Kestler after Rutherford, et al. (1985).	48
Table 3.1	Summary of seasonally posted low volume road field test sites.	57
Table 3.2	Laboratory properties of in-situ material at Kennebec Road, Hampden/Dixmont, Maine.	59
Table 3.3	Laboratory properties of in-situ material at Lakeside Landing Road, Glenburn, Maine.	60
Table 3.4	Laboratory properties of in situ subbase material at Stinson Lake Road, Rumney, New Hampshire.	62
Table 3.5	Laboratory properties of in situ material at Buffalo Road, Rumney, New Hampshire.	63
Table 3.6	Laboratory properties of in situ material at Crosstown Road, Berlin, Vermont.	65
Table 3.7	Laboratory properties of in situ material at Knapp Airport Parking Lot, Berlin, Vermont.	66
Table 3.8	Laboratory index properties of cohesive subgrade material at Witter Farm Road, Orono, Maine (Lawrence, et al., 2000).	69

Table 3.9	Laboratory index properties of subgrade material at Route 126, Monmouth/Litchfield, Maine (Helstrom and Humphrey, 2005).	72
Table 3.10	Water contents at thermocouple location on Route 1A Frankfort/Winterport, Maine (Fetten and Humphrey, 1998).	75
Table 3.11	Test Section description of Route 11, Wallagrass Plantation, Maine (Bouchédid and Humphrey, 2004).	76
Table 3.12	Test Section description of Route 167, Presque Isle/Fort Fairfield, Maine (Bouchédid and Humphrey, 2004).	76
Table 3.13	Summary of compaction control field test sites	77
Table 3.14	Summary of Marshall Stability tests on field samples at Commercial Paving & Recycling test site, Scarborough, Maine.	82
Table 3.15	Summary of instruments spring thaw field test sites	83
Table 3.16	Summary of thermocouple locations at spring thaw field test sites	85
Table 3.17	Summary of thermistor locations at spring thaw field test sites	86
Table 3.18	Summary of frost tube locations at spring thaw field test sites	87
Table 3.19	Summary of vibrating wire piezometer locations at spring thaw field test sites.	91
Table 3.20	Summary of standpipe piezometer locations at spring thaw field test sites	93
Table 3.21	TDR probe locations at Stinson Lake Road and USFS Parking Lot, Rumney, New Hampshire.	94
Table 3.22	Summary of test point locations at Witter Farm Road, Route 126, and Route 1A	97
Table 3.23	Prima 100 PFWD input parameters	99
Table 3.24	FLEX testing plan drop sequence used at Berlin, Vermont test sites (LTTP, 2000).	103
Table 3.25	FLEX testing plan target loads used at Berlin, Vermont test sites (LTTP, 2000).	104
Table 4.1	Summary of frost penetration measurements made on asphalt surfaced test sites.	115

Table 4.2	Summary of frost penetration measurements made on gravel surfaced test sites.	116
Table 4.3	Summary of standpipe piezometer measurements.....	119
Table 4.4	Summary of time domain reflectometry probe water content readings.....	119
Table 4.5	Summary of manual vibrating wire piezometer measurements.....	120
Table 4.6	Summary of PFWD and FWD composite moduli at the end of thawing and during recovery periods.....	128
Table 4.7	FWD and PFWD mean composite moduli for different asphalt thicknesses.	148
Table 4.8	Summary of the effects of reduced drop height on PFWD composite modulus for different asphalt thicknesses.....	174
Table 4.9	Summary of the effects of reduced drop height on PFWD composite moduli for different asphalt thicknesses.	177
Table 4.10	Comparison of the first, second, and third measurements with successive measurements at Route 126, Monmouth/Litchfield, Maine.	181
Table 4.11	Prima 100 PFWD input parameters.	184
Table 4.12	Summary of load restrictions for spring thaw field test sites.....	186
Table 5.1	Summary of laboratory samples	195
Table 5.2	Summary of laboratory measurements.	196
Table 5.3	Summary of field samples	199
Table 5.4	Summary of the correlations between percent compaction and composite modulus for laboratory samples.	204
Table 5.5	Summary of the correlations between percent compaction and composite modulus for field samples.	212
Table 5.6	Summary of the correlations between water content and composite modulus for laboratory samples.....	217
Table 5.7	Summary of the correlations between water content and composite modulus for field samples.....	222

Table 5.8	Summary of multivariate linear regression analyses on laboratory samples.....	227
Table 5.9	Summary of multivariate linear regression analyses on field tests on granular base.....	227
Table 5.10	Comparison of average composite moduli associated with varying degrees of compaction.	231
Table 5.11	Comparison of composite moduli from USFS and UMaine Prima 100 PFWDs.....	238
Table 5.12	Comparison of Prima 100 PFWD composite moduli and CIH moduli	239
Table 5.13	Comparison of Prima 100 PFWD composite moduli determined by different users.	242
Table 5.14	Tentative equivalences between percent compaction and composite modulus at optimum water content for base and subbase course aggregate.....	244
Table 5.15	Factor to correct composite modulus measured at field water content to equivalent value at optimum water content.	244
Table 5.16	Prima 100 PFWD input parameters.	245
Table C.1	Summary of Connecticut crushed gravel raw laboratory data.	295
Table C.2	Summary of New Hampshire sand raw laboratory data.	296
Table C.3	Summary of New Hampshire gravel raw laboratory data.	297
Table C.4	Summary of Owen J. Folsom gravel raw laboratory data.	298
Table C.5	Summary of Wardwell gravel raw laboratory data.....	299

LIST OF FIGURES

Figure 2.1	Nuclear density and water content determination: (a) direct transmission; (b) backscatter; (c) air gap (Holtz and Kovacs, 1981).....	8
Figure 2.2	Keros Prima 100 PFWD.	12
Figure 2.3	Keros Prima 100 PFWD.	12
Figure 2.4	Profile of load cell and geophone.	13
Figure 2.5	Bottom view of geophone.....	13
Figure 2.6	Additional geophones.	14
Figure 2.7	Prima 100 PFWD PDA display after one measurement.....	15
Figure 2.8	Loadman PFWD (Livneh, et al., 1997).....	16
Figure 2.9	Loadman PFWD display after one measurement.	17
Figure 2.10	Comparison of Loadman and FWD at various test points (Gros, 1993).	19
Figure 2.11	Correlation between Loadman and FWD (Gros, 1993).....	19
Figure 2.12	Comparison of Loadman and FWD at various test points (Gros, 1993).	20
Figure 2.13	Correlation between Loadman and FWD (Gros, 1993).....	20
Figure 2.14	Comparison of Loadman and FWD at various test points (Whaley, 1994).	21
Figure 2.15	Correlation between Loadman and FWD (Whaley, 1994).	21
Figure 2.16	Comparisons of Loadman, FWD, and Benkelman Beam (SHT, 1998).	23
Figure 2.17	(a) Uncorrected and (b) corrected relationship between FWD modulus and PFWD modulus using the double testing technique (Livneh, 1997).	25
Figure 2.18	Loadman PFWD deflection versus Benkelman Beam deflection (Livneh, et al., 1998).....	26
Figure 2.19	Comparison of multiple FWD and PFWD measurements at one location (Honkanen, 1991).	26

Figure 2.20	Comparison of Loadman and FWD at various test points (Gros, 1993).....	28
Figure 2.21	Correlation between Loadman and FWD (Whaley, 1994).....	28
Figure 2.22	Comparison of FWD, Loadman PFWD, Benkelman Beam, and Clegg Hammer at various test points (Whaley, 1994).....	29
Figure 2.23	Moduli versus location for granular base material (Siekmeier, et al., 2000).....	30
Figure 2.24	Correlation between Loadman and FWD moduli (Pidwerbesky, 1997).....	32
Figure 2.25	Relationship between stiffness modulus determined by the portable dynamic plate test devices and the FWD (on subgrade and 400 mm thick granular capping) (Fleming, et al., 2000).	34
Figure 2.26	Comparison of k value from Prima 100 and HFWD at multiple test locations (Kamiura, et al., 2000).....	36
Figure 2.27	Comparison of the variation in deflection ratio with the number of drops at one location (Kamiura, et al., 2000).....	37
Figure 2.28	Prima 100 PFWD measured increase in stiffness due to increased compactive effort and time (Nazzal, 2003).	39
Figure 2.29	Correlations between Prima 100 PFWD, FWD, and PLT (Nazzal, 2003).....	39
Figure 2.30	Typical signage associated with placing load restrictions (Janoo and Cortez, 1998).	41
Figure 2.31	Methods for determining when to place and remove load restrictions (Kestler, et al., 2000).	43
Figure 2.32	Length of time over which load restrictions are placed (Kestler, et al., 2000).....	44
Figure 2.33	Comparison in the ability of the Loadman PFWD and Benkelman Beam to track strength change through spring thaw (Davies, 1997).....	51
Figure 3.1	Typical condition of Kennebec Road, Hampden/Dixmont, Maine in April, 2003.....	56
Figure 3.2	Approximate geographic location of spring thaw test sites.....	58
Figure 3.3	Typical road condition of Lakeside Landing Road, Glenburn, Maine in April, 2003.....	60

Figure 3.4	Typical road condition of Stinson Lake Road, Rumney, New Hampshire in July, 2003.	61
Figure 3.5	Existing site conditions at USFS Parking Lot, Rumney, New Hampshire.	64
Figure 3.6	Existing conditions at Crosstown Road, Berlin, Vermont in March 2004	65
Figure 3.7	Plan view of test sections at Witter Farm Road (Lawrence, et al., 2000).	67
Figure 3.8	Cross section of test sections at Witter Farm Road, Orono, Maine (Lawrence, et al., 2000).	68
Figure 3.9	Test section layout of Route 126 Monmouth/Litchfield, Maine (Helstrom and Humphrey, 2005).	71
Figure 3.10	Test section layout of Route 1A Frankfort/Winterport, Maine (Fetten and Humphrey, 1998).	74
Figure 3.11	I-84 test section, Southington, Connecticut.	77
Figure 3.12	Route 25 Test Section 1, Effingham/Freedom, New Hampshire.	79
Figure 3.13	Route 25 Test Section 2, Effingham/Freedom, New Hampshire.	79
Figure 3.14	Route 26 test section, New Gloucester, Maine.	80
Figure 3.15	Thermocouple string detail	84
Figure 3.16	Frost tube detail.	87
Figure 3.17	Thermocouple/thermistor section view.	88
Figure 3.18	Placement of thermocouple string in auger hole.	89
Figure 3.19	Standpipe piezometer detail.	92
Figure 3.20	Standpipe piezometer detail for Witter Farm Road, Orono, Maine (Lawrence, et al., 2000).	92
Figure 3.21	Kennebec Road and Lakeside Landing Road test point layout.	96
Figure 3.22	Stinson Lake Road, Buffalo Road, and Crosstown Road test point layout	96
Figure 3.23	Variable drop heights (a) 850 mm, (b) 630 mm, and (c) 420 mm.	98

Figure 3.24	MaineDOT JILS Model 20 C FWD.....	101
Figure 3.25	CRREL Dynatest 8000 FWD.....	102
Figure 3.26	VAOT Dynatest 8000 FWD.	103
Figure 3.27	Test point layout for compaction control field test sites.....	105
Figure 3.28	CPN MC-1 Portaprobe NDM	106
Figure 3.29	Troxler 3430 NDM.	106
Figure 3.30	Laboratory test box.	108
Figure 3.31	Bosch 11304 hammer with modified flat plate attachment	109
Figure 3.32	Laboratory test point layout	110
Figure 4.1	Formation of ice lenses within a pavement structure (WSDOT).....	118
Figure 4.2	Route 126 (Section 3), Monmouth/Litchfield, Maine automated pore water pressure measurements.	121
Figure 4.3	Route 126 (Section 8), Monmouth/Litchfield, Maine automated pore water pressure measurements.	121
Figure 4.4	Evercalc 5.0 general file data entry screen (WSDOT, 2001).	125
Figure 4.5	Evercalc 5.0 raw FWD data conversion screen (WSDOT, 2001).	126
Figure 4.6	Evercalc 5.0 FWD deflection data file screen (WSDOT, 2001).....	126
Figure 4.7	Stiffness variation at Kennebec Road (Section 1), Hampden/Dixmont, Maine.	129
Figure 4.8	Stiffness variation at Kennebec Road (Section 2), Hampden/Dixmont, Maine.	130
Figure 4.9	Stiffness variation at Buffalo Road, Rumney, New Hampshire	130
Figure 4.10	Stiffness variation at Stinson Lake Road, Rumney, New Hampshire	131
Figure 4.11	Stiffness variation at Knapp Airport Parking Lot, Berlin, Vermont.....	131
Figure 4.12	Stiffness variation at Witter Farm Road (Control Section), Orono, Maine	132
Figure 4.13	Stiffness variation at Witter Farm Road (Section 2), Orono, Maine.	132

Figure 4.14	Stiffness variation at Witter Farm Road (Section 1), Orono, Maine	133
Figure 4.15	Stiffness variation at Route 126 (Section 3), Monmouth/Litchfield, Maine	133
Figure 4.16	Stiffness variation at Route 126 (Section 8), Monmouth/Litchfield, Maine	134
Figure 4.17	Stiffness variation at Route 126 (Section 12), Monmouth/Litchfield, Maine	134
Figure 4.18	Stiffness variation at Route 1A (Section D-1), Frankfort/Winterport, Maine	135
Figure 4.19	Stiffness variation at Route 1A (Section D-2), Frankfort/Winterport, Maine	135
Figure 4.20	Stiffness variation at Route 1A (Section D-3), Frankfort/Winterport, Maine	136
Figure 4.21	Stiffness variation at Lakeside Landing Road (Section 1), Glenburn, Maine	137
Figure 4.22	Detailed stiffness variation at Lakeside Landing Road (Section 1), Glenburn, Maine	138
Figure 4.23	Stiffness variation at Lakeside Landing Road (Section 2), Glenburn, Maine	138
Figure 4.24	Detailed stiffness variation at Lakeside Landing Road (Section 2), Glenburn, Maine	139
Figure 4.25	2003 stiffness variation at USFS Parking Lot, Rumney, New Hampshire	139
Figure 4.26	2004 stiffness variation at USFS Parking Lot, Rumney, New Hampshire	140
Figure 4.27	2004 detailed stiffness variation at USFS Parking Lot, Rumney, New Hampshire	140
Figure 4.28	Stiffness variation at Crosstown Road, Berlin, Vermont.....	141
Figure 4.29	Detailed stiffness variation at Crosstown Road, Berlin, Vermont.....	141
Figure 4.30	Modulus versus test location at Route 11 (Test Pit 1), Wallagrass Plantation, Maine	143

Figure 4.31	Modulus versus test location at Route 11 (Test Pit 2), Wallagrass Plantation, Maine	143
Figure 4.32	Modulus versus test location at Route 11 (Test Pit 3), Wallagrass Plantation, Maine	144
Figure 4.33	Modulus versus test location at Route 11 (Test Pit 4), Wallagrass Plantation, Maine	144
Figure 4.34	Modulus versus test location at Route 167 (Test Pit 1), Presque Isle/Fort Fairfield, Maine	145
Figure 4.35	Modulus versus test location at Route 167 (Test Pit 2), Presque Isle/Fort Fairfield, Maine	145
Figure 4.36	Modulus versus test location at Route 167 (Test Pit 3), Presque Isle/Fort Fairfield, Maine	146
Figure 4.37	Modulus versus test location at Route 167 (Test Pit 4), Presque Isle/Fort Fairfield, Maine	146
Figure 4.38	Comparison of FWD and PFWD composite moduli at Kennebec Road, Hampden/Dixmont, Maine	148
Figure 4.39	Comparison of FWD and PFWD composite moduli at Route 126, Monmouth/Litchfield, Maine	149
Figure 4.40	Comparison of FWD and PFWD composite moduli at Witter Farm Road, Orono, Maine	149
Figure 4.41	Comparison of FWD and PFWD composite moduli at Route 11, Wallagrass Plantation, Maine	150
Figure 4.42	Comparison of FWD and PFWD composite moduli at Route 167, Presque Isle/Fort Fairfield, Maine	150
Figure 4.43	Comparison of FWD and PFWD composite moduli at Route 1A, Frankfort/Winterport, Maine	151
Figure 4.44	Comparison of FWD and PFWD composite moduli for asphalt thicknesses ≤ 127 mm (5 in.)	151
Figure 4.45	Comparison of FWD and PFWD composite moduli for asphalt thicknesses equal to 152 mm (6 in.)	152
Figure 4.46	Comparison of FWD and PFWD composite moduli for asphalt thicknesses equal to 152 mm (6 in.) and moduli ≤ 4000 MPa	152

Figure 4.47	Comparison of FWD and PFWD composite moduli for all asphalt surfaced test sites	153
Figure 4.48	Comparison of FWD and PFWD composite moduli for all asphalt surfaced test sites and moduli ≤ 4000 MPa	153
Figure 4.49	Comparison of FWD and PFWD composite moduli at Lakeside Landing Road, Glenburn, Maine.	154
Figure 4.50	Comparison of FWD subbase moduli and PFWD composite moduli at Kennebec Road, Hampden/Dixmont, Maine	155
Figure 4.51	Comparison of FWD subbase moduli and PFWD composite moduli at Stinson Lake Road, Rumney, New Hampshire	156
Figure 4.52	Comparison of FWD subbase moduli and PFWD composite moduli at Buffalo Road, Rumney, New Hampshire	156
Figure 4.53	Comparison of FWD subbase moduli and PFWD composite moduli at Knapp Airport Parking Lot, Berlin, Vermont.....	157
Figure 4.54	Comparison of FWD subbase moduli and PFWD composite moduli at Witter Farm Road, Orono, Maine	157
Figure 4.55	Comparison of FWD subbase moduli and PFWD composite moduli at Route 126, Monmouth/Litchfield, Maine	158
Figure 4.56	Comparison of FWD subbase moduli versus PFWD composite moduli at Route 1A, Frankfort/Winterport, Maine.....	158
Figure 4.57	Comparison of FWD subbase moduli and PFWD composite moduli for asphalt thicknesses ≤ 127 mm (5 in.).....	159
Figure 4.58	Comparison of FWD subbase moduli and PFWD composite moduli for asphalt thickness ≤ 127 mm (5 in.) and moduli ≤ 5000 MPa	159
Figure 4.59	Comparison of FWD subbase moduli and PFWD composite moduli for all asphalt surfaced test sites	160
Figure 4.60	Comparison of FWD subbase moduli and PFWD composite moduli for all asphalt surfaced test sites and moduli ≤ 5000 MPa	160
Figure 4.61	Comparison of FWD subbase moduli and PFWD composite moduli at Crosstown Road, Berlin, Vermont.....	161
Figure 4.62	Comparison of FWD and PFWD ISM at Kennebec Road, Hampden/Dixmont, Maine	162

Figure 4.63	Comparison of FWD and PFWD ISM at Stinson Lake Road, Rumney, New Hampshire.....	163
Figure 4.64	Comparison of FWD and PFWD ISM at Buffalo Road, Rumney, New Hampshire.....	163
Figure 4.65	Comparison of FWD and PFWD ISM at Knapp Airport Parking Lot, Berlin, Vermont.....	164
Figure 4.66	Comparison of FWD and PFWD ISM at Witter Farm Road, Orono, Maine.....	164
Figure 4.67	Comparison of FWD and PFWD ISM at Route 126, Monmouth/Litchfield, Maine.....	165
Figure 4.68	Comparison of FWD and PFWD ISM at Route 1A, Frankfort/Winterport, Maine.....	165
Figure 4.69	Comparison of FWD and PFWD ISM for test sites with asphalt thicknesses ≤ 127 mm (5 in.).....	166
Figure 4.70	Comparison of FWD and PFWD ISM for test sites with asphalt thicknesses equal to 152 mm (6 in.).....	166
Figure 4.71	Comparison of FWD and PFWD ISM for all asphalt surfaced test sites.....	167
Figure 4.72	Comparison of FWD and PFWD ISM at Lakeside Landing Road, Glenburn, Maine.....	167
Figure 4.73	Comparison of FWD and PFWD ISM at Crosstown Road, Berlin, Vermont.....	168
Figure 4.74	Comparison of FWD and PFWD ISM at USFS Parking Lot, Rumney, New Hampshire.....	168
Figure 4.75	Comparison of FWD and PFWD ISM for all gravel surfaced test sites.....	169
Figure 4.76	Comparison of FWD derived subbase moduli to Loadman and Prima 100 PFWD composite moduli on asphalt surfaced test sites.....	171
Figure 4.77	Effect of drop weight and loading plate diameter on Prima 100 PFWD composite moduli.....	172
Figure 4.78	Effect of drop height on PFWD composite moduli at Witter Farm Road, Orono, Maine.....	174

Figure 4.79	Effect of drop height on PFWD composite moduli at Route 126, Monmouth/Litchfield, Maine.....	175
Figure 4.80	Effect of drop height on PFWD composite moduli at Route 1A, Frankfort/Winterport, Maine	175
Figure 4.81	Comparison of FWD composite moduli to PFWD composite moduli derived from different geophones at Kennebec Road, Hampden/Dixmont, Maine	177
Figure 4.82	Comparison of FWD composite moduli to PFWD composite moduli derived from different geophones at Route 126, Monmouth/Litchfield, Maine.....	178
Figure 4.83	Comparison of FWD composite moduli to PFWD composite moduli derived from different geophones at Route 1A, Frankfort/Winterport, Maine	178
Figure 4.84	Effect of consecutive drops on composite modulus on May 12, 2004 at Route 126 (Section 3), Monmouth/Litchfield, Maine	179
Figure 4.85	Effect of consecutive drops on composite modulus values on April 22, 2004 at Route 126 (Section 12), Monmouth/Litchfield, Maine	180
Figure 4.86	Buffalo Road, Rumney, New Hampshire.	187
Figure 4.87	Knapp Airport Parking Lot, Berlin, Vermont.....	187
Figure 4.88	USFS Parking Lot, Rumney, New Hampshire.	188
Figure 4.89	Crosstown Road, Berlin, Vermont.....	188
Figure 5.1	Comparison of oven dried and NDM water contents.	197
Figure 5.2	Comparison of percent compaction determined from sand cone and NDM tests.....	198
Figure 5.3	Effect of percent compaction on composite modulus, Connecticut crushed gravel.....	200
Figure 5.4	Effect of percent compaction on composite modulus, New Hampshire sand.....	201
Figure 5.5	Effect of percent compaction on composite modulus, New Hampshire gravel.....	201
Figure 5.6	Effect of percent compaction on composite modulus, OJF gravel.....	202

Figure 5.7	Effect of percent compaction on composite modulus, Wardwell gravel.	202
Figure 5.8	Comparison of percent compaction and composite modulus, Connecticut crushed gravel.....	204
Figure 5.9	Comparison of percent compaction and composite modulus, New Hampshire sand.....	205
Figure 5.10	Comparison of percent compaction and composite modulus, New Hampshire gravel.....	205
Figure 5.11	Comparison of percent compaction and composite modulus, OJF gravel.	206
Figure 5.12	Comparison of percent compaction and composite modulus, Wardwell gravel.....	206
Figure 5.13	Comparison of percent compaction and composite modulus for all laboratory samples.	207
Figure 5.14	Comparison of percent compaction and composite modulus for three laboratory samples.	207
Figure 5.15	Comparison of percent compaction and composite modulus for laboratory tests with water contents dry of the OWC.....	208
Figure 5.16	Comparison of percent compaction and composite modulus for selected laboratory samples with water contents dry of the OWC.....	209
Figure 5.17	Comparison of percent compaction and composite modulus for laboratory tests with water contents wet of the OWC.	209
Figure 5.18	Comparison of percent compaction and composite modulus for selected laboratory samples with water contents wet of the OWC.....	210
Figure 5.19	Comparison of percent compaction and composite modulus of crushed gravel tested at I-84, Southington, Connecticut.	213
Figure 5.20	Comparison of dry density and composite modulus of subgrade tested at I-84, Southington, Connecticut.....	213
Figure 5.21	Comparison of percent compaction and composite modulus of construction sand tested at Route 25, Effingham/Freedom, New Hampshire.....	214
Figure 5.22	Comparison of percent compaction and composite modulus of gravel tested at Route 25, Effingham/Freedom, New Hampshire.	214

Figure 5.23	Comparison of percent compaction and composite modulus of subgrade tested at CPR, Scarborough, Maine.....	215
Figure 5.24	Comparison of percent compaction and composite modulus for materials tested at Route 25 and I-84 field test sites.....	215
Figure 5.25	Change in moduli with time at CPR test site, Scarborough, Maine.	216
Figure 5.26	Change in moduli with time at Route 201 test site, The Forks, Maine.....	216
Figure 5.27	Comparison of water content and composite modulus, Connecticut crushed gravel.	218
Figure 5.28	Comparison of water content and composite modulus, New Hampshire sand.....	218
Figure 5.29	Comparison of water content and composite modulus, New Hampshire gravel.....	219
Figure 5.30	Comparison of water content and composite modulus, OJF gravel.	219
Figure 5.31	Comparison of water content and composite modulus, Wardwell gravel.	220
Figure 5.32	Comparison of water content and composite modulus for all laboratory samples.	220
Figure 5.33	Prima 100 PFWD measurement on Wardwell gravel wet of optimum	221
Figure 5.34	Prima 100 PFWD measurement on Wardwell gravel wet of optimum	221
Figure 5.35	Comparison of water content and composite modulus of crushed gravel tested at I-84, Southington, Connecticut.....	223
Figure 5.36	Comparison of water content and composite modulus of subgrade tested at I-84, Southington, Connecticut.....	223
Figure 5.37	Comparison of water content and composite modulus of sand tested at Route 25, Effingham/Freedom, New Hampshire.	224
Figure 5.38	Comparison of water content and composite modulus of gravel tested at Route 25, Effingham/Freedom, New Hampshire.	224
Figure 5.39	Comparison of water content and composite modulus of subgrade tested at CPR, Scarborough, Maine.	225
Figure 5.40	Comparison of water content and composite modulus for all field test sites.....	225

Figure 5.41	Composite modulus predicted by regression equations at 4% dry of optimum.	229
Figure 5.42	Composite modulus predicted by regression equations at optimum.	229
Figure 5.43	Composite modulus predicted by regression equations at 4% wet of optimum.	230
Figure 5.44	Effect of percent compaction and water content on predicted composite modulus based on laboratory results for Connecticut crushed gravel, New Hampshire sand, and Wardwell gravel.	230
Figure 5.45	Typical shapes of coarse grained bulky particles (Holtz and Kovacs, 1981).	233
Figure 5.46	Poorly graded New Hampshire sand.	233
Figure 5.47	Well graded Connecticut crushed gravel.	234
Figure 5.48	Testing with USFS and UMaine Prima 100 PFWDs.	235
Figure 5.49	Change in composite modulus with subsequent drops for two PFWDs at the same test point for OJF gravel at 100% compaction and optimum water content (TP #1).	236
Figure 5.50	Change in composite modulus with subsequent drops for two PFWDs at the same test point for Wardwell gravel at 100% compaction and optimum water content (TP #1).	237
Figure 5.51	Comparison of USFS and UMaine Prima 100 PFWD composite moduli.	237
Figure 5.52	Change in composite modulus with subsequent drops for different devices at the same test point for OJF gravel at 100% compaction and optimum water content (TP #1).	239
Figure 5.53	Clegg Impact Hammer measurement on New Hampshire sand.	240
Figure 5.54	Comparison of Clegg Impact Hammer and UMaine Prima 100 PFWD composite moduli.	240
Figure 5.55	MaineDOT representative (operator #2) performing laboratory PFWD measurements.	242
Figure A.1	Grain size distribution of Connecticut crushed gravel.	279

Figure A.2	Grain size distribution of New Hampshire sand.	279
Figure A.3	Grain size distribution of New Hampshire gravel.	280
Figure A.4	Grain size distribution of bottom 1 ft of OJF gravel.....	280
Figure A.5	Grain size distribution of Owen J. Folsom gravel.	281
Figure A.6	Grain size distribution of Wardwell gravel.....	281
Figure A.7	Grain size distribution of crushed gravel tested at I-84, Southington, Connecticut.	282
Figure A.8	Grain size distribution of existing subgrade material tested at I-84, Southington, Connecticut.	282
Figure A.9	Grain size distribution of construction sand tested at Route 25, Effingham/Freedom, New Hampshire.	283
Figure A.10	Grain size distribution of gravel tested at Route 25, Effingham/Freedom, New Hampshire.	283
Figure A.11	Grain size distribution of MaineDOT Type D gravel tested at Route 26, New Gloucester, Maine.	284
Figure A.12	Grain size distribution of MaineDOT Type E gravel tested at Route 26, New Gloucester, Maine.	284
Figure A.13	Grain size distribution of existing subgrade tested at CPR, Scarborough, Maine.	285
Figure A.14	Grain size distribution of existing subgrade material at Route 126 (Section 3), Monmouth/Litchfield, Maine.	285
Figure A.15	Grain size distribution of existing subgrade material at Route 126 (Section 8), Monmouth/Litchfield, Maine.	286
Figure A.16	Grain size distribution of existing subbase material at Stinson Lake Road, Rumney, New Hampshire.	286
Figure A.17	Grain size distribution of tire chip / soil mixtures at Witter Farm Road, Orono, Maine (Lawrence, et al., 2000).	287
Figure A.18	Grain size distribution of MaineDOT Type D subbase used at Witter Farm Road, Orono, Maine (Lawrence, et al., 2000).	287
Figure A.19	Grain size distribution of MaineDOT Type D subbase used at Witter Farm Road, Orono, Maine (Lawrence, et al., 2000).	288

Figure A.20	Grain size distribution of subbase material at Route 1A, Frankfort/Winterport, Maine (Fetten and Humphrey, 1998).....	288
Figure B.1	Connecticut crushed gravel moisture density curve.	289
Figure B.2	New Hampshire sand moisture density curve.....	289
Figure B.3	New Hampshire gravel moisture density curve.	290
Figure B.4	Owen J. Folsom #1 moisture density curve.	290
Figure B.5	Owen J. Folsom #2 moisture density curve.	291
Figure B.6	Wardwell gravel moisture density curve.	291
Figure B.7	Moisture density curve of sand tested at Route 25, Effingham/Freedom, New Hampshire.....	292
Figure B.8	Moisture density curve of gravel tested at Route 25, Effingham/Freedom, New Hampshire.	292
Figure B.9	Moisture density curve of MaineDOT Type D at Route 26, New Gloucester, Maine.....	293
Figure B.10	Moisture density curve of MaineDOT Type E at Route 26, New Gloucester, Maine.....	293
Figure B.11	Moisture density curve of existing subgrade material at CPR, Scarborough, Maine.....	294

(BLANK PAGE)

CHAPTER 1

INTRODUCTION

1.1 BACKGROUND

Modulus (stiffness) is one of the primary inputs into mechanistic pavement design procedures and provides insight into long term pavement performance. Based on layer stiffness and thickness, stresses and strains are computed to investigate whether they are below critical limits needed to achieve adequate pavement performance during the design life (Van Gurp, et al., 2000). Despite the importance of modulus, some aspects of pavement construction and management are still based on measurement of parameters that are not directly connected with long-term performance or on empirical based judgments. Two critical areas that do not make use of modulus are evaluating the support capacity of pavements during the spring thaw for the purposes of restricting truck loading and evaluating the adequacy of subgrade and base compaction during construction. These topics are the focus of this study.

Pavements in areas with seasonal freezing and thawing often undergo frost heave and thaw weakening in addition to load-induced pavement distress. To minimize damage, many road maintenance agencies impose load restrictions during damage-susceptible periods. Spring thaw adversely affects pavement life while load restrictions impose local economic hardships throughout the northern United States and Canada. Although the maximum allowable load and the duration of the reduced load period vary widely among agencies, they try to strike a balance between minimizing the disruption to the local economy caused by the load restrictions and minimizing road damage.

Although modulus is a key parameter in determining damage-susceptibility of pavements, the imposition of spring-thaw load restrictions are often based on visual observation combined with the pavement manager's judgment. Modulus could be monitored during spring thaw and through recovery using a trailer-mounted falling weight deflectometers (FWD). However, FWD purchase, operation, and maintenance is expensive. Second, even if a state owns a FWD, it can only cover so many roads within the spring thaw period. As a result, determining when the road has thawed and recovered sufficient strength to remove the restriction is left to personal experience and subjective judgment.

Virtually all state highway departments use dry density as the principal criterion for judging the quality of compacted earthwork. This criterion implies that increased dry density produces improved engineering properties in the material. Although the use of dry density for field control can be easily accomplished, particularly with the increasing use of nuclear devices, its value as a usable criterion is only valid insofar as the dry density does, in fact, indicate the critical engineering properties of the material such as stiffness (Langfelder and Nivargikar, 1967). At present, there is no viable alternative to density as a method for compaction control since there is no well-established method to measure the stiffness of compacted materials that would be practical to use during construction.

The purpose of this project is to investigate a practical method of measuring stiffness of pavement structures during the spring thaw and of compacted subgrade soil and base aggregate during construction. The premise is that this can be accomplished using a portable falling weight deflectometer (PFWD). The PFWD operates on the same

principle as the full-size FWD, but it is small enough that it can be easily moved by one person.

1.2 SCOPE OF STUDY

There are two main objectives for this research project. The first objective was to investigate the ability of portable falling weight deflectometers (PFWD) to track seasonal stiffness variations. Measurements were taken on paved and unpaved low volume roads during the spring thaw. Comparisons were made to the traditional FWD as well as other portable devices. Correlations were developed to compare performance. Recommendations were made for field testing techniques.

The second objective was to investigate the ability of the PFWDs to serve as an alternative to traditional compaction control devices. A relationship between PFWD composite moduli and percent compaction for soil types representative of New England base and subbase aggregates was established. The effect of water content was also investigated. Comparisons were made to other portable devices and correlations were developed. Recommendations were made for field testing techniques.

1.3 ORGANIZATION OF THE REPORT

This report is divided into six chapters, and is organized as follows. Chapter 2 is a literature review covering several topics relevant to the evaluation of the PFWD. PFWD and other portable testing devices are described. Past test programs, results, and recommendations for use on both asphalt and gravel surfaces are presented. Current methods to evaluate thaw weakening of roads are discussed. Results and

recommendations for using the PFWD to track seasonal stiffness variations are made for asphalt surfaced test sites. A questionnaire to determine current usage of the PFWD as an alternative to traditional compaction control devices and as a tool to evaluate thaw weakening of roads was distributed to transportation agencies, the results of which are presented.

Chapter 3 describes the field and laboratory testing techniques. Field test site locations are presented including: current road condition, subsurface conditions, and cross sections of the test sites. Instrumentation descriptions, and installation and monitoring procedures are presented. Descriptions of the field testing procedures and data gathered for both the study of seasonally posted low volume paved and unpaved roads and the field and laboratory study of the compaction of subgrades and construction materials are provided. Finally, data analysis techniques that were employed are discussed.

Chapter 4 presents the analysis, field test results, and recommendations for utilizing the PFWD as tool to track seasonal stiffness variations in paved and unpaved low volume roads.

Chapter 5 presents the analysis, laboratory and field test results, and recommendations for utilizing the PFWD as an alternative to traditional compaction control devices.

Chapter 6 summarizes all aspects of the research project and provides conclusions and recommendations for future work.

CHAPTER 2

LITERATURE REVIEW

2.1 INTRODUCTION

This literature review focuses on the use of a Portable Falling Weight Deflectometer (PFWD) as an alternative to traditional compaction control methods and as a tool to evaluate thaw weakening of roads. Several studies have been conducted pertaining to the use, reliability, and accuracy of the PFWD. The PFWD has been compared to traditional in situ testing devices and is discussed below. A questionnaire was developed and distributed to state departments of transportation as well as international organizations currently utilizing PFWDs, the results of which are also discussed.

2.2 PFWD AS ALTERNATIVE FOR COMPACTION CONTROL

2.2.1 Current Compaction Control Methods

Traditional compaction control methods can be costly, require considerable time for field tests, and some have extensive training and safety requirements. Devices used to monitor compaction measure one of two things, density or modulus (stiffness). Stiffness is a qualitative term meaning a general resistance to deformation. It is often used interchangeably with elastic modulus, modulus of subgrade reaction, and resilient modulus. It largely determines the strains and displacements of the subgrade as it is loaded and unloaded (Newcomb and Birgisson, 1999). During construction major emphasis has traditionally been placed on achieving the specified dry density and little

consideration is given to the engineering properties desired of the compacted fill. Dry density and water content correlate well with the engineering properties, and thus they are convenient construction control parameters (Holtz and Kovacs, 1981). Therefore, instruments that measure density are used for quality assurance. However, modulus is one of the primary inputs into any pavement design procedure, and provides insight into long term pavement performance. Based on layer stiffness and thickness, critical stresses and strains are computed to investigate whether they are below critical limits needed to achieve adequate pavement performance during the design life (Van Gorp, et al., 2000). Such stiffness measurements are more fundamentally sound from an engineering perspective than the now universally accepted moisture-density measurements used for compaction control (Lenke, et al., 2003). Stiffness measurements on pavement structures make it possible to treat it in the same manner as other civil engineering structures by using mechanistically based design methods. Selecting the type of rehabilitation to be implemented on a given pavement is of considerable economic significance. To reach that decision with inadequate knowledge of the structural condition of the pavement may result in unnecessary costly repairs (Dynatest, 2004).

2.2.1.1 Density Measurement

Many in-situ testing devices exist that monitor density. Until recently, the sand cone method (AASHTO T 191) and to a lesser extent the rubber balloon method (AASHTO T 205) were used to measure density and provide quality control for construction. However, both methods are labor intensive, time is required to dig holes, and there is time delay in obtaining water content. In practice, both of these devices have

been replaced by the nuclear moisture density meter (NDM) (AASHTO T 238). The NDM emits gamma rays and neutrons from two radioactive materials (Cesium-137 and Americium-241) housed within the device. The gamma rays emitted by the Cesium-137 penetrate the layers through a probe inserted into the ground from beneath the unit and interact with electrons in the material. A Geiger Detector housed within the unit counts the gamma rays that reach it from the source. A calibration chart, provided by the manufacturer, relates the count to density. Similarly, Americium-241 produces high energy (fast) neutrons that collide with nuclei in the material. The neutrons that collide with hydrogen nuclei slow down much quicker than those that collide with other, larger nuclei. The Geiger Detector counts only low energy (slow) neutrons, thus the detector count is proportional to the number of hydrogen atoms present. Since water (H₂O) contains many hydrogen atoms, the detector count is proportional to moisture content. A calibration chart, provided by the manufacturer relates the count to moisture content. Operation of the device is shown in Figure 2.1.

Nuclear tests can be conducted rapidly as compared with destructive methods, with results known within minutes. Such rapidity allows the contractor and field engineer to know results quickly, allowing corrective action to be taken as necessary before additional earthwork has been placed (Lenke, et al., 2003). However, the NDM has several drawbacks:

1. Relatively high initial cost.
2. Operation is limited to certified operators.

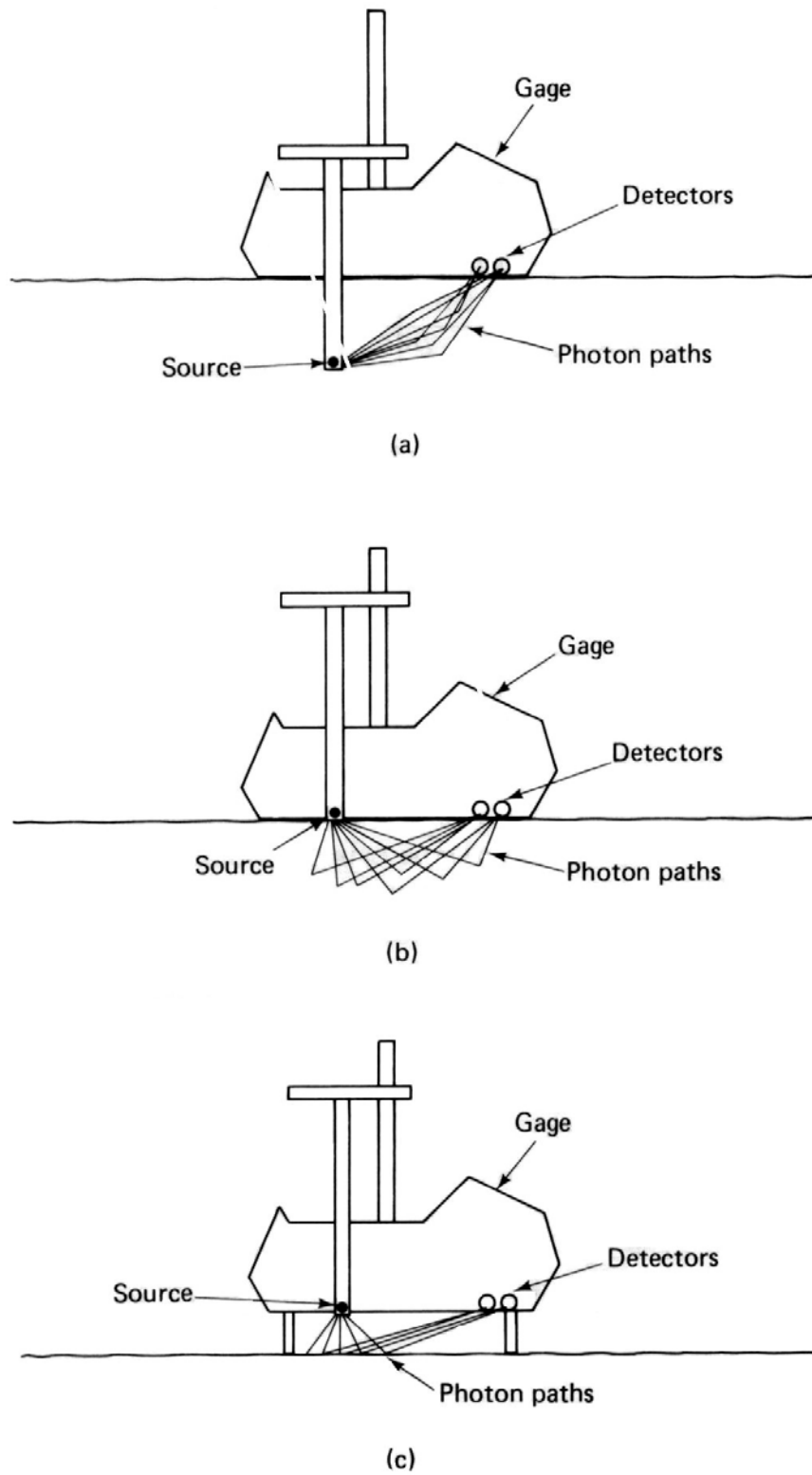


Figure 2.1 Nuclear density and water content determination: (a) direct transmission; (b) backscatter; (c) air gap (Holtz and Kovacs, 1981).

3. Those working with and around the device are required to wear film badges that must periodically be submitted and checked for radioactive exposure dosage in response to operational manuals, women of child-bearing age are frequently discouraged by their supervisors from using this equipment.
4. Shipping and transport of the device over borders and state lines requires significant monetary investment, paperwork, and therefore time.
5. Disposal at the end of the gauge's useful life is extremely difficult.

2.2.1.2 Alternative Portable Device Measurement

It is for the reasons given above that a new method for evaluating compaction is desirable. The disadvantages have prompted transportation agencies to look for nonnuclear methods for compaction control. Such alternatives must eliminate the safety and regulatory concerns of nuclear methods yet provide comparable speed and precision during field testing. Any alternative must also provide an engineering measurement that is related to the engineering properties and engineering performance of the soil evaluated (Lenke, et al., 2003).

There are several portable test devices that attempt to measure the in situ modulus of highway foundation material (Fleming, et al., 2002). The Clegg Impact Tester (ASTM D 5874) utilizes a hammer of known mass dropped from a predetermined height to evaluate the modulus. An accelerometer is used to measure the deceleration of the weight as it impacts the underlying material, and is reported on a digital readout as an

impact value that may be correlated to stiffness (Thompson and Garcia, 2003). The Dynamic Cone Penetrometer (DCP) test measures the penetration resistance as the cone of the device is driven into the pavement structure. A cone on the bottom of an anvil is driven into the ground by means of a hammer dropped from a standard height. The amount of penetration per blow is monitored. The penetration is a function of the shear strength of the material. The Humboldt Soil Stiffness Gauge (SSG) is a recently developed nondestructive testing device that measures the in situ stiffness. The SSG imparts very small displacements to the soil at 25 steady state frequencies between 100 and 196 Hz (Thompson and Garcia, 2003). It then measures the stress imparted to the surface and resulting surface velocity as a function of time, from which, stiffness may be calculated. The final type of device is the Portable Falling Weight Deflectometer (PFWD), and is discussed in detail in the following sections.

2.2.2 PFWD Equipment

The PFWD is a light, portable device that has been developed to measure stiffness of construction layers including subgrades, base courses, and pavements. Various models have been developed and used significantly in Europe. The PFWD creates a non-destructive shock-wave through the soil as a result of the impact of a falling weight. Sensors such as velocity transducers or accelerometers are used to measure surface movement, from which deflection is determined. A load cell is used to measure the impact force of the falling weight. Boussinesq developed equations for the state of stress within a homogeneous, isotropic, linearly elastic half-space for a point load acting

perpendicular to the surface (Holtz and Kovacs, 1981). Manipulation of this theory provides a means for determining the modulus from the two measurements.

2.2.2.1 Prima 100 PFWD

The first model is the Prima 100, manufactured by Keros Technology and Carl Bro Pavement Consultants, both of Denmark. This model is versatile in that it allows more flexibility in the stress applied to the underlying material by varying the falling mass (10, 15, and 20 kg (22, 33, and 44 lb)) as well as varying the drop height (10 to 850 mm (0.4 to 33.5 in.)). Three different loading plates may be used, 100, 200, and 300 mm (3.9, 7.9, and 11.8 in.). The Prima 100 has a load impulse of between 15 and 20 ms and a load range of 1 to 15 kN (224.8 to 3372.1 lbf), i.e. up to 200 kPa (29 psi) with its 300 mm (11.8 in.) diameter bearing plate (Fleming, et al., 2000). The unit is shown in Figures 2.2 and 2.3.

The Prima 100 uses two types of sensors: a load cell for measuring the impact force from the falling weight, and a geophone that measures the velocity of the surface from which deflection is determined by integration (Christensen, 2003). With this model, the reaction of the soil to the shock-waves can be measured by up to three geophones that extend radially outward from the unit. The load cell and geophones are shown in Figures 2.4, 2.5, and 2.6.

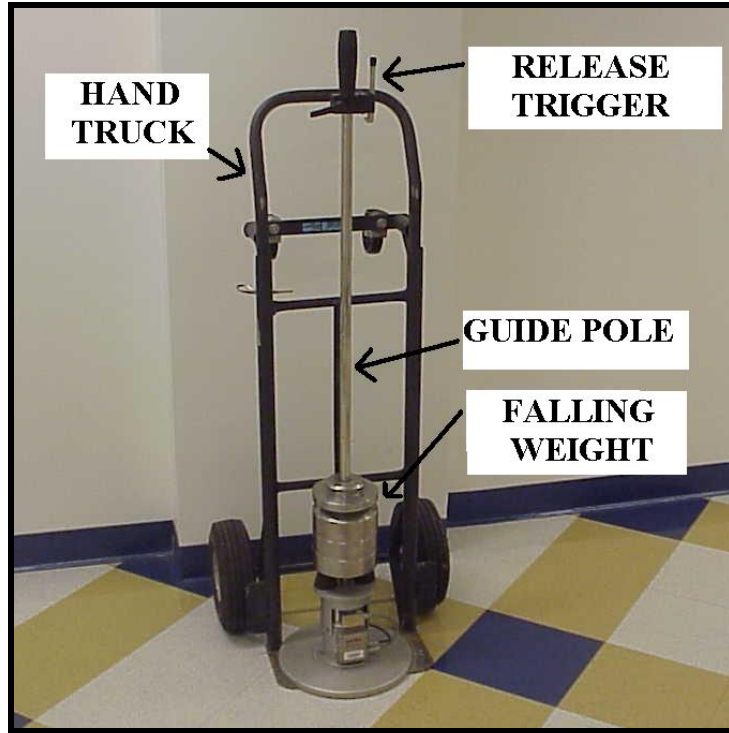


Figure 2.2 Keros Prima 100 PFWD.

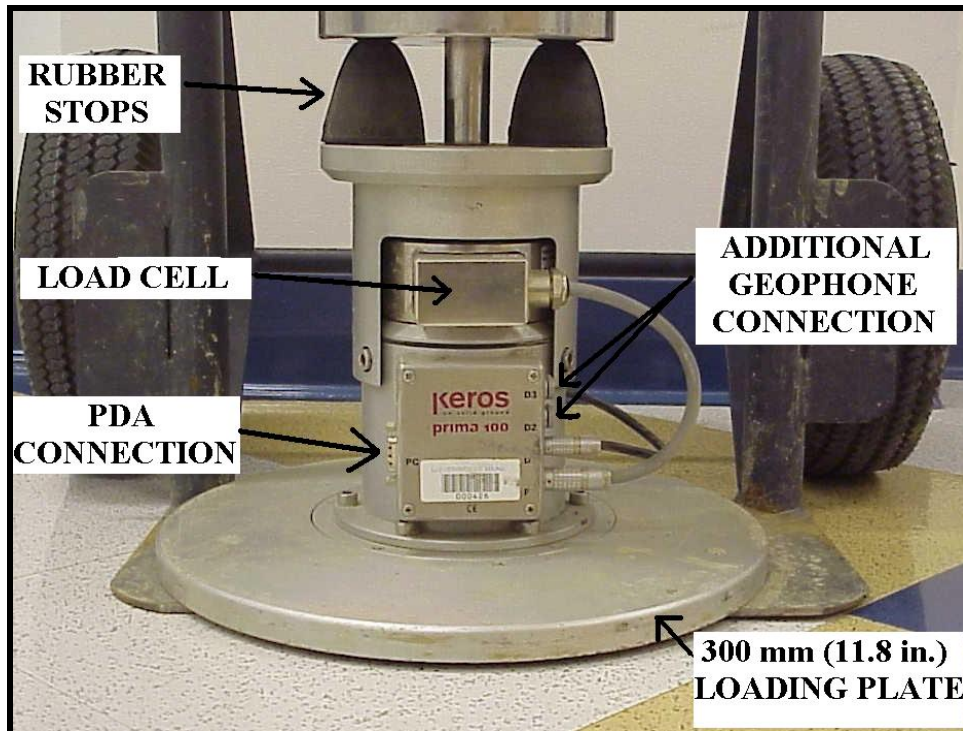


Figure 2.3 Keros Prima 100 PFWD.

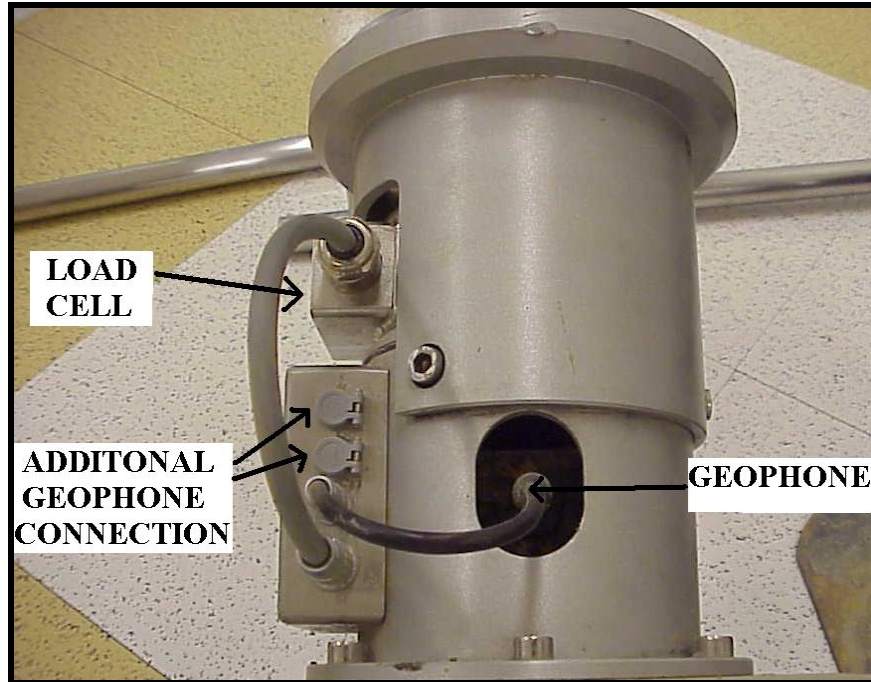


Figure 2.4 Profile of load cell and geophone.

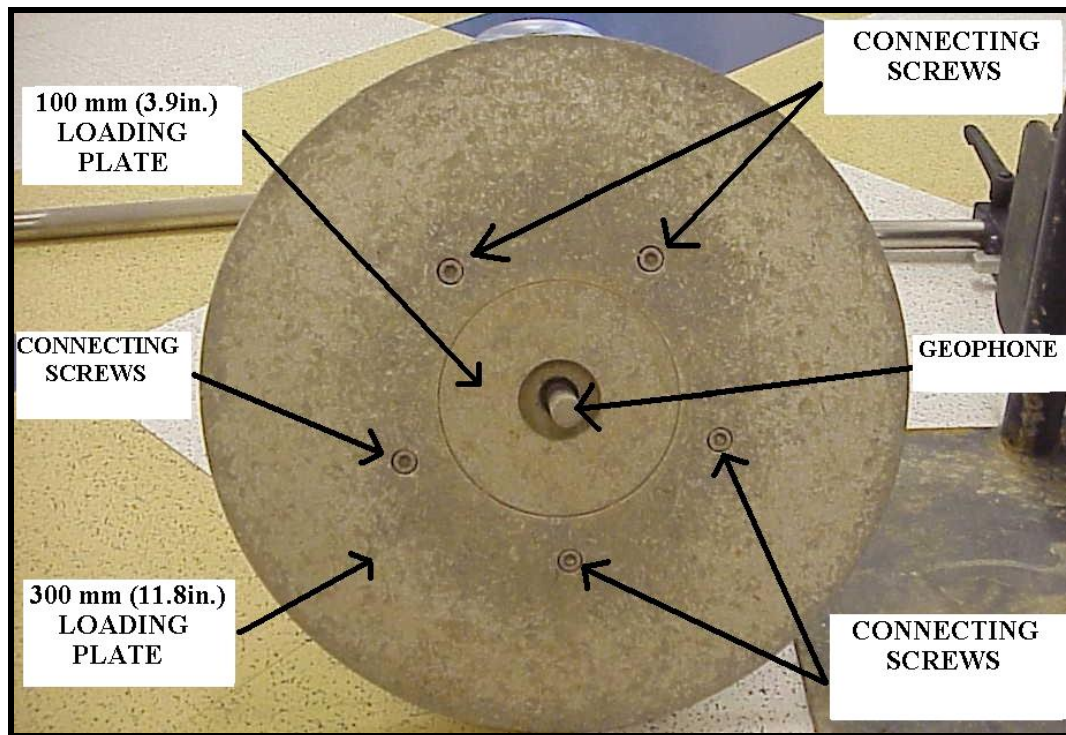


Figure 2.5 Bottom view of geophone.



Figure 2.6 Additional geophones.

The Prima 100 PFWD records values of force, pressure, and deflection with respect to time and is recorded automatically by a Personal Digital Assistant (PDA). Based on these measurements, the software calculates the elastic modulus according to Equation 2.1. For modulus values at distances of more than two radii from the center of the load may be determined by Equation 2.2 (Christensen, 2003). A sample of the output screen for one measurement is shown in Figure 2.7.

$$E = \frac{f \cdot (1 - \nu^2) \cdot \sigma_0 \cdot a}{d_0} \quad \text{Eqn. 2.1}$$

Where: E = Surface Modulus
 μ = Poisson's ratio (default: 0.5)
 σ_0 = Applied stress at surface
 a = Radius of loading plate
 d_0 = Deflection
 f = Factor that depends on the stress distribution

Uniform: $f = 2$ (default)
 Rigid plate: $f = \pi/2$
 Parabolic, granular: $f = 8/3$
 Parabolic, cohesive: $f = 4/3$

$$E = \frac{(1 - \nu^2) \cdot \sigma_0 \cdot a^2}{r \cdot d_0(r)} \quad \text{Eqn. 2.2}$$

Where: r = Distance from center
 $d_0(r)$ = Deflection at the distance r from the center

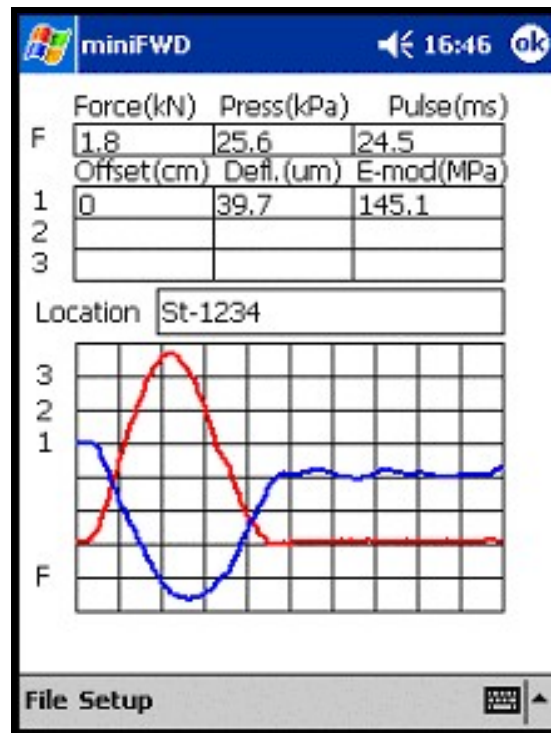


Figure 2.7 Prima 100 PFWD PDA display after one measurement.

2.2.2.2 Loadman PFWD

The Loadman PFWD was originally developed in Finland by AI-Engineering Oy (Honkanen, 1991) for the testing of granular base courses and its use has been extended to bound layers. It has been adopted by over 60 research organizations, universities, consultants, road agencies, contractors and local authorities in Canada, Estonia, Finland,

India, Israel, Italy, Pakistan, Russia, Sweden, the United Kingdom and other countries located throughout the world (Pidwerbesky, 1997). It is not as versatile as the Prima 100 model. The device utilizes a single 10 kg weight that is dropped from a fixed height of 800 mm (2.6 ft). The Loadman has loading plate sizes of 132, 200, and 300mm (5.2, 7.9, and 11.8 in.). The device is believed to be capable of measuring deflections ranging from 0 to 5 mm (0 to 0.2 in.), with an approximate time of loading of between 25 and 30 milliseconds (ms) and maximum dynamic load of roughly 23 kN (5171 lbf) (Gros, 1993). The Loadman PFWD is shown in Figure 2.8.

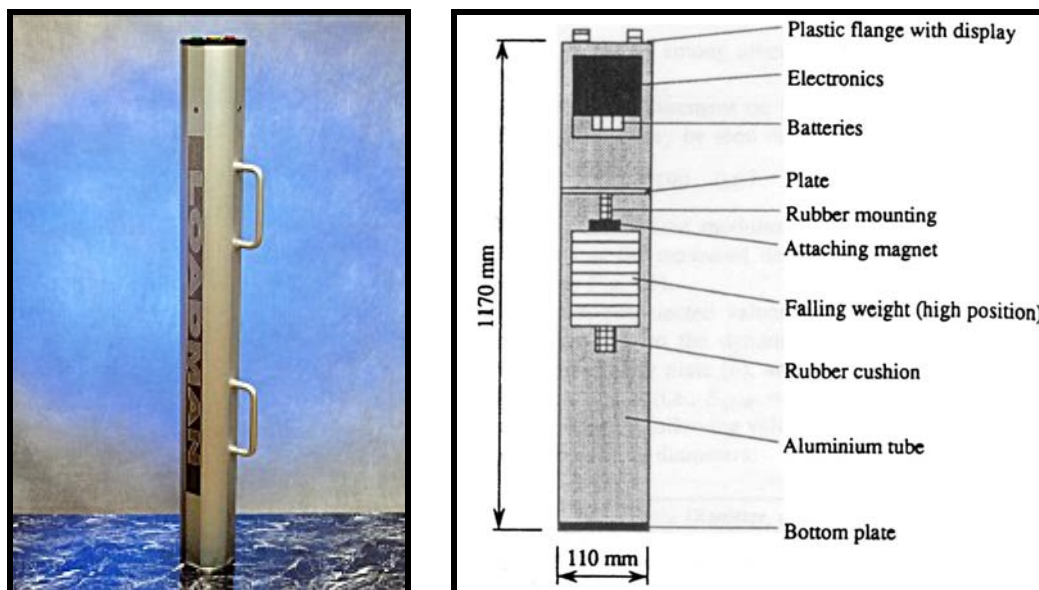


Figure 2.8 Loadman PFWD (Livneh, et al., 1997).

The Loadman PFWD uses two types of sensors, a load cell and an accelerometer. Manipulation of Boussinesq's equations provides an equation to determine modulus from the results measured by the Loadman (Pidwerbesky, 1997). Equation 2.3 is used by the device to determine elastic modulus.

$$E = 1.5 \times \frac{pa}{\Delta} \quad \text{Eqn. 2.3}$$

Where: Δ = deflection under Loadman plate
 p = unit load on circular plate
 a = radius of base plate
 E = modulus of elasticity

For each measurement, the Loadman displays the maximum deflection, calculated bearing capacity modulus, length of the loading impulse, percentage of the rebound deflection compared to the maximum deflection, and the compaction ratio, which is defined as the deflections measured on second and subsequent drops divided by the deflection measured on the first drop (Al-Engineering Oy). A sample of the output screen after one measurement is shown in Figure 2.9.

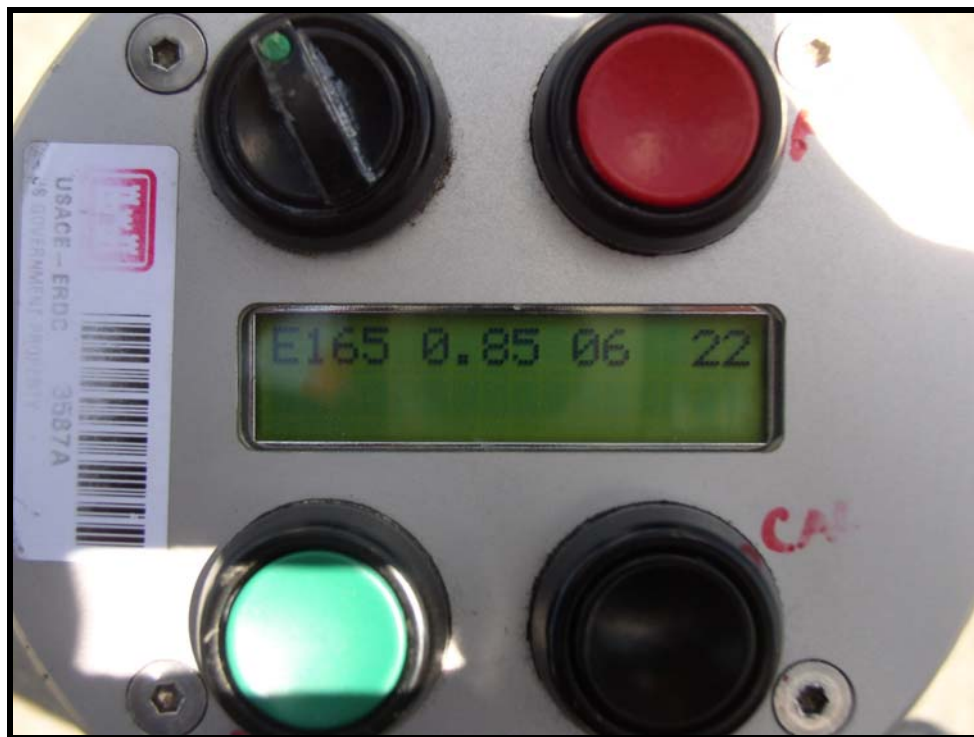


Figure 2.9 Loadman PFWD display after one measurement.

2.2.3 Past Test Programs, Results, and Recommendations

Several test programs have been conducted outside of the United States (US) over the last several years with an increasing but still limited number of studies within the US. Generally, the primary purpose of the test programs was to determine whether the PFWD was suitable for use as a measuring instrument for quality assurance purposes in road construction. Most researchers developed relationships between the PFWD and other, more traditional measuring devices. The studies yielded encouraging results. Testing was conducted on pavement and unbound aggregate layers and each are discussed separately below.

2.2.3.1 Pavement Layers

PFWD evaluations on pavement layers have been conducted by several investigators. Flexible pavements and thin membrane surfaced roads were tested by Gros (1993), Livneh (1997), Whaley (1994), and Davies (1997). Correlations to other traditional measures of stiffness and comparison between PFWD devices have been made and are discussed.

Gros (1993) performed tests on pavement sections consisting of asphalt concrete (AC), thickness unknown, underlain by 0 to 64 mm (0 to 2.5 in.) of crushed gravel or crushed rock, and 0 to 32 mm (0 to 1.25 in.) of gravel. Multiple Loadman PFWD and Falling Weight Deflectometer (FWD) measurements were taken. Gros (1993) recommended that when testing asphalt pavement, two measurements at each measuring point are necessary. For the majority of points tested, the Loadman produced higher modulus values than the FWD. Correlation coefficients between devices range from 0.03 to 0.44 with an average of 0.27. Typical results are shown in Figures 2.10 through 2.13.

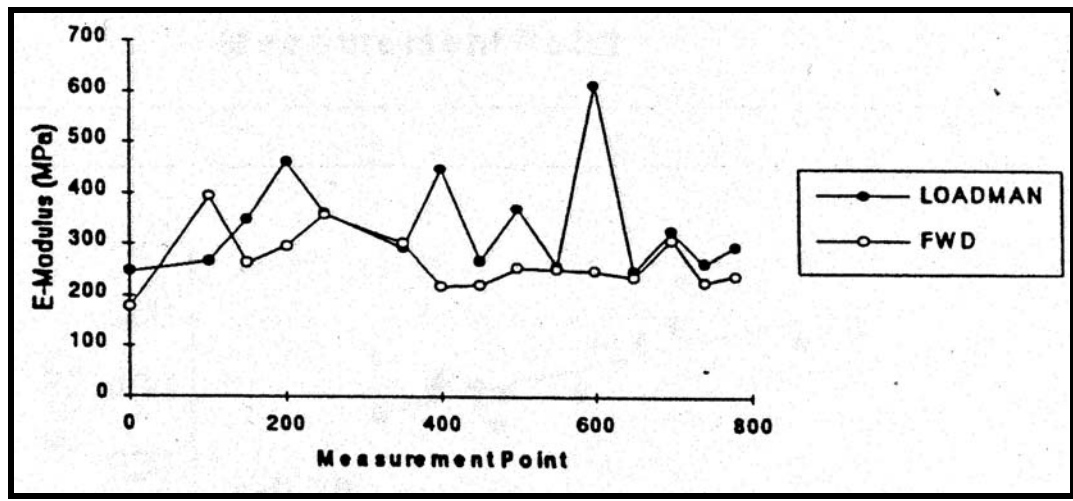


Figure 2.10 Comparison of Loadman and FWD at various test points (Gros, 1993).

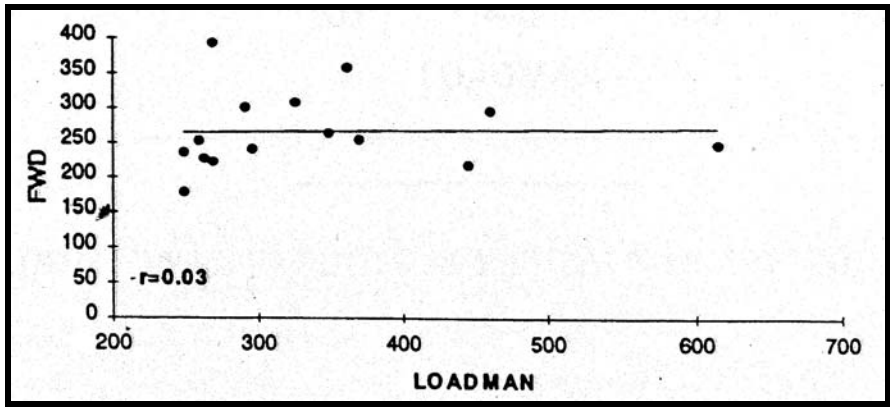


Figure 2.11 Correlation between Loadman and FWD (Gros, 1993).

Results of testing on bound layers indicated that the PFW and FWD correlate poorly with one another, typically differing by 20% to 30%. Gros attributes the “irregularity” of the Loadman curve to the fact that it is more sensitive to heterogeneous layers because its depth of influence is less. He notes that larger stone particles can cause peaks, and the influence of a stone will be higher for Loadman because the “spheres” of stress levels are smaller.

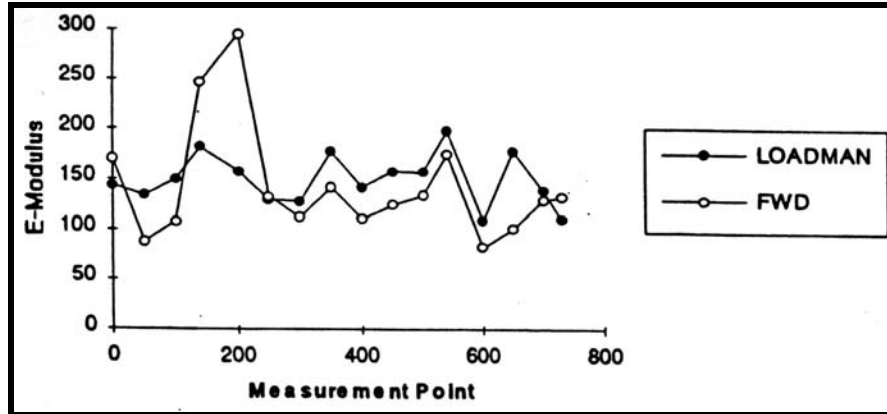


Figure 2.12 Comparison of Loadman and FWD at various test points (Gros, 1993).

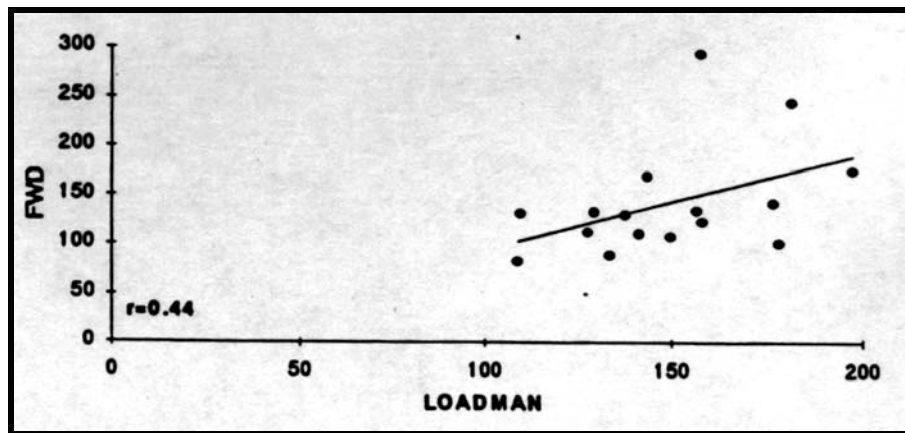


Figure 2.13 Correlation between Loadman and FWD (Gros, 1993).

Similarly, Whaley (1994) directly compared the results of the Loadman PFWD with the FWD to determine its effectiveness when testing deflection and layer moduli of AC layers. The tested pavement section consisted of an 80 mm (3.2 in.) asphalt concrete surface, 200 mm (7.9 in.) base course, 1220 mm (48 in.) subbase, and a rigid layer at 1500 mm (59 in.) depth (Whaley, 1994). Like Gros (1993), Whaley (1994) concluded that the Loadman yielded higher moduli than the modulus values backcalculated from the FWD measurements at all test points, with a difference of roughly 200 MPa between

FWD and Loadman results. The correlation coefficient was 0.2. The overall results of the testing are shown in Figures 2.14 and 2.15.

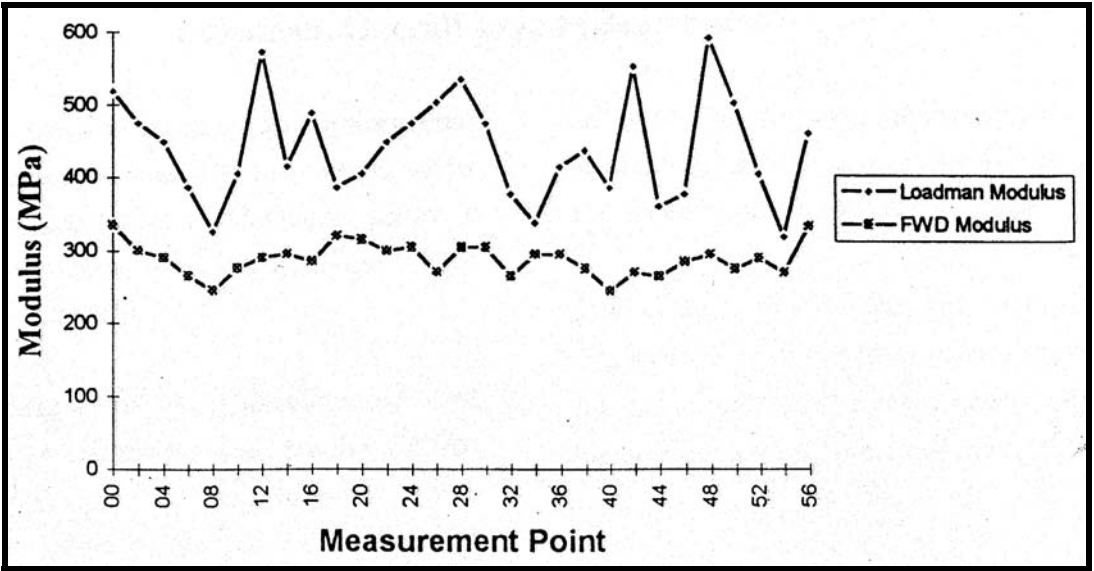


Figure 2.14 Comparison of Loadman and FWD at various test points (Whaley, 1994).

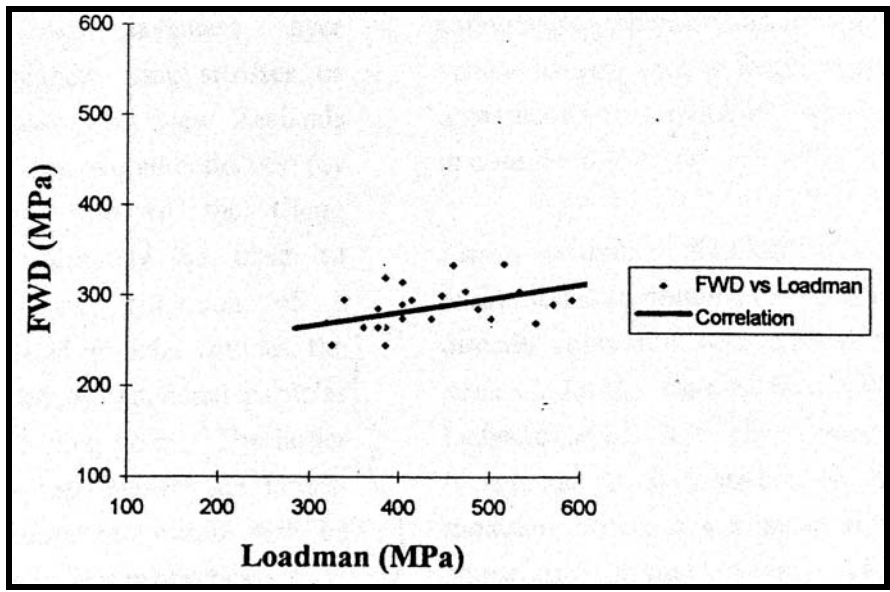


Figure 2.15 Correlation between Loadman and FWD (Whaley, 1994).

Despite the low correlation coefficient, it is noticed that both the FWD and the Loadman follow the same overall trend. Whaley (1994) explains the poor correlation (low correlation coefficient) to the fact that only the upper portion of the pavement section was loaded with the Loadman, whereas the FWD loaded all layers resulting in a lower modulus, representing the stiffness of all layers, not just the AC layer. Additionally, the significant variations between the two devices may be caused by the presence of large aggregate directly beneath the loading plate of the Loadman. These conclusions are mirrored by Gros (1993).

Davies (1997) investigated similarities between the Loadman PFWD, Benkelman Beam, and FWD on two thin membrane surface (TMS) roads. More detailed results of this study are provided by Saskatchewan Highways & Transportation (SHT) (1998). The TMS roads consisted of a 20 to 25 mm (0.79 to 0.98 in.) layer of oil treatment (cold mix) for surfacing, with the application of a minimum of three to six sand seals since construction. This was underlain by a graded/compacted subgrade (Davies, 1997). Each test section consisted of 20 test points. The FWD was the first instrument over the test point followed by the Benkelman Beam and the Loadman. Three seating drops and four drops with each of four weights were used with the FWD. One measurement was taken with the Benkelman Beam and ten measurements were taken with the Loadman. The average of all ten Loadman measurements was plotted in addition to the first Loadman measurement, the FWD measurement, and the Benkelman Beam measurement. The Benkelman Beam produced the largest deflections at virtually all points tested followed by the FWD and Loadman, all following similar trends, with few exceptions. The overall results are shown in Figure 2.16.

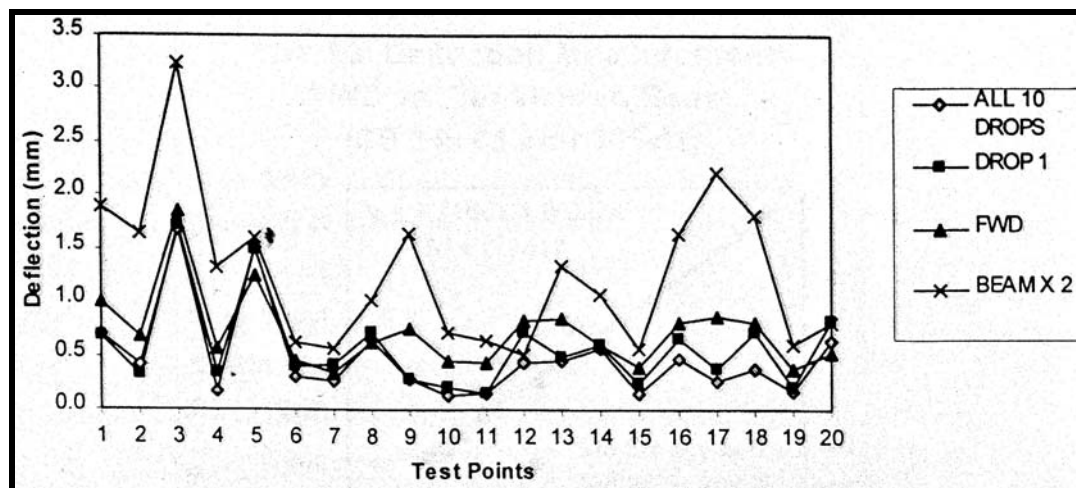


Figure 2.16 Comparisons of Loadman, FWD, and Benkelman Beam (SHT, 1998).

There was a relatively good correlation between the Loadman PFWD and FWD with a correlation coefficients of 0.86, significantly greater than obtained by Gros (1993) and Whaley (1994). However, the PFWD and Benkelman Beam did not correlate as well, yielding a correlation coefficient of 0.62. Additional results are shown in Table 2.1.

Table 2.1 Correlation coefficients of 20 test points on two TMS structures (SHT, 1998).

	<i>FWD</i>	<i>BB</i>	<i>Loadman(10)</i>	<i>Loadman(5)</i>	<i>Loadman(4)</i>
<i>FWD</i>	1.00				
<i>BB</i>	0.86	1.00			
<i>Loadman(10)</i>	0.86	0.62	1.00		
<i>Loadman(5)</i>	0.85	0.59	1.00	1.00	
<i>Loadman(4)</i>	0.85	0.59	1.00	1.00	1.00
<i>Loadman(1st)</i>	0.85	0.59	0.97	0.98	0.97

From the results shown, Davies (1997) reasoned that the PFWD did well to differentiate between surfaces whose stiffness' may be characterized as "soft" and "hard" but lacked the ability to differentiate between surfaces that were of "hard" and medium stiffness.

Furthermore, Davies (1997) noted several other differences between devices that may

have contributed to the skewed results. The depth of the road structure that is measured by each device is different. Thus, a device measuring only the upper portions of the road structure will have a higher deflection than one measuring to a significantly greater depth, paralleling the thoughts of Whaley (1994). Fleming and Rogers (1995) determined that the zone “significantly stressed” was roughly equal to 1.5 to 2.0 times the diameter of the loading plate. Also noted was the possibility that the Loadman is unable to deflect, thus measure stiffness, above a certain level of stiffness. Davies (1997) suggests that this may be the tradeoff of having an instrument small enough and light enough for one person to use.

Livneh (1997) developed a double testing method to determine asphalt layer moduli. Two measurements were necessary, one on the asphalt surface, and one at the same point once the asphalt layer had been cored to its bottom. Utilizing this method, the modulus of all the structural layers could be measured as well as the partial surface modulus of all the layers not including the upper drilled asphaltic layer. The tested section consisted of 120 to 250 mm (4.7 to 9.8 in.) thick asphalt layer underlain by approximately 100 mm (3.9 in.) of variable size granular base and subbase layers. The backcalculated FWD modulus values were larger than the modulus values determined from the PFWF double testing, contradicting the results obtained by Gros (1993), Whaley (1994), and Davies (1997). To compensate for differences in geometry, contact pressure, and pulse loading between the two devices, correction factors were applied.

Original and corrected results are shown in Figure 2.17. Encouraging results were gained only from the double PFWF testing (Livneh, 1997).

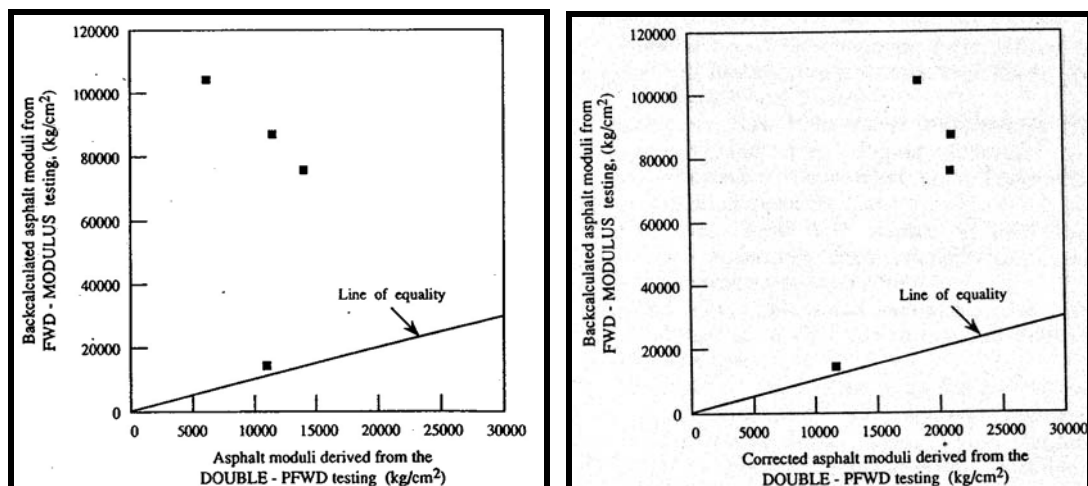


Figure 2.17 (a) Uncorrected and (b) corrected relationship between FWD modulus and PFWD modulus using the double testing technique (Livneh, 1997).

Livneh, et al. (1998) conducted tests aimed at developing correlations between the deflection obtained with the Loadman PFWD and the central deflection obtained by means of the Benkelman Beam. Side by side tests were completed at three different sites. Site A consisted of 80 mm (3.1 in.) of asphalt underlain with 320 mm (12.6 in.) of granular material. Site B consisted of 100 mm (3.9 in.) of asphalt and 450 mm (17.7 in.) of granular material, and Site C had 160 mm (6.3 in.) of asphalt underlain by 1050 mm (41.3 in.) of gravel. The results from each of the three sites are presented in Figure 2.18. The results of the regression analysis indicate that the deflections obtained from the two units correlated poorly with one another. The author attributed the differences to the fact that the Loadman PFWD is only capable of measuring the properties of pavements of limited thickness. The effect of deep layers on the surface deflection is a function of the ratio between the layer thickness and the loading plate radius.

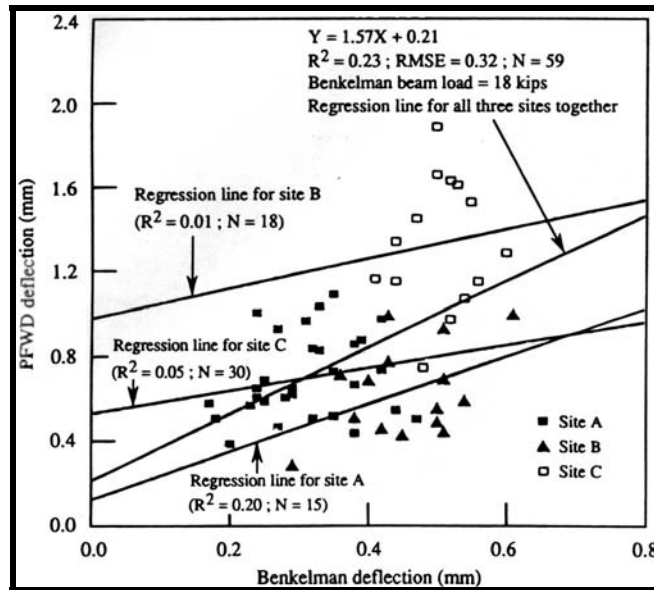


Figure 2.18 Loadman PFWD deflection versus Benkelman Beam deflection (Livneh, et al., 1998).

Honkanen (1991) performed a comparison of the Loadman and FWD on a gravel road bound by oil. The results were consistent with other investigators. Loadman produced higher modulus values than the FWD, with both instruments following a similar trend, as seen in Figure 2.19.

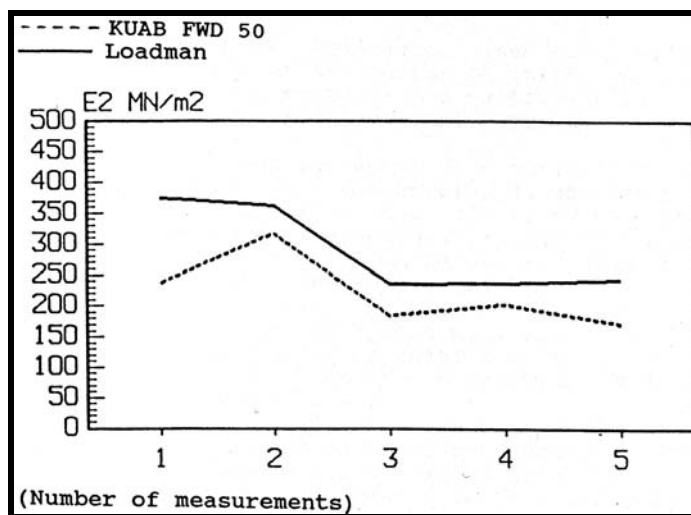


Figure 2.19 Comparison of multiple FWD and PFWD measurements at one location (Honkanen, 1991).

2.2.3.2 Unbound Layers

Honkanen (1991) and Gros (1993) compared FWD, plate bearing tests, and Loadman PFWD measurements on unbound surfaces. Honkanen (1991) completed procedures on multiple test beds of equal length, differing thickness, and varying grain size. Test results on sections with varying thicknesses revealed that as layer thickness increases, modulus values from each instrument approach one another. Honkanen found that to achieve sufficient reliability of the Loadman, it was necessary to perform multiple measurements at each test point, a conclusion reiterated by Gros (1993) and Groenendijk, et al. (2000). Honkanen (1993) indicated that at least four measurements should be obtained at each test location. Of the four measurements, the first two should be discarded and the remaining two should be averaged and used as a representative value.

Gros (1993) conducted tests on unbound aggregate containing sand, gravel, and crushed gravel. Excluding errant test results, the correlation coefficients between the Loadman and FWD ranged from 0.31 to 0.99 with an average of 0.77, which is higher than for most of the studies with pavement layers. The Loadman and plate bearing test yielded almost identical results. Modulus values given by the Loadman were at all points larger than those given by the FWD and plate bearing unit. Results for unbound material were shown to correlate well with one another, as shown in Figures 2.20 and 2.21. Both the Loadman and the FWD follow the same trend with the FWD resulting in higher modulus values on all points tested.

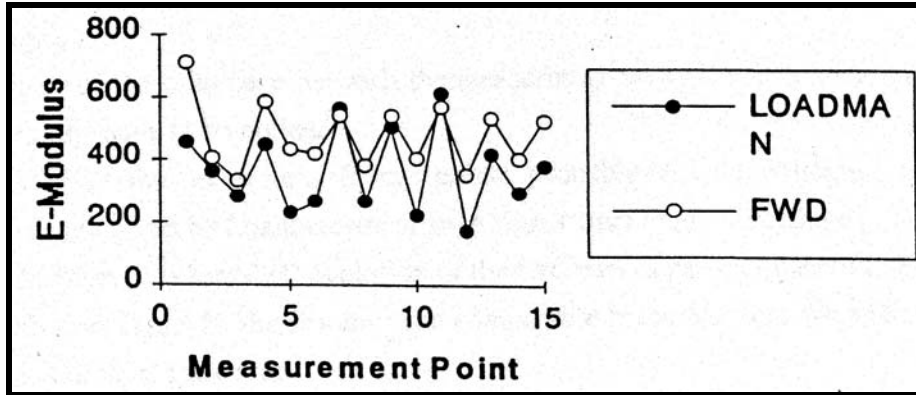


Figure 2.20 Comparison of Loadman and FWD at various test points (Gros, 1993).

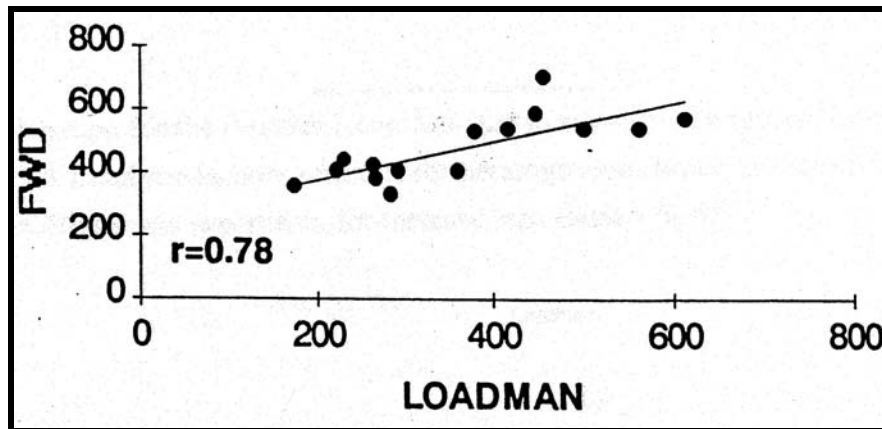


Figure 2.21 Correlation between Loadman and FWD (Whaley, 1994).

Whaley (1994) also compared the results of testing the Loadman PFWD with the FWD, Clegg Hammer, and Benkelman Beam to determine its efficiency when testing deflection and layer moduli of base course layers. A comparison of all devices is shown in Figure 2.22.

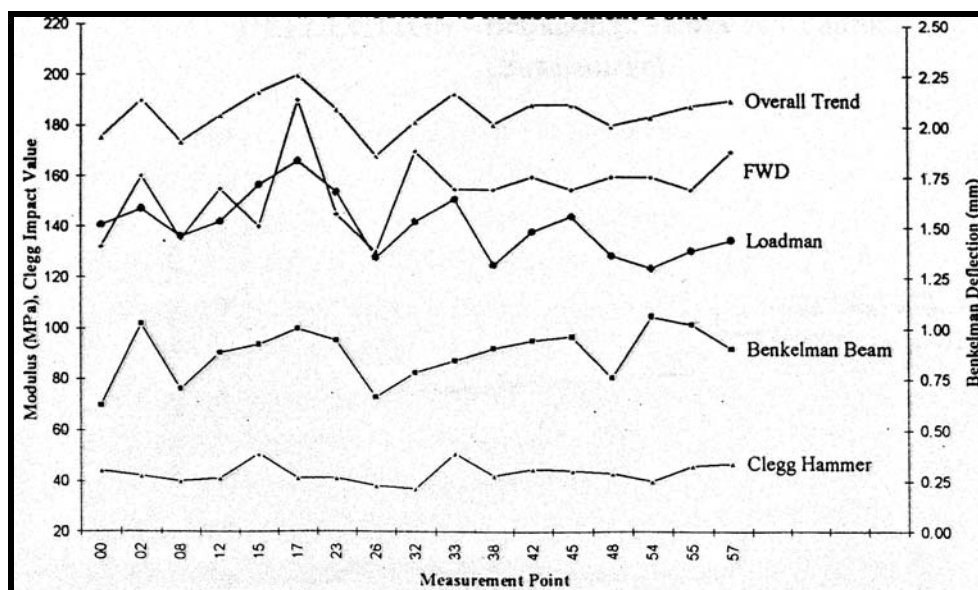
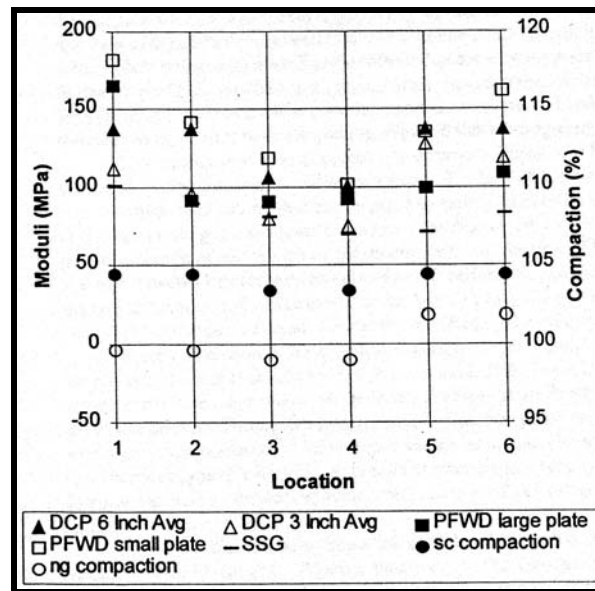


Figure 2.22 Comparison of FWD, Loadman PFWD, Benkelman Beam, and Clegg Hammer at various test points (Whaley, 1994).

Whaley (1994) concluded that the Loadman and FWD were best suited for this application while the Benkelman Beam showed some discrepancies. The Clegg Hammer showed no relation to the other devices. Comparing the FWD and Loadman, the correlation is very near ideal, almost returning an error free 1 to 1 correlation (Whaley, 1994). The FWD moduli were slightly larger than those of the Loadman at 86% of points tested, possibly due to the stress dependent nature of the aggregate.

Siekmeier, et al. (2000) performed comparative testing utilizing the PFWD for the Minnesota Department of Transportation (Mn/DOT). Siekmeier, et al. (2000) completed testing for 13 different sections utilizing the DCP, Loadman PFWD, SSG, and Dynatest FWD. Test locations were primarily composed of a sand and gravel mixture with less than 10 percent fines. Sand cone and nuclear density gauge density tests were conducted. For the DCP testing, the penetration for each drop was recorded. With the PFWD, for each test location, five tests were performed and recorded with the average of the last

three used for the modulus calculation. For the SSG, two tests were conducted for each test location with the second being used for calculation purposes. If the two tests differed by more than 3 percent, the tests were repeated at a new location. Results are shown in Figure 2.23.



(ng = nuclear gage; sc = sand cone)

Figure 2.23 Moduli versus location for granular base material (Siekmeier, et al., 2000).

Locations 1 and 2 were beneath the inside wheel path, 3 and 4 between wheel paths, and 5 and 6 beneath the outside wheel path. The results indicated that all of the devices used detected a variation in stiffness at each location, and all displayed a similar trend, differing only in magnitude. Siekmeier, et al. (2000) explained the differences as a result of the stress condition imposed by the instrument used. The lower the vertical stress induced by the device, the lower the resulting modulus. Tests were also performed on a mixture of clayey and silty sand fill. Like previous tests, each instrument showed a similar trend. Siekmeier, et al. (2000) determined there was a strong correlation between

the instruments designed to measure modulus and that it is important to consider the stress imposed by the instrument when stress dependent materials are used.

There was little agreement between percent compaction and modulus values. Siekmeier, et al. (2000) explained that it is not realistic to know the Proctor maximum density for every soil type found on a construction site. During the time of the testing twelve Proctor tests had been completed covering typical soil types, however, did not perfectly match each soil mixture that could be found at the location of an in situ density test. The best available Proctor value was used, and as a result the agreement was poor. It was concluded that compaction tests could be compared to in situ modulus tests only when the material is uniform with respect to a single maximum Proctor density (Siekmeier, et al., 2000).

Pidwerbesky (1997) completed a study utilizing the Clegg Hammer, FWD, NDM and Loadman PFWD to determine their suitability for quantifying the present condition and predicting the rutting potential of unbound granular base courses. The pavement structure consisted of 90 mm (3.5 in.) of hot mix asphalt (HMA) over 200 mm (7.9 in.) of crushed rock base course over a silty clay subgrade with a California Bearing Ratio (CBR) of 12% (Pidwerbesky, 1997). The laboratory resilient modulus of the subgrade and base course material was 105 MPa and 280 MPa, respectively. A Simulated Loading and Vehicle Emulator (SLAVE) was used to load the pavement structure for approximately one year. Once loading was complete, trenches were cut through the layers for measuring density and modulus of the base course and subgrade. The backcalculated moduli from FWD measurements were larger than the Loadman moduli at 86% of all points tested. Like the results given by Whaley (1994), the Clegg Hammer did

not correlate well with any of the other testing devices. The Loadman is not capable of differentiating the moduli of various layers within a multi-layered pavement system, but it can give an indication of the modulus of the layer being tested (Pidwerbesky, 1997). A regression analysis of Loadman and FWD moduli was performed and shown in Figure 2.24.

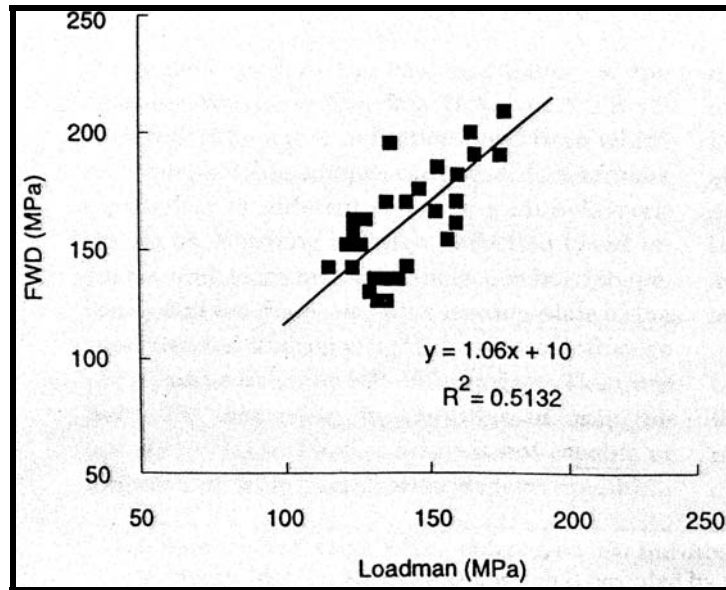


Figure 2.24 Correlation between Loadman and FWD moduli (Pidwerbesky, 1997).

Pidwerbesky (1997) reported that the Loadman is substantially faster than NDM methods, enabling increases in testing area and frequency. Further, Loadman is also simpler to operate and interpret (a trained technician is not required), and does not have to be calibrated for each material, which should be done with NDM tests.

Fleming, et al. (2000) performed FWD, German Dynamic Plate (GDP), TRL Foundation Tester (TFT), and Prima 100 PFWD tests on two specially constructed trial foundations. The GDP apparatus consists of a 10 kg (22 lb) falling mass impacting a rubber buffer connected to a bearing plate. The drop height of the falling mass is set such

that the peak applied force is 7.07 kN (1589 lbf), i.e. 100 kPa (14.5 psi) stress. The falling mass is guided by a vertical rod. The loading plate houses a velocity transducer that measures the impact signal (Fleming, et al., 2000). The TFT consists of a 10 kg (22 lb) falling mass inside a guide tube that impacts a 300 mm (11.8 in.) load plate. The drop height may be varied up to a maximum of 1 m (3.3 ft). The loading plate can be reduced to 200 mm (7.9 in.) in diameter in order to vary the maximum contact stress, and to provide a range of approximately 20 to 400 kPa (2.9 to 58 psi). A load cell and velocity transducer is used to measure the force and surface deflection.

Typically, the sites tested consisted of a granular subbase at a depth of 37.5 mm (1.5 in.) and/or crushed rock granular capping at a depth of 75 mm (3 in.), and a clayey subgrade. Ten test locations were used at each site. The correlation coefficient and coefficient of variation was determined for each test location (Fleming, et al., 2002). Results are shown in Table 2.2 and 2.3.

Table 2.2 Summary of correlations between the FWD and GDP, TFT, and Prima 100 PFWD at Mountsorrel and Bardon test sites (Fleming, et al., 2000).

Subgrade	Formation Details Capping	Test	GDP		TFT		Prima 100 PFWD	
			CC	R ²	CC	R ²	CC	R ²
Silty Clay	150 mm subbase over up to 450 mm 6F1 capping	subgrade	0.59	0.83	0.96	0.922	-	-
Gravelly Silty Clay		capping	0.63	0.33	1.13	0.37	0.97	0.6

Table 2.3 Summary of correlations between the Prima 100 PFWD and GDP and TFT at Mountsorrel and Bardon test sites (Fleming, et al., 2000).

Subgrade	Formation Details Capping	Test	GDP		TFT		Prima 100 PFWD	
			CC	R ²	CC	R ²	CC	R ²
Silty Clay	150 mm subbase over up to 450 mm 6F1 capping	subgrade	-	-	-	-	-	-
Gravelly Silty Clay		capping	0.63	0.38	1.13	0.53	-	-

Fleming, et al. (2000) determined that the Prima 100 PFWD correlates reasonably with the FWD, yielding a coefficient of variation of 0.6 at the same site where the TFT and GDP yielded 0.37 and 0.33. A typical set of data for tests on 400 mm (15.7 in.) of capping and the clayey subgrade is shown by Fleming, et al. (2002) in Figure 2.25.

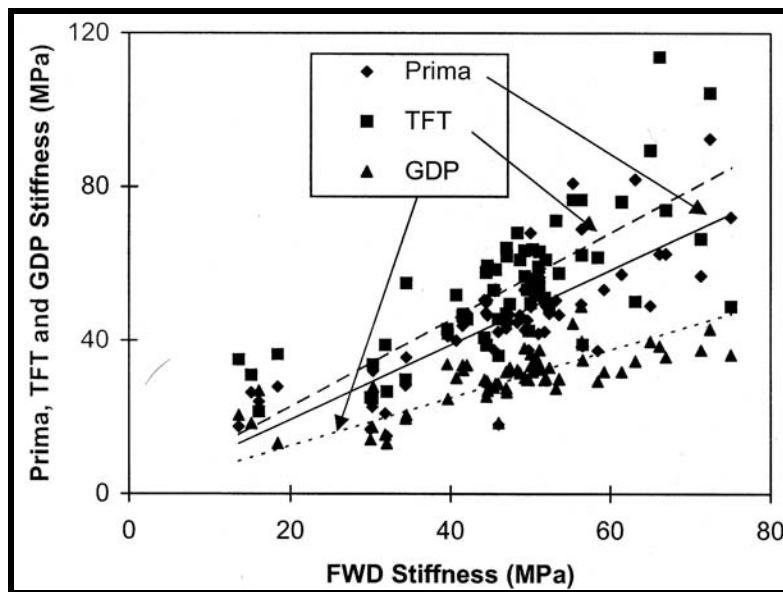


Figure 2.25 Relationship between stiffness modulus determined by the portable dynamic plate test devices and the FWD (on subgrade and 400 mm thick granular capping) (Fleming, et al., 2000).

Thom and Fleming (2002) present a theoretical model that predicts the response of a dynamic plate test. The dynamic model uses the $K\theta$ non-linear model for unbound

materials (modulus = $K_1\theta^{K_2}$, where θ is the sum of the principal stresses and K_1 and K_2 are constants). The second simplification is the use of a “load spread angle” technique for stress analysis, which effectively turns the problem into a 1 dimensional one (Thom and Fleming, 2002).

Four devices (FWD, Prima 100 PFWD, German Dynamic Plate, and TFT) were theoretically applied to eight different foundations described in Table 2.4, and results from the tests are shown in Table 2.5.

Table 2.4 Description of foundations applied to theoretical model (Thom and Fleming, 2002).

A:	450 mm of good granular ($K_1 = 30, K_2 = 0.3$) over soft soil ($K_1 = 10, K_2 = 0.1$)
B:	Uniform soft soil ($K_1 = 10, K_2 = 0.1$)
C:	Uniform very soft soil ($K_1 = 1, K_2 = 0.3$)
D:	Uniform highly non-linear very soft soil ($K_1 = 0.2, K_2 = 0.6$)
E:	Uniform linear elastic very soft soil ($E = 10$ MPa)
F:	150 mm of granular ($K_1 = 10, K_2 = 0.3$) over soft soil ($K_1 = 2, K_2 = 0.3$)
G:	150 mm of soft soil ($K_1 = 2, K_2 = 0.3$) over granular ($K_1 = 10, K_2 = 0.3$)
H:	150 mm of granular ($K_1 = 10, K_2 = 0.3$) over 450 mm of poor granular ($K_1 = 8, K_2 = 0.3$) over soft soil ($K_1 = 2, K_2 = 0.3$)

Table 2.5 Predicted surface moduli from different dynamic plate test devices (Thom and Fleming, 2002).

Foundation	Predicted surface modulus (MPa)				Range as % of mean
	FWD	Prima	ZGF-01	TRL Tester	
A	128.0	123.2	128.0	128.8	4.4
B	26.8	28.2	29.4	29.8	10.5
C	11.7	12.7	14.4	14.2	20.4
D	13.4	12.3	14.3	14.1	14.8
E	16.8	19.9	21.0	21.2	22.3
F	36.1	36.5	38.6	39.0	7.7
G	25.5	22.7	24.4	24.7	11.5
H	65.5	58.8	61.3	61.6	10.8
Time to peak load (msecs):	13.6–16.3	14.0–14.1	10.1–10.2	20.2	

It may be noted that there are some variations in the results presented above, however, for the most part, there is uniformity. Primarily, the TFT predicts the highest modulus, while for most test sections; the FWD presents the lowest modulus.

Kamiura, et al. (2000) conducted a series of tests with two different kinds of PFWD's (Handy Type Falling Weight Deflectometer (HFWD), Prima 100 PFWD) and a static bearing test on a sandy soil and subbase. He found that the modulus depended on the strain of the surface beneath the loading plate. Kamiura, et al. (2000) reports that modulus values would be relatively the same for each subgrade material if the strain levels were in the range of 10^{-3} to 10^{-4} percent. Kamiura, et al. (2000) used a k value to evaluate subgrade stiffness. The k value is the ratio of the stress induced by a 300 mm (11.8 in.) loading plate to the deflection of the ground surface equal to 0.125 cm (0.05 in.). Comparison of k values for the Prima 100 and HFWD at multiple test locations is shown in Figure 2.26. Figure 2.27 displays the comparison of deflection ratio at different test locations for the Prima and HFWD.

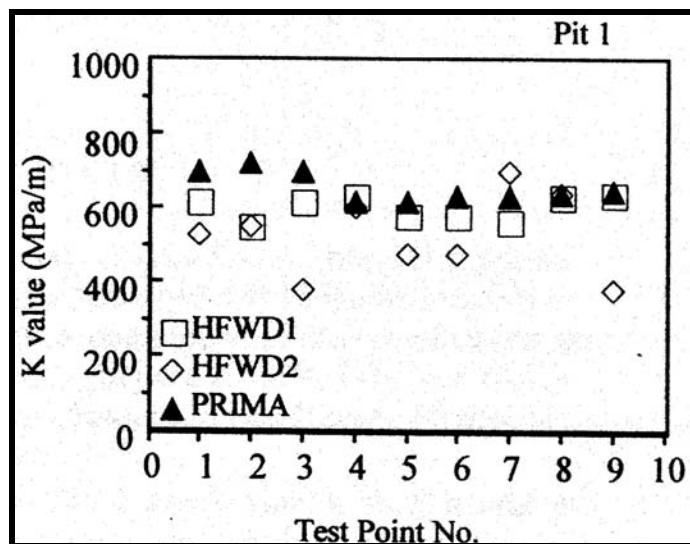


Figure 2.26 Comparison of k value from Prima 100 and HFWD at multiple test locations (Kamiura, et al., 2000).

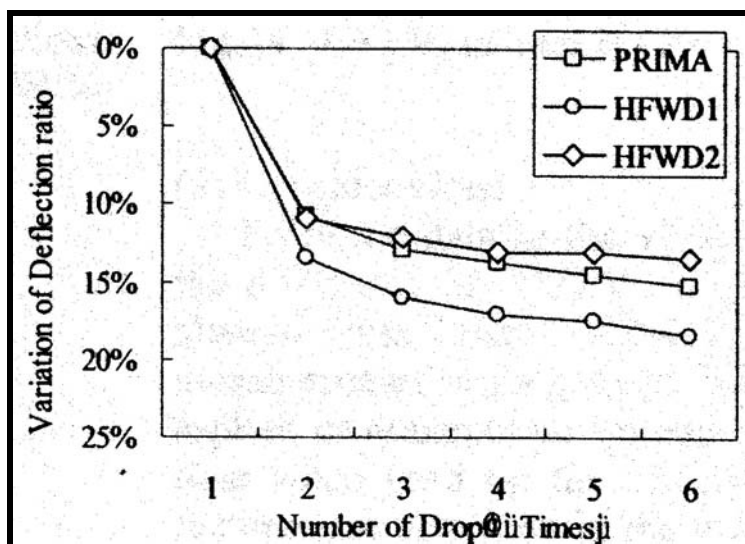


Figure 2.27 Comparison of the variation in deflection ratio with the number of drops at one location (Kamiura, et al., 2000).

Nazzal (2003) evaluated the potential use of the SSG, DCP, and Prima 100 PFWD as reliable means to measure the stiffness characteristics of highway materials for possible application in the quality control quality assurance (Q_C/Q_A) procedures during and after the construction of pavement layers and embankments. In addition to these devices, FWD, PLT, and laboratory CBR tests were performed. Laboratory tests were conducted to determine the zone influenced by the SSG and Prima 100 PFWD. Regression analyses were performed to develop correlations between devices.

Field tests were performed at four separate locations. Conditions on U.S. Highway 190 consisted of 200 mm (8 in.) of crushed limestone base on top of 200 mm (8 in.) of lime treated subgrade. Testing was also completed on four sections of Louisiana State Highway 182. Measurements on existing subgrade material were completed in Section 1. Section 2 consisted of 250 mm (10 in.) of cement treated base overlying 300 mm (12 in.), Section 3 consisted of 300 mm (12 in.) of cement treated subbase atop

subgrade, and Section 4 was made up of 300 mm (12 in.) of lime treated subbase atop subgrade. Testing on U.S. Highway 61 was completed during the compaction of a 300 mm (12 in.) thick layer of untreated subbase. Finally, six sections were constructed at the Louisiana Department of Transportation and Development (LA-DOTD) Accelerated Load Facility (ALF). These sections included: one clayey silt soil, two cement stabilized soils, one lime treated soil, one calcium sulfate hemihydrate (39.2% Calcium Oxide, 51.15% Sulfur Trioxide, 0.6% Silicon Dioxide, 0.75% Phosphorous Pent Oxide, 0.38% Potassium, and 0.81% Aluminum Oxide), and one crushed limestone section (Nazzal, 2003). All layers were 300 mm (12 in.) in thickness and were constructed on existing subgrade with the exception of the clayey silt material which was 100 mm (4 in.) thick. Additionally, three trench sections (crushed limestone, sand, and recycled asphalt pavement) were constructed at the ALF site to evaluate the devices for control of trench backfill.

Test results from the ALF site indicated that the Prima 100 PFWD modulus increased with increasing compactive effort as well as time after construction was completed. This is shown in Figure 2.28. Similar moduli were obtained for the Prima 100 PFWD and the SSG. Results of the statistical analysis show that good correlations do exist between the devices under evaluation (SSG, DCP, and Prima 100 PFWD) and the standard tests (FWD, PLT, and CBR). Some of the results are shown in Figure 2.29.

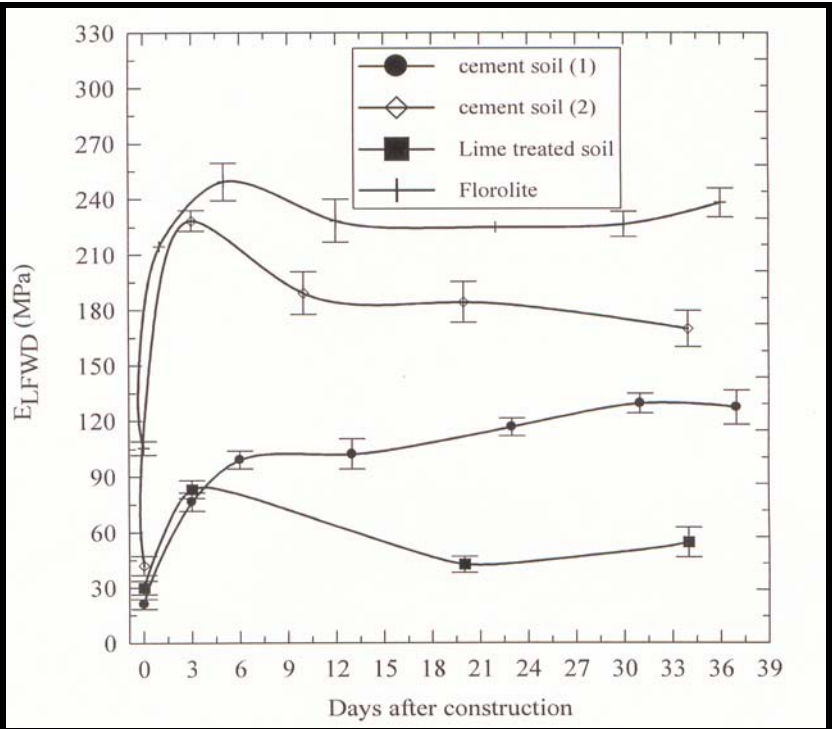


Figure 2.28 Prima 100 PFWD measured increase in stiffness due to increased compactive effort and time (Nazzal, 2003).

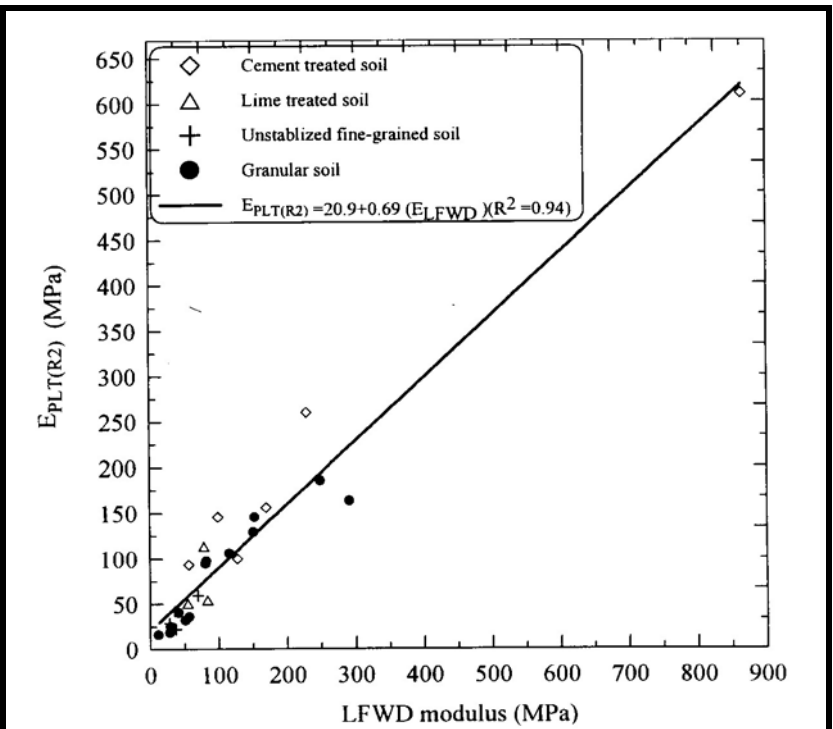


Figure 2.29 Correlations between Prima 100 PFWD, FWD, and PLT (Nazzal, 2003).

All regression models had an adjusted R^2 value and a significance level greater than 0.8 and 99.9% respectively (Nazza, 2003). Laboratory results indicated that the depth influenced by the SSG ranged from 180 to 190 mm (7.5 to 8.0 in.), while the Prima 100 PFWD influenced a depth of approximately 267 to 280 mm (10.5 to 11.0 in.). It was the opinion of the author that the three devices in question could be reliably used to predict the moduli obtained from PLT, FWD, and CBR values, and could be used to evaluate the stiffness/strength parameters of different pavement layers and embankments.

2.3 PFWD AS TOOL TO EVALUATE THAW WEAKENING OF ROADS

Pavements in areas with seasonal freezing and thawing often undergo frost heave and thaw weakening in addition to load-induced pavement distress. Vehicle traffic can cause significant damage to roads that are weakened during the spring thaw. To minimize damage, many road maintenance agencies impose load restrictions during damage-susceptible periods. This is shown in Figure 2.30.

Spring thaw adversely affects pavement life while load restrictions impose local economic hardships throughout the northern United States and Canada. Although the maximum allowable load and the duration of the reduced load period vary widely among agencies, they try to strike a balance between minimizing the disruption to the local economy caused by the load restrictions and minimizing road damage.

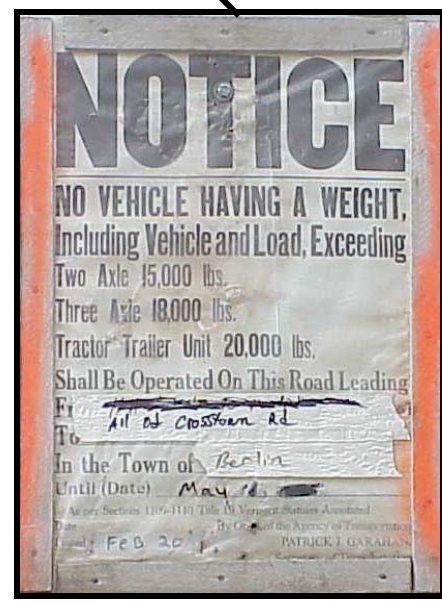
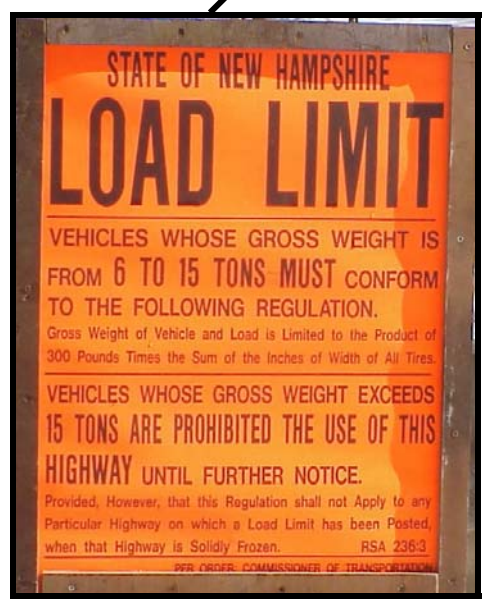
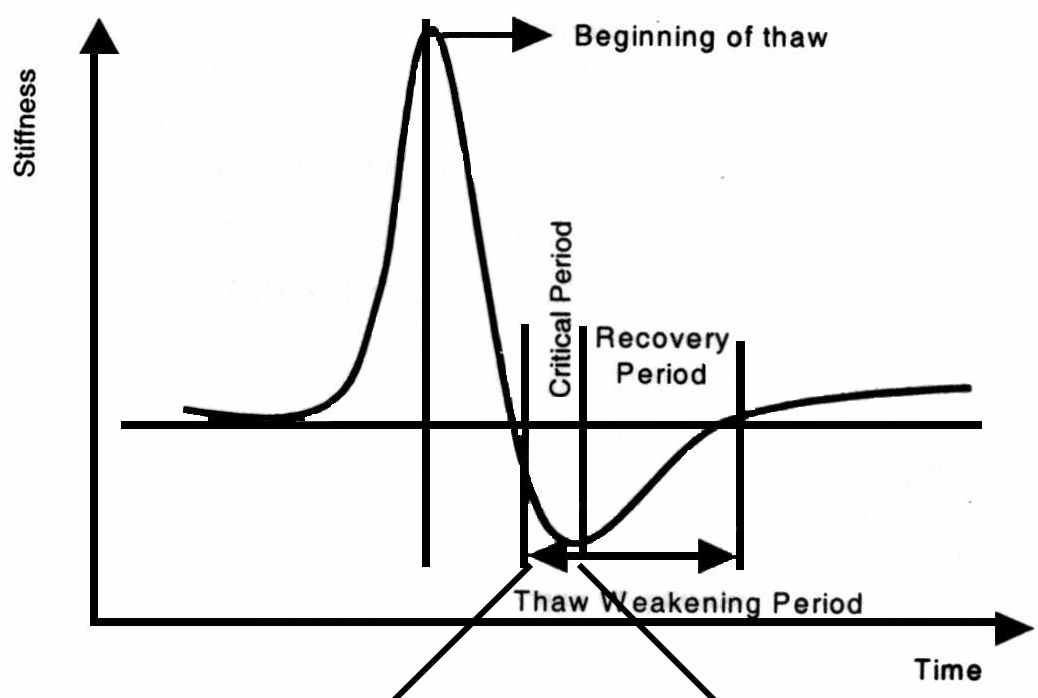


Figure 2.30 Typical signage associated with placing load restrictions (Janoo and Cortez, 1998).

2.3.1 Current Methods to Evaluate Thaw Weakening of Roads

Pavement modulus is a key parameter in determining damage-susceptibility of pavements. This can be monitored during spring thaw and through recovery using a FWD. However, FWD purchase, operation, and maintenance is expensive. Second, even if a state owns a FWD, it can only cover so many roads within a given time frame. As a result, determining when the road has thawed and recovered sufficient strength to remove the restriction is left to personal experience and subjective judgment.

Kestler, et al. (2000) distributed a survey to 45 state DOTs and multiple U.S. Department of Agriculture Forest Service offices. The survey was aimed at determining current load restriction practices. Of the 45 state DOTs that were solicited, 36 responded. Three USFS regional offices also replied. Figure 2.31 shows a breakdown of methods used for determining when to impose and when to remove load restrictions (Kestler, et al., 2000). Kestler, et al. (2000) observed a majority of the respondents that post load restrictions used subjective techniques, such as observation, to both place and remove load restrictions. Additionally, many of the states indicated that they posted restrictions only after the first signs of pavement distress are observed. Many also indicated that their preference would be to switch from current subjective methods to more quantitative methods (such as a FWD) if adequate resources were available (Kestler, et al., 2000). Twenty four percent of responding DOTs were currently using quantitative methods to place load restrictions and only 14% used the same methods to remove load restrictions. The remaining 10%, who use quantitative methods to place load restrictions, simply keep restrictions in place for a specific length of time or remove restrictions subjectively.

Roughly one quarter of the responding states use dates to impose restrictions. Some roads were being restricted for as long as one third of one year. The length of seasonal load restrictions for respondents is shown in Figure 2.32.

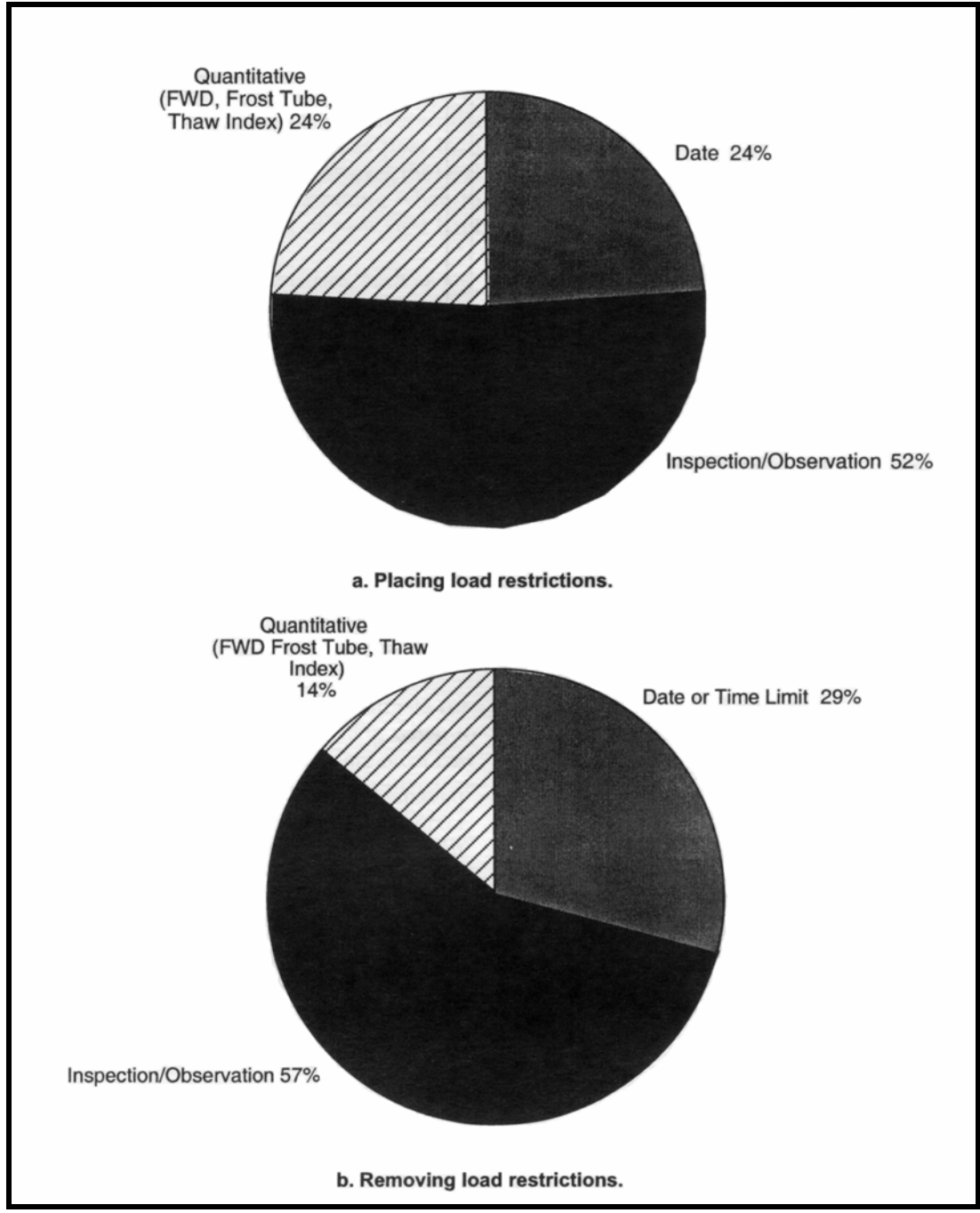


Figure 2.31 Methods for determining when to place and remove load restrictions (Kestler, et al., 2000).

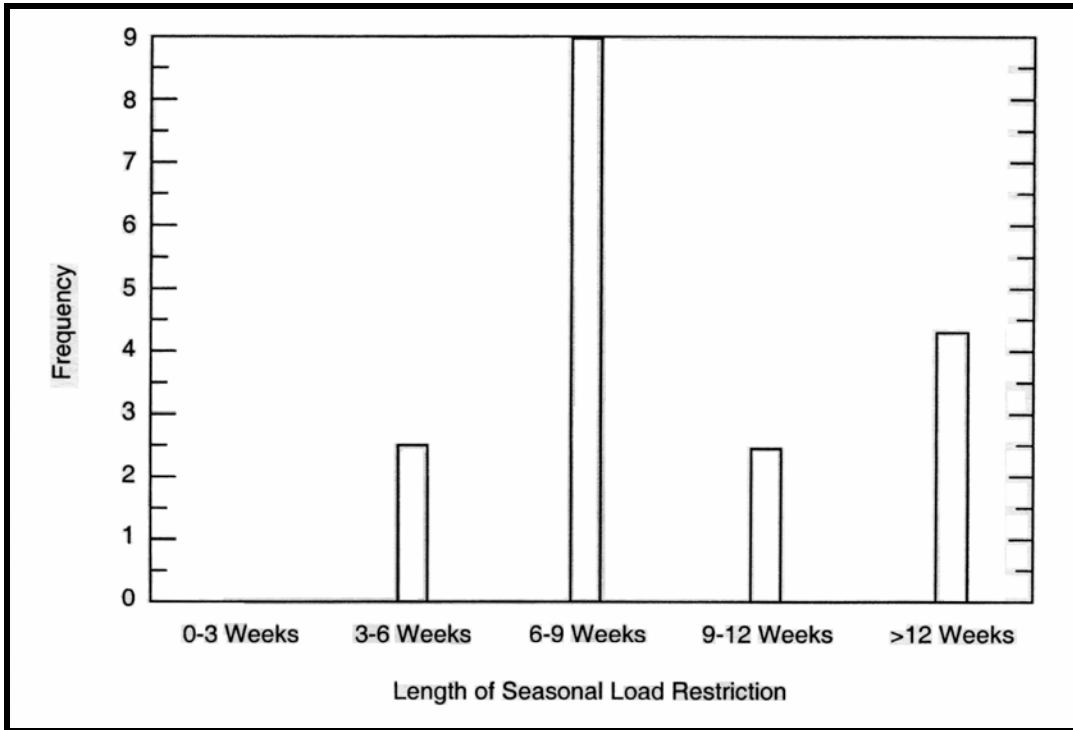


Figure 2.32 Length of time over which load restrictions are placed (Kestler, et al., 2000).

According to most respondents, the longer the load restrictions are in place, the more complaints were received from loggers and contractors. Table 2.6 lists typical DOT responses regarding user feedback (Kestler, et al., 2000).

Table 2.6 Road user feedback to DOTs and USFS on spring thaw load (Kestler, et al., 2000).

- Restricting the flow of goods makes shipping inconvenient.
- Some routes too restrictive; length of time too long.
- Numerous complaints from contractors and loggers.
- "Don't post my road."
- Haulers want restrictions lifted as soon as possible and more frequent FWD testing done in these areas.
- DOT met with trucking industry association, and they have jointly funded research on load restrictions.
- Using quantitative methods for shutting down roads but using subjective and arbitrary methods for determining when to reopen roads.

The United States Federal Highway Administration (FHWA) investigated the benefits of seasonal load restrictions in 1990. Table 2.7 shows the expected increase in pavement life associated with varying pavement load restrictions. It is clear that seasonal load restrictions can significantly extend the useful pavement life.

Table 2.7 Benefits from seasonal load restrictions (FHWA, 1990).

Pavement Load Reduction During Thaw (%)	Expected Pavement Life Increase (%)
20	62
30	78
40	88
50	95

Although seasonal weight restrictions extend pavement life, they also affect the productivity of the trucking industry. In 1982, The Alaska Department of Transportation and Public Facilities reported the statewide loss in revenue to the trucking industry was approximately \$100,000 USD per restricted day (1982 dollars). However, the associated damage to state roads imposed when load restrictions were not enforced was roughly \$158,000 USD per day (C-SHRP, 2000).

The Canadian Strategic Highway Research Program (C-SHRP) prepared a technical brief summarizing a series of presentations that were made to discuss policies of seasonal pavement load restrictions in Canadian provinces, the United States and various European countries. The methods used to determine when to place and remove the weight restrictions are similar to those discussed by Kestler, et al. (2000). Direct methods include the use of frost tubes or deflection testing, while indirect methods include the use of historical databases, weather forecasts, prediction models or expert

judgment (C-SHRP, 2000). The report notes that each Canadian province utilizes weight restrictions during spring thaw in an attempt to minimize damage. However, the regulations vary not only in duration and extent but also on technical criteria and agency practices. Most Canadian agencies impose spring load restrictions during March, and remove the restrictions in May. Deflection testing is used by 7 of the 10 provinces, while frost tubes are used primarily in British Columbia and Quebec (C-SHRP, 2000).

According to the brief, in the United States, 19 states have adopted the use of load restrictions but there is no consistency between states in terms of where and when to use the restrictions, how to apply them, and by how much to restrict the loads (C-SHRP, 2000). Finally, spring load restrictions are also used in France and several Scandinavian countries. The amount of the load restrictions are presented, however, there is no discussion of the methods used to develop them or methods used to determine when to place and remove the restrictions.

Van Deusen (1998) reports on improved predictive equations for estimating thaw duration based on deflection and environmental data collected from eight different low-volume flexible pavement test sections in the state of Minnesota. Various studies have found that air and subsurface temperatures can be used to identify thawing events. A significant amount of research in this area has come from work done in the state of Washington (Rutherford, et al., 1985; Mahoney, 1985; Rutherford, 1989), where it was found that the onset of the critical period could be estimated with the air temperature thawing index and that air temperature (air freezing index) can be used to predict the duration of the thaw (Van Deusen, 1998). Results from the Minnesota test sites were used to develop an equation to determine the duration of the thaw in terms of the freezing

index, and compare the results to those obtained by using the equation developed in Washington. As a result, an improved thaw duration prediction relationship was developed including the effects of frost depth. The predicted thaw durations from the Washington equation appeared to be conservative in comparison to those determined from the new Minnesota equation. It was recommended that the equation be validated with one more winter/spring season of data (Van Deusen, 1998).

Research conducted by Rutherford, et al. (1985) in cooperation with the Federal Highway Administration (FHWA) and the Washington State Department of Transportation (WSDOT) aimed at providing procedures that would aid in determining the amount of the restriction, where to apply them, and when to place and remove them. The researchers investigated relationships between the Freezing Index (FI), Thaw Index (TI), and thaw duration. Regression equations were developed from heat flow simulations and are shown in Equations 2.4 and 2.5.

$$D = 25 + 0.018(FI) \quad \text{Eqn 2.4}$$

Where: D = thaw duration (days)
 FI = Freezing Index (°C days)

$$TI = 0.3(FI) \quad \text{Eqn 2.5}$$

Where: FI = Freezing Index (°C days)

The authors found that using the equations predicted the thaw duration to be longer than the actual duration, however, WSDOT adopted the technique and used the equations to predict the length of the thaw for Washington State. In addition, the researchers found that as the amount of load reduction is increased there is an increase in pavement life.

Furthermore, thin or flexible pavements and unpaved roads require greater load reduction during the spring thaw. The remainder of the findings are provided in Table 2.8.

Table 2.8 Summary of recommendations made by Kestler after Rutherford, et al. (1985).

Which pavements require load restrictions?
<ul style="list-style-type: none"> • Pavement with surface deflections 45-50% higher during spring thaw than summer.
<ul style="list-style-type: none"> • Pavements with frost susceptible base and subgrade materials.
<ul style="list-style-type: none"> • Pavements with subgrade soils classified as ML, MH, CL, and CH.
<ul style="list-style-type: none"> • Pavements where local experience so indicates. This includes poor ditch drainage, high groundwater levels, etc.
<ul style="list-style-type: none"> • Pavement in which distress has been observed (fatigue cracking and rutting).
When should vehicle load restrictions be placed?
<ul style="list-style-type: none"> • When pavement surface deflections reach values 40-50% higher than summer values.
<ul style="list-style-type: none"> • When the air thaw index accumulates to values that correspond to thaw depths in frost susceptible materials.
<ul style="list-style-type: none"> • When the thaw depth enters the frost susceptible subgrade materials as shown by temperature measurements, frost tubes, or electric resistance gauges.
What magnitude of load restrictions should be required?
<ul style="list-style-type: none"> • Allow only load levels that limit pavement deflections and strains to those estimated for summer conditions.
<ul style="list-style-type: none"> • Use load reductions that correlate with the desired increase in service life
When should load restrictions be removed?
<ul style="list-style-type: none"> • When measured pavement surface deflections have returned to summer values (or design values).

The Minnesota Department of Transportation (Mn/DOT) conducted a study aimed at evaluating the criteria used to predict when to place and remove load restrictions. The approach was used to evaluate Minnesota's load restriction practice, and suggest improvements that would result in a more simple and accurate procedure. More specifically, the objectives of the study were to (1) develop improved predictive equations for estimating when to begin and end load restrictions, (2) investigate changes

in pavement strength in relation to freeze-thaw events, and (3) compare aggregate base strength-recovery characteristics and assess their performance.

Eight test sections at the Mn/Road test facility were used for the study. Hot mix asphalt (HMA) thicknesses range from 75 to 150 mm (3 to 6 in.). Six of the eight sections are conventional designs with varying base and subbase thickness and two sections are full-depth HMA sections. The base and subbase materials are dense-graded sand and gravel mixtures of varying quality (Ovik, et al., 2000). In addition, environmental data consisting of air temperature, frost depth, and subsurface temperature were analyzed to determine the dates, on which the thaw began and ended, and to determine the actual frost and thaw depth during spring-thaw. Finally, deflection data from Mn/ROAD was used to determine the reduction in stiffness for the base and subgrade materials during spring thaw (Ovik, et al., 2000).

Using the Freezing and Thaw Index data as well as the observed thaw duration, the prediction equations developed by WSDOT were adjusted to more accurately predict the thaw duration for conditions in Minnesota. This is shown below. Using Equations 2.4 and 2.5 directly proved that they predict thaw too late in Minnesota.

$$D = 0.15 + 0.010FI + 19.1P - 12090 \cdot \frac{P}{FI} \quad \text{Eqn. 2.6}$$

Where: D = thaw duration (days)
 P = frost depth (m)
 FI = Freezing Index (°C days)

In addition, historical posting dates from 1986 through 1998 were compared to the posting dates predicted using the new technique. It was found that there was typically a week or more delay from the time that load restrictions should be placed until restrictions were actually posted (Ovik, et al., 2000).

The final result of the study was the adoption of a new procedure for placing load restrictions in Minnesota. The policy uses actual and forecasted average daily temperatures to determine when the restrictions should be placed (Ovik, et al., 2000).

2.3.2 Past Test Programs, Results, and Recommendations

Davies (1997) investigated the ability of the Loadman PFWD to track strength changes through the spring thaw for Saskatchewan Highways & Transportation (SHT). Five thin membrane surfaces (TMS) of varying age, construction history, annual maintenance costs, and traffic volumes were tested. Each surface contained between three and six test points, totaling 21 points. SHT currently utilizes the Benkelman Beam, which is the standard against which the Loadman was measured. For each test point, five Loadman measurements were taken and averaged for comparison to the Benkelman Beam. Peak frost free strengths were established in late fall and testing continued once the spring thaw began. After an evaluation of the initial regression analysis, it was determined that temperature correction was required to compare the Loadman data collected through the different seasons. As a result, data points were separated into three groups based on their regression coefficients, deflection values observed at 20°C, and DCP/coring information and field observations. The categories are as follows:

1. seal-on-subgrade
2. Thick, (relatively) soft mat; and
3. Thick, (relatively) hard mat.

A temperature correction of 10 °C was applied to all of the field values by means of best fit equations for the respective category. Davies (1997) found this necessary in

order to compare the Loadman results through the seasons. Results are shown below in Figure 2.33.

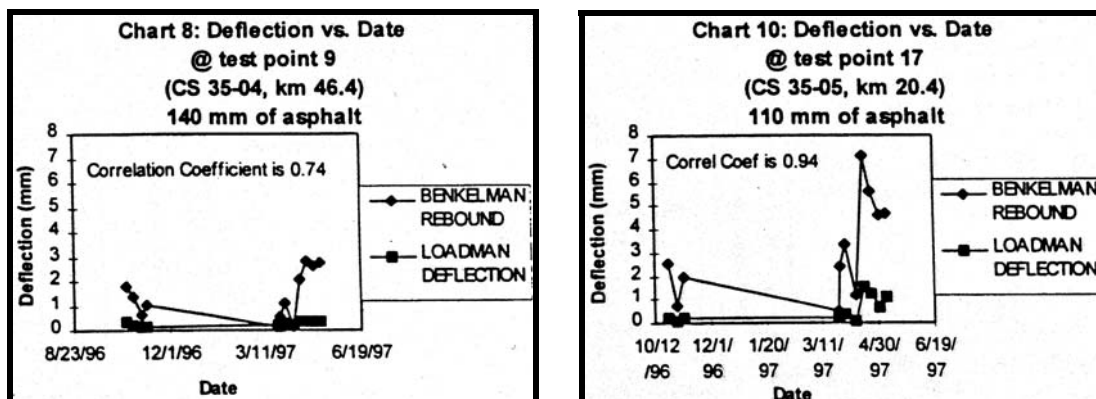


Figure 2.33 Comparison in the ability of the Loadman PFWD and Benkelman Beam to track strength change through spring thaw (Davies, 1997).

Davies (1997) noted “significant differences” in the ability of the PFWD to track strength change, citing the varying layer thicknesses at the test locations as the prime reason.

Fleming and Rogers (1995) determined that the zone “significantly stressed” was roughly equal to 1.5 to 2.0 times the diameter of the loading plate. From this, he concluded that the Loadman follows the change in strength if the asphalt thickness is less than one half (<100 mm) of the Loadman’s zone of influence.

2.4 PFWD QUESTIONNAIRE

In February 2003 and May 2004 a questionnaire, aimed at determining current usage of the PFWD as an alternative to traditional compaction control devices and as a tool to evaluate thaw weakening of roads, was distributed to each of the 50 state Departments of Transportation (DOTs). The following sections describe the results of the survey.

2.4.1 2003 Results

The survey distributed in March, 2003 had a response rate of 56%. Of the 28 states that responded, none had past or present experience in using the PFWD. However, four of the respondents, or ~15%, were aware of current usage by other organizations.

2.4.2 2004 Results

The survey distributed in May, 2004 had a response rate of 36%. Of the 18 states that responded, one (Minnesota) has past or present experience in using the PFWD.

2.5 SUMMARY

The PFWD compared marginally with other devices when testing on pavement layers. Correlation coefficients relating the PFWD to other devices were relatively low. The portable devices generally result in higher modulus values than the FWD, possibly due to the thickness influenced. Several investigators have reported that the zone of influence for the different models lies primarily between one and two loading plate diameters. Large aggregate particles beneath the loading plate of the portable devices also have been shown to affect the results, as the particles increase the resulting modulus values.

The PFWD compared reasonably with other devices when testing on unbound layers. The PFWD reported higher modulus values than the FWD and plate bearing unit when used on granular soils. The range of correlation coefficients was similar to those obtained on pavement layers. The differences between Loadman and the FWD for

measurements obtained on a bound surface were reversed on an unbound surface; however, correlations between devices were much closer.

Few researchers have examined the methods used to evaluate when to place and remove load restrictions. Kestler, et al. (2000) distributed a survey aimed at determining current load restriction practices. A majority of respondents use subjective techniques to aid in determining when load restrictions should be applied and removed. The lengths of the restrictions ranged from as little as three weeks to, according to some respondents, greater than 12 weeks. The Canadian Strategic Highway Research Program also summarized its findings from a survey similar to the one distributed by Kestler, et al. (2000). The findings were similar. The Washington and Minnesota Departments of Transportation developed equations using the freezing and thawing indices to determine the duration of spring thaw period and have had varying degrees of success putting them into practice.

Davies (1997) performed testing aimed at determining the ability of the PFWD to track seasonal stiffness variations. He concluded that the PFWD did adequately follow strength change through spring thaw. This, however, is only valid if the asphalt thickness is less than one half of the zone of influence of the PFWD.

(BLANK PAGE)

CHAPTER 3

FIELD & LABORATORY TEST PROTOCOL

3.1 INTRODUCTION

This test protocol presents the procedures for the field and laboratory evaluation of the Portable Falling Weight Deflectometer (PFWD). This protocol includes the following:

1. Field test site locations.
2. Current road condition, subsurface conditions, and cross sections of field test sites.
3. Instrumentation description, and installation and monitoring procedures.
4. Descriptions of the field testing procedures and data gathered for the study of seasonally posted low volume paved and unpaved roads.
5. Descriptions of testing procedures, materials tested, and data gathered for the field and laboratory study of the compaction of subgrades and construction materials.

3.2 FIELD TEST SITE LOCATIONS

3.2.1 Seasonally Posted Low Volume Roads

The performance of seven paved and three gravel surfaced roads were monitored during the spring of 2004. This portion of the project made use of existing instrumented test sites. Three of the instrumented test sites were part of previous or ongoing New England Transportation Consortium (NETC) and Maine Department of Transportation (MaineDOT) projects constructed under the direction of Dr. Dana N. Humphrey. One of

the instrumented sites was part of ongoing research by the United States Forest Service (USFS) under the direction of Maureen Kestler. Additional sites were selected in consultation with NETC, USFS, MaineDOT, and the Vermont Agency of Transportation (VAOT). A summary of each site is provided in Table 3.1 with approximate geographic locations shown in Figure 3.1. Details are discussed in the following subsections.

3.2.1.1 Kennebec Road – Hampden/Dixmont, Maine

Kennebec Road is a seasonally posted, low volume, hot mix asphalt (HMA) surfaced road. The road is owned and maintained by the State of Maine. This road was selected because it has a relatively low traffic volume, is posted for seasonal weight restrictions, and is in close proximity to the University of Maine campus. The conditions at the site consist of approximately 152 mm (6 in.) of HMA pavement, and approximately 203 mm (8 in.) of subbase material. Typical road condition is shown in Figure 3.1.



Figure 3.1 Typical condition of Kennebec Road, Hampden/Dixmont, Maine in April, 2003.

Table 3.1 Summary of seasonally posted low volume road field test sites.

Project Name	Location	HMA Thickness mm (in.)	Subbase Aggregate Thickness mm (in.)	Subgrade Type	Instrumentation & Field Measurements
Kennebec Rd	Hampden / Dixmont, Me.	152 (6)	203 (8)	Silty Sand	Thermocouples, Piezometers, FWD
Lakeside Landing Rd	Glenburn, Me.	NA	203 (8)	Sandy Silt	Thermocouples, Piezometers, FWD
Stinson Lake Rd	Rumney, N.H.	127 (5)	305-381 (12-15)	Silty Clay To Silty Sand	Thermistors, Waterwell, TDR, FWD
Buffalo Rd	Rumney, N.H.	127 (5)	300 (12)	Silty Sand	Thermocouple, Frost Tube, FWD
USFS Parking Lot	Rumney, N.H.	NA	180 (7)	Sandy Silt	Thermistors, TDR, Waterwells, FWD
Crosstown Rd	Berlin, Vt.	NA	300 (12)	Silty Sand	Thermocouple, FWD
Knapp Airport Parking Lot	Berlin, Vt.	127 (5)	300 (12)	Silty Sand	Frost Tube, FWD
Witter Farm Road	Orono, Me.	127 (5)	483 (19) 288 (11.3)	Silty Clay	Thermocouples, Piezometers, FWD
		127 (5)	483 (19) 326 (12.8)	Silty Clay	Thermocouples, Piezometers, FWD
		127 (5)	635 (25)	Silty Clay	Thermocouples, Piezometers, FWD
Route 126	Monmouth / Litchfield, Me.	150 (6)	600 (24)	Silty Clay to Silty Sand	Thermocouples, Piezometers, FWD
		150 (6)	300 (12)	Silty Clay to Silty Sand	Thermocouples, Piezometers, FWD
		150 (6)	150 (6) grindings	Silty Clay to Silty Sand	Thermocouples, Piezometers, FWD
Route 1A	Frankfort / Winterport, Me.	180 (7)	640 (25)	Silty Clay to Sandy Gravel	Thermocouples, Piezometers, FWD
		180 (7)	640 (25)	Silty Clay to Sandy Gravel	Thermocouples, Piezometers, FWD
		180 (7)	640 (25)	Silty Clay to Sandy Gravel	Thermocouples, Piezometers, FWD

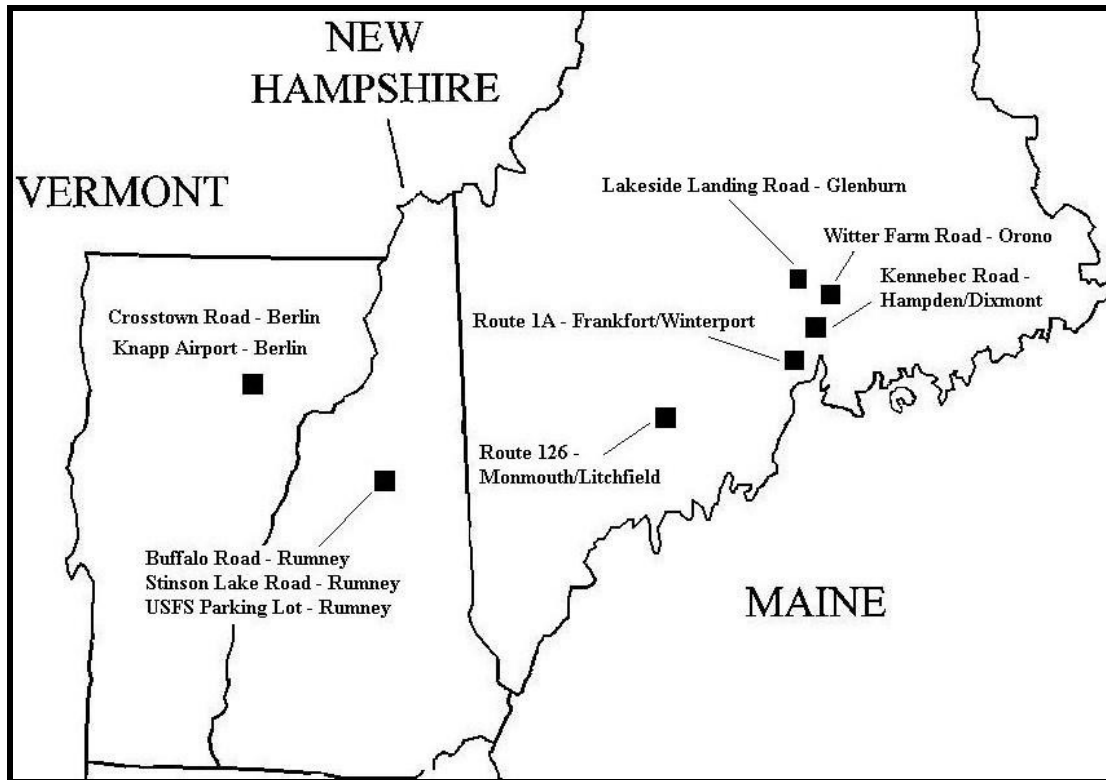


Figure 3.2 Approximate geographic location of spring thaw test sites.

Two separate sections were chosen for testing. Each section was instrumented with one thermocouple and two standpipe piezometers on November 14, 2003. Groundwater was not encountered during installation of instruments in Section 1. The groundwater table at Section 2 at the time of instrument installation was approximately 1.5 to 1.8 m (5 to 6 ft) beneath top of pavement. Results of laboratory tests on field samples obtained during instrumentation are provided in Table 3.2. Details of the instruments, as well as, installation and monitoring methods are described in subsequent sections.

Table 3.2 Laboratory properties of in-situ material at Kennebec Road, Hampden/Dixmont, Maine.

Section 1				Section 2			
Boring No.	Depth (m)	Water Content (%)	Visual Classification	Boring No.	Depth (m)	Water Content (%)	Visual Classification
PZ 1	0.2 – 0.4	4.1	fine to medium gravel	PZ 3	0.2 – 0.4	8.5	medium to coarse sand with a trace of silt
PZ 1	0.4 – 0.8	7.8		PZ 3	0.4 – 0.5	11.0	
TH 1	0.2 – 0.4	3.7	fine to medium gravel	PZ 3	0.5 – 0.8	11.7	
TH 1	0.4 - 0.8	10.1		TH 2	0.2 – 0.3	8.5	medium to coarse sand with a trace of silt
TH 1	0.8 – 1.4	11.9	fine to medium sand with a trace of silt	TH 2	0.3 – 0.5	10.8	medium sand with a trace of silt
TH 1	1.4 – 1.6	10.7		TH 2	1.1 – 1.2	13.6	
TH 1	2.0 – 2.3	18.1		TH 2	1.5 – 1.8	23.7	
TH 1	2.3 – 2.6	14.8		TH 2	1.8 – 2.1	18.3	
PZ 2	0.2 – 0.4	4.4		fine to medium gravel	TH 2	2.1 – 2.4	20.6
PZ 2	0.4 – 0.8	5.3	PZ 4		0.2 – 0.5	7.6	medium to coarse sand with a trace of silt

3.2.1.2 Lakeside Landing Road – Glenburn, Maine

Lakeside Landing Road is a seasonally posted, low volume, gravel surfaced road. The road is owned and maintained by the Town of Glenburn. This road was selected because it has a low traffic volume, is posted for seasonal weight restrictions, is in close proximity to the University of Maine campus, and conditions significantly deteriorate during spring thaw as shown in Figure 3.3. The road section consists of approximately 0.2 m (8 in.) of gravel overlying a geotextile placed on subgrade.



Figure 3.3 Typical road condition of Lakeside Landing Road, Glenburn, Maine in April, 2003.

Two separate sections of the road were chosen for testing. Each section was instrumented with one thermocouple and two standpipe piezometers on November, 7, 2003. Groundwater was not encountered during installation. Results of laboratory tests on samples obtained during instrumentation are provided in Table 3.3. Details of the instruments, as well as, installation and monitoring methods are described in subsequent sections.

Table 3.3 Laboratory properties of in-situ material at Lakeside Landing Road, Glenburn, Maine.

Boring No.	Depth (m)	Water Content (%)	Visual Classification
TH 1	0.2 – 0.8	7.4	fine to medium sandy gravel with a trace of silt
TH 2	0.2 – 0.8	8.9	

3.2.1.3 Stinson Lake Road– Rumney, New Hampshire

Stinson Lake Road is a seasonally posted, low volume, HMA surfaced road. The road is owned by the Town of Rumney and is maintained by the State of New Hampshire. The site was selected because of its close proximity to an existing test site at the USFS Parking Lot. The conditions at the site consist of approximately 127 mm (5 in.) of HMA pavement, and approximately 305 to 381 mm (12 to 15 in.) of subbase material.



Figure 3.4 Typical road condition of Stinson Lake Road, Rumney, New Hampshire in July, 2003.

Two thermistor probes, five time domain reflectometry (TDR) probes, and one standpipe piezometer were installed on July 24, 2003. The groundwater table was encountered during instrumentation at approximately 0.9 m (3 ft) beneath top of pavement. Results of laboratory tests on field samples obtained during instrumentation

are shown in the Table 3.4. Details of the instruments, as well as, installation and monitoring procedures are provided in a later section.

Table 3.4 Laboratory properties of in situ subbase material at Stinson Lake Road, Rumney, New Hampshire.

Boring No.	Depth (m)	Water Content (%)	Visual Classification
T2	0.0 - 0.5	4.2	fine to medium gravel and some sand
	0.5 - 0.9	6.8	
	0.9 - 1.4	14.3	fine sandy gravel with a trace of silt
	1.4 - 1.8	14.0	
	1.8 - 2.2	15.7	

3.2.1.4 Buffalo Road – Rumney, New Hampshire

Buffalo Road is a seasonally posted, low volume, HMA surfaced road. The road is owned and maintained by the Town of Rumney. Like Stinson Lake Road, Buffalo Road was chosen for this project due to its closeness to the USFS Parking Lot site. The conditions at the site consist of approximately 127 mm (5 in.) of HMA pavement, overlying a silty sand subgrade. One thermocouple and one frost tube were installed in December 2004. Results of laboratory tests on field samples obtained during instrumentation are provided in Table 3.5. Details of the installation are described elsewhere.

Table 3.5 Laboratory properties of in situ material at Buffalo Road, Rumney, New Hampshire.

Boring No.	Depth (m)	Water Content (%)	Visual Classification
TH 1	0.0 – 0.3	11.7	fine to medium silty sand
	0.3 – 0.9	15.3	
	0.9 – 1.2	21.2	
	1.2 – 1.5	19.4	
	1.5 – 1.8	24.3	
	1.8 – 2.1	27.1	
	2.1 – 2.4	28.6	
	2.4 – 2.7	26.3	

3.2.1.5 USFS Parking Lot – Rumney, New Hampshire

The gravel surfaced parking lot, located at the Rumney Rocks recreational area, is owned and maintained by the USFS. The conditions at the site consist of approximately 178 mm (7 in.) of gravel overlying a sandy silt subgrade. The subgrade material is classified as SP-SM according to the USCS. Existing site conditions are shown in Figure 3.5. One thermistor probe, two TDR probes, and two standpipe piezometers were installed during the winter of 2003 by the USFS. A gradation of the subbase material is provided in the Appendix A.



Figure 3.5 Existing site conditions at USFS Parking Lot, Rumney, New Hampshire.

3.2.1.6 Crosstown Road – Berlin, Vermont

Crosstown Road is a seasonally posted gravel surfaced road. It is owned and maintained by the Town of Berlin. This site was selected in consultation with VAOT due to its close proximity to their offices and due to the extreme deterioration the road experiences during spring thaw. Existing conditions are shown in Figure 3.6. The road conditions consist of 305 mm (12 in.) of gravel overlying subgrade.



Figure 3.6 Existing conditions at Crosstown Road, Berlin, Vermont in March 2004.

One thermocouple and one frost tube were installed in February 2004.

Groundwater was not encountered during instrumentation. Results of laboratory tests on field samples obtained during instrumentation are shown in Table 3.6. Installation details are described elsewhere.

Table 3.6 Laboratory properties of in situ material at Crosstown Road, Berlin, Vermont.

Boring No.	Depth (m)	Water Content (%)	Visual Classification
TH 1	0.0 – 0.6	10.2	fine to medium sandy gravel
	0.6 – 1.2	10.4	
	1.2 – 1.8	14.5	medium to coarse sand and some silt
	1.8 – 2.4	27.8	
	2.4 – 2.7+	25.4	

3.2.1.7 Knapp Airport Parking Lot – Berlin, Vermont

This site was selected because the VAOT utilizes space at the airport for housing their FWD. In addition, it is in close proximity to the Crosstown Road test site. The parking lot consists of 127 mm (5 in.) of HMA pavement and approximately 300 mm (12 in.) of subbase material overlying subgrade soil. One frost tube was installed in February 2004. No groundwater was encountered during installation. Laboratory test results on samples obtained during installation are provided in the Table 3.7. Instrumentation details are described in subsequent sections.

Table 3.7 Laboratory properties of in situ material at Knapp Airport Parking Lot, Berlin, Vermont.

Boring No.	Depth (m)	Water Content (%)	Visual Classification
F1	0.0 – 0.6	8.4	medium to coarse sand and some silt
	0.4 – 1.2	14.9	
	1.2 – 1.8	14.6	
	1.8 – 2.4	13.97	

3.2.1.8 Witter Farm Road – Orono, Maine

Reconstruction of a 77 m (255 ft) section of Witter Farm Road in the town of Orono was completed in 1997 as part of NETC Project No. 95-1. The full scale field trial was constructed to investigate the use of tire chip/soil mixtures to reduce frost penetration and improve drainage of paved roads (Lawrence, et al., 2000). The project was divided into six 12.2 m (40 ft) long paved sections. Three of the sections (Section 1, Section 2, and Control Section) were used for this study. A plan view is shown in Figure 3.7.

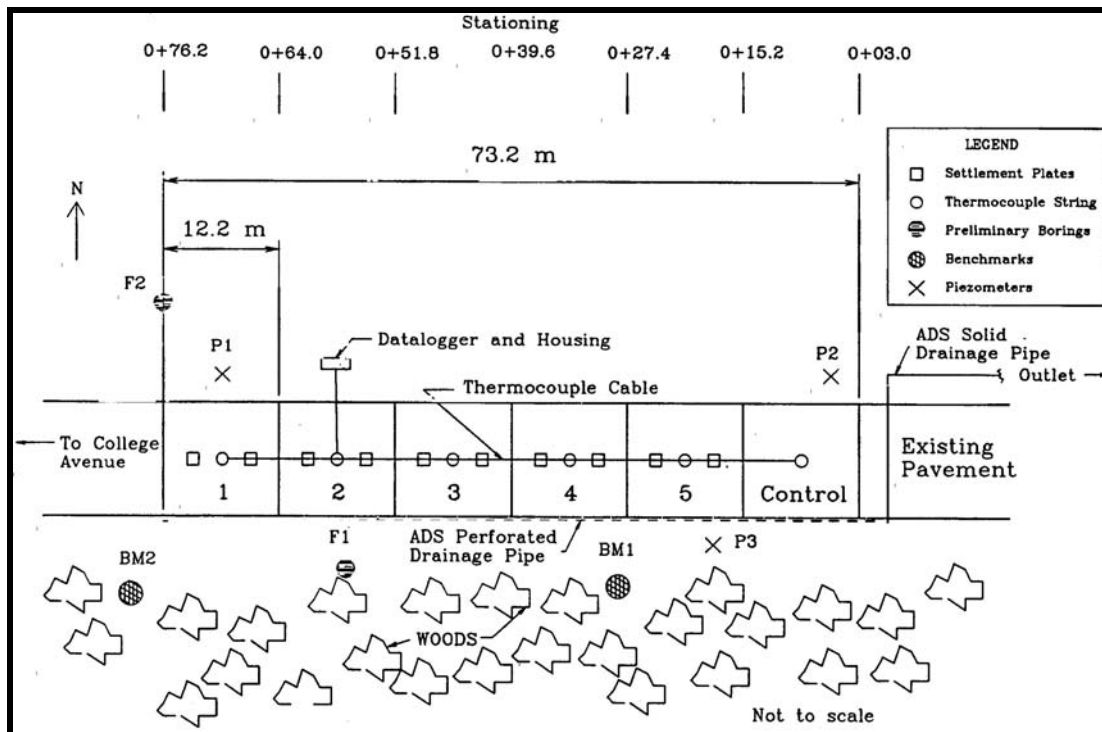


Figure 3.7 Plan view of test sections at Witter Farm Road (Lawrence, et al., 2000).

Each of the three sections contains 127 mm (5 in.) of HMA bituminous pavement. Section 1 contains 483 mm (19 in.) of gravel subbase (MaineDOT Type D) overlying 326 mm (12.8 in.) of a 33% / 67% tire chip/gravel mixture. Section 2 contains 483 mm (19 in.) of gravel subbase (MaineDOT Type D) overlying 288 mm (11.3 in.) of 67% / 33% tire chip/gravel mixture. The Control Section contains 635 mm (25 in.) of gravel subbase (MaineDOT Type D) and has no tire chips. Cross sections for each test section are shown in Figure 3.8.

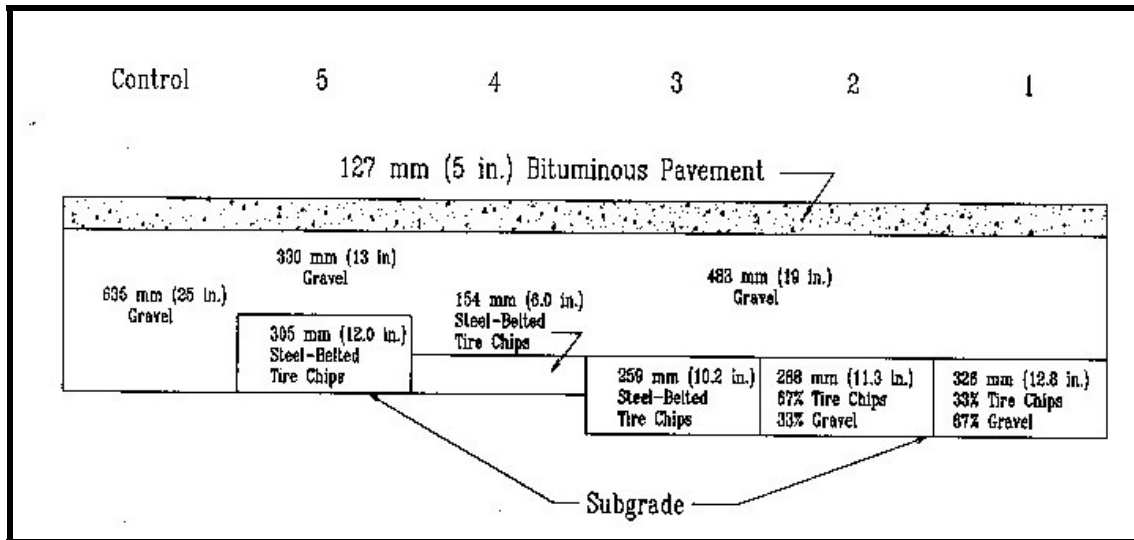


Figure 3.8 Cross section of test sections at Witter Farm Road, Orono, Maine (Lawrence, et al., 2000).

The granular subbase met MaineDOT Specification 703.06, Type D (152 mm (6 in.) maximum size, 25 to 70% passing the 6.4 mm ($\frac{1}{4}$ in.), 30% maximum passing the No. 40, and 7% maximum fines). This material was used for subbase over the tire chips, tire chip/soil mixtures, and for the subbase course in the Control Section (Lawrence, et al., 2000). Gradation curves for this material as well as the tire chip/soil mixtures are provided in Appendix A. The subgrade soil was classified as CL according to the USCS and A-4(8) according the AASHTO classification system. Laboratory test results on subgrade samples are shown in the Table 3.8. Gradations of subbase and subgrade samples can be found in Appendix A.

Table 3.8 Laboratory index properties of cohesive subgrade material at Witter Farm Road, Orono, Maine (Lawrence, et al., 2000)

Sample Type	Location	Depth (m)	Water Content (%)	Plastic Limit	Liquid Limit	Plasticity Index	Specific Gravity
Boring	F1	0.6	23.8				
	F2	0.6	21.1				
	F2	1.2	21.7				2.72
	F2	1.8	22.0				2.74
Bulk Subgrade	Section 1		20.4				
	Section 2		24.1	24	32	8	2.64
	Control		17.7	21	27	6	
Auger	Section 1	0.0 – 0.9	20.4				
	Section 1	0.9 – 1.5	15.5				
	Section 2	0.0 – 0.9	20.7				
	Section 2	0.9 – 1.5	14.4				
	Control	0.0 – 0.9	20.7				
	Control	0.9 – 1.5	32.1				

Each test section contains one thermocouple string. Three standpipe piezometers were installed at locations P1, P2, and P3 shown in Figure 3.7. Instrumentation details are discussed in the following sections.

3.2.1.9 Route 126 – Monmouth/Litchfield, Maine

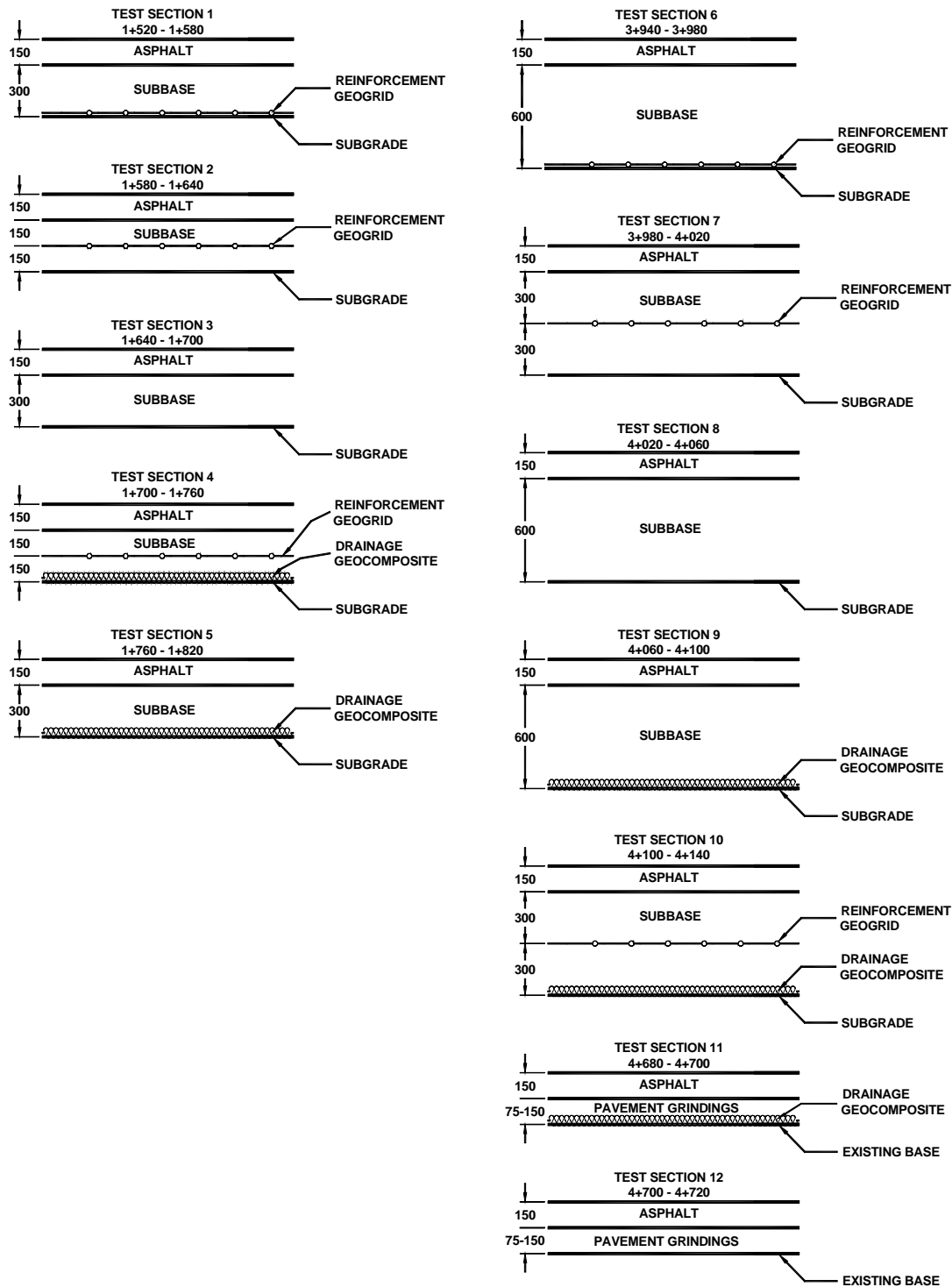
Reconstruction of a 9.5 km (5.9 mile) section of Route 9 in the towns of Monmouth and Litchfield, Maine was completed in 2002 as part of NETC Project No. 00-8. The purpose of the full scale field trial was to investigate the effectiveness of geogrid and drainage geocomposite with thin pavement sections and soft subgrade soils in cold regions (Helstrom and Humphrey, 2005). The project was divided into 12 sections. Sections 1 through 5 are 60 m (196.8 ft) long, Sections 6 through 10 are 40 m

(131.2 ft) long, and Sections 11 and 12 are 20 m (65.6 ft) long. Three control sections (Section 3, Section 8, and Section 12) were used for this study.

Each control section contains 150 mm (6 in.) of HMA pavement. Sections 3 and 8 contain 300 mm (12 in.) and 600 mm (24 in.) of subbase (MaineDOT Type D aggregate), respectively. Section 12 serves as one of two reclaim sections for this project. This section contains 76 to 152 mm (3 to 6 in.) of reclaimed asphalt grindings overlying existing subbase material. Cross sections of all sections are shown in Figure 3.9.

The granular subbase met MaineDOT Specification 703.06, Type D (152 mm (6 in.) maximum size, 25 to 70% passing the 6.4 mm ($\frac{1}{4}$ in.), 30% maximum passing the No. 40, and 7% maximum fines). It is classified as A-1-a according to the AASHTO classification system. Gradation curves for this material are provided in Appendix A.

A subsurface investigation reported very poor subgrade soils throughout the length of the project (Fogg, 2002). These soils are moist and plastic with standard penetration blow counts as low as 10. The water content, liquid limit, plasticity index, and classification of the subgrade samples taken during the investigation are summarized in Table 3.9. Grain size distributions of the subgrade samples are given in Appendix A.



*All dimensions shown are in millimeters

Figure 3.9 Test section layout of Route 126 Monmouth/Litchfield, Maine (Helstrom and Humphrey, 2005).

Table 3.9 Laboratory index properties of subgrade material at Route 126, Monmouth/Litchfield, Maine (Helstrom and Humphrey, 2005).

Boring & Sample ID	Test Section	Station (m)	Offset (m)	Depth (m)	WC	LL	PI	Classification	
								USCS	AASHTO
HB-MONM 103/TS3-1	3	1+670	RT	Subgrade	14.0	--	--	CL-ML	A-4
HB-MONM 103/TS3-2	3	1+670	RT	Subgrade	21.1	27	10	CL	A-4
8-3	8	4+040	0.9RT	1.5-1.8	23.3	N	P	CL-ML	A-4
8-4	8	4+040	0.9RT	1.8-3.0	27.3	24	6	CL-ML	A-4
12-2	12	4+710	0.9RT	2.4-3.0	--	--	--	--	--

Each test section contains one thermocouple string and two vibrating wire piezometers, details of which are presented elsewhere.

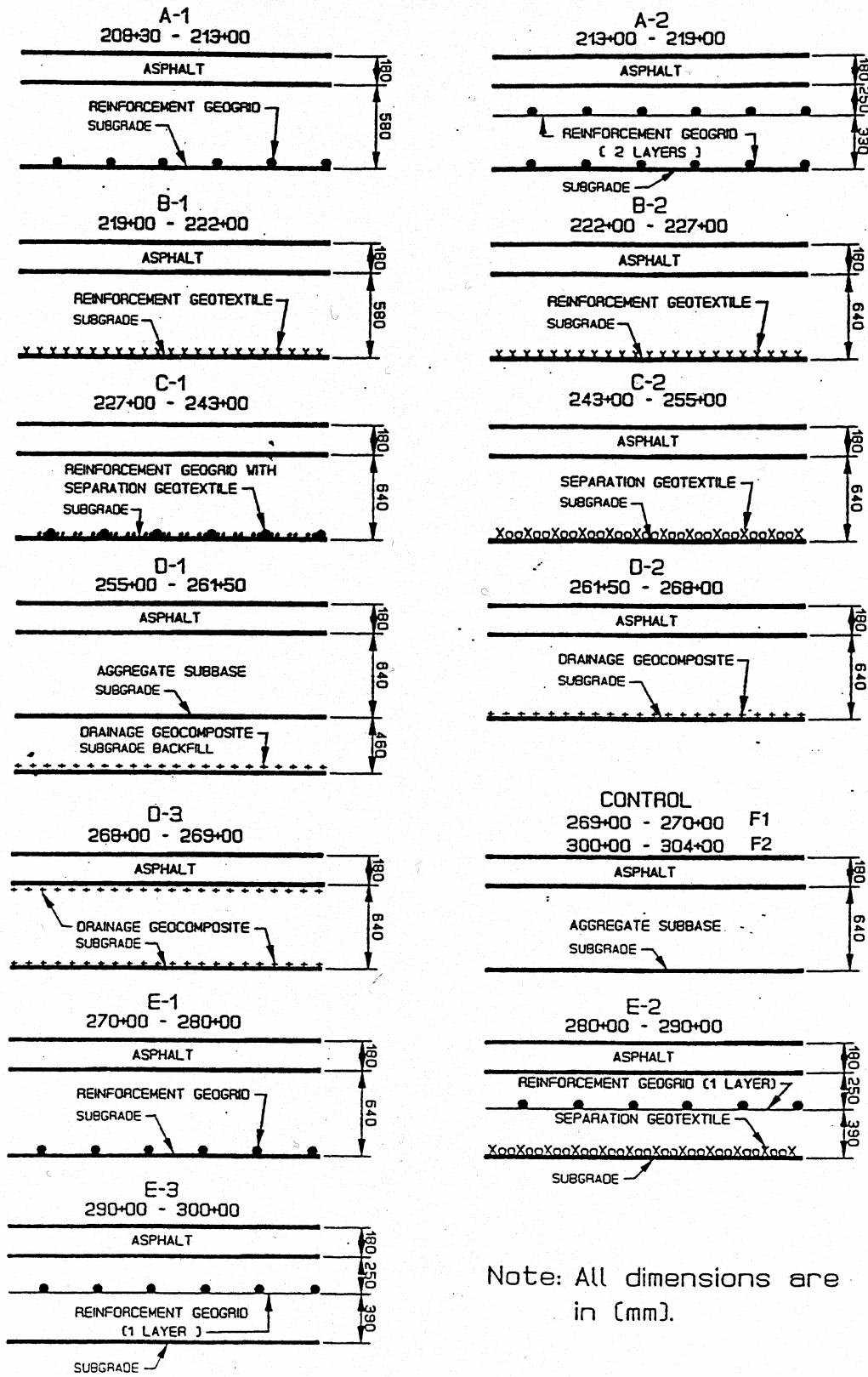
3.2.1.10 Route 1A – Frankfort/Winterport, Maine

Reconstruction of a 3.06 km (1.9 mile) section of Route 1A in the towns of Winterport and Frankfort was completed in 1997 as part of a MaineDOT research project. Reinforcement geogrid, reinforcement geotextile, separation geotextile, and high compressive strength geocomposite drainage net were used in this project to evaluate their reinforcement, separation, filtration, and drainage performance for Maine soil and climatic conditions (Fetten and Humphrey, 1998). The project was divided into six sections, each with different geosynthetic applications. Three of the sections (D-1, D-2, and E-3) were used for this study.

The test sections considered for this study have 180 mm (7 in.) of HMA pavement and 640 mm (25 in.) of aggregate subbase. Section D-1 has a drainage geocomposite located 460 mm (18 in.) beneath the subbase / subgrade interface. Section D-2 has a drainage geocomposite on subgrade, and Section E-3 has one layer of reinforcement geogrid 250 mm (9.8 in.) beneath the asphalt / subbase interface. Cross sections of the sections are shown in Figure 3.10.

The subbase aggregate used for this project was uniformly graded sandy gravel. Approximately 50% of the soil is between 12 mm and 75 mm (0.47 in. and 3.0 in.). It is classified as an A-1-a soil according to the AASHTO classification system. The gradation of this material is shown in Appendix A.

A subsurface investigation (Hayden, 1996) reported poor subgrade soil conditions along the entire length of the project. Moist clay soils were the dominant soil type encountered. The material is plastic with water contents greater than 20% in some areas and liquid limits as high as 37 and plasticity indexes of 17. Natural water contents for samples taken at thermocouple locations are provided in Table 3.10. The samples were classified as A-6 according to the AASHTO classification system. Three laboratory CBR tests were conducted on representative samples at Modified Proctor optimum moisture contents. These tests produced values of 2.6, 3.2, and 3.6 (Fetten and Humphrey, 1998).



Note: All dimensions are in (mm).

Figure 3.10 Test section layout of Route 1A Frankfort/Winterport, Maine (Fetten and Humphrey, 1998).

Table 3.10 Water contents at thermocouple location on Route 1A Frankfort/Winterport, Maine (Fetten and Humphrey, 1998).

Section	Station (m)	Offset (m)	Depth (m)	Water Content (%)
E-3	88+85	NA	1.04	7.5
			1.65	7.7
			2.26	7.0
D-1	78+00	CL	0.2	21.5
			0.6	23.1
		2R	0.2	21.7
			0.2 – 0.6	21.7
			0.6 – 1.1	22.7
		2L	0.2	21.0
			0.2 – 1.1	23.3

NA – information not available.

Section D-2 contains two vibrating wire piezometers. The U.S. Army Corps of Engineers Cold Regions Research and Engineering Laboratory (CRREL) also installed two thermocouple strings.

3.2.1.11 Route 11, Wallgrass Plantation, Maine and Route 167, Presque Isle/Fort Fairfield, Maine.

Routes 11 and 167 were used for testing on one day during the spring of 2003 as part of an ongoing MaineDOT research project (Bouchédid and Humphrey, 2004). Four test sections were used at each site. A detailed description of each test section is provided in Table 3.11 and 3.12.

Table 3.11 Test Section description of Route 11, Wallagrass Plantation, Maine (Bouchédid and Humphrey, 2004).

Location	Asphalt Thickness mm (in.)	Subbase Thickness mm (in.)	Underlying Material
Test Pit 1	118 (4.6)	647 (25.5)	Fill
Test Pit 2	103 (4.1)	797 (31.4)	Fill
Test Pit 3	128 (5)	803 (31.6)	Subgrade
Test Pit 4	136 (5.4)	617 (24.3)	Ledge

Table 3.12 Test Section description of Route 167, Presque Isle/Fort Fairfield, Maine (Bouchédid and Humphrey, 2004).

Location	Asphalt Thickness mm (in.)	Subbase Thickness mm (in.)	Underlying Material
Test Pit 1	135 (5.3)	730 (28.7)	Subgrade
Test Pit 2	120 (4.7)	773 (30.4)	Ledge
Test Pit 3	118 (4.6)	895 (35.2)	Ledge
Test Pit 4	127 (5)	750 (29.5)	subgrade

3.2.2 Compaction Control Field Test Sites

The field sites for evaluation of subgrades and construction materials were located with the assistance of the NETC Technical Committee assigned to this project and MaineDOT. Field sites are summarized in Table 3.13, and each is discussed separately in the following subsections.

Table 3.13 Summary of compaction control field test sites.

Project Name	Location	Material Types Tested	Measurements
I-84 Reconstruction	Southington, Ct.	Crushed Gravel, Subgrade	PFWD, NDM
Rt. 25 Realignment	Effingham/Freedom, N.H.	Construction Sand, Gravel	PFWD, NDM
Rt. 26 Bypass	New Gloucester, Me.	MaineDOT Type D & E	PFWD, NDM
Rt. 201 Reconstruction	The Forks, Me.	Reclaimed Asphalt	FWD, PFWD, NDM
Commercial Paving & Recycling	Scarborough, Me.	Subgrade, Flexpave	PFWD, NDM

3.2.2.1 I-84 Reconstruction – Southington, Connecticut

Reconstruction of several sections of I-84 in Southington, Connecticut took place in the fall of 2003. One section was used for this project. Conditions consisted of variable depths of crushed gravel overlying existing subgrade. Thicknesses ranged from 102 to 356 mm (4 to 14 in.), some of which had been subjected to varying degrees of compaction. The test section is shown in Figure 3.11.



Figure 3.11 I-84 test section, Southington, Connecticut.

The crushed gravel was classified as A-1-a by the AASHTO classification system. The crushed gravel has a maximum dry density of 2.31 Mg/m^3 (144 lb/ft^3) at an optimum water content of 7.4% as determined by AASHTO T 180. Gradations of both materials are provided in Appendix A.

3.2.2.2 Route 25 Realignment – Effingham/Freedom, New Hampshire

The realignment of a portion of Route 25 in the towns of Effingham and Freedom, New Hampshire, took place in conjunction with a bridge replacement project. Two sections were used for testing. Section 1, shown in Figure 3.12, was used for testing crushed gravel meeting NHDOT Specification 304.3 (75 mm (3 in.) maximum size, 95-100% passing the 50 mm (2 in.) sieve, 55-85% passing the 25 mm (1 in.) sieve, 27-52% passing the No. 40 sieve, and 12% maximum fines). Section 1 consisted of 203 mm (8 in.) of crushed gravel overlying 203 mm (8 in.) of material meeting NHDOT Specification 304.1 (70-100% passing the No. 40 sieve, and 12% maximum fines). Section 2, shown in Figure 3.13, consisted of 305 mm (12 in.) of sand overlying subgrade. Both materials were classified as SW according to the USCS and A-1-a according to AASHTO. The crushed aggregate has a maximum dry density of 1.92 Mg/m^3 (120 lb/ft^3) at an optimum moisture content of approximately 12%. The sand aggregate has a maximum dry density of 2.17 Mg/m^3 (135 lb/ft^3) at an optimum moisture content of 11%. Gradation and moisture density curves for each material are shown in Appendixes A and B, respectively.



Figure 3.12 Route 25 Test Section 1, Effingham/Freedom, New Hampshire.



Figure 3.13 Route 25 Test Section 2, Effingham/Freedom, New Hampshire.

3.2.2.3 Route 26 Bypass – New Gloucester, Maine

Several kilometers of road were constructed to bypass an unsafe section of Route 26 in New Gloucester, Maine. The subbase material consisted of 229 mm (9 in.) of MaineDOT Type D aggregate overlying 229 mm (9 in.) of MaineDOT Type E aggregate. Type D aggregate meets MaineDOT Specification 703.06 (152 mm (6 in.) maximum size, 25 to 70% passing the 6.4 mm (¼ in.), 0 to 30% passing the No. 40, and 7% maximum fines). Type E aggregate meets MaineDOT Specification 703.06 (152 mm (6 in.) maximum size, 25 to 100% passing the 6.4 mm (¼ in.), 0 to 50% passing the No. 40, and 7% maximum fines).



Figure 3.14 Route 26 test section, New Gloucester, Maine.

The Type D aggregate was classified A-1-a according to the AASHTO classification system. It has a maximum dry density of 1.99 Mg/m^3 (124 lb/ft^3) at an

optimum water content of 12%. The Type E aggregate was classified A-1-b according to the AASHTO system. It has a maximum dry density of 1.94 Mg/m^3 (121 lb/ft^3) at an optimum water content of 11%. Gradation and moisture density curves for both materials are provided in Appendix A and B.

3.2.2.4 Route 201 Reconstruction – The Forks, Maine

A 20 km (12.41 mi) section of Route 201 in the town of The Forks, Maine, was reconstructed during the summer of 2003 due to progressive pavement deterioration. The existing pavement thickness ranged from 88.9 mm to 127 mm (3.5 in. to 5 in.). A cold in place (CIP) technique was used to rehabilitate the existing pavement. The CIP process begins by milling the existing pavement down. A 7 km (4.35 mi.) section was reclaimed to a depth of 111 mm (3 in.), 8.2 km (5.08 mi) of 102 mm (4 in.), 3.8 km (2.35 mi) of 19 mm (0.75 in.) overlay, and 1 km (0.63 mi) of variable gravel. Each lane was completed in one pass. The millings are conveyed to a crusher and passed over a 38 mm (1.5 in.) screen. Material passing the screen is conveyed to a pugmill. Dry cement, water, and emulsified asphalt are added in the following percentages based on dry weight: 0.5% Portland cement; 2.8% water; and 1.7% emulsion. The material is mixed and conveyed to a paver for laydown. Once the material was placed, it was rolled with a 10 ton steel drum roller and a 20 ton pneumatic tired roller. The compaction process continued until the pavement had a density of 98% of the target density. The target density of 2.0 Mg/m^3 (126 lb/ft^3) was established from a 91 m (300 ft) trial section. A 38 mm (1.5 in.) hot mix asphalt (HMA) surface was placed over the CIP after a 10 day curing period. All testing was done prior to the placement of the HMA surface.

3.2.2.5 Commercial Paving & Recycling – Scarborough, Maine

Commercial Paving & Recycling Co., Inc. (CPR) constructed a 67 m (220 ft) test section at its recycling facility in Scarborough, Maine in October, 2003. CPR developed a paving material known as Flexpave. This material is cold mix-asphalt made from waste materials such as roofing shingles, bottom ash, fly ash, recycled glass, recycled asphalt pavement (RAP), and virgin emulsified asphalt (MS-4). A 63 mm (2.5 in.) layer of Flexpave was used to surface an existing gravel road and monitor its performance. The mix used for the test section consisted of 61% roofing shingles, 30% bottom ash, and 9% MS-4, by weight. Results from Marshall Stability tests on field samples are shown in Table 3.14.

Table 3.14 Summary of Marshall Stability tests on field samples at Commercial Paving & Recycling test site, Scarborough, Maine.

Beginning of Test Section		End of Test Section	
Average Max. Load (kg)	Flow (%)	Average Max. Load (kg)	Flow (%)
252	15	210	18

The subgrade material was classified A-1-b according to the AASHTO system of classification. The material has a maximum dry density of 2.05 Mg/m³ (128 lb/ft³) at an optimum water content of approximately 6%. Gradation and moisture density curves are provided in the Appendices.

3.3 INSTRUMENTATION

Instrumentation was used for the spring thaw monitoring portion of this project to quantify the condition of the test sections on days when measurements were made.

Instrumentation included: thermocouples, thermistors, frost tubes, vibrating wire piezometers, standpipe piezometers, and TDR probes. Only selected instruments were installed in each project as listed in Table 3.15.

Table 3.15 Summary of instruments spring thaw field test sites.

Field Test Site	Instrumentation
Kennebec Road	Thermocouples, Standpipe Piezometers
Lakeside Landing Road	Thermocouples, Standpipe Piezometers
Stinson Lake Road	Thermistors, Frost Tube, TDR probes
Buffalo Road	Thermocouples, Frost Tube
USFS Parking Lot	Thermistors, Standpipe Piezometers, TDR probes
Crosstown Road	Thermocouples, Frost Tube
Knapp Airport Parking Lot	Frost Tube
Witter Farm Road	Thermocouples, Standpipe Piezometer
Route 126	Thermocouples, Vibrating Wire Piezometers
Route 1A	Thermocouples, Standpipe Piezometers, Vibrating Wire Piezometers

3.3.1 Frost Penetration Measurement

Thermocouples, thermistors, and/or frost tubes were installed and used to monitor frost penetration during the winter and subsequent spring thaw. Thermocouples were installed at Kennebec Road, Lakeside Landing Road, Buffalo Road, and Crosstown Road. Thermistors were installed at the USFS Parking Lot site and at Stinson Lake Road. Frost tubes were also installed at Buffalo Road, Crosstown Road, and Knapp

Airport Parking Lot. Thermocouple strings installed as part of previous projects were used at the Witter Farm Road, Route 126, and Route 1A test sites.

3.3.1.1 Thermocouple Characteristics

The thermocouples used for this project were 20 gage copper constantan (Type T). A bi-metal reaction occurs where the copper and constantan wires are joined at their terminus in the ground. Measurement of the resulting electrical potential allows the temperature to be determined. The thermocouples installed for this project were attached to 2.4 m (8 ft) long by 25 mm (1 in.) diameter wooden dowels. Eleven sensors were placed vertically every 152 mm (6 in.) to a depth of 0.9 m (3 ft), where spacing was increased to 0.3 m (1 ft) for the remaining length of the probe. The twelfth sensor is a flyer, which is not attached to the dowel and was placed in the soil directly beneath the pavement layer, above the top of the dowel. Thermocouple string configuration is shown in Figure 3.15. Thermocouple location at each site is provided in Table 3.16.

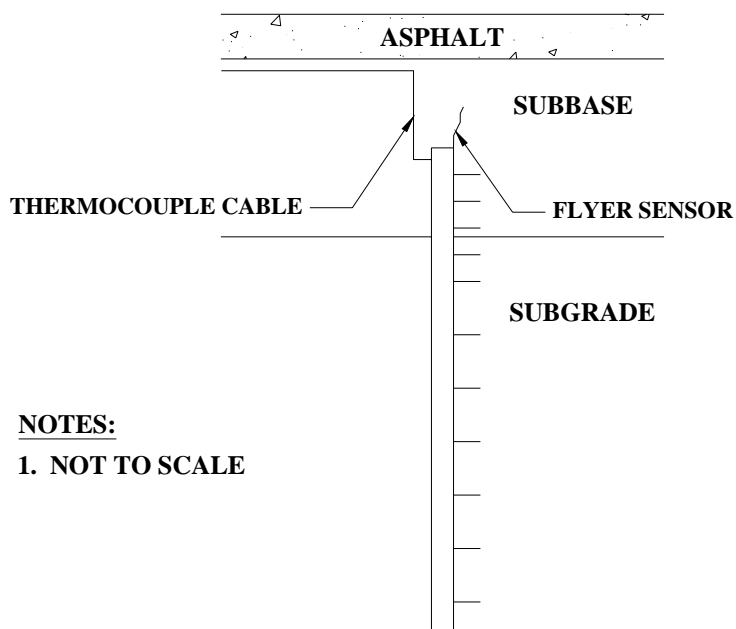


Figure 3.15 Thermocouple string detail.

Table 3.16 Summary of thermocouple locations at spring thaw field test sites.

Test Site	Test Section	Station (m)	Offset From C/L (m)	Approximate Depth of Top Sensor From Finish Grade mm (in.)	Approximate Depth of Flyer Sensor From Finish Grade mm (in.)
Kennebec Road	1	NA	2.7 RT	305 (12)	152 (6)
	2	NA	2.7 RT	305 (12)	
Lakeside Landing Road	1	NA	2.7 RT	432 (17)	152 (6)
	2	NA	2.7 RT	203 (8)	152 (6)
Buffalo Road	1	NA	2.7 RT	238 (8)	152 (6)
Crosstown Road	1	NA	2.7 RT	152 (6)	102 (4)
Witter Farm Road	Control	0+09.1	CL	248 (10)	NFS
	1	0+70.1	CL	333 (13)	
	2	0+57.9	CL	422 (17)	
Route 126	3	1+670	2.9 RT	305 (12)	NFS
	8	4+040	2.9 RT	460 (18)	
	12	4+710	2.9 RT	152 (6)	
Route 1A	D-1	255+50	CL	203 (8)	NFS
		258+50	CL		
	D-2	267+50	CL		
		268+50	CL		
E-3	88+85	7.5 RT	430 (17)		

NFS – no flyer sensors.

3.3.1.2 Thermistor Characteristics

The thermistors used for this project are YSI epoxy encapsulated thermistors. The temperature dependant resistors allow for a direct measurement of resistance. One thermistor probe was installed in the USFS parking lot site in Rumney, N.H. in the fall of 2002. The probe is approximately 1.5 m (5 ft) long and consists of 8 thermistors. The thermistors are located within the probe and are spaced roughly 191 mm (7.5 in.) apart. Three thermistors are flyers and are located above the top of the probe, at various depths beneath the ground surface.

Two thermistor probes were installed at the Stinson Lake Road site during the summer of 2003. Each probe is 1.6 m (5.25 ft) in length and contains 12 thermistors, 11

within the probe, and one flyer attached to the top of the probe. Two additional flyers were installed with each thermistor string and are not attached to the probe. The thermistors within the probes are spaced at 102 mm (4 in.) to a depth of 914 mm (35.5 in.) where spacing then increases to 152 mm (6 in.) for the remaining length of the probe. Thermistor location at each site is shown in Table 3.17.

Table 3.17 Summary of thermistor locations at spring thaw field test sites.

Test Site	Instrument No.	Offset From C/L (m)	Approximate Depth of Top of Probe From Finish Grade mm (in.)	Approximate Depth of Flyer Sensors From Finish Grade mm (in.)
USFS Parking Lot	T1	NA	334 (13)	70 (3)
				134 (5)
				194 (8)
Stinson Lake Road	T1	2.7 RT	393 (15)	85 (3)
				152 (6)
				186 (7)
	T2	2.7 RT	405 (16)	79 (3)
				165 (7)
				195 (8)

NA – no centerline present in parking lot.

3.3.1.3 Frost Tube Characteristics

Frost tubes used for this project were approximately 1.8 m (6 ft) long, 18 mm ($\frac{1}{2}$ in.) plastic tubing. Within the plastic tubing is a blue colored fluid. When freezing conditions exist, the blue color precipitates out leaving a colorless material. The depth of frost penetration is determined by measuring the length of colorless material. The frost tube is housed within a 19.1 mm ($\frac{3}{4}$ in.) PVC pipe. The frost tubes used for this project are shown in Figure 3.16. Frost tube locations are shown in Table 3.18.



Figure 3.16 Frost tube detail.

Table 3.18 Summary of frost tube locations at spring thaw field test sites.

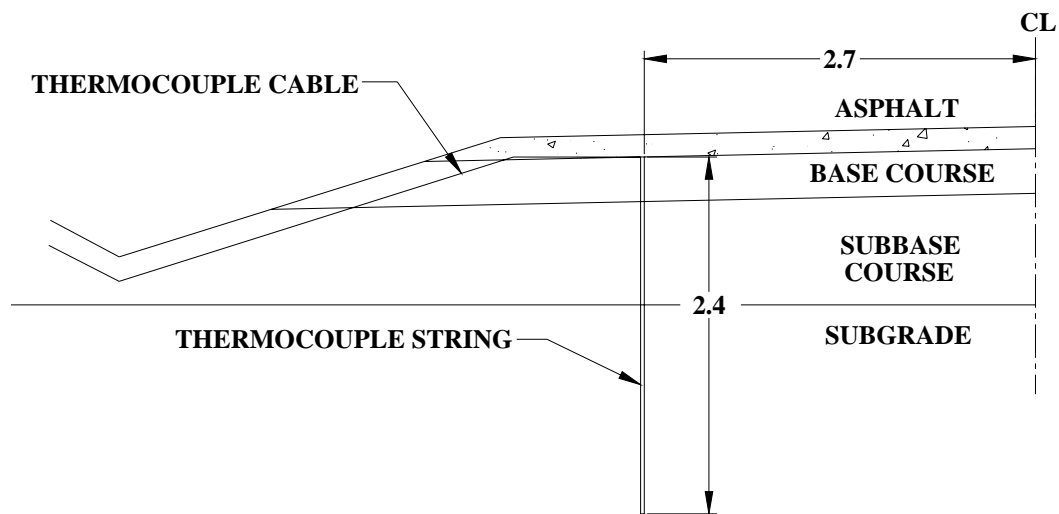
Test Site	Instrument No.	Offset From C/L (m)
Buffalo Road	F1	2.7 RT
Knapp Airport Parking Lot	F1	NA

NA – no centerline in parking lot.

3.3.1.4 Installation & Monitoring

Thermocouple strings, thermistor probes, and/or frost tubes were installed in the outside wheel path, approximately 2.7 m left or right of centerline as shown in Figure 3.17. A drill rig was required for installation. The drill rig augured a 102 mm (4 in.)

diameter hole to approximately 2.7 m (9 ft) below the road surface. Samples were taken for water content, Atterberg Limit, and/or gradation laboratory tests as appropriate for the soil type recovered. The strings/tubes were inserted and backfilled with native material as shown in Figure 3.18.



1. ALL DIMENSIONS GIVEN ARE IN METERS.

Figure 3.17 Thermocouple/thermistor section view.

A groove approximately 51 mm (2 in.) wide by 152 mm (6 in.) deep was jack-hammered in the pavement to run the thermocouple/thermistor wire to the edge of the pavement. After placement in the groove, the wire was covered with cold patch and compacted. Beyond the edge of the pavement the wire was placed in PVC conduit and buried in a 152 mm (6 in.) deep trench and run to the outside of the ditch line.



Figure 3.18 Placement of thermocouple string in auger hole.

Manual thermocouple readings were taken weekly during the spring thaw with a hand held electronic readout unit (Omega Type HH201A). The accuracy of the readings was improved by keeping the readout device at a constant temperature. This was done by taking readings inside of a heated vehicle. The constant temperature is used a reference temperature by the handheld unit to determine the temperature at the location of that particular thermocouple pair. Lead wires from the thermocouples were installed with adequate length to extend from the outside of the ditch line to the side of the road.

Thermocouple strings previously installed in Witter Farm Road, Route 1A, and Route 126 are read automatically by a Campbell Scientific data acquisition system. The thermistor probes installed to monitor the USFS sites are also read by automated data acquisition systems. All data acquisition systems are read hourly for daily average

temperature determination. Data was downloaded approximately weekly during the spring thaw. Frost tubes were also monitored weekly.

3.3.2 Pore Water Pressure Measurement

Standpipe piezometers were installed to monitor pore water pressures. At sites where piezometers were not already present, four standpipe piezometers were installed. In addition, time domain reflectometry (TDR) probes were installed in two USFS sites under the direction of Maureen Kestler. Previously installed vibrating wire piezometers were used in Route 1A and Route 126. Previously installed standpipe piezometers were used at the Witter Farm Road and USFS Parking Lot.

3.3.2.1 Vibrating Wire Piezometer Characteristics

Vibrating wire piezometers were installed in Route 1A in the towns of Frankfort and Winterport, Maine during the summer of 1997 and 1998. RocTest PWS vibrating wire piezometers were used for this project. They have a low air entry sintered ceramic porous stone and a 34 kPa (5 psi) range of measurement. Piezometers are located beneath the break down lane, 3.7 m (12 ft) right of centerline. RocTest PWL vibrating wire piezometers were installed in Route 126 in the towns of Monmouth and Litchfield, Maine during the fall of 2001 and the summer of 2002. A summary of vibrating wire piezometer locations is provided in Table 3.19.

Table 3.19 Summary of vibrating wire piezometer locations at spring thaw field test sites.

Test Site	Test Section	Station (m)	Offset From C/L (m)	Subbase or Subgrade	Approximate Depth From Finish Grade mm (in.)
Route 126	3	1 + 673	3.7 RT	Subbase	405 (16)
		1 + 673		Subgrade	660 (26)
	8	4 + 042	3.7 RT	Subbase	710 (28)
		4 + 042		Subgrade	965 (38)
	12	4 + 712	3.7 RT	Subbase	255 (10)
		4 + 712		Subgrade	510 (20)
Route 1A	D-1	78 + 79	3.7 RT	Subbase	468 (18)
				Subgrade	950 (37)
				Subgrade	NA
	D-2	81 + 53	3.7 RT	Subbase	481 (19)
				Subgrade	715 (28)
				Subgrade	887 (35)
E-3	88 + 15	3.7 RT	Subbase	NA	
			Subgrade	NA	

NA – information not available.

3.3.2.2 Standpipe Piezometer Characteristics

For projects that did not already have piezometers, standpipe piezometers were used. The piezometers are 25 mm (1 in.) diameter schedule 40 black iron pipe. The piezometers extend approximately 76 mm (30 in.) into the road base material. The lower 300 mm (12 in.) of the pipe is slotted. Two pieces of 25 mm (1 in.) by 6.4 mm (¼ in.) by 300 mm (12 in.) steel were welded on opposing sides of the piezometer. This was done to add resistance to aid in removing the top plug during measurement. The black iron pipe was wrapped with geosynthetic fabric to prevent migration of soil particles into the well. The top of the piezometer consists of a plug that is unscrewed to take measurements. A detailed view of standpipe piezometers is shown in Figure 3.19.

Standpipe piezometers used at the Witter Farm Road are shown in Figure 3.20.

Piezometer location is shown in Table 3.20.

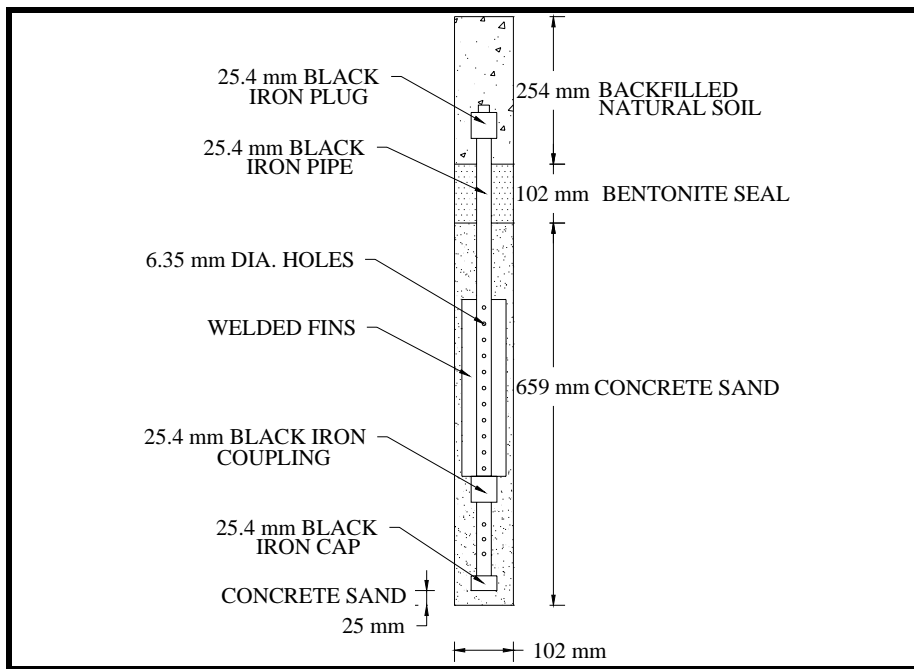


Figure 3.19 Standpipe piezometer detail.

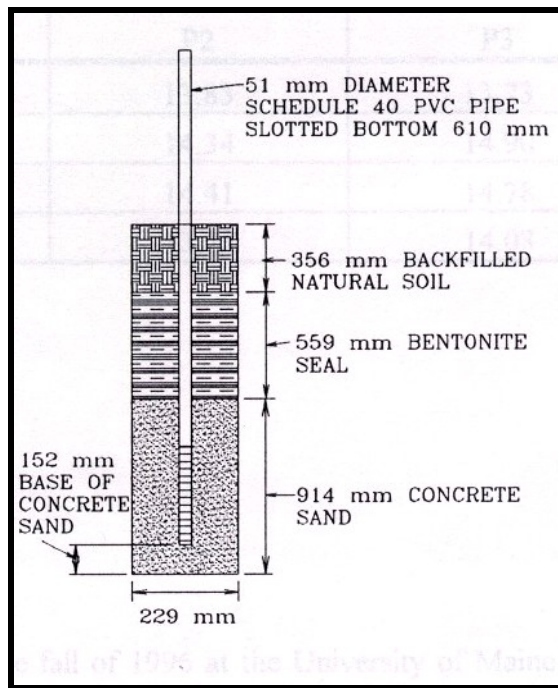


Figure 3.20 Standpipe piezometer detail for Witter Farm Road, Orono, Maine (Lawrence, et al., 2000).

Table 3.20 Summary of standpipe piezometer locations at spring thaw field test sites.

Test Site	Test Section	Station (m)	Instrument No.	Offset From C/L (m)	Approximate Depth of Top of Piezometers From Finish Grade mm (in.)
Kennebec Road	1	NA	P1	2.7 RT	76 (3)
			P2		
	2	NA	P3		
			P4		
Lakeside Landing Road	1	NA	P1	2.7 RT	152 (6)
			P2		
	2	NA	P3		
			P4		
Witter Farm Road	1	0+70.1	P1	LT	NA
	Control	0+3.1	P2	RT	
	5	0+18.3	P3	LT	
Route 1A	D-1	255+50	P1	13.1 LT	NA
		256+75	P2	11.6 RT	
		261+00	P3	10.8 LT	

NA – information not available.

Standpipe piezometers were installed at the USFS parking lot site in Rumney, N.H. in the fall of 2002. They extend to approximately 1.8 m (6 ft) below the ground surface. This type of piezometer consists of a filtered tip connected to a riser pipe. The standpipe piezometers are 3 m (10 ft) long, 51 mm (2 in.) diameter PVC pipe. The perforated section is covered with geosynthetic fabric to prevent migration of particles into the well. The riser pipe is terminated above the ground surface and covered with a vented cap.

3.3.2.3 TDR Probe Characteristics

The TDR probes used for this project are Soilmoisture 6005L2 Buriable Waveguides. A frequency electromagnetic pulse is generated and sent down a line

comprised of two waveguides. The velocity of propagation of the high frequency, broad band 3GHz wave in soil is determined primarily by the water content. The wave is reflected from the open ends of the waveguides and returns along the original path. By microprocessor, the travel time of the wave is used to directly calculate the dielectric constant of the soil. TDR probe locations are shown in Table 3.21.

Table 3.21 TDR probe locations at Stinson Lake Road and USFS Parking Lot, Rumney, New Hampshire.

Test Site	Instrument No.	Offset From C/L (m)	Approximate Depth of Probe From Finish Grade mm (in.)
Stinson Lake Road	TDR 1	2.7 RT	677 (27)
	TDR 2		561 (22)
	TDR 4		427 (17)
	TDR 5		268 (11)
	TDR 6		143 (6)
USFS Parking Lot	TDR 1		NA
	TDR 2		NA

NA – information not available.

3.3.2.4 Installation & Monitoring

Installation of vibrating wire piezometers used at Routes 1A and 126 and standpipe piezometers used at the Witter Farm Road and USFS Parking Lot are not discussed.

The standpipe piezometers were installed in the outside wheel path, approximately 2.7 m (9 ft) left or right of centerline. A drill rig was required for installation. The drill rig augured a 102 mm (4 in.) diameter hole. The piezometers were inserted into the augured hole and backfilled according to the specification illustrated in

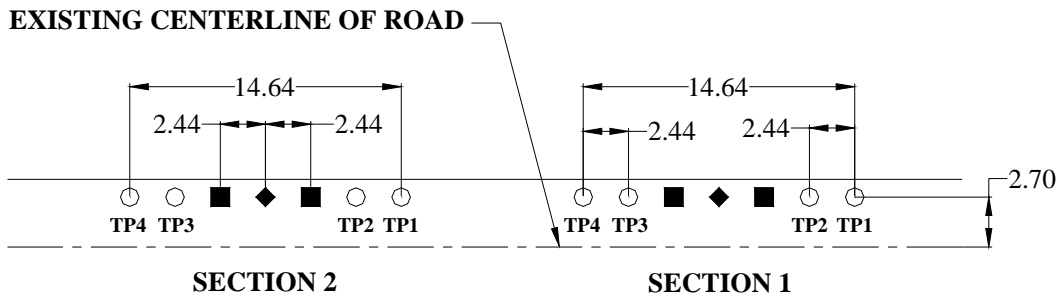
Figure 3.19. Bentonite powder/pellets were used to minimize infiltration of surface water.

All monitoring was done approximately weekly during the spring thaw. The top plug was removed and the depth to the water surface from the top of pavement was measured and recorded. Vibrating wire piezometers used in Section 3 and Section 8 on Route 126 are read automatically by a Campbell Scientific data acquisition system. Vibrating wire piezometers in Section 12, Route 126, and those used at Route 1A were read manually with a RocTest MB-6T unit. TDR probes were read with a Trase system 6050X1 measuring unit.

3.4 FIELD TESTING PROCEDURES

3.4.1 Spring Thaw Monitoring

At each field site, device measurements were performed at a minimum of eight locations. Measurements were taken approximately weekly during the spring thaw period. Test point locations for Kennebec Road and Lakeside Landing Road field sites are shown in Figures 3.21. Test point locations for Stinson Lake Road, Buffalo Road, and Crosstown Road are shown in Figure 3.22. Test point locations for USFS Parking Lot and Knapp Airport Parking Lot are shown in Figure 3.23. Table 3.22 provides test point locations for Witter Farm Road, Route 126, and Route 1A.



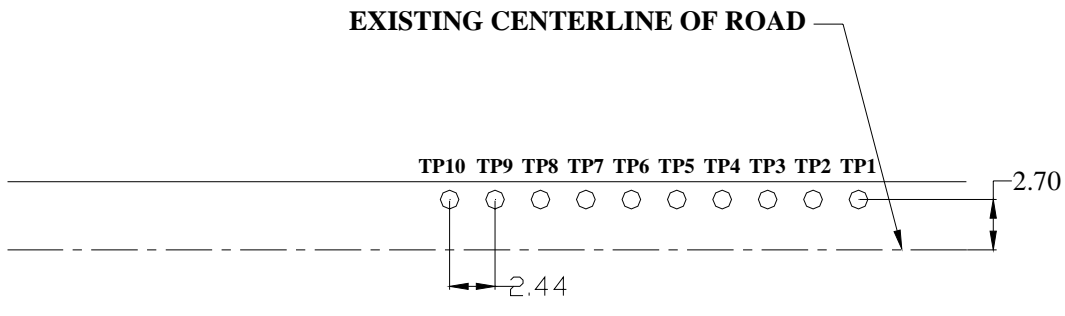
NOTES:

1. ALL DIMENSIONS SHOWN ARE IN METERS

LEGEND:

- = FWD & PFWD TEST POINT LOCATION
- = STANDPIPE PIEZOMETER
- ◆ = THERMOCOUPLE STRING

Figure 3.21 Kennebec Road and Lakeside Landing Road test point layout.



NOTES:

1. ALL DIMENSIONS SHOWN ARE IN METERS

LEGEND:

- = FWD & PFWD TEST POINT LOCATION

Figure 3.22 Stinson Lake Road, Buffalo Road, and Crosstown Road test point layout.

Table 3.22 Summary of test point locations at Witter Farm Road, Route 126, and Route 1A.

Witter Farm Road			Route 126			Route 1A		
Test Section	Station (m)	Offset From C/L (m)	Test Section	Station (m)	Offset From C/L (m)	Test Section	Station (m)	Offset From C/L (m)
Control Section	0+3	1.2RT	Section 3	1+652	2.7RT	Section D-1	255+50	2.7RT
		0.6LT		1+664			256+50	
	0+6	0.6RT		1+676			257+50	
		1.2LT		1+688			258+50	
	0+9	1.2RT	Section 8	4+028			259+00	
		0.6LT		4+036			260+50	
Section 2	0+55	0.6RT	4+044	Section D-2		262+00		
		1.2LT	4+052			263+00		
	0+58	1.2RT	Section 12			4+704	264+00	
		0.6LT				4+708	265+00	
	0+61	0.6RT	4+712			266+00		
		1.2LT	4+716			267+00		
Section 1	0+67	0.6RT				Section E-3	291+00	
		1.2LT					292+00	
	0+70	1.2RT					293+00	
		0.6LT					294+00	
	0+73	0.6RT					295+00	
		1.2LT						

3.4.1.1 Portable Device Measurements

Several portable measuring devices were used for testing during the spring of 2004. Prima 100 PFWD measurements were taken at all test sites. Loadman PFWD measurements were taken at spring thaw test sites in Rumney, New Hampshire. Clegg Impact Hammer and Humboldt Soil Stiffness Gauge measurements were taken at the USFS Parking Lot during the spring of 2003 and 2004. Each device is discussed separately in the following sections.

3.4.1.1.1 Prima 100 PFWD

The Prima 100 is a light, portable device that has been developed to measure stiffness of construction layers including subgrades, base courses, and pavements.

Details regarding the mode of operation are provided in Section 2.2.2.1. With the Prima 100 PFWD, six measurements were taken at each of three different drop heights, at each test location. Additional drop heights were approximately equal to 850, 630, and 420 mm (34, 25, and 17 in.). This is illustrated in Figure 3.23. Additional deflection sensors were used with spacing as follows (as measured from the center of the loading plate): 0, 207, and 407 mm (0, 8, and 16 in.). The PFWD measurements were taken utilizing a 20 kg (44 lb) drop weight and a 300 mm (11.8 in.) loading plate. In all cases, the first reading was neglected and the average of the remaining five was used for analysis and comparison. These, as well as other input parameters are summarized in Table 3.23.

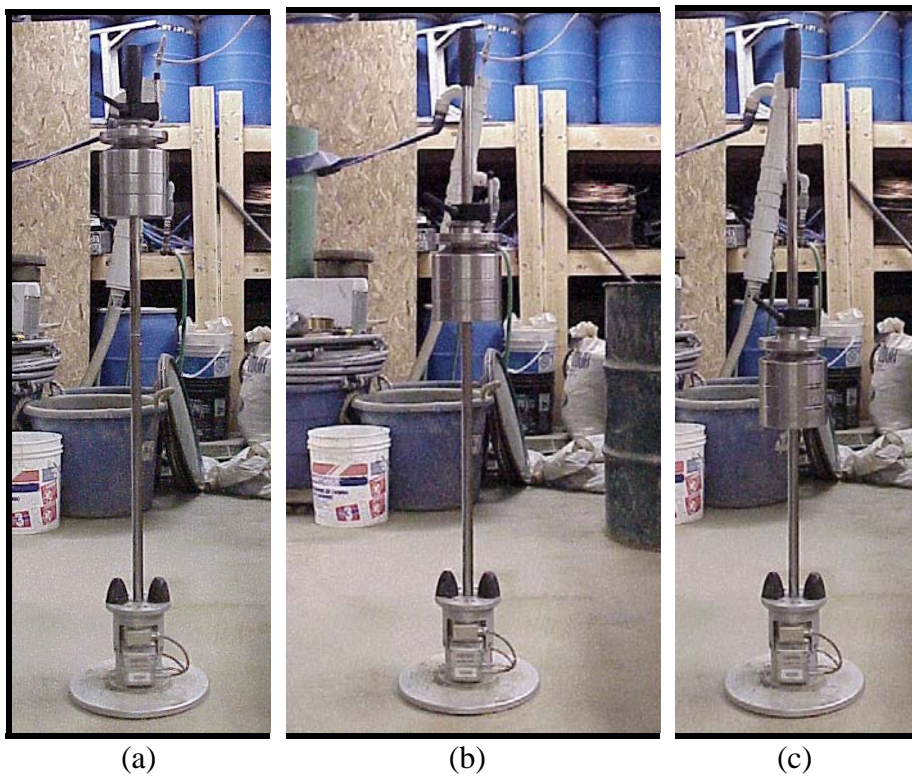


Figure 3.23 Variable drop heights (a) 850 mm, (b) 630 mm, and (c) 420 mm.

Table 3.23 Prima 100 PFWD input parameters.

Setup Menu Item	Input Parameter	Asphalt Surfaced Test Sites	Gravel Surfaced Test Sites
Trigger	Pretrig time (ms)	10*	
	Pulsebase (%)	24*	
	Trig Level (kN)	0.90*	
View	Sample Time (ms)	60*	
Mechanical	Load Plate Radius (mm)	150	
	Number of sensors	3	
	D ₍₁₎ offset (cm)	0	
	D ₍₂₎ offset (cm)	20.7	
	D ₍₃₎ offset (cm)	40.7	
Formula	Poisson's Ratio	0.35**	0.35**
	Stress Distribution	2.0	2.67

* - default values.

** - Huang, 2004.

3.4.1.1.2 Loadman PFWD

A detailed description of the Loadman PFWD and its mode of operation is provided in Section 2.2.2.2. A total of five measurements were taken at each test location. In all cases, the first drop was neglected and an average of the remaining drops was used for analysis and comparison.

3.4.1.1.3 Clegg Impact Hammer

A detailed description of the Clegg Impact Hammer and its mode of operation is provided in Section 2.2.1. Four drops were made at each test location. The first drop was excluded and the average of the remaining drops was averaged. The average of the values was taken and correlated to stiffness using Equation 3.1. This value was used for analysis and comparison.

$$E = 0.088 \cdot CIV^2 \quad \text{Eqn. 3.1}$$

Where: E = Elastic Modulus (MPa)

CIV = Clegg Impact Value

3.4.1.1.4 Humboldt Soil Stiffness Gauge

The Humboldt Soil Stiffness Gauge (SSG) was used for testing at the USFS Parking Lot site in Rumney, New Hampshire during the spring of 2003. A detailed description of the SSG is provided in Section 2.2.1. One measurement was taken at each test location.

3.4.1.2 Falling Weight Deflectometer Testing

The MaineDOT provided a falling weight Deflectometer (FWD) for seasonally posted roads in Maine. The United States Army Corps of Engineers Cold Regions Research and Engineering Laboratory (CRREL) provided a FWD for test sites in Rumney, New Hampshire. The Vermont Agency of Transportation (VAOT) provided a FWD for seasonally posted low volume roads in Vermont. Each agency utilized different units and had different testing techniques. As a result, each is discussed separately below.

3.4.1.2.1 MaineDOT FWD

The MaineDOT utilizes a JILS Model 20C Falling Weight Deflectometer manufactured by Foundation Mechanics, Inc. The unit has a constant drop weight of 340.2 kg (750 lb). The load capacity ranges from 9 to 120 kN (2,000 to 27,000 lbf) with a loading plate diameter of 304.8 mm (12 in.). Deflection sensors are spaced at 0, 305, 457, 610, 914, 1219, and 1524 mm (0, 12, 18, 24, 36, 48, and 60 in.). The unit is shown in Figure 3.24.



Figure 3.24 MaineDOT JILS Model 20 C FWD.

Prior to testing the FWD operator conducts a force calibration. During the calibration, the software determines the drop heights required to produce predetermined forces based on layer response. One drop each at six different loads is performed. The loading sequence is as follows: 26.7, 40.0, 53.4, and 71.2 kN (6, 9, 12, 16, 9, and 9 kips).

3.4.1.2.2 CRREL FWD

CRREL uses a Dynatest Model 8000 Falling Weight Deflectometer. The Model 8000 FWD has a loading range of 7 to 120 kN (1.5 to 27.0 kips). The unit has a loading plate diameter of 457 mm (18 in.). Deflection sensors are spaced at 0, 305, 610, 914, 1219, 1524, and 1829 mm (0, 12, 24, 36, 48, 60, and 72 in.). The unit is shown in Figure 3.25. The CRREL test program targeted four drops at each of four different drop heights.



Figure 3.25 CRREL Dynatest 8000 FWD.

3.4.1.2.3 VAOT FWD

The VAOT utilizes a Dynatest® Model 8000 Falling Weight Deflectometer. The Model 8000 FWD has a loading range of 7 to 120 kN (1.5 to 27.0 kips). The unit has a loading plate diameter of 300 mm (11.8 in.) and deflection sensor spacing of 0, 203, 305, 457, 610, 914, 1219, 1524, and 1829 mm (0, 8, 12, 18, 24, 36, 48, 60, 72 in.) The unit is shown in Figure 3.26.



Figure 3.26 VAOT Dynatest 8000 FWD.

VAOT FWD testing followed the Strategic Highway Research Program (SHRP) FWD testing protocol administered by the Long Term Pavement Performance (LTPP) division of the Federal Highway Administration (FHWA). This testing procedure includes three seating drops and four drops each at four different drop heights that target four different loads. The procedure is shown in Table 3.24 and Table 3.25.

Table 3.24 FLEX testing plan drop sequence used at Berlin, Vermont test sites (LTPP, 2000).

No. of Drops	Height (mm)	Data Stored
3	3 (200)	No*
4	1 (50)	Peaks
4	2 (100)	Peaks
4	3 (200)	Peaks
4	4 (390)	Peaks & History

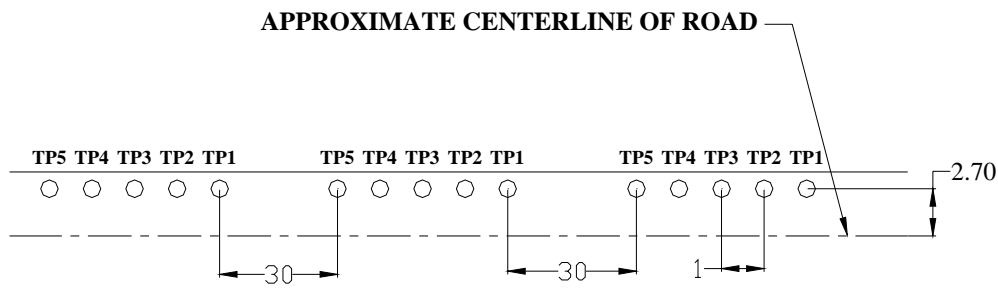
* - no data stored, seating drop only. Deflection and load data are printed but not stored.

Table 3.25 FLEX testing plan target loads used at Berlin, Vermont test sites (LTTP, 2000).

Height (mm)	Target Load kN (kips)	Acceptable Range kN (kips)
1 (50)	27 (6.0)	24.0 to 29.4 (5.4 to 6.6)
2 (100)	40 (9.0)	36.0 to 44.0 (8.1 to 9.9)
3 (200)	53 (12.0)	48.1 to 58.7 (10.8 to 13.2)
4 (390)	71 (16.0)	64.1 to 78.3 (14.4 to 17.6)

3.4.2 Subgrades and Construction Materials

The field component included tests on two subgrades, one construction sand product, two aggregates, and one reclaimed stabilized base product. At each field site, tests were performed utilizing both the Prima 100 PFWD and Nuclear Moisture Density Gauge (NDM) (AASHTO T 238). Multiple tests were performed at a minimum of 12 locations using each instrument. Test point locations for measurements in Southington, Connecticut were similar to those depicted in Figure 3.32. Test point locations for all other sites are shown in Figure 3.27. Samples were taken at each site for sieve analysis, maximum dry density, and optimum water content determination.

**NOTES:**

1. ALL DIMENSIONS SHOWN ARE IN METERS
2. NOT TO SCALE

LEGEND:

○ = PFWD & NDM TEST POINT LOCATION

Figure 3.27 Test point layout for compaction control field test sites.

With the Prima 100 PFWD, six measurements were taken at each test location. The maximum drop height of 850 mm (33.5 in.) was used throughout. Setup input parameters are shown in Table 3.23. In all cases, the first reading was neglected and the average of the remaining five was used for analysis and comparison.

For field test sites in Maine, NDM measurements were taken with a MC-1 Portaprobe manufactured by Campbell Pacific Nuclear International. The device is shown in Figure 3.28. NHDOT and Connecticut Department of Transportation provided NDM's for field sites in their respective states. Both departments provided Troxler 3430 gauges. This device is shown in Figure 3.29. Five NDM measurements were taken at depths of 203, 152, 102, 51, and 0 mm (8, 6, 4, 2, and 0 in.) at each test location. Density measurements taken at 203 mm (8 in.) depths were used for analysis and comparison.

Water content values determined from surface measurements were used for analysis and comparison.



Figure 3.28 CPN MC-1 Portaprobe NDM.



Figure 3.29 Troxler 3430 NDM.

3.5 LABORATORY TESTING PROCEDURES

3.5.1 Spring Thaw Monitoring

During instrumentation installation samples were taken for water content, Atterberg Limit, and/or gradation laboratory tests as appropriate for the soil type recovered. Laboratory tests followed procedures outlined by AASHTO.

3.5.2 Subgrades and Construction Materials

The primary purpose of the laboratory component of this project is to determine a relationship between PFWD results and percent compaction under carefully controlled conditions. Five different material types were used. Each aggregate was compacted in the container to approximately 90, 95, and 100% of the maximum dry density. The effect of water content was determined at 95% of the maximum dry density. Measurements were taken at optimum water content as well as $\pm 3\%$ of the optimum water content. Layer construction and testing procedures are discussed below.

3.5.2.1 Test Section Construction

The large-scale laboratory study to correlate PFWD results to percent compaction was constructed in the geotechnical research laboratory at the University of Maine. The tests were conducted in a 1.8 m x 1.8 m x 0.9 m (6 ft x 6 ft x 3 ft) deep test container as shown in Figure 3.30.



Figure 3.30 Laboratory test box.

The bottom 203 mm (8 in.) of material met MaineDOT Type D Aggregate specifications and was left in-place throughout the testing. This base layer was placed in two, approximately equal lifts and compacted to 100% of the maximum dry density and optimum moisture content. To differentiate between the base layer and the overlying layers which would be changed with each test, geogrid and/or geotextile were added on top of the lower layer. Material was then added in three 152 mm (6 in.) lifts. NDM readings were taken at 152 mm (6 in.) depths at two to three locations after each lift was added in order to determine whether predetermined compaction and water content requirements had been met. Each lift was compacted in the container to approximately 90, 95, and 100% of the maximum dry density (AASHTO T 180). Compaction was achieved by means of a Bosch 11304 Brute Breaker Hammer. Two different tamper

plates were used; both were Bosch HS2124 152 mm (6 in.) square tamper plates. One of the plates was modified; a 305 mm x 305 mm x 6 mm (12 in. x 12 in. x ¼ in.) steel plate was welded to the smaller tamper plate. The outfitted jackhammer with modified flat plate attachment is shown in Figure 3.31.

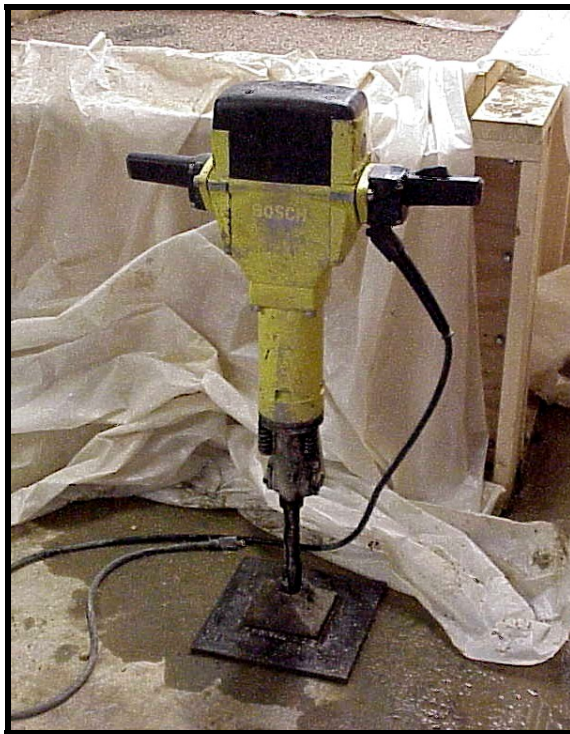


Figure 3.31 Bosch 11304 hammer with modified flat plate attachment.

3.5.2.2 Portable Device Measurements

Once construction of the test sections was completed multiple portable devices were used. Devices used for testing included Prima 100 PFWD, Clegg Impact Hammer, NDM, and Dynamic Cone Penetrometer (DCP). Measurements were taken at five locations in a pattern similar to the one shown in Figure 3.32.

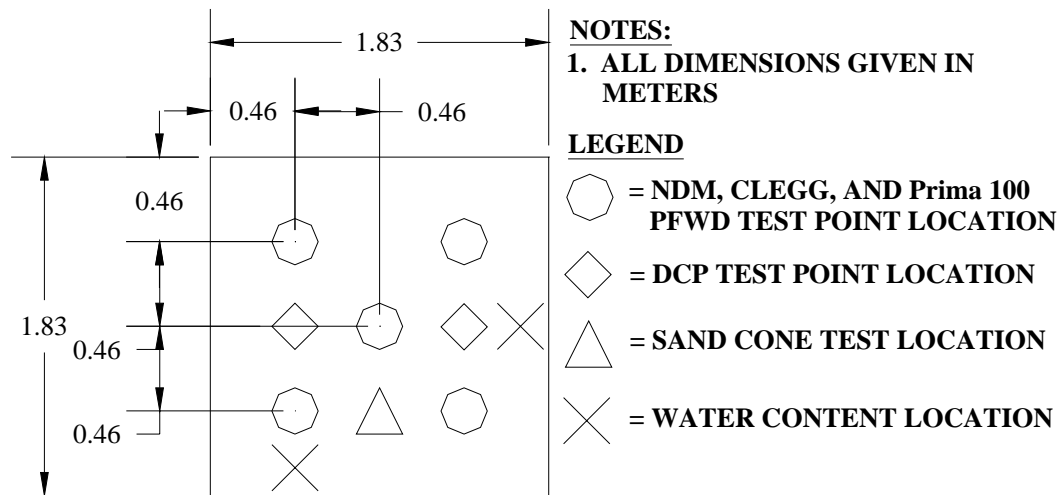


Figure 3.32 Laboratory test point layout.

Prima 100 and Clegg Impact Hammer measurements were taken following the procedures outlined in Sections 3.4.1.1.1 and 3.4.1.1.3. NDM measurements were taken following procedures outlined in Section 3.4.2.1 with a MC-1 Portaprobe NDM. Two water content samples were taken from the surface at locations indicated in Figure 3.27 and used to compare with those obtained with the NDM. One sand cone test was completed for each trial to compare with densities obtained with the NDM. Lastly, two dynamic cone penetrometer (DCP) tests were completed for each trial and followed procedures outlined by AASHTO.

3.6 SUMMARY

The performance of seven paved and three gravel surfaced roads were monitored during the spring of 2004 to evaluate the effectiveness of the Prima 100 PFWD in tracking seasonal stiffness variations. Field test sites were located in Maine, New Hampshire, and Vermont. Some sites were part of previous or ongoing NETC research projects. The remainder of the sites were chosen by the researchers with aid from MaineDOT and VAOT. Test sites were instrumented with thermocouples, thermistors, and frost tubes to monitor subsurface temperatures. Vibrating wire and standpipe piezometers as well as TDR probes were installed to monitor pore water pressure in the subbase and subgrade layers and water content. Instruments were read manually approximately weekly during the spring thaw period. Selected sites contained automated data acquisition systems which monitored hourly. Data was downloaded approximately weekly. Traditional and portable FWD's, as well as other portable devices were used at multiple locations at each test site through the spring and into early summer of 2004.

Five field sites were used for the evaluation of subgrades and construction materials. Different aggregate types were tested at each field site. Field test sites were located in Maine, New Hampshire, and Connecticut. Sites were located with the assistance of the NETC Technical Committee assigned to this project and MaineDOT. Prima 100 PFWD and NDM measurements were taken at multiple locations at each site.

Laboratory tests were performed on five different material types representative of typical New England subbase materials. Each lift was compacted in the container to approximately 90, 95, and 100% of the maximum dry density. The effect of water content was determined at 95% of the maximum dry density. Measurements were taken

at optimum water content as well as $\pm 3\%$ of the optimum water content. Each material was added to the test box in approximately equal lifts. Materials were compacted with a hand tamper and electric jackhammer until the predetermined compaction criteria had been met. Prima 100 PFWD, Clegg Impact Hammer, NDM, and DCP measurements were taken at multiple locations for each trial and material tested.

CHAPTER 4

SPRING THAW MONITORING

4.1 INTRODUCTION

This chapter presents the analysis and results of monitoring seasonal stiffness variations in paved and unpaved, seasonally posted, low volume roads. The objective of this portion of the research project was to investigate the ability of the Prima 100 Portable Falling Weight Deflectometer (PFWD) to track seasonal stiffness variations.

Comparisons were made to the traditional Falling Weight Deflectometer (FWD) as well as other portable devices. Correlations were developed to compare performance.

Recommendations are made for field testing techniques.

The performance of seven paved and three gravel surfaced roads were evaluated during the spring and early summer of 2004. Portable and traditional FWD tests were performed at multiple locations at each site beginning in early March with the last set of readings taking place in late June. Additional measurements were taken at the United States Forest Service (USFS) Parking Lot during the spring of 2003. One set of measurements was taken on Route 11, Wallagrass Plantation, Maine and Route 167, Presque Isle/Fort Fairfield, Maine during the spring of 2003. These results are presented separately.

This chapter is organized as follows. Frost penetration and pore water pressure measurements are presented first, followed by seasonal stiffness variations measured with the FWD and PFWD. Portable and traditional FWD derived moduli are compared. Comparisons are made to other portable measuring devices used at selected sites.

Finally, field testing techniques are evaluated and appropriate recommendations are presented.

4.2 FROST PENETRATION

Subsurface temperatures were measured at each field site during the end of the freezing season, throughout the thawing period, and into the recovery period. These results are presented first to provide the context for interpretation of PFWD and FWD results in subsequent sections. Temperature readings were generally taken weekly, however, at a few sites readings were taken hourly by an automatic datalogger. Details of the instrumentation installed to measure subsurface temperatures are given in Section 3.3.1.

The subsurface temperature measurements were used to determine the maximum depth of the 0°C (32°F) isotherm. This was assumed to be the maximum depth of frost penetration, ignoring factors such as the salinity of the porewater that can alter the freezing point of water. Thawing occurs both from the surface down and bottom up, although the former tends to be the dominant factor. The initiation of surface thawing was indicated by the first date that the temperature sensor closest to the surface had a reading above 0°C (32°F). The surface may undergo several cycles of thawing and refreezing during the thawing season in response to daily and diurnal temperature fluctuations. When all temperature sensors in the vertical string were above 0°C (32°F), it was assumed that the location was completely thawed. Since the temperature readings at most of the sites were taken weekly, the dates of maximum depth of frost penetration,

initiation of surface thawing, and completion of thawing could only be determined approximately.

The maximum depth of frost penetration, initiation of surface thawing, and the completion of thawing are summarized in Table 4.1 for paved sites, and Table 4.2 for gravel surfaced sites. Measurements taken at asphalt surfaced test sites indicated freezing temperatures penetrated to their maximum depths between February 17 and March 24. Maximum depths ranged from a minimum of 866 mm (34 in.) at Stinson Lake Road to a maximum of 1930 mm (76 in.) at Route 1A (Section D-2). Complete thaw occurred at all test sites between mid-March and mid-April.

Table 4.1 Summary of frost penetration measurements made on asphalt surfaced test sites.

Field Test Site	Test Section	Date of Maximum Frost Penetration	Depth of Maximum Frost Penetration mm (in.)	First Day Top Sensor Reads >0°C	Date of Complete Thaw
Kennebec Road	1	3/24/2004	1852 (73)	3/12/2004	4/17/2004
	2	3/10/2004	1372 (54)	3/12/2004	4/17/2004
Buffalo Road	1	3/11/2004	1846 (73)	3/3/2004	4/8/2004
Stinson Lake Road	1	2/28/2004	866 (34)	3/1/2004	4/19/2004
Knapp Airport Parking Lot	1	3/4/2004	1372 (54)	NA	4/16/2004
Route 126	3	3/17/2004	1214 (48)	3/26/2004	4/14/2004
	8	2/17/2004	1158 (46)	3/21/2004	4/7/2004
Witter Farm Road	Control	3/1/2004	1594 (63)	3/3/2004	4/20/2004
	2	2/20/2004	1135 (45)	3/15/2004	3/25/2004
	1	2/26/2004	1518 (60)	3/16/2004	4/16/2004
Route 1A	D-1	3/12/2004	1575 (62)	3/16/2004	3/30/2004
	D-2	3/12/2004	1930 (76)	3/12/2004	3/16/2004
	E-3	3/2/2004	1725 (68)	3/16/2004	3/23/2004

NA – not available, frost tube measurements made.

Measurements taken at gravel surfaced test sites indicated freezing temperatures penetrated to their maximum depths between March 1 and April 21. Maximum depths ranged from a minimum of 1128 mm (44 in.) at the USFS Parking Lot to a maximum of 2134 mm (84 in.) at Crosstown Road. Complete thaw had occurred at all sites between early April and mid May.

Table 4.2 Summary of frost penetration measurements made on gravel surfaced test sites.

Field Test Site	Test Section	Date of Maximum Frost Penetration	Depth of Maximum Frost Penetration mm (in.)	First Day Top Sensor Reads >0°C	Date of Complete Thaw
Lakeside Landing Road	1	4/21/2004	1803 (71)	3/12/2004	5/11/2004
	2	3/16/2004	1422 (56)	3/2/2004	4/6/2004
USFS Parking Lot	1	3/1/2004	1128 (44)	2/22/2004	4/23/2004
Crosstown Road	1	4/16/2004	2134 (84)	4/2/2004	5/14/2004

4.3 PORE WATER PRESSURE

Pore water pressures were measured in the subbase layer at each field site throughout the thawing and into the recovery period. At some sites, pore water pressures were also measured in the subgrade layer. These results, like subsurface temperatures, are provided for interpretation of the PFWD and FWD results presented in the following sections. Pore water pressure measurements were taken approximately weekly, however, at some sites readings were taken hourly by an automated data acquisition system.

Details of the instrumentation installed to measure subbase and subgrade pore water pressures are provided in Section 3.3.2.

The pore water pressure measurements were used in conjunction with the subsurface temperature readings to examine the extent to which the road had thawed and recovered. Water, located in the pore space between soil particles, freezes as heat is removed from the soil. The ice crystals grow by incorporating nearby water into the crystal as more heat is removed. Capillary action draws water from the groundwater table to the freezing front (0°C (32°F) isotherm). The ice crystals grow and merge together to form ice lenses. This process reduces the density of the soil as it expands to make room for the ice lenses, also creating frost heaves. This is illustrated in Figure 4.1. Thawing predominantly occurs from the ground surface downward. Once some surface thawing has occurred, water may be trapped above the underlying soil that is still frozen and is not able to drain. As a result, a temporary loss of bearing capacity occurs. An undrained loading condition can be created from passing traffic (Janoo and Cortez, 2002). This phenomenon is known as thaw weakening. Once the entire road section has thawed, water is able to drain and strength is regained, this is known as the recovery period.

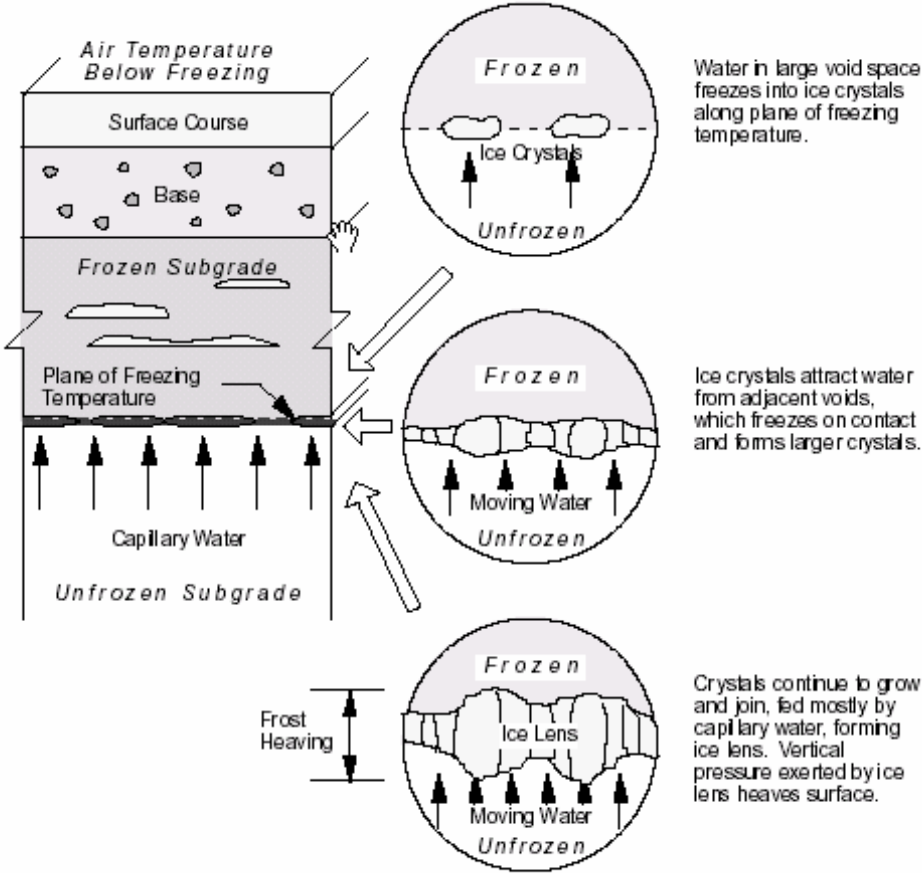


Figure 4.1 Formation of ice lenses within a pavement structure (WSDOT).

Manual standpipe piezometer readings are provided in Table 4.3. Two of four standpipe piezometers installed at Kennebec Road became inoperable in late spring. The reasons for this are that the top plug jammed on one and could not be removed, while frost action heaved the top of the other up above the road surface and it was clipped off by a snow plow. A summary of time domain reflectometry probe readings is provided in Table 4.4. Manual vibrating wire piezometer measurements are presented in Table 4.5. Figures 4.2 and 4.3 present the pore water pressure readings taken by the automated data acquisition system at Route 126, Monmouth/Litchfield, Maine.

The highest water levels observed in standpipe piezometers roughly correspond to the date of complete thaw for that particular site. This is true for both asphalt and gravel surfaced test sections. Time Domain Reflectometry (TDR) moisture sensors used at the USFS Parking Lot and Stinson Lake Road also indicate an increase in moisture content at or near the date of complete thaw.

Table 4.3 Summary of standpipe piezometer measurements.

Date	Kennebec Road				Lakeside Landing Road				Witter Farm Road			Route 1A			
	P1	P2	P3	P4	P1	P2	P3	P4	P1	P2	P3	P1	P2	P3	
3/2	0.9N	0.9N	0.4F	0.4F	0.9N	0.9N	1.0N	1.0N	1.9	2.2	2.1	0.2	3.2	1.3	
3/10	0.9F	0.9N	0.4F	0.4F	0.9N	0.9N	1.0N	1.0N	0.5	0.7	1.5	NA	NA	NA	
3/12	0.9F	0.9N	0.4F	0.4F	0.9N	0.9N	1.0N	0.9N	0.4	0.6	1.3	0.2	2.7	1.0	
3/16	NA	NA	NA	NA	0.9N	0.9N	0.6	0.8	0.5	0.6	0.9	0.2	2.6	0.8	
3/19	0.9F	0.9N	0.4F	0.4F	NA	NA	NA	NA	0.5	0.6	1.1	0.2	2.5	1.0	
3/23	NA	NA	Inoperable	NA	NA	NA	0.6	0.6	0.4	0.5	1.0	0.2	2.5	0.9	
3/24	NA	NA		0.4	NA	NA	NA	NA	NA	NA	NA	NA	NA	NA	NA
3/30	NA	NA		NA	0.4	0.4	0.4	0.3	0.4	0.5	0.6	0.2	2.1	0.8	
3/31	0.4	0.4		0.2	NA	NA	NA	NA	NA	NA	NA	NA	NA	NA	NA
4/6	NA	NA		NA	0.4	0.3	0.3	0.4	0.4	0.5	0.5	0.3	2.0	0.8	
4/7	0.4	0.4		0.1	NA	NA	NA	NA	NA	NA	NA	NA	NA	NA	NA
4/17	Inoperable	0.9		0.2	NA	NA	NA	NA	NA	NA	NA	NA	1.0	1.8	0.9
4/18		NA		NA	0.1	0.1	0.3	0.4	NA	NA	NA	NA	NA	NA	NA
4/21		NA		NA	NA	0.1	0.2	0.3	0.4	0.5	0.5	0.6	0.7	1.7	1.0
4/22		N		NA	0.2	NA	NA	NA	NA	NA	NA	NA	NA	NA	NA
4/27		NA	NA	NA	0.1	0.1	NA	0.5	0.5	0.5	0.6	0.7	1.8	1.2	
4/28		N	NA	0.4	NA	NA	NA	NA	NA	NA	NA	NA	NA	NA	NA
5/11		NA	NA	NA	0.9	0.9	NA	NA	0.7	0.6	0.5	NA	NA	NA	NA

*** Values indicate depth (m) to water in piezometer measured from the ground surface.

N = no water, F = frozen, NA = not available

Table 4.4 Summary of time domain reflectometry probe water content readings.

Date	USFS Parking Lot		Stinson Lake Road			
	TDR 1 (%)	TDR 2 (%)	TDR 1 (%)	TDR 4 (%)	TDR 5 (%)	TDR 6 (%)
3/3	4.0	7.8	9.5	12.7	20.7	29.8
3/11	6.0	8.8	11.7	23.7	19.6	24.2
3/18	12.9	8.5	13.5	25.1	18.6	20.2
3/25	12.8	8.2	14.8	25.8	16.8	19.4
4/1	24.6	28.6	17.1	NA	NA	NA
4/8	19.6	15.8	27.7	33.5	30.3	27.4
4/15	20.8	13.6	34.6	33.7	30.3	26.9
4/29	13.3	12.4	34.8	33.0	29.5	20.9
5/13	10.5	11.6	NA	NA	NA	NA
6/9	11.2	10.2	32.3	24.4	30.9	16.6

NA – not available.

The relationship between manual vibrating wire piezometer measurements and the date of complete thaw is less clear. Manual readings do not show a trend. Manual readings represent the conditions at the time the measurements were taken whereas automated readings were taken hourly and averaged over a 24 hour period. Trends exhibited by automated vibrating wire piezometer measurements roughly correspond with partially and completely thawed states. Pore water pressure measurements during the frozen state provide no meaningful information. Converting maximum subbase and subgrade pore water pressure measurements into feet of head indicates that these readings are unreasonable as the water surface lies above the finished road surface. Prior to the onset of thaw, pressure reduces to roughly 2 kPa (0.67 ft of water) in Section 3 and 1 kPa (0.33 ft of water) in Section 8. Subbase pore water pressure remains relatively constant through the end of the monitoring period. Subgrade pore water pressure in both sections begins to increase just prior to the beginning of thaw and continue to increase to a maximum value of nearly 20 kPa (6.6 ft of water) at the end of the monitoring period.

Table 4.5 Summary of manual vibrating wire piezometer measurements.

Pore Water Pressure (kPa)*							
Date	Route 1A				Date	Route 126	
	Section D-1 (STA 258+50)		Section D-2 (STA 267+25)			Section 12 (STA 4+712)	
	subbase	subgrade	subbase	subbase		subbase	subgrade
3/2	5.88	6.17	-1.86	1.78	3/27	-0.02	0.41
3/12	4.65	5.73	3.99	1.80	3/31	-0.15	0.46
3/16	4.77	5.54	2.45	1.20	4/16	-0.07	0.51
3/19	4.97	7.22	1.46	0.67	4/28	-0.02	1.19
3/23	4.71	7.97	1.65	0.87	5/12	0.14	1.04
3/30	4.28	6.05	2.28	0.71			
4/6	4.76	3.92	2.72	0.85			
4/17	4.66	3.79	1.81	1.46			
4/21	4.55	1.65	0.00	1.52			
4/27	4.39	4.34	1.63	1.27			

* - 1 kPa \approx 0.33 ft of water.

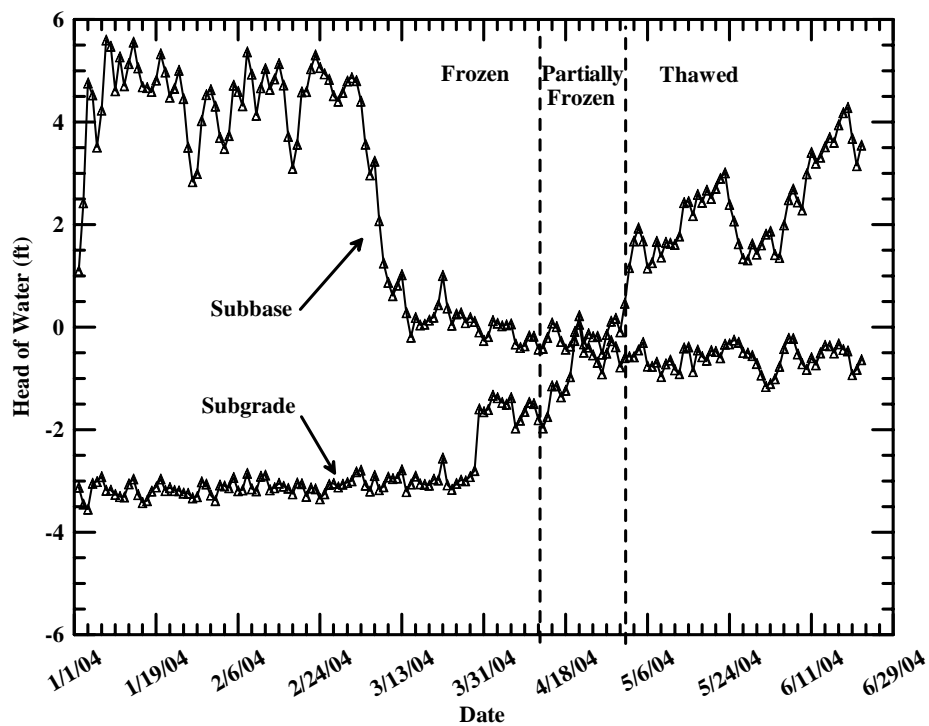


Figure 4.2 Route 126 (Section 3), Monmouth/Litchfield, Maine automated pore water pressure measurements.

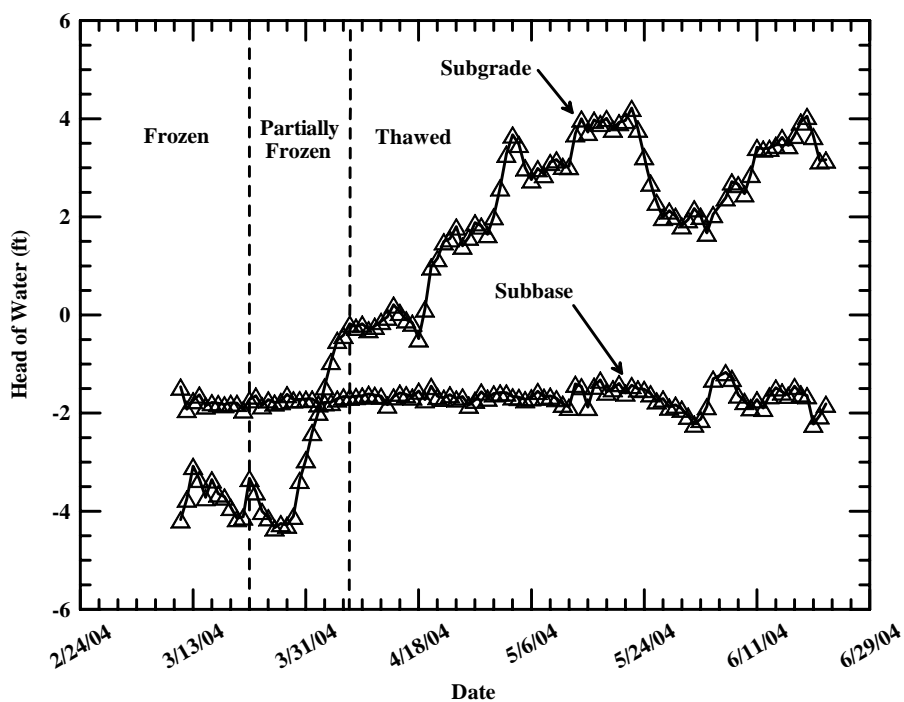


Figure 4.3 Route 126 (Section 8), Monmouth/Litchfield, Maine automated pore water pressure measurements.

4.4 SEASONAL STIFFNESS VARIATIONS

The seasonal variation in modulus as measured by the conventional and portable FWDs are presented and assessed in this section. Details regarding backcalculation analysis of FWD data are presented first, followed by the presentation and discussion of results for asphalt surfaced roads. Lastly, the results derived from testing on gravel surfaced roads are presented.

4.4.1 Backcalculation of Layer Moduli

Backcalculation is the process by which pavement layer moduli are determined by matching measured and calculated surface deflection basins (FHWA, 1999).

Backcalculation of pavement layer moduli was performed for FWD test results and used as the basis for comparison for the PFWD. MaineDOT provided FWD backcalculation analysis for Maine test sites using DARWin. In addition, backcalculation was performed on FWD data from all test sites using Evercalc. Details are discussed below.

4.4.1.1 Mid-Depth Asphalt Temperature Determination

Deflection measurements taken on all pavements are dependent on seasonal variations that affect the underlying aggregate and subgrade. The results from asphalt pavements are also dependent on the temperature of the asphalt. In order to meaningfully analyze the deflection results, the deflections or deflection analysis results, must be adjusted to account for the seasonal and temperature effects (FHWA, 2000).

The BELLS temperature prediction model was developed after work done by Southgate (1959). Subsequently, several modifications were made to the BELLS model

that resulted in an improved model called BELLS2. The Seasonal Monitoring Program (SMP) of the Long Term Pavement Performance (LTTP) program developed the most comprehensive temperature and deflection data set ever to be assembled. The data was used to develop a model that can be used to predict the temperature within an asphalt layer from surface temperature data collected during routine deflection testing (FHWA, 2000). This model is the BELLS3 model and was used for this research project. Mid-depth asphalt temperatures can be determined from Equation 4.1.

$$T_d = 0.95 + 0.892(IR) + (\log(d) - 1.25) \cdot [(-0.448(IR) + 0.621(1 - \text{day}) + 1.83 \sin(hr_{18} - 15.5))] + 0.042(IR) \sin(hr_{18} - 13.5) \quad \text{Eqn. 4.1}$$

where: T_d = Pavement temperature at depth d , °C
 IR = Infrared surface temperature, °C
 \log = base 10 logarithm
 d = depth at which mat temperature is to be predicted, mm
 1-day = Average air temperature the day before testing
 \sin = Sine function on an 18-hr clock system, with 2π radians equal to one 18-hr cycle
 hr_{18} = Time of day, in 24-hr clock system, but calculated using an 18-hr asphalt concrete (AC) temperature rise-and fall-time

Mid-depth asphalt temperatures were determined and input into the Evercalc program. Evercalc then adjusts all the deflection measurements to a standard temperature of 25°C (77°F).

4.4.1.2 DARWin

AASHTOWare DARWin v. 3.1.002 software was used by the MaineDOT to backcalculate composite and subgrade moduli. This program is based on AASHTO deflection analysis procedures. DARWin does not provide individual layer moduli, only a composite modulus for asphalt and subbase layers and a modulus for the subgrade

layer. This was beneficial because the Prima 100 PFWD also provides composite moduli, which allowed for a direct comparison. However, it was necessary to select another program for backcalculation analysis to differentiate between moduli associated with asphalt, subbase, and subgrade structural layers.

4.4.1.3 Evercalc

Evercalc 5.0, developed by the Washington State Department of Transportation (WSDOT) was used for backcalculating FWD data to obtain individual layer moduli. Evercalc is a pavement analysis computer program that estimates the “elastic” moduli of pavement layers. Evercalc estimates the elastic modulus for each pavement layer, determines the coefficients of stress sensitivity for unstabilized materials, stresses and strains at various depths, and optionally normalizes asphalt concrete modulus to a standard laboratory condition (temperature). Evercalc uses an iterative approach in changing the moduli in a layered elastic solution to match theoretical and measured deflections (WSDOT, 1999).

The Evercalc program uses WESLEA (provided by the Waterways Experiment Station, U.S. Army Corps of Engineers) as the layered elastic solution to compute the theoretical deflections and a modified Augmented Gauss-Newton algorithm for optimizations. Basic assumptions of layered elastic theory include the following:

- Layers are infinitely long in the horizontal directions
- Layers have uniform thickness
- Bottom layer is semi infinite in the vertical direction
- Layers are composed of homogeneous, isotropic, linearly elastic materials, characterized by elastic modulus and Poisson’s ratio.

To begin the backcalculation process a general file must be created. The general file allows for basic input parameters including but not limited to the following: loading plate radius, number of sensors, sensor spacing, number of layers, and Poisson's ratio. Additional input parameters are shown in Figure 4.4. Locations are selected or deselected for analysis and layer thicknesses are input. Options pertaining to the treatment of multiple drops at several different load levels are available. This is shown in Figure 4.5. Once the raw data file has been converted, a deflection data file is created. This is shown in Figure 4.6. The deflection data may be modified if the measurements do not follow a descending pattern moving radially outward from the center sensor.

The screenshot shows the 'General Data Entry' dialog box for Evercalc 5.0. The window title is 'General Data Entry - C:\ENGINE~1\EVERSERS\EVERCALC\555.GEN'. The form includes the following fields and options:

- Title:** [Text Field]
- No of Layers:** [Text Field]
- No of Sensors:** [Text Field]
- Plate Radius (cm):** [Text Field]
- Units:** Metric, US Units
- Temp. Measurement:** Direct Method, Southgate Method
- Seed Moduli:** Internal, User Supplied
- Stiff Layer:**
- Temp. Correction:**
- Sensor Weigh Factor:** Uniform, Inverse First Sensor, User Supplied
- Sensor No:** 1, 2, 3, 4, 5, 6, 7, 8, 9, 10
- Radial Offset (cm):** [Text Fields for each sensor number]
- Layer Information Table:**

No	Layer ID	Poisson' Ratio	Initial Modulus (MPa)	Min. Modulus (MPa)	Max. Modulus(MPa)
1	0	0.00	0.0	0.0	0.0
- Max. Iteration:** [Text Field]
- RMS Tol. (%):** [Text Field]
- Modulus Tol. (%):** [Text Field]
- Buttons:** Stress and Strain Location..., Save, Save As, Cancel

Figure 4.4 Evercalc 5.0 general file data entry screen (WSDOT, 2001).

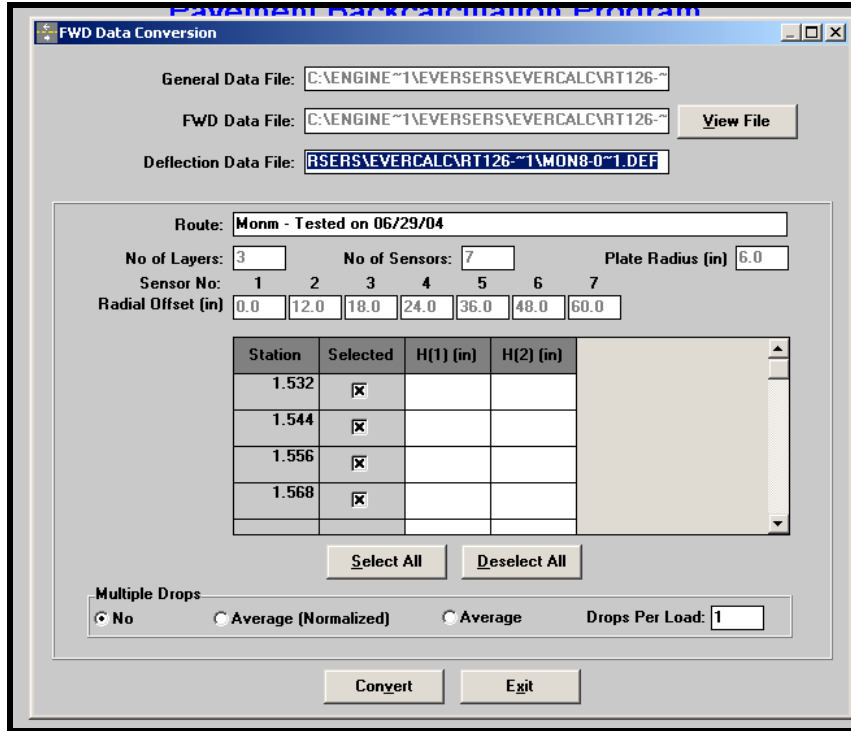


Figure 4.5 Evercalc 5.0 raw FWD data conversion screen (WSDOT, 2001).

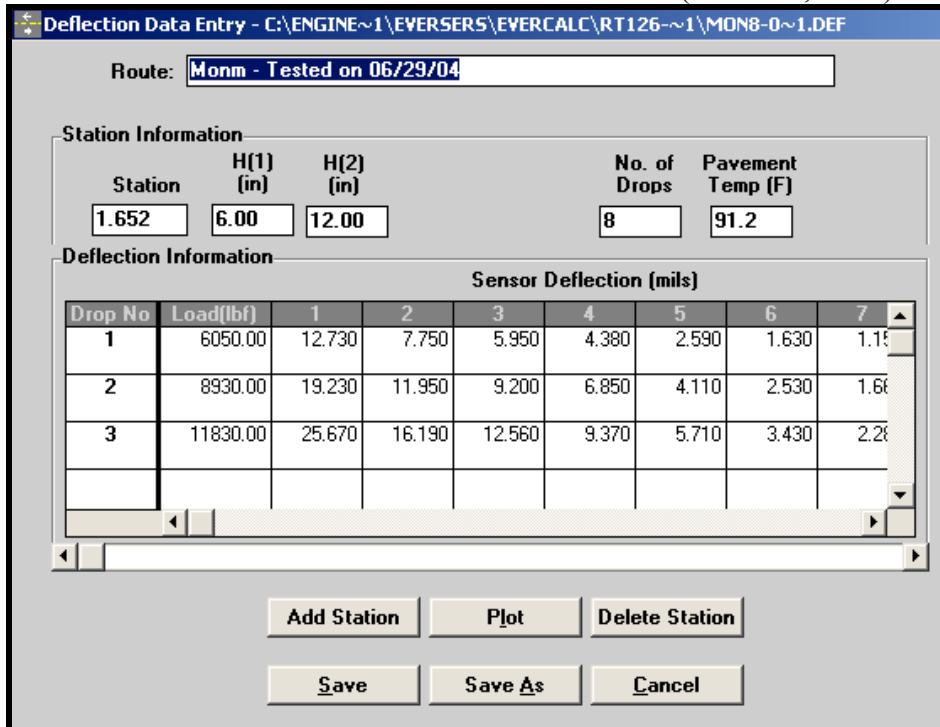


Figure 4.6 Evercalc 5.0 FWD deflection data file screen (WSDOT, 2001).

4.4.2 Asphalt Surfaced Roads

Asphalt surfaced roads used for tracking seasonal stiffness variations include: Kennebec Road, Buffalo Road, Stinson Lake Road, Knapp Airport Parking Lot, Witter Farm Road, Route 126, and Route 1A. Backcalculation procedures are described in the previous sections.

Prima 100 PFWD composite modulus, and for sites where it is available, FWD asphalt, subbase, subgrade, and composite modulus and Loadman PFWD composite modulus values are plotted versus date in Figures 4.7 through 4.20. In general, the moduli are high when the pavement section is frozen and during the early part of the period when section is partially thawed. At some field sites there are significant differences in moduli from nearby test locations and from one week to the next. This behavior was especially evident at Kennebec Road (Figures 4.7 and 4.8), Witter Farm Road (Figures 4.12 through 4.14), and Route 126 (Figure 4.15).

As air temperatures fluctuate, the rate at which heat is added and/or removed from the roadway changes. As a result, thawing and re-freezing may occur causing the modulus to also change. This behavior was noticeable at Kennebec Road (Figure 4.3 and 4.4), Witter Farm Road (Figure 4.8 through 4.10), and Route 1A (Figure 4.14 through 4.16). At these sites partial thawing occurred at or near March 16, 2004 before the return of freezing temperatures. A distinct increase in modulus occurred at each site on approximately March 24, 2004. All three sites are located within a 32 km (20 mi) radius of Bangor, Maine.

The composite moduli generally decreased as thawing progressed. It was anticipated that a distinct minimum modulus would be reached near the end of the

thawing period followed by increasing modulus due to drainage of excess water in the subbase and subgrade soils. This behavior was observed at the Buffalo Road (Figure 4.9), Knapp Airport Parking Lot (Figure 4.11), and to a lesser extent, the Stinson Lake Road (Figure 4.10) test sites. All three sites reached distinct minimum values at or near the end of March. At the remaining sites, the composite modulus at the end of the thawing period was approximately equal to, or in some cases greater than, the value measured in late June or early July. To better illustrate this behavior, the average PFWD and FWD composite moduli at the end of the thawing period and in mid to late June are summarized in Table 4.6.

Table 4.6 Summary of PFWD and FWD composite moduli at the end of thawing and during recovery periods.

Field Test Site	Test Section	Modulus on Date of Complete Thaw			Modulus in mid to late June		
		Date of Complete Thaw	Average Prima 100 PFWD Composite Modulus (MPa)	Average FWD Composite Modulus (MPa)	Date of Final Reading	Average Prima 100 PFWD Composite Modulus (MPa)	Average FWD Composite Modulus (MPa)
Witter Farm Road	Control	4/20	524	446	6/28	434	476
	2	3/25	999	751		291	252
	1	4/16	466	347		348	351
Route 126	3	4/14	427	533	6/29	280	468
	8	4/7	362	410		263	446
Route 1A	D-1	3/30	636	506	6/28	469	586
	D-2	3/16	438	413		308	403
	E-3	3/23	457	474		319	551
Stinson Lake Road	1	4/19	279	NA	6/9	179	NA

NA – no composite modulus for spring thaw field test sites outside of Maine.

Backcalculated layer moduli are used as the basis for FWD comparison. FWD derived moduli indicate that Kennebec Road, Buffalo Road, and Knapp Airport Parking Lot exhibited some degree of thaw weakening and recovery. Moduli derived from Prima 100 FWD measurements also follow similar trends. Prima 100 FWD moduli also followed similar trends to FWD moduli at test sites where no thaw weakening occurred. Three of these test sites: Witter Farm Road, Route 126, and Route 1A were all fully reconstructed within the last ten years. Each test site was constructed with non frost susceptible materials and as a result, none experienced thaw weakening as shown in plots corresponding to those test sites. Based on these observations, the Prima 100 FWD can be used as a tool to aid in determining both when to apply and remove load restrictions.

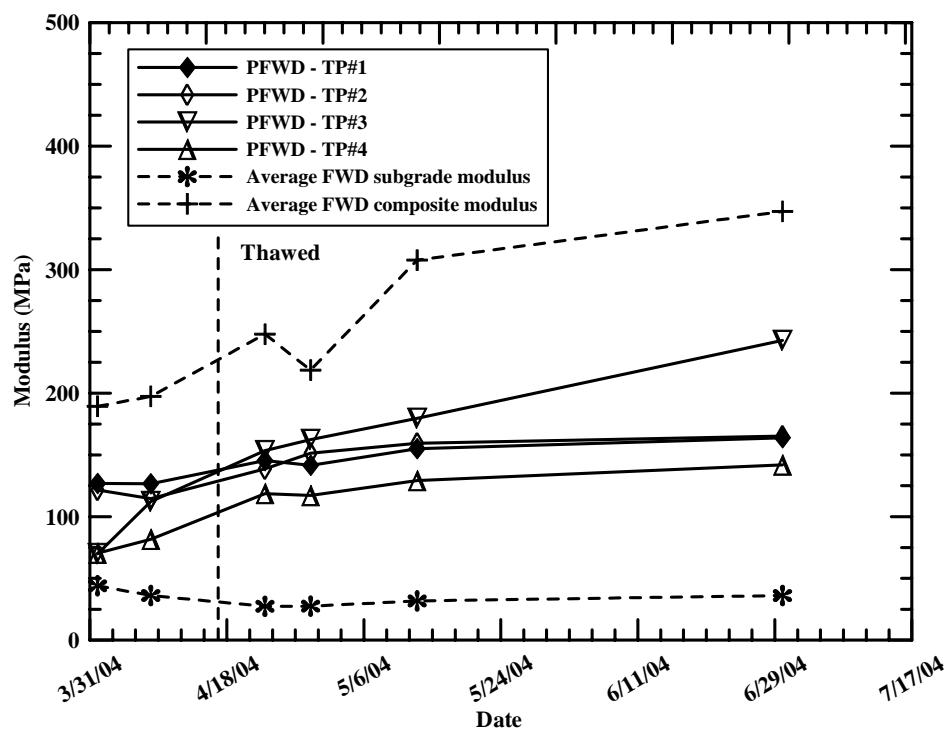


Figure 4.7 Stiffness variation at Kennebec Road (Section 1), Hampden/Dixmont, Maine.

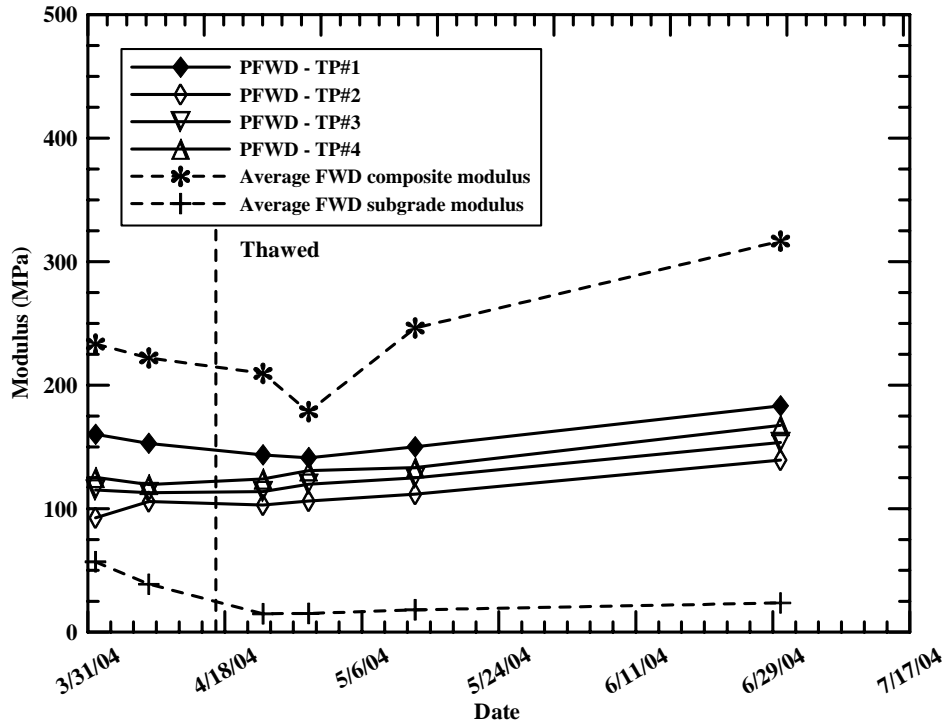


Figure 4.8 Stiffness variation at Kennebec Road (Section 2), Hampden/Dixmont, Maine.

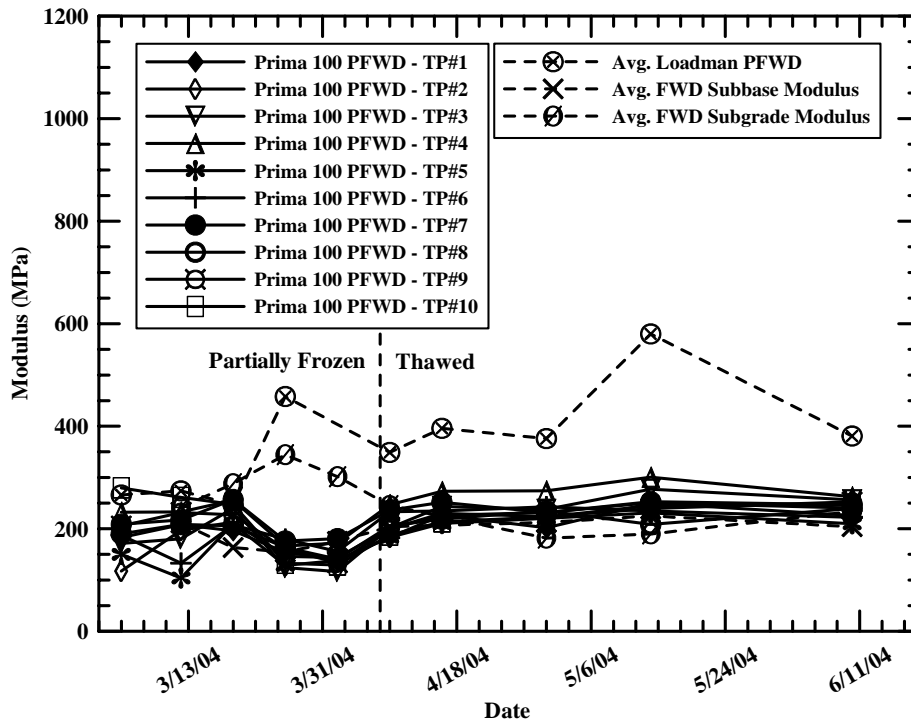


Figure 4.9 Stiffness variation at Buffalo Road, Rumney, New Hampshire.

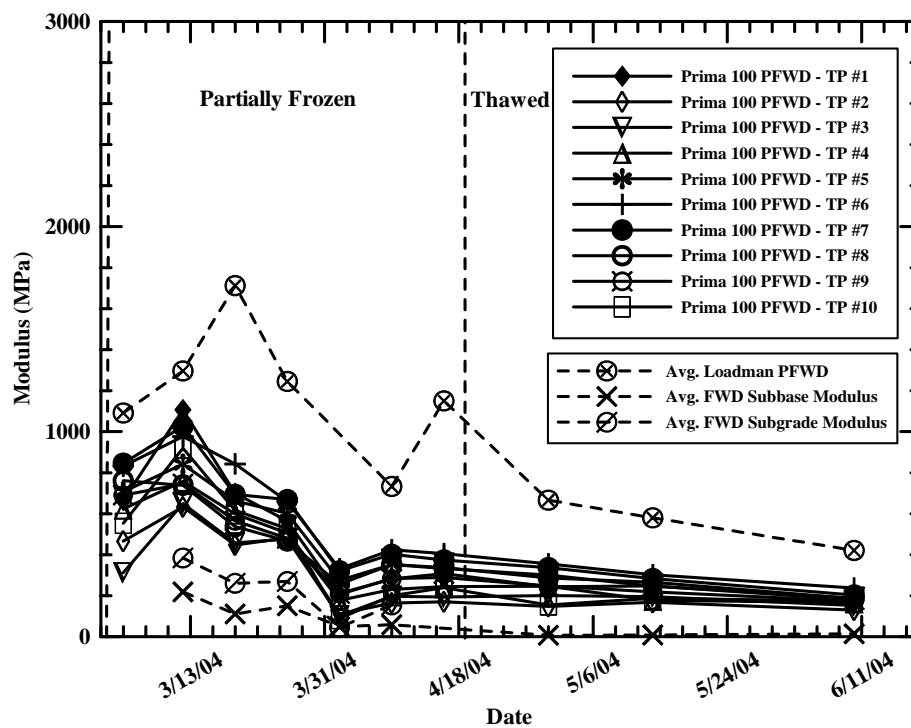


Figure 4.10 Stiffness variation at Stinson Lake Road, Rumney, New Hampshire.

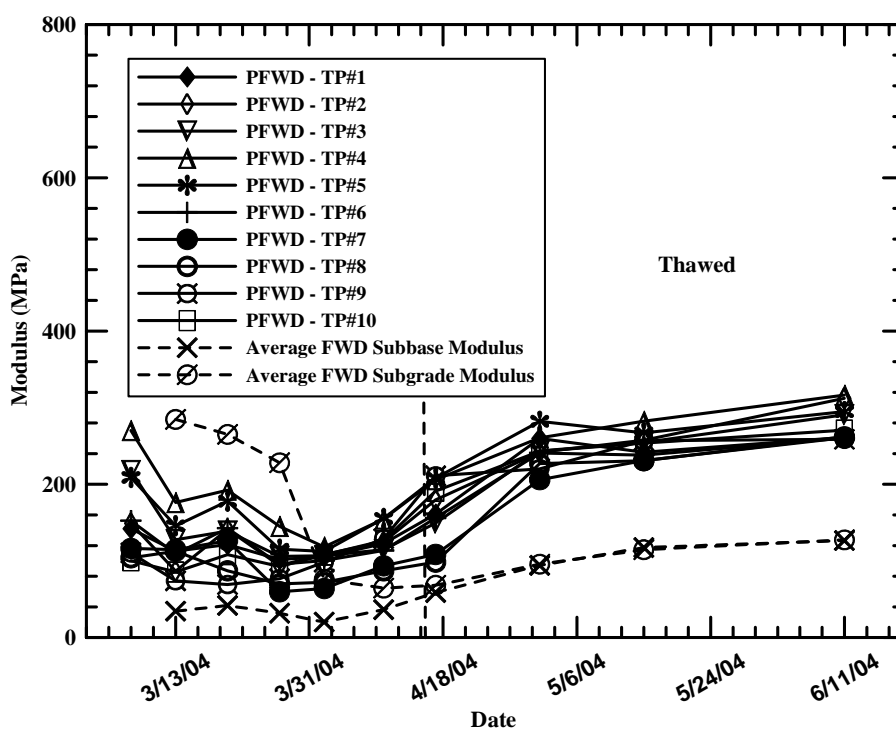


Figure 4.11 Stiffness variation at Knapp Airport Parking Lot, Berlin, Vermont.

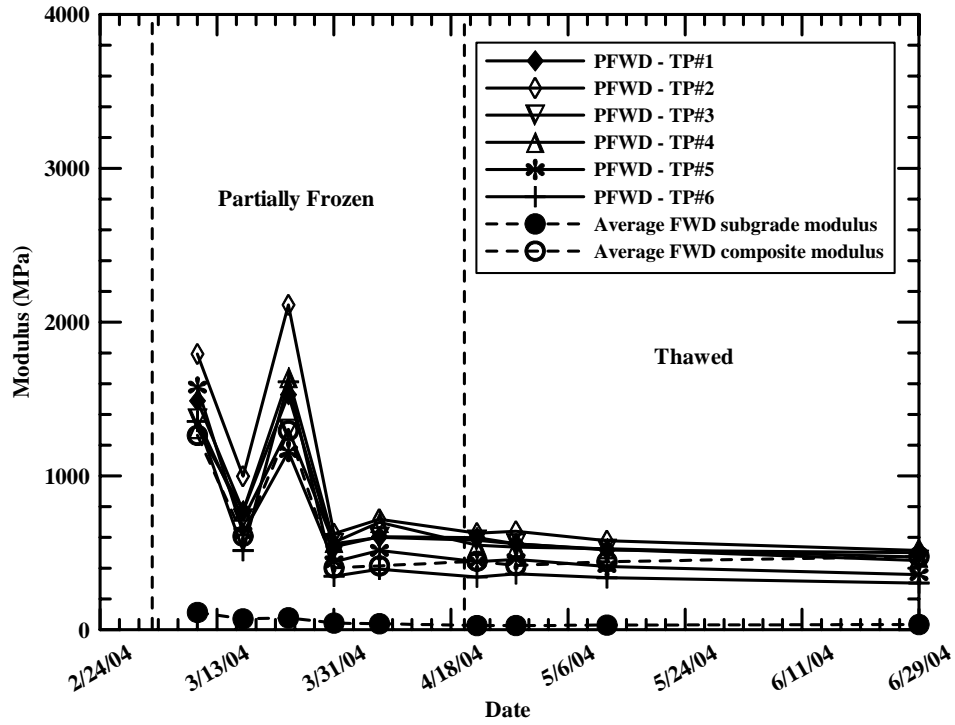


Figure 4.12 Stiffness variation at Witter Farm Road (Control Section), Orono, Maine.

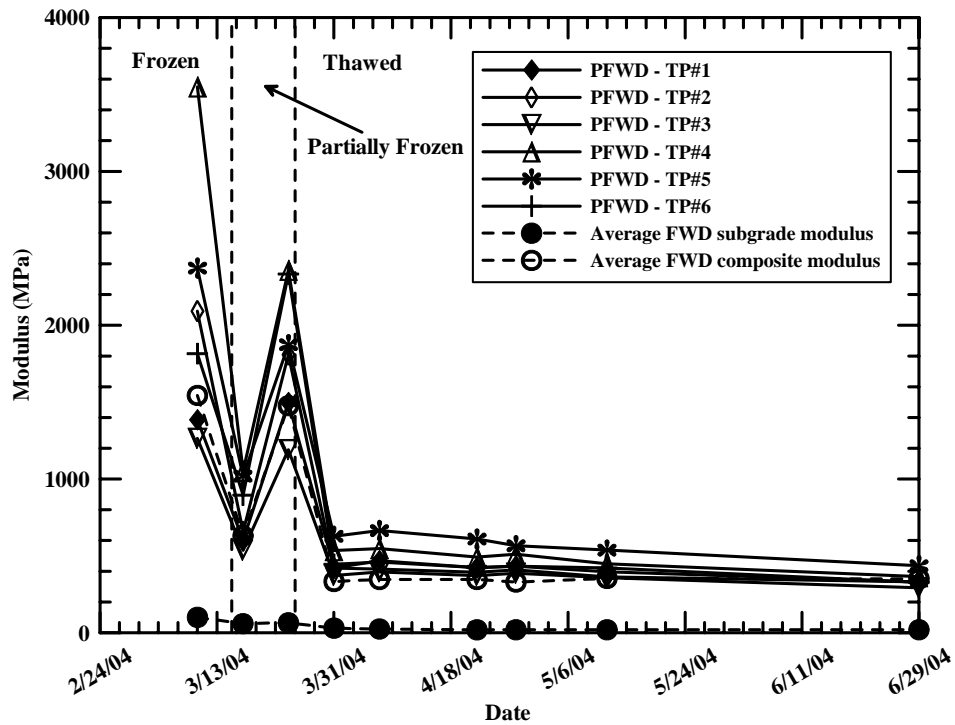


Figure 4.13 Stiffness variation at Witter Farm Road (Section 2), Orono, Maine.

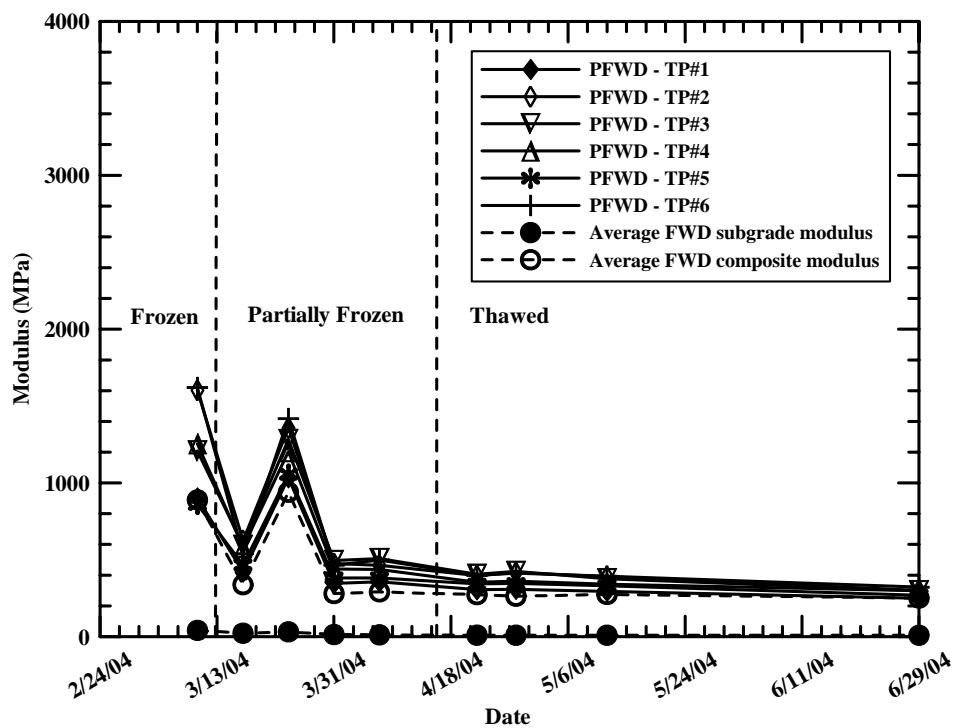


Figure 4.14 Stiffness variation at Witter Farm Road (Section 1), Orono, Maine.

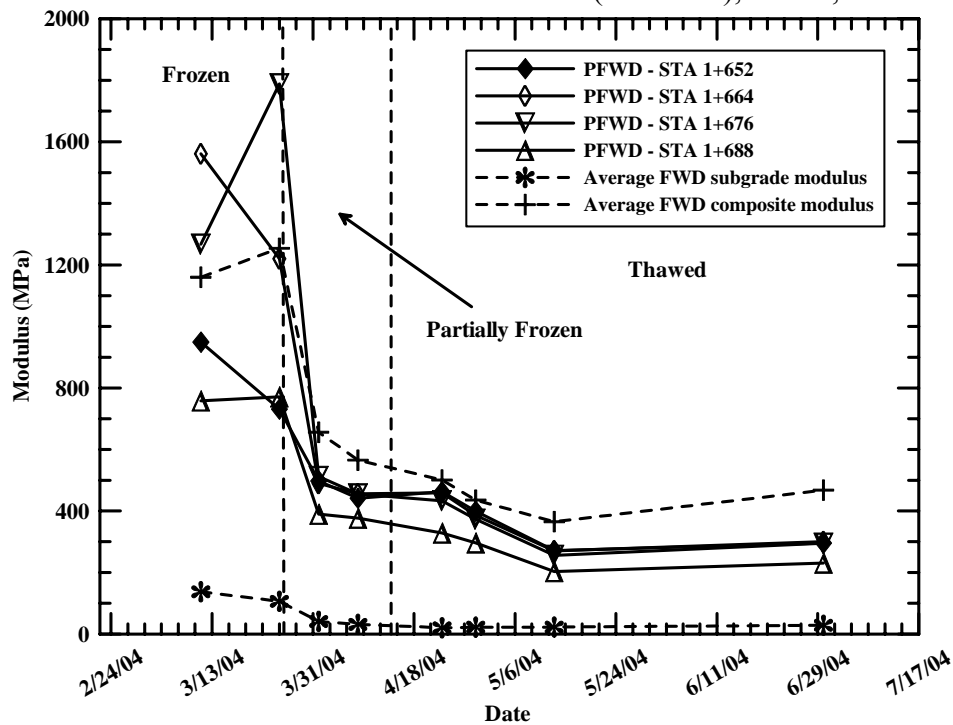


Figure 4.15 Stiffness variation at Route 126 (Section 3), Monmouth/Litchfield, Maine.

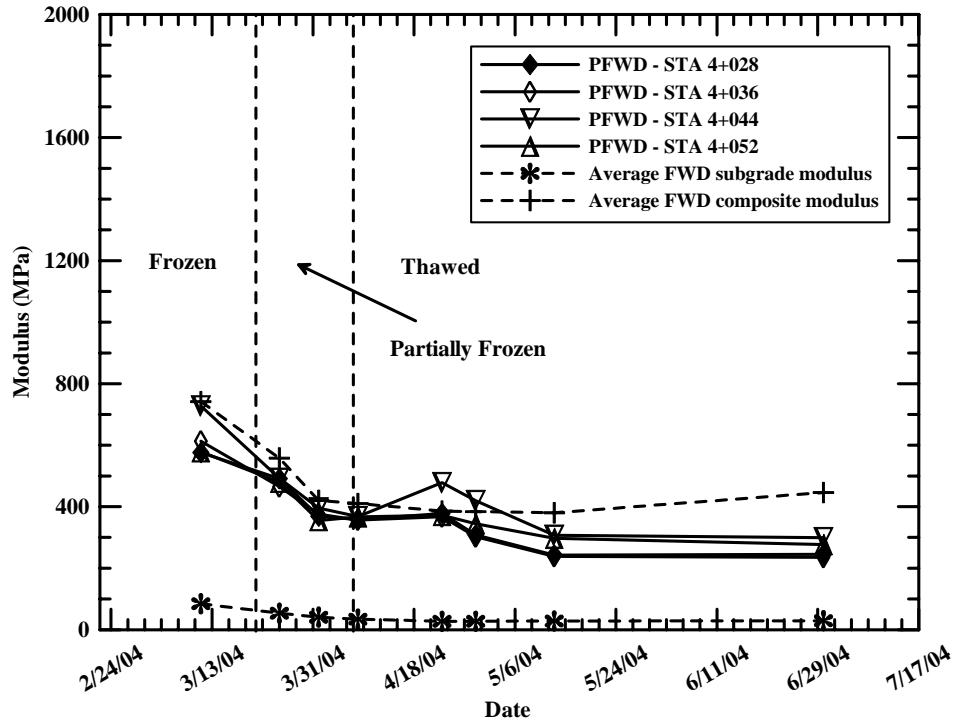


Figure 4.16 Stiffness variation at Route 126 (Section 8), Monmouth/Litchfield, Maine.

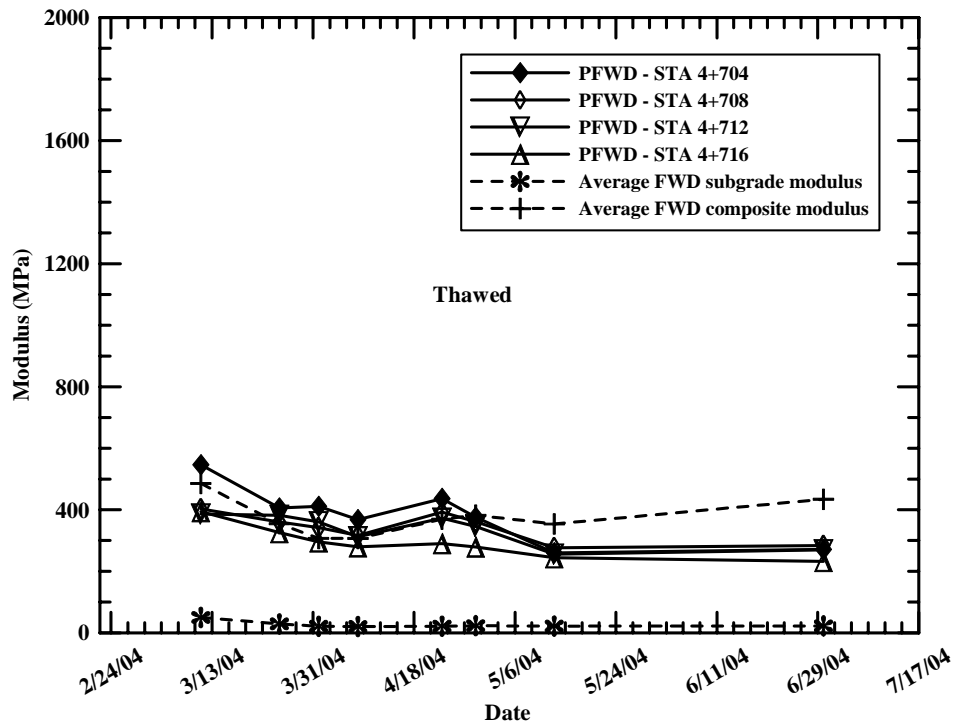


Figure 4.17 Stiffness variation at Route 126 (Section 12), Monmouth/Litchfield, Maine.

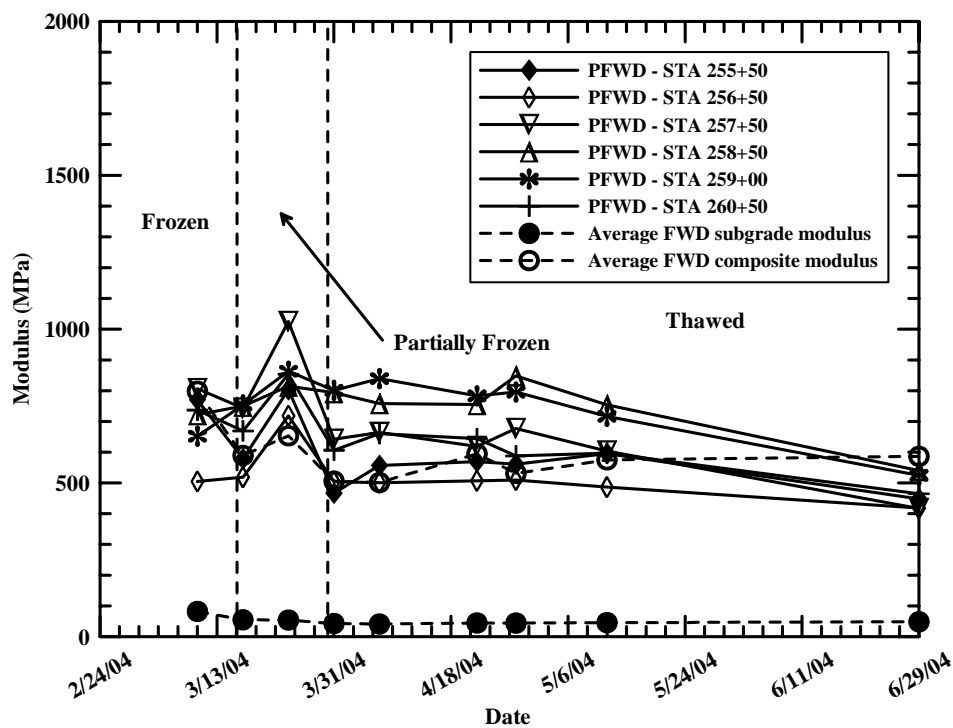


Figure 4.18 Stiffness variation at Route 1A (Section D-1), Frankfort/Winterport, Maine.

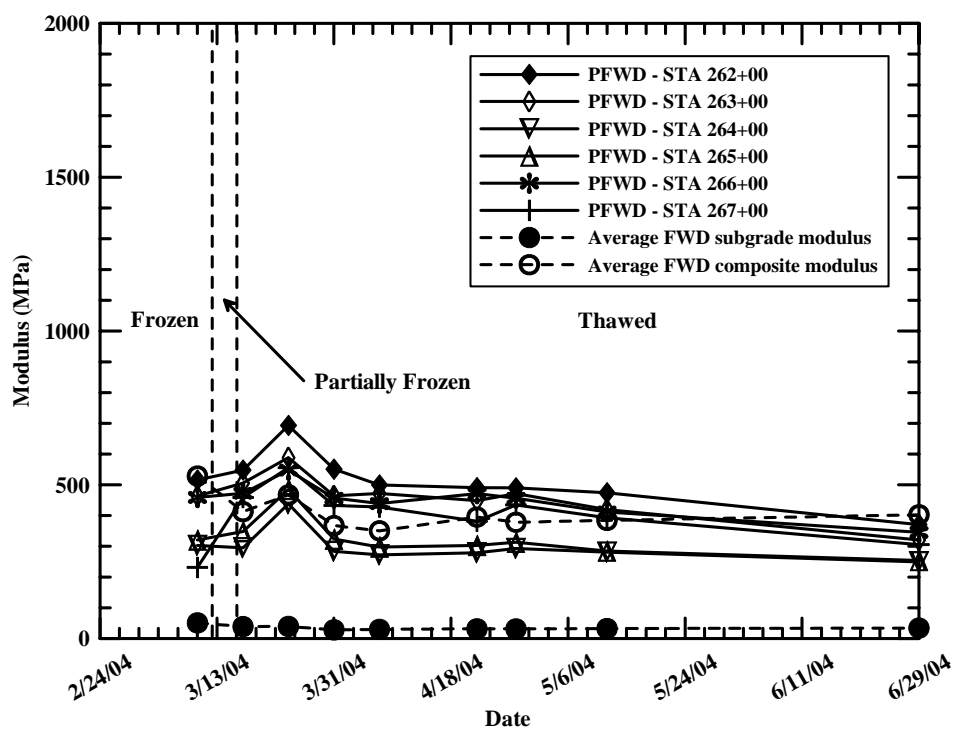


Figure 4.19 Stiffness variation at Route 1A (Section D-2), Frankfort/Winterport, Maine.

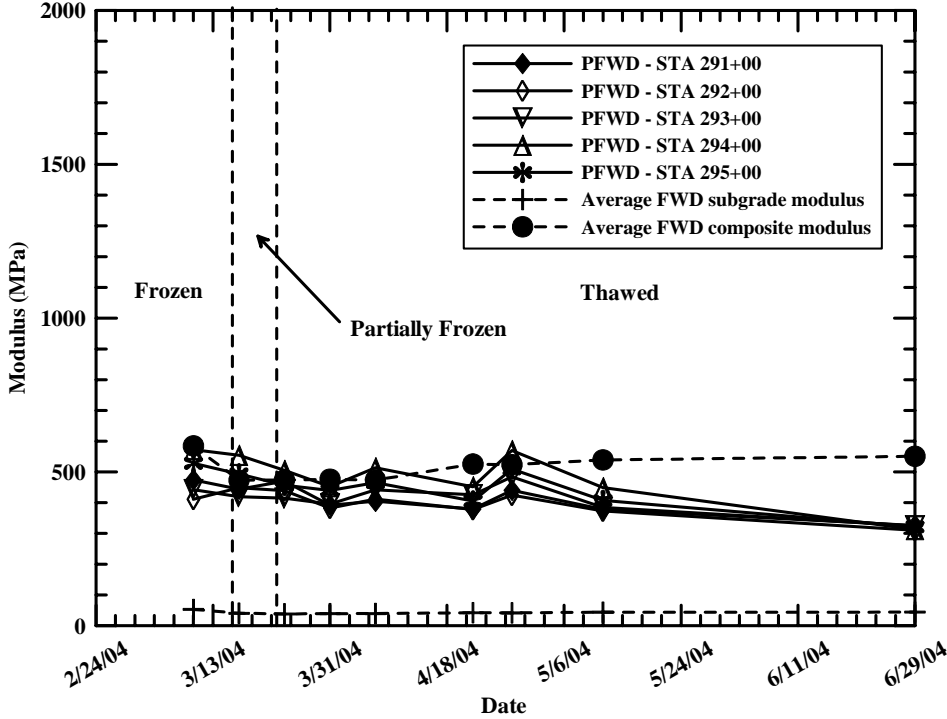


Figure 4.20 Stiffness variation at Route 1A (Section D-3), Frankfort/Winterport, Maine.

4.4.3 Gravel Surfaced Roads

Gravel surfaced roads tested for seasonal stiffness variations include Lakeside Landing Road (Glenburn, Maine), Crosstown Road (Berlin, Vermont), and the USFS Parking Lot (Rumney, New Hampshire). Additional portable device measurements were taken at the USFS Parking Lot during the spring of 2003, these results are also presented.

Prima 100 PFWD composite modulus, and for sites where it is available, FWD composite, subbase, and subgrade moduli are plotted versus date in Figures 4.17 through 4.23. In general, the moduli are high when the section is frozen and during the early part of the period when section is partially thawed. At some field sites there are significant differences in moduli from nearby test locations and from one week to the next. This is more apparent in gravel surfaced test sites compared to asphalt surfaced test sites.

The composite moduli generally decreased as thawing progressed. It was anticipated that a distinct minimum modulus would be reached near the end of the thawing period followed by increasing modulus due to drainage of excess water in the base and subgrade soils. This behavior was more apparent in the gravel surfaced test sites where environmental factors and material uniformity have an increased effect on measured moduli. The composite modulus measured in late June was approximately equal to, or in most cases greater than, the value measured during the thaw period. Measurements taken at the USFS Parking Lot in the spring of 2003 do not show the same trends. The first set of measurements was taken at the end of April after the thawing period had occurred. Thus, Figure 4.25 only illustrates a small portion of the recovery period. Similar to asphalt surfaced test sites, gravel surfaced sites also showed the effects of re-freezing. This was noticeable at the Lakeside Landing Road, USFS Parking Lot (2004), and Crosstown Road test sites.

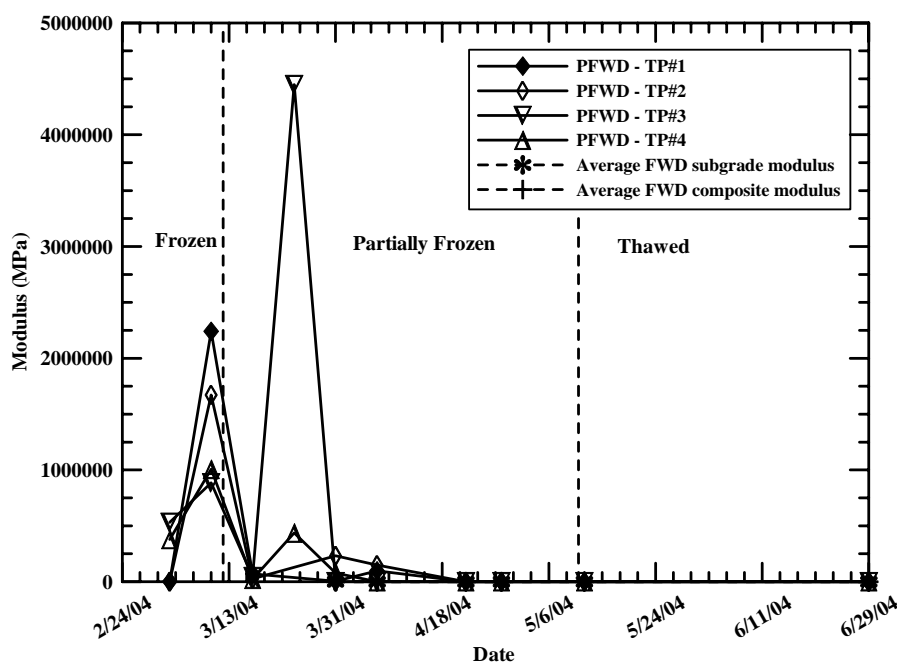


Figure 4.21 Stiffness variation at Lakeside Landing Road (Section 1), Glenburn, Maine.

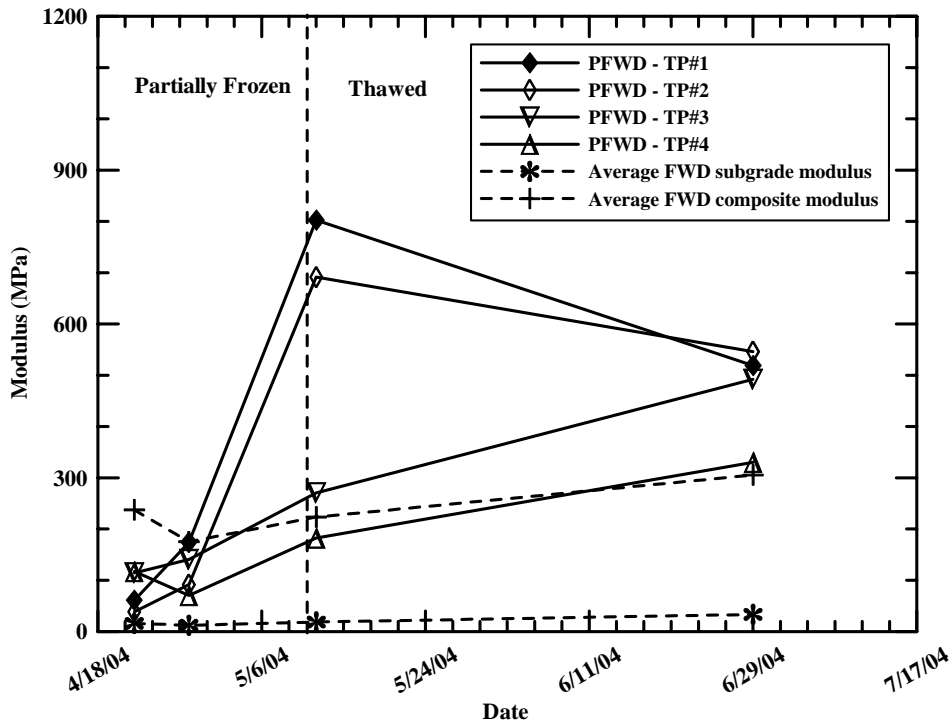


Figure 4.22 Detailed stiffness variation at Lakeside Landing Road (Section 1), Glenburn, Maine.

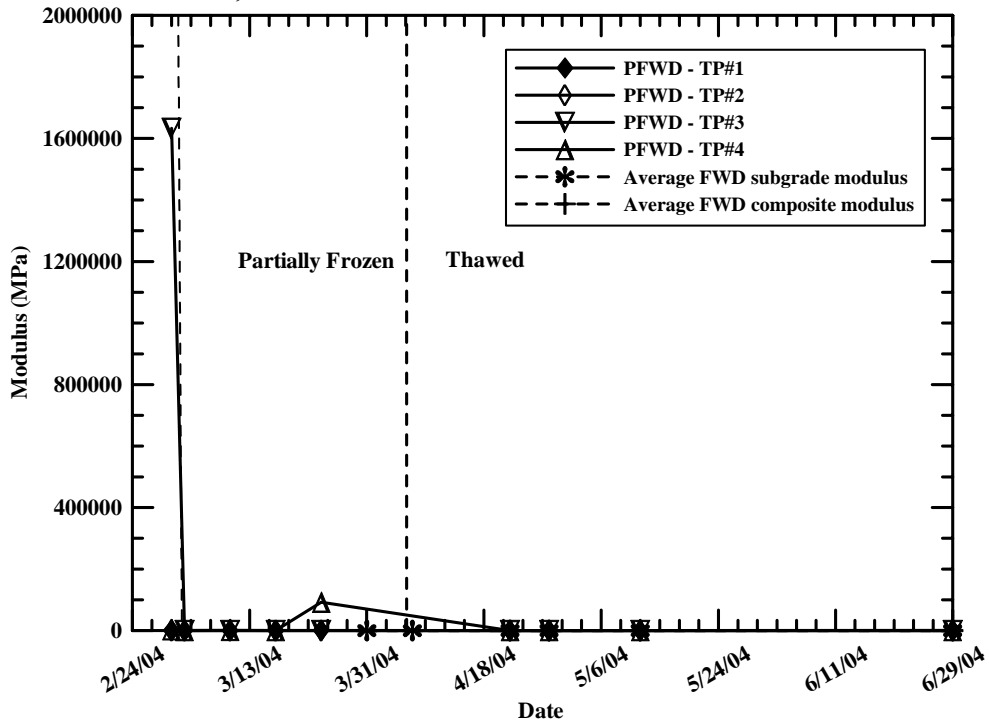


Figure 4.23 Stiffness variation at Lakeside Landing Road (Section 2), Glenburn, Maine.

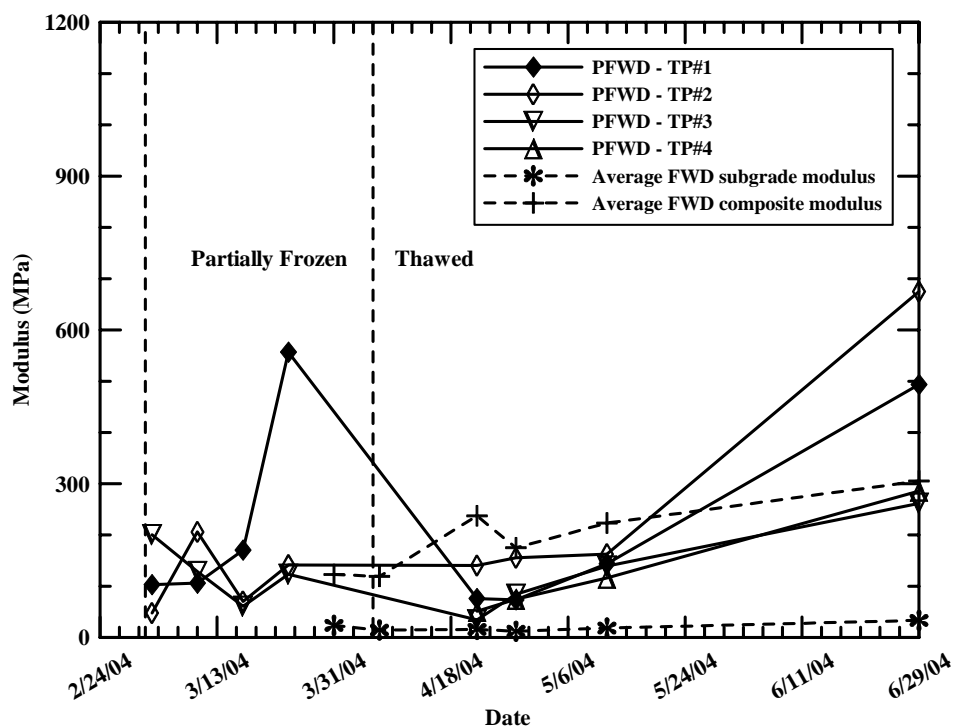


Figure 4.24 Detailed stiffness variation at Lakeside Landing Road (Section 2), Glenburn, Maine.

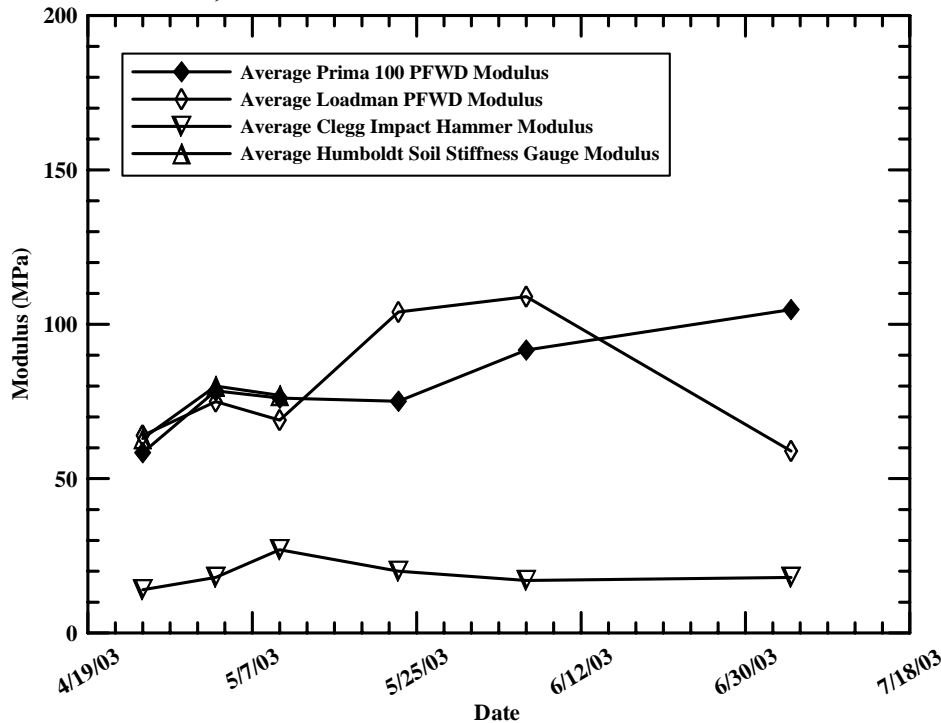


Figure 4.25 2003 stiffness variation at USFS Parking Lot, Rumney, New Hampshire.

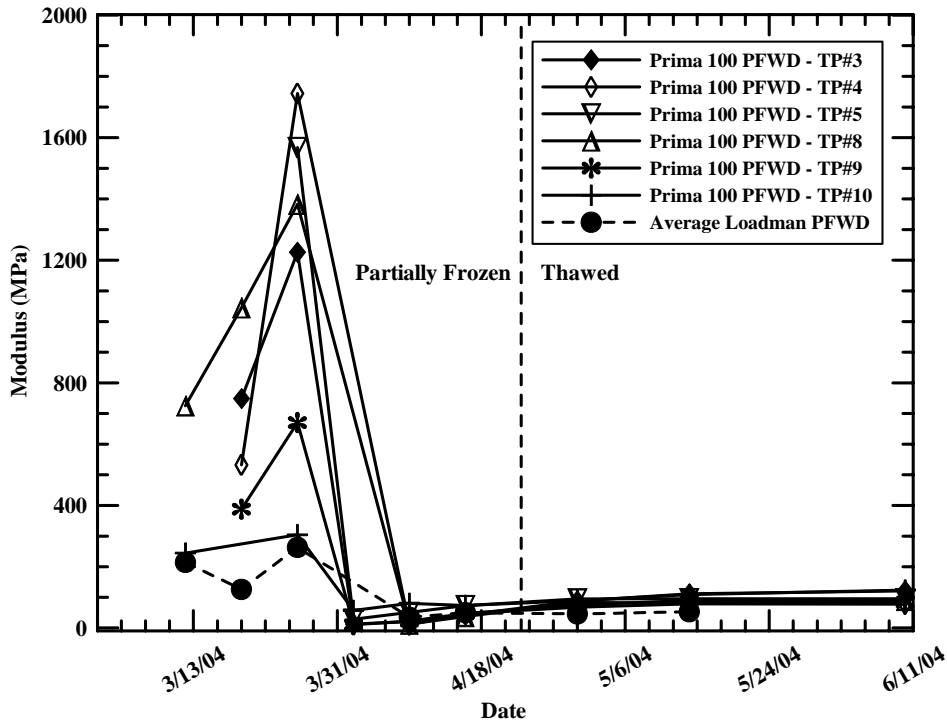


Figure 4.26 2004 stiffness variation at USFS Parking Lot, Rumney, New Hampshire.

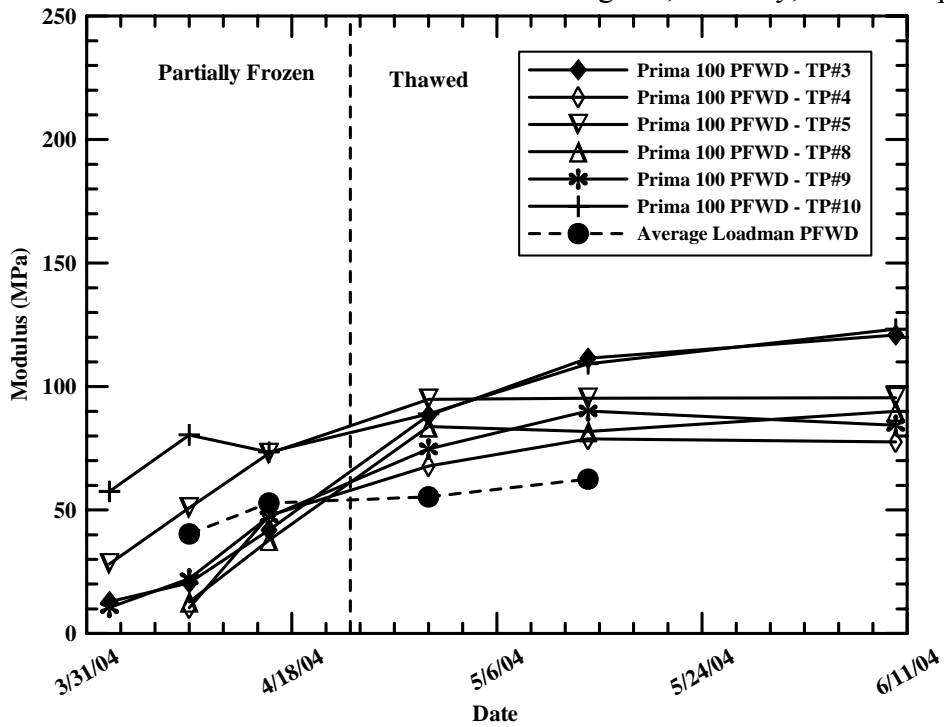


Figure 4.27 2004 detailed stiffness variation at USFS Parking Lot, Rumney, New Hampshire.

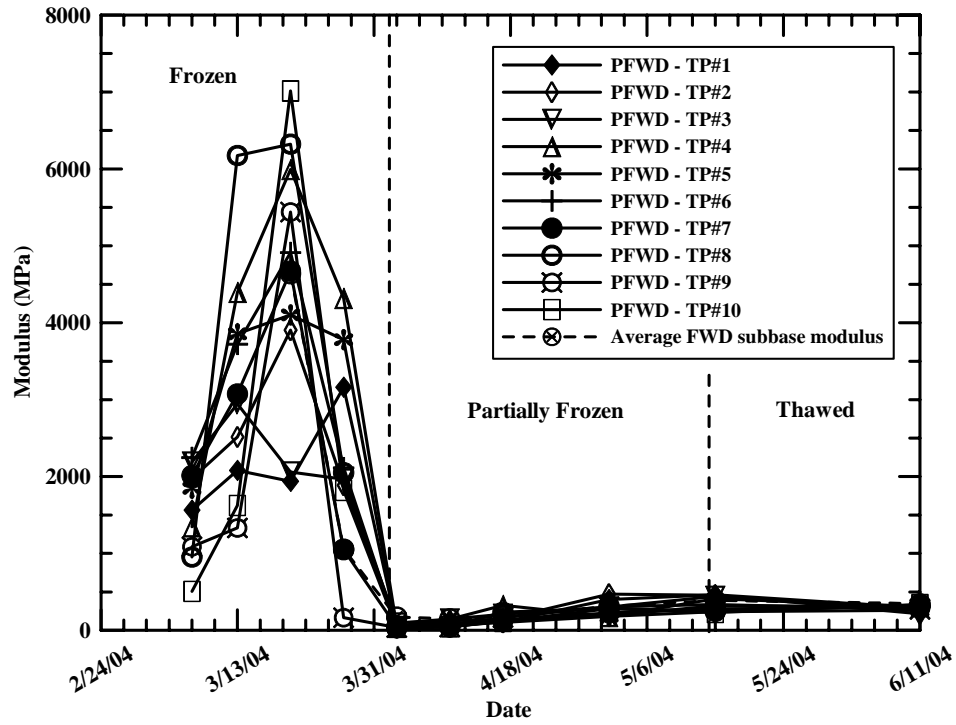


Figure 4.28 Stiffness variation at Crosstown Road, Berlin, Vermont.

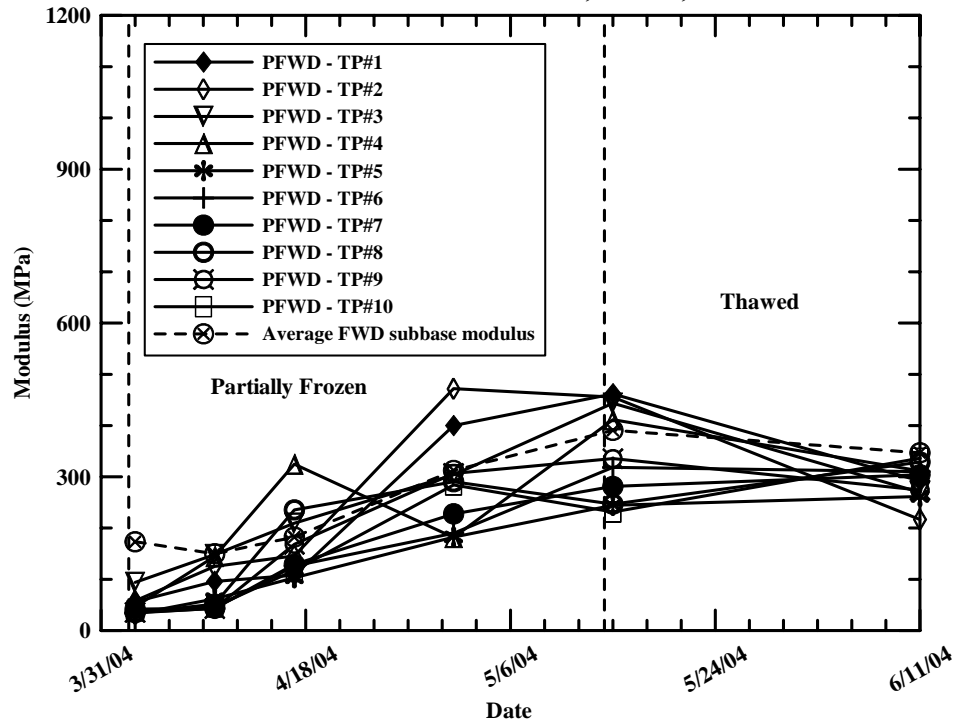


Figure 4.29 Detailed stiffness variation at Crosstown Road, Berlin, Vermont.

4.5 COMPARISON OF PFWD AND FWD MODULI

Portable and traditional FWD derived moduli for the Route 11 and Route 167 test sites are presented and assessed in this section. In addition, Prima 100 PFWD derived composite moduli are compared to FWD derived composite and subbase moduli for both asphalt and gravel surfaced test sites. Finally, portable and traditional FWD derived impact stiffness moduli are compared for asphalt and gravel surfaced test sites.

4.5.1 Route 11 & Route 167 Field Test Sites

A single set of Prima 100 PFWD and FWD measurements were taken on Routes 11 in Wallagrass Plantation and Route 167 in Presque Isle/Fort Fairfield, Maine in May 2003 as part of an ongoing MaineDOT research project (Bouchédid and Humphrey, 2004). Composite modulus values derived from both PFWD and FWD as well as subgrade moduli are plotted versus test location for each site. These results are presented in Figures 4.30 through 4.37.

Prima 100 PFWD composite moduli follow a similar trend to that of the traditional FWD at each test location at both test sites. Prima 100 PFWD composite moduli are less than the composite moduli backcalculated from FWD data at all test points. Prima 100 PFWD composite moduli are greater than subgrade moduli backcalculated from FWD data at all test locations.

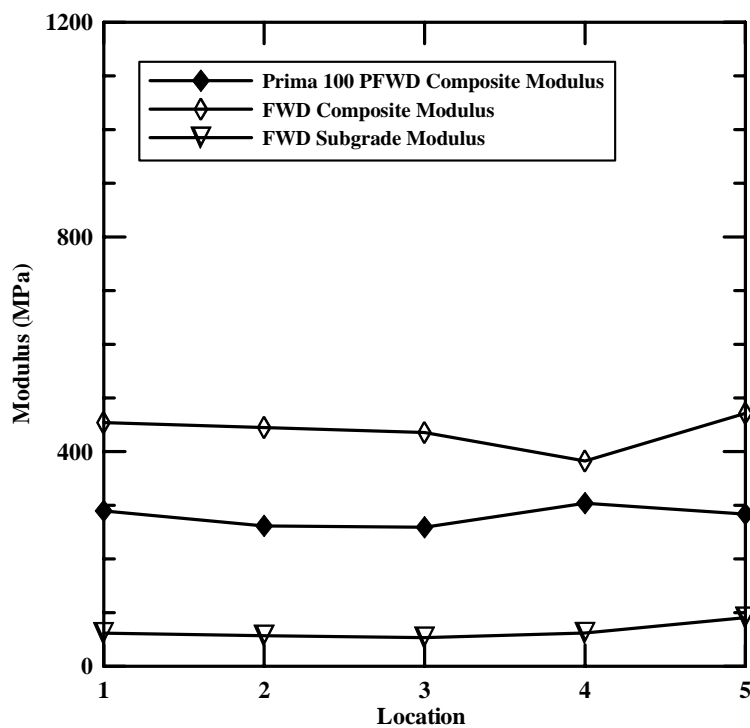


Figure 4.30 Modulus versus test location at Route 11 (Test Pit 1), Wallgrass Plantation, Maine.

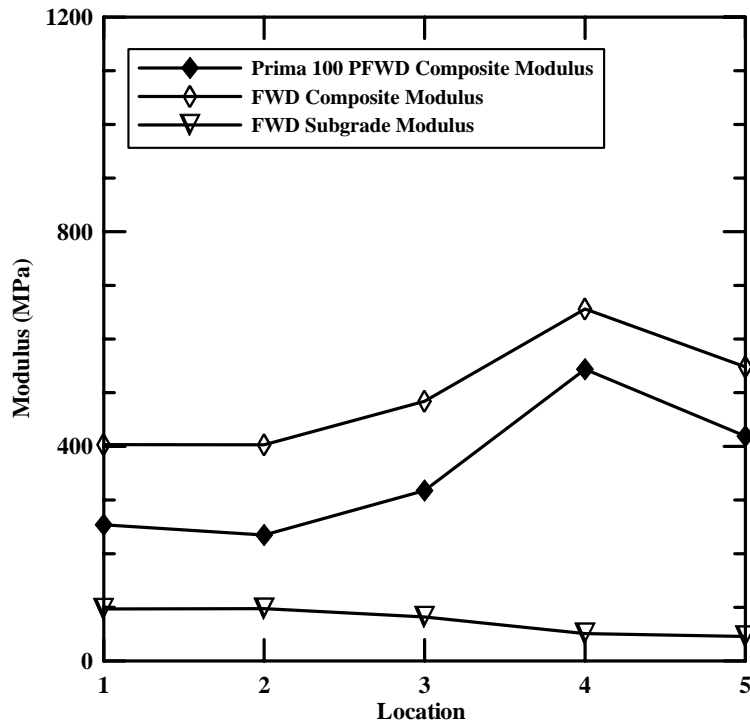


Figure 4.31 Modulus versus test location at Route 11 (Test Pit 2), Wallgrass Plantation, Maine.

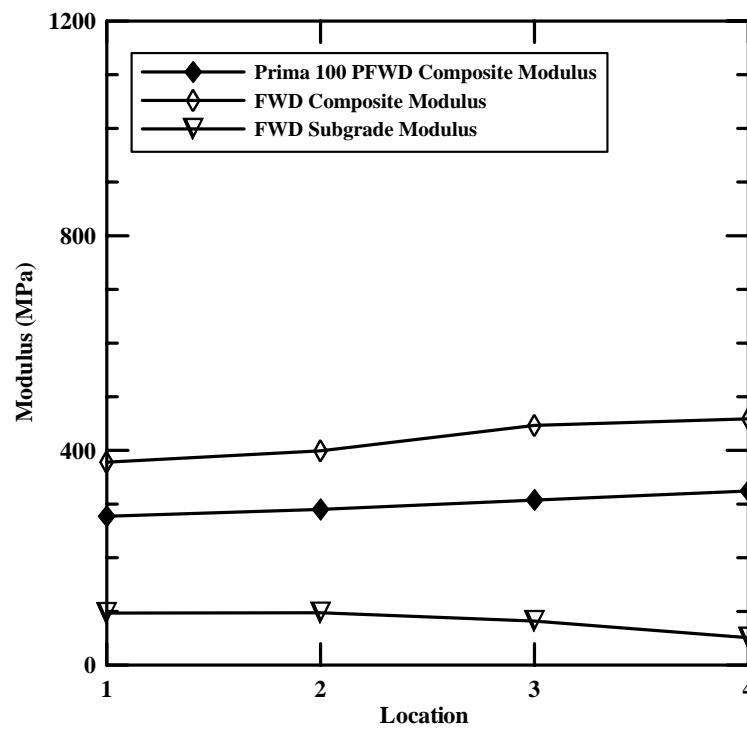


Figure 4.32 Modulus versus test location at Route 11 (Test Pit 3), Wallgrass Plantation, Maine.

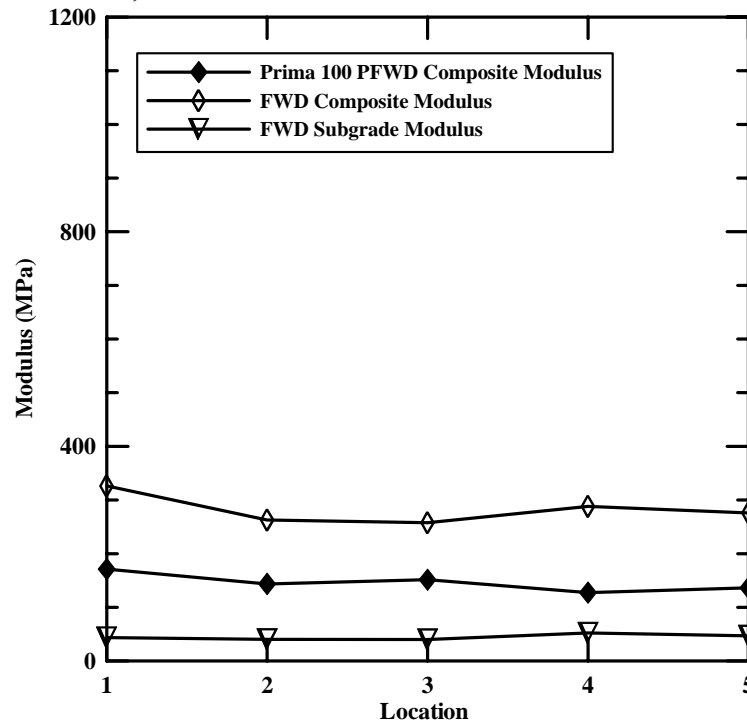


Figure 4.33 Modulus versus test location at Route 11 (Test Pit 4), Wallgrass Plantation, Maine.

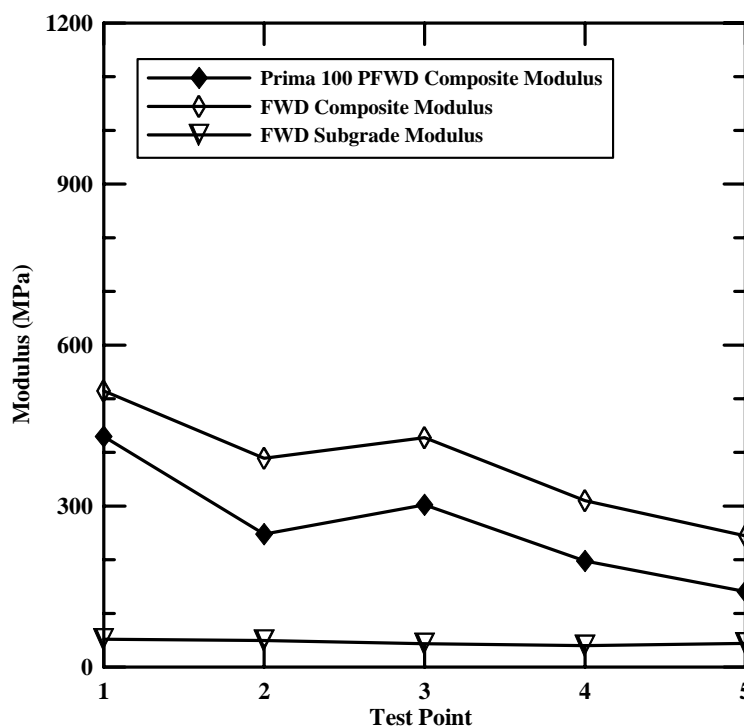


Figure 4.34 Modulus versus test location at Route 167 (Test Pit 1), Presque Isle/Fort Fairfield, Maine.

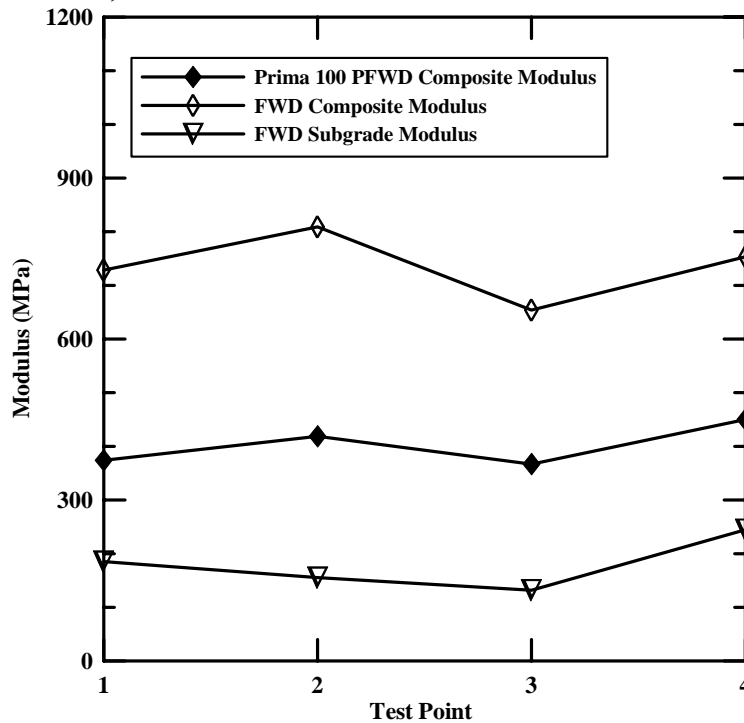


Figure 4.35 Modulus versus test location at Route 167 (Test Pit 2), Presque Isle/Fort Fairfield, Maine.

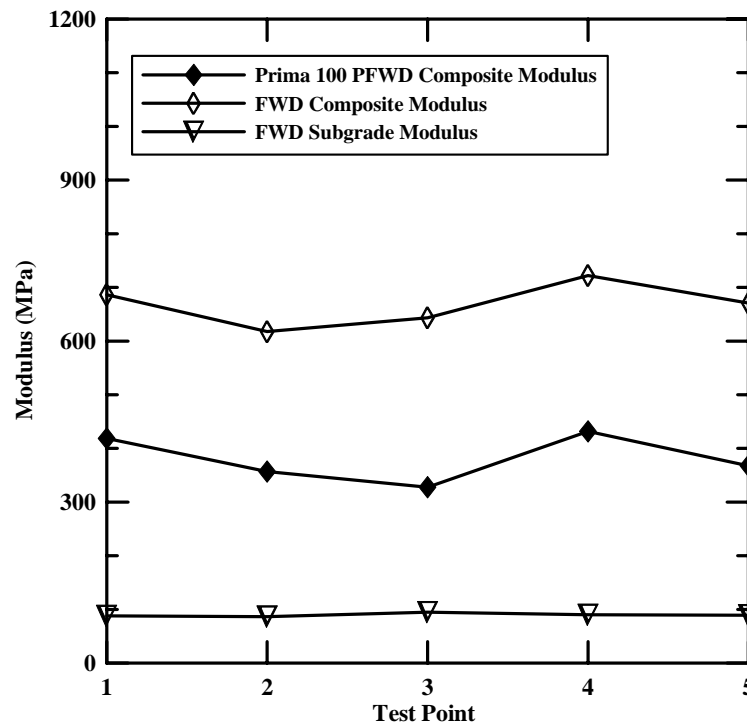


Figure 4.36 Modulus versus test location at Route 167 (Test Pit 3), Presque Isle/Fort Fairfield, Maine.

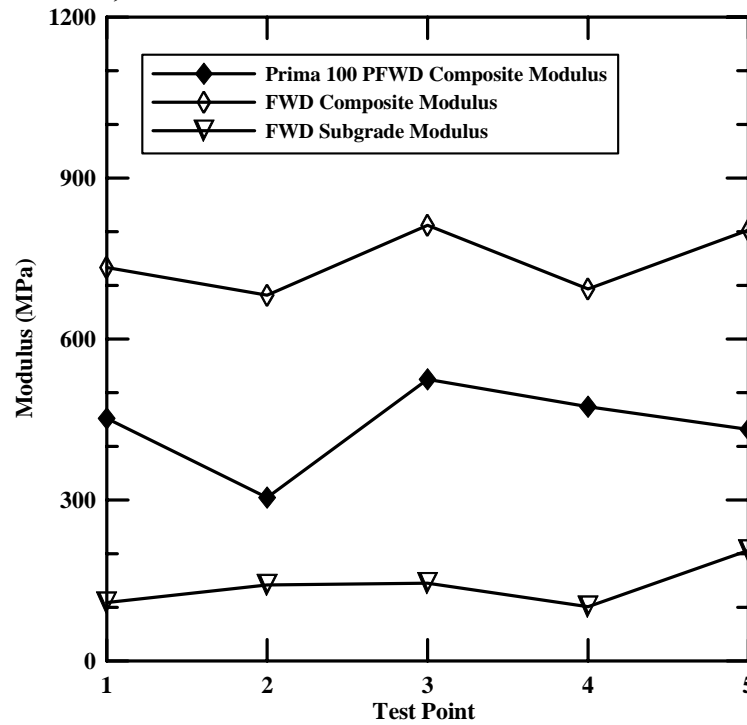


Figure 4.37 Modulus versus test location at Route 167 (Test Pit 4), Presque Isle/Fort Fairfield, Maine.

4.5.2 Composite Modulus

Composite moduli derived from traditional FWD measurements were supplied to the researchers by MaineDOT for asphalt and gravel surfaced test sites located in the State of Maine. For each site, backcalculated moduli are plotted against composite moduli as measured with the Prima 100 PFWD in Figure 4.38 through 4.43. Regression analyses yielded correlation coefficients ranging from 0.336 (Route 1A) to 0.950 (Witter Farm Road). In general terms, correlation coefficients tended to increase as pavement thickness decreased. To better illustrate this, separate plots were developed for sites with different asphalt thicknesses. These are presented in Figures 4.44 through 4.46 and Figure 4.43. Three test sites with asphalt thicknesses less than or equal to 127 mm (5 in.) produced the best correlation with $r^2 = 0.873$. Two test sites with an asphalt thickness of 152 mm (6 in.) followed with $r^2 = 0.559$. However, when excluding moduli greater than 4000 MPa the correlation improves with $r^2 = 0.802$. Route 1A served as the single test site with a 180 mm (7 in.) asphalt thickness and produced the poorest correlation with $r^2 = 0.336$. Data from all paved sites is presented in Figure 4.47. Regression analysis yielded a correlation coefficient of 0.531, however, when excluding all moduli greater than 4000 MPa (Figure 4.48), the correlation improved with $r^2 = 0.809$. Results from the Lakeside Landing Road test site are shown in Figure 4.49. Regression analysis yielded an r^2 of 0.446. Overall, a strong correlation exists between the Prima 100 PFWD composite moduli and FWD derived composite moduli for asphalt surfaced roads. A marginal correlation exists for gravel surfaced test sites.

Mean moduli for individual asphalt thicknesses are presented in Table 4.7. The FWD and PFWD composite moduli are lower for the 178 mm (7 in.) asphalt thickness

than the 127 mm (5 in.) thickness. This is contrary to expectations, since thicker pavements would be expected to yield higher composite moduli.

Table 4.7 FWD and PFWD mean composite moduli for different asphalt thicknesses.

Asphalt Thickness mm (in.)	Prima 100 PFWD Mean Composite Modulus (MPa)	FWD Mean Composite Modulus (MPa)
127 (5)	645	557
150 (6)	483	658
180 (7)	503	505

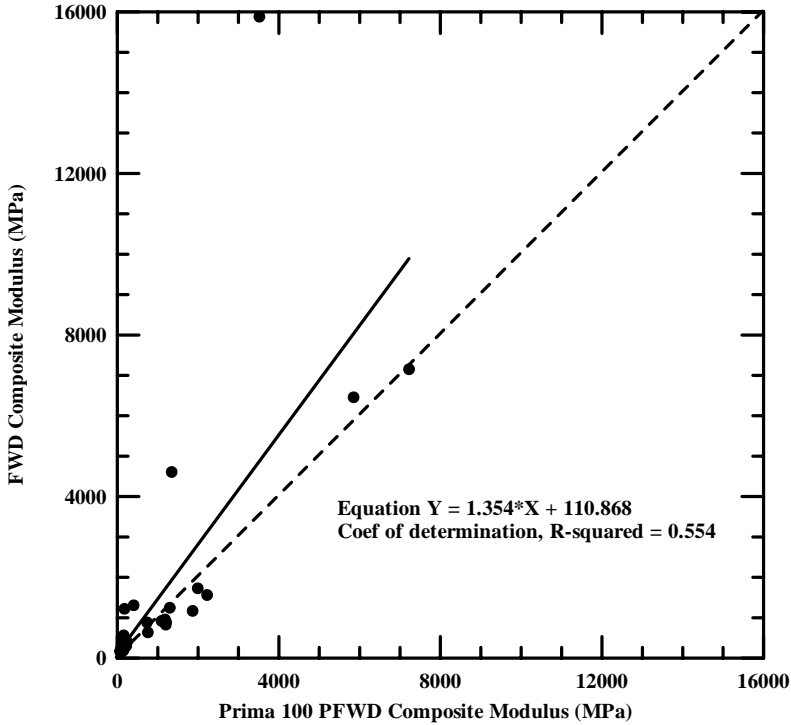


Figure 4.38 Comparison of FWD and PFWD composite moduli at Kennebec Road, Hampden/Dixmont, Maine.

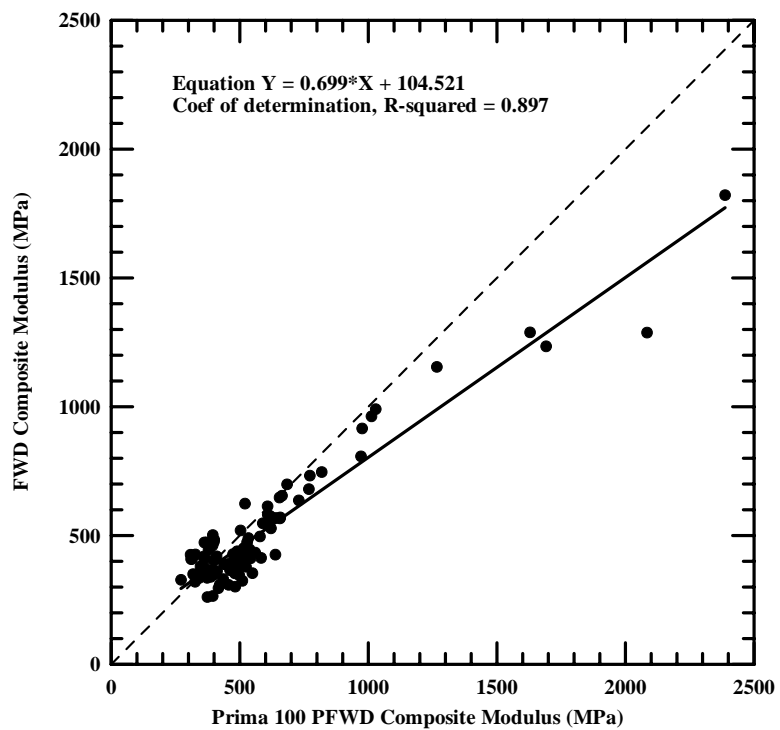


Figure 4.39 Comparison of FWD and PFWD composite moduli at Route 126, Monmouth/Litchfield, Maine.

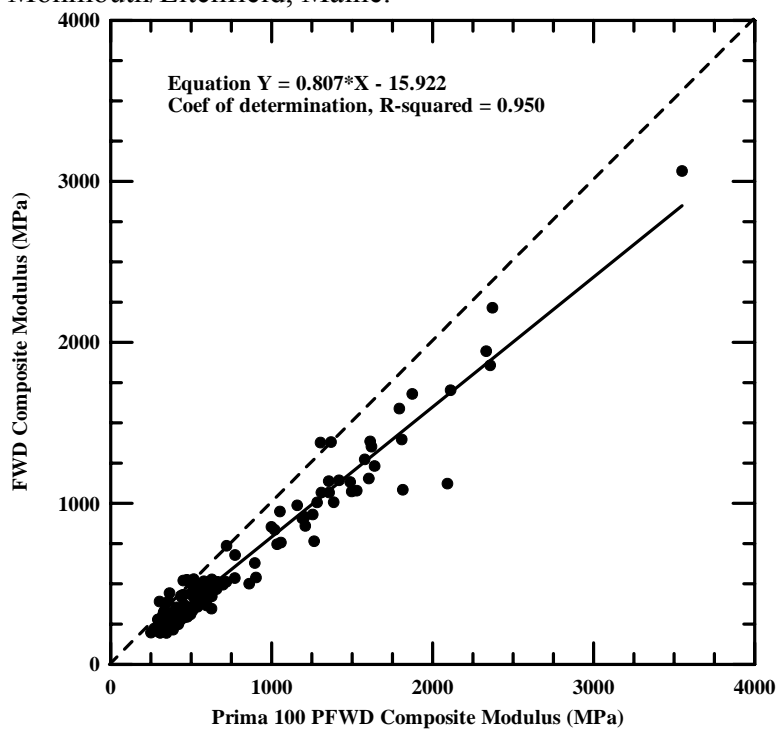


Figure 4.40 Comparison of FWD and PFWD composite moduli at Witter Farm Road, Orono, Maine.

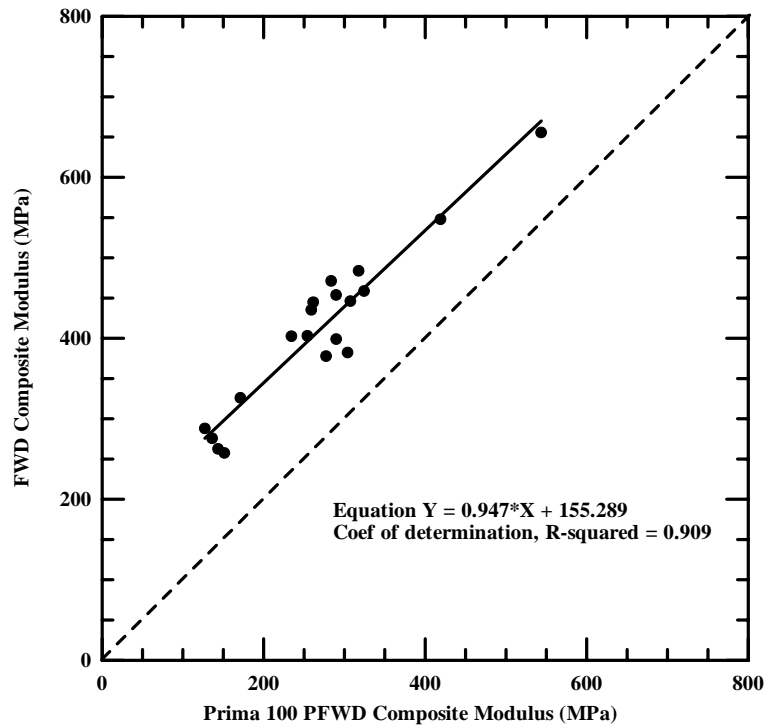


Figure 4.41 Comparison of FWD and PFWD composite moduli at Route 11, Wallgrass Plantation, Maine.

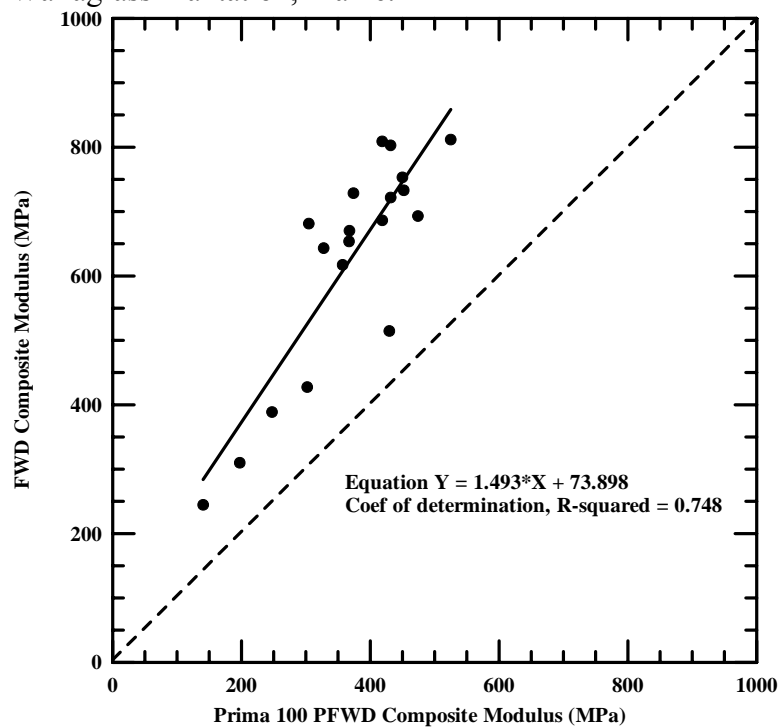


Figure 4.42 Comparison of FWD and PFWD composite moduli at Route 167, Presque Isle/Fort Fairfield, Maine.

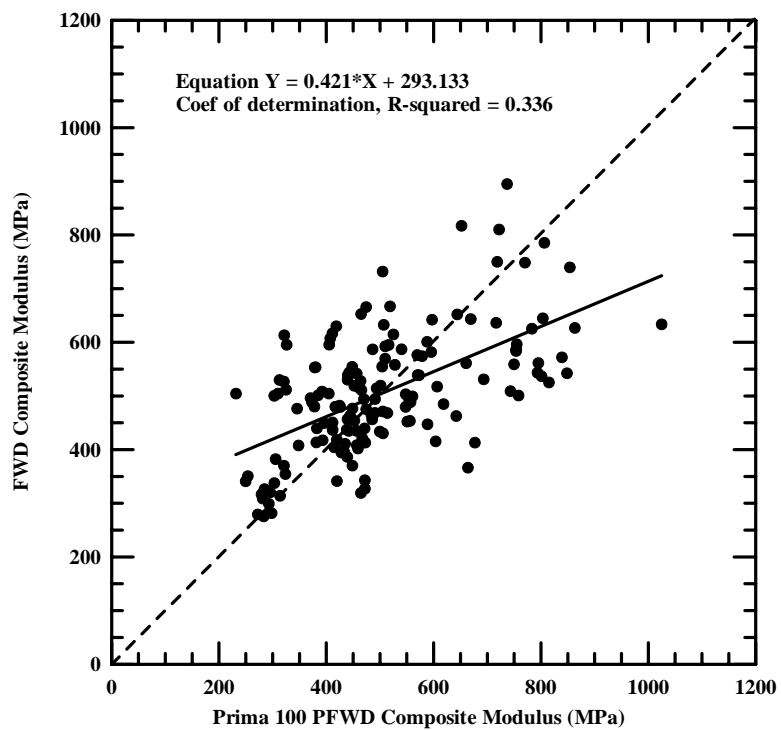


Figure 4.43 Comparison of FWD and PFWD composite moduli at Route 1A, Frankfort/Winterport, Maine.

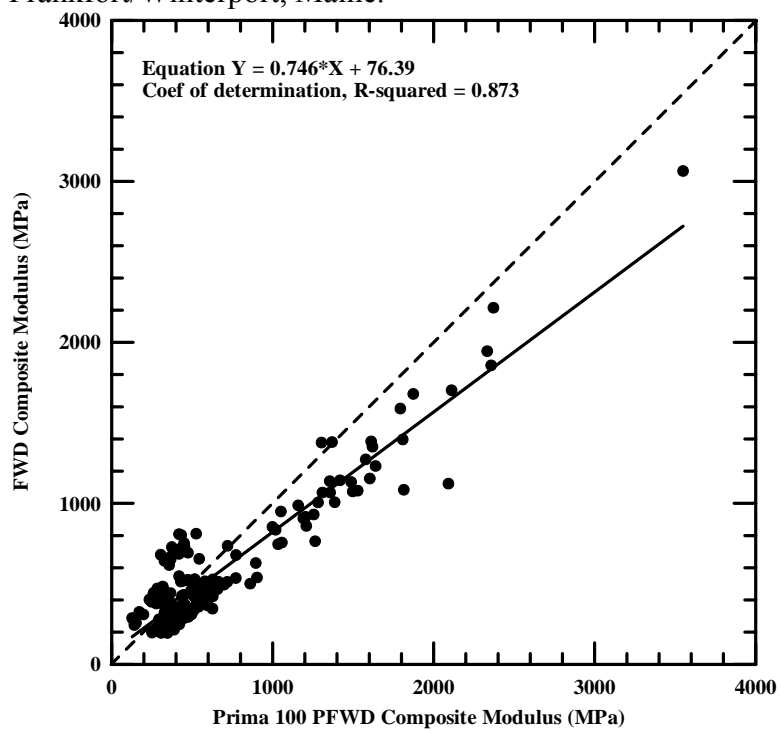


Figure 4.44 Comparison of FWD and PFWD composite moduli for asphalt thicknesses ≤ 127 mm (5 in.).

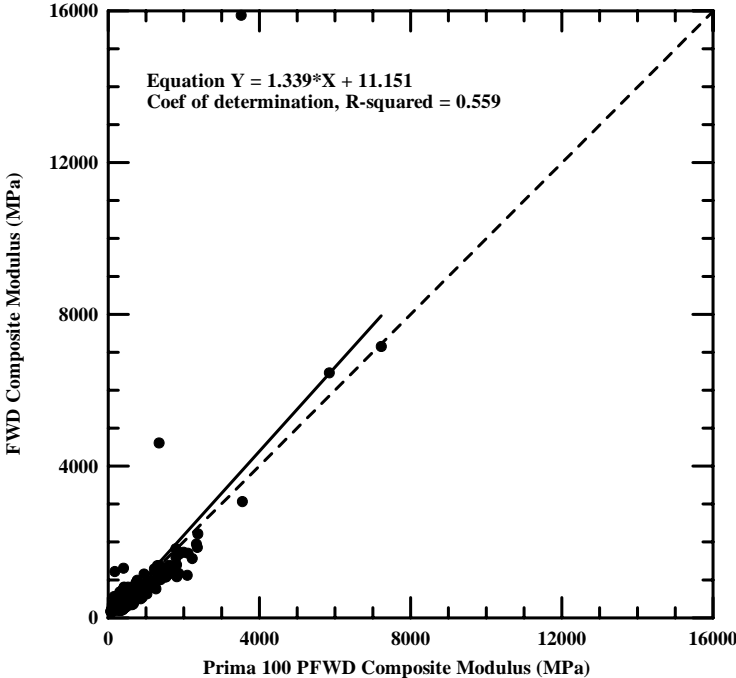


Figure 4.45 Comparison of FWD and PFWD composite moduli for asphalt thicknesses equal to 152 mm (6 in.).

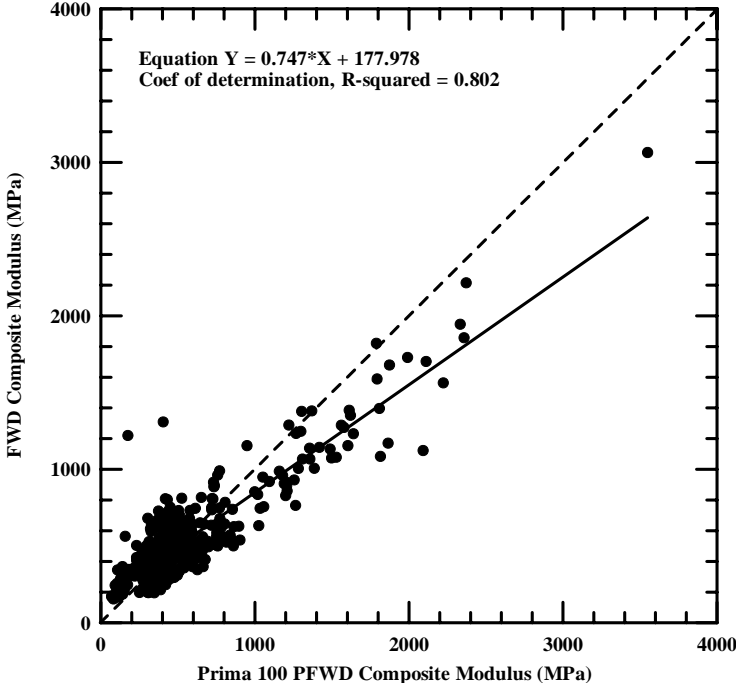


Figure 4.46 Comparison of FWD and PFWD composite moduli for asphalt thicknesses equal to 152 mm (6 in.) and moduli ≤ 4000 MPa.

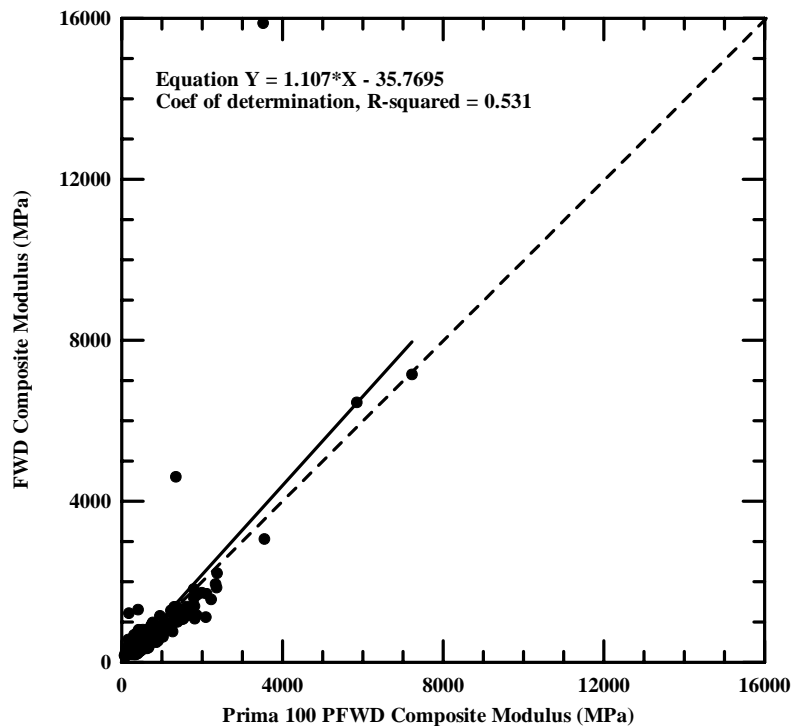


Figure 4.47 Comparison of FWD and PFWD composite moduli for all asphalt surfaced test sites.

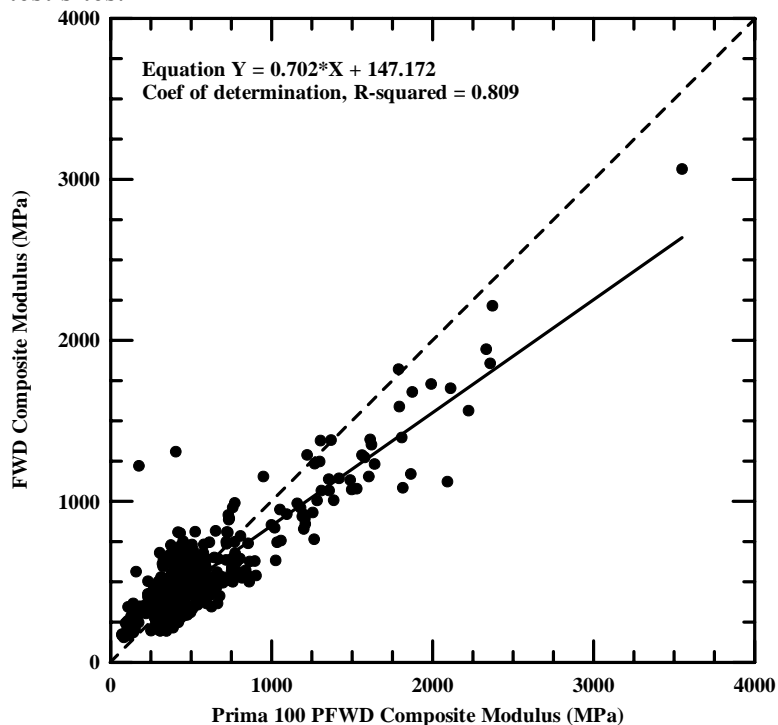


Figure 4.48 Comparison of FWD and PFWD composite moduli for all asphalt surfaced test sites and moduli ≤ 4000 MPa.

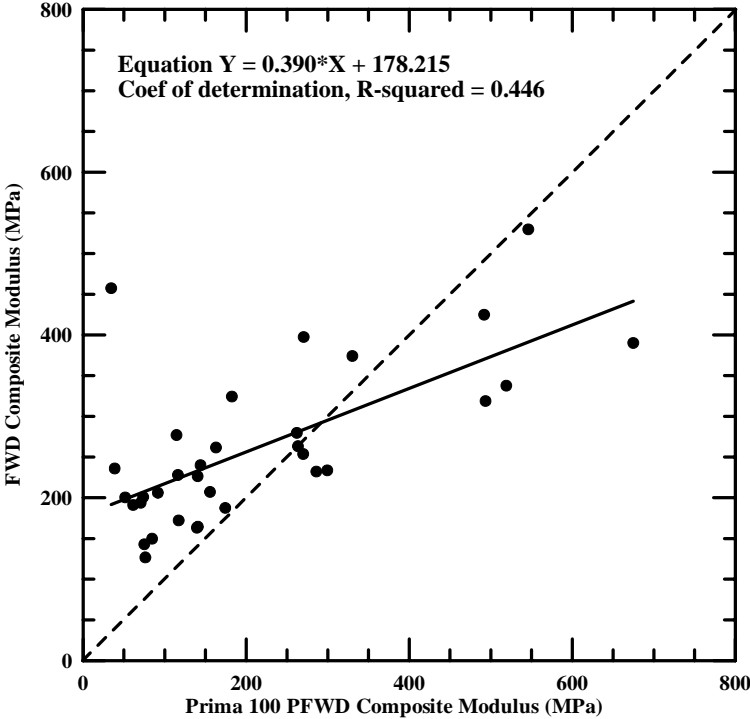


Figure 4.49 Comparison of FWD and PFWD composite moduli at Lakeside Landing Road, Glenburn, Maine.

4.5.3 Subbase Modulus

Subbase moduli were derived from traditional FWD data using Evercalc backcalculation software. For each site, subbase moduli are plotted against composite moduli as measured with the Prima 100 PFWD. These are presented in Figure 4.50 through 4.56. Regression analyses yielded correlation coefficients ranging from 0.163 (Route 1A) to 0.807 (Knapp Airport Parking Lot). In general, correlation coefficients tended to decrease as pavement thickness increased. With thin asphalt layers, the subbase modulus has an increased affect on PFWD composite moduli whereas with thick asphalt layers, composite moduli are heavily influenced by the pavement layer. To better illustrate this, separate plots were developed for sites with different asphalt thicknesses. Five test sites with an asphalt thicknesses equal to 127 mm (5 in.) followed with $r^2 =$

0.508. However, when excluding moduli greater than 5000 MPa, the correlation improves with $r^2 = 0.693$. This is shown in Figures 4.57 and 4.58. One test site (Route 126) with a 150 mm (6 in.) asphalt thickness, shown in Figure 4.55, produced the best correlation with $r^2 = 0.698$. Route 1A served as the single test site with a 180 mm (7 in.) asphalt thickness, shown in Figure 4.56, and produced the poorest correlation with $r^2 = 0.363$. Data from all paved sites is presented in Figure 4.59. Regression analysis yielded a correlation coefficient of 0.485, however, when excluding all moduli greater than 5000 MPa (Figure 4.60), the correlation improved with $r^2 = 0.654$. The results from the Crosstown Road, gravel surfaced test site are presented in Figure 4.61. Composite and subbase moduli compared marginally with $r^2 = 0.327$. In general terms, PFWD composite moduli had a reasonable correlation with FWD derived subbase moduli, suggesting that the Prima 100 composite moduli are influenced at least in part by the subbase layer.

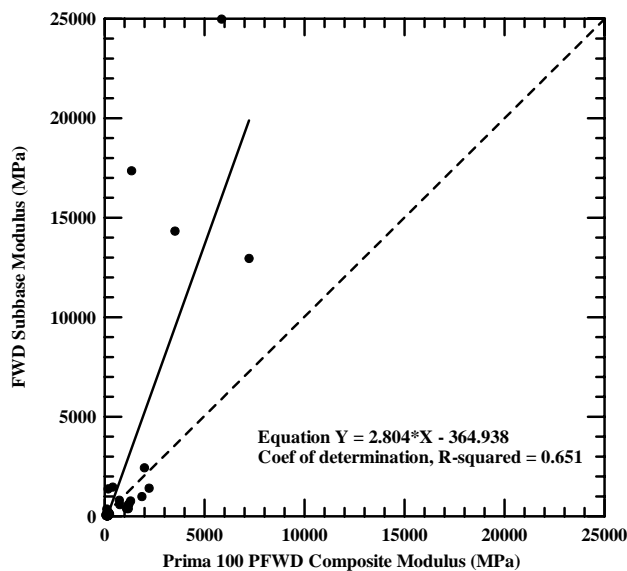


Figure 4.50 Comparison of FWD subbase moduli and PFWD composite moduli at Kennebec Road, Hampden/Dixmont, Maine.

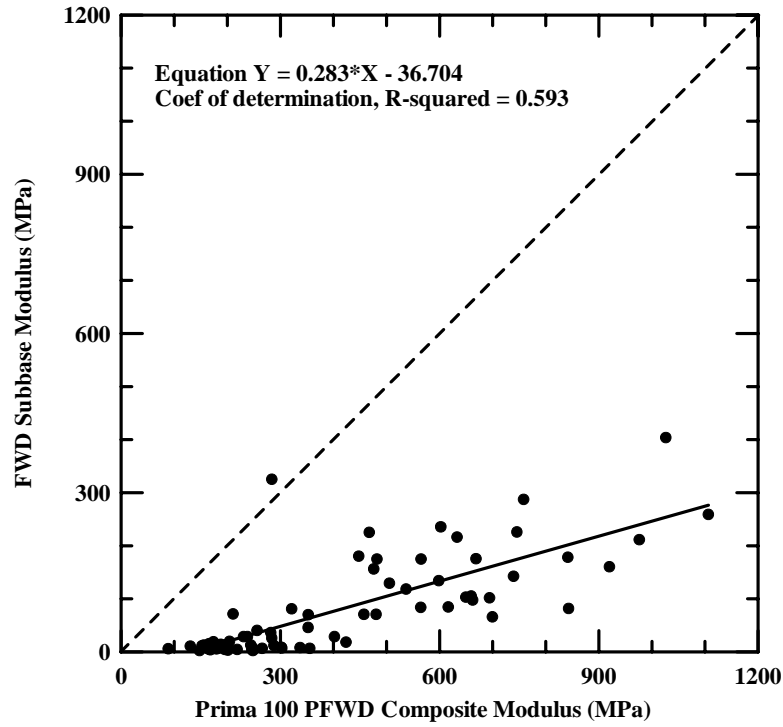


Figure 4.51 Comparison of FWD subbase moduli and PFWD composite moduli at Stinson Lake Road, Rumney, New Hampshire.

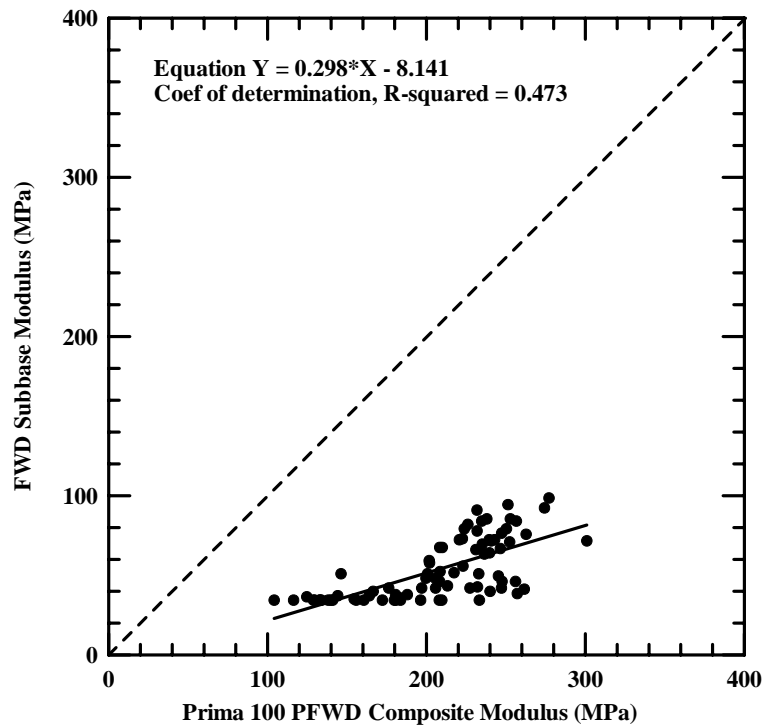


Figure 4.52 Comparison of FWD subbase moduli and PFWD composite moduli at Buffalo Road, Rumney, New Hampshire.

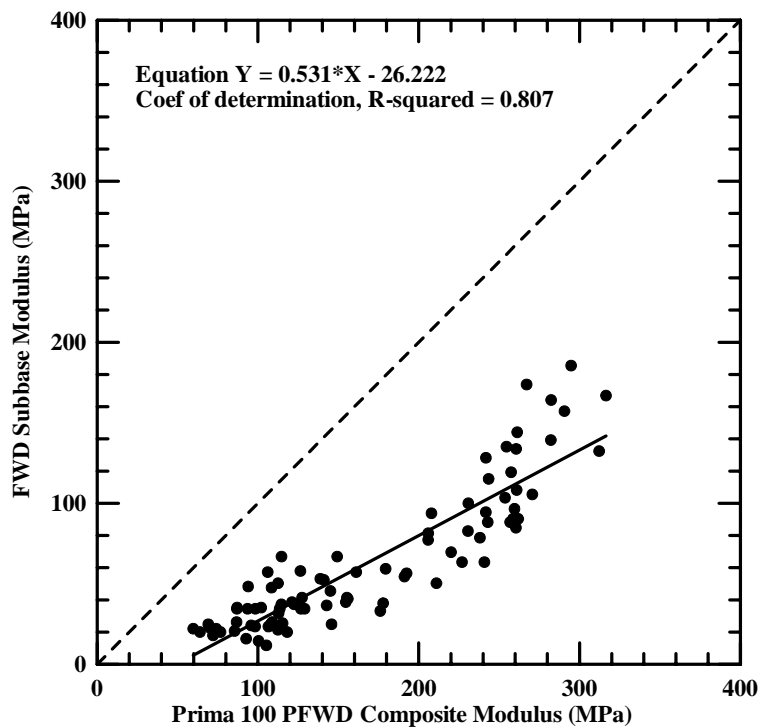


Figure 4.53 Comparison of FWD subbase moduli and PFWD composite moduli at Knapp Airport Parking Lot, Berlin, Vermont.

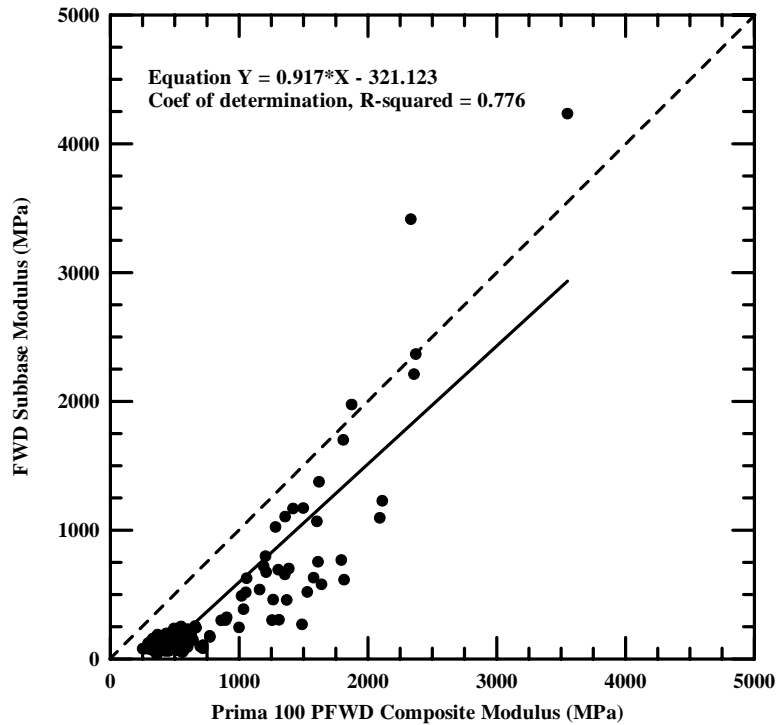


Figure 4.54 Comparison of FWD subbase moduli and PFWD composite moduli at Witter Farm Road, Orono, Maine.

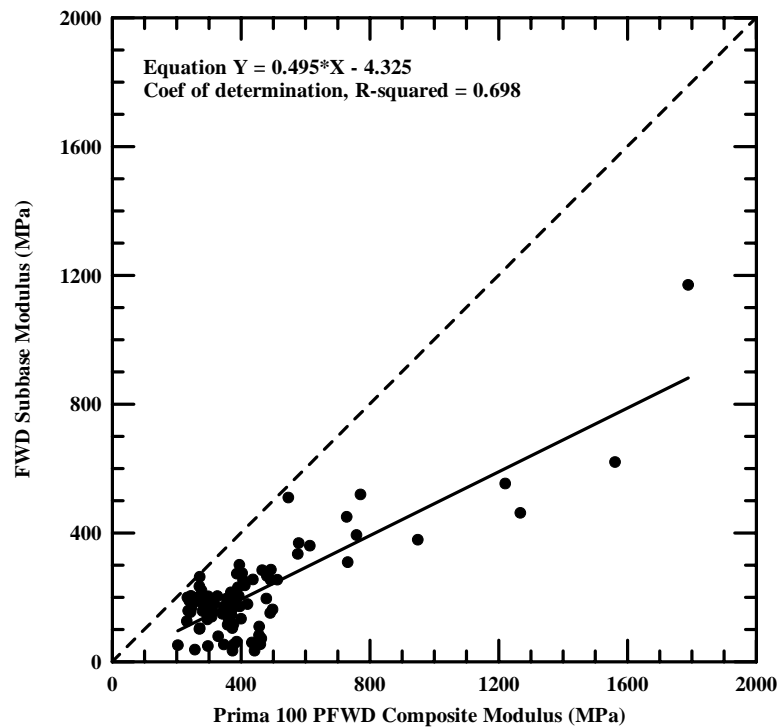


Figure 4.55 Comparison of FWD subbase moduli and PFWD composite moduli at Route 126, Monmouth/Litchfield, Maine.

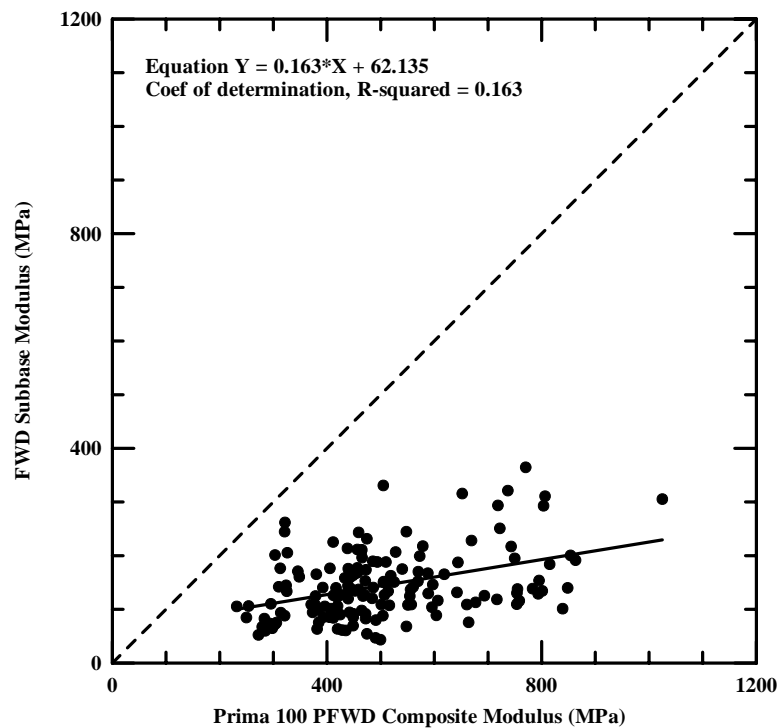


Figure 4.56 Comparison of FWD subbase moduli versus PFWD composite moduli at Route 1A, Frankfort/Winterport, Maine.

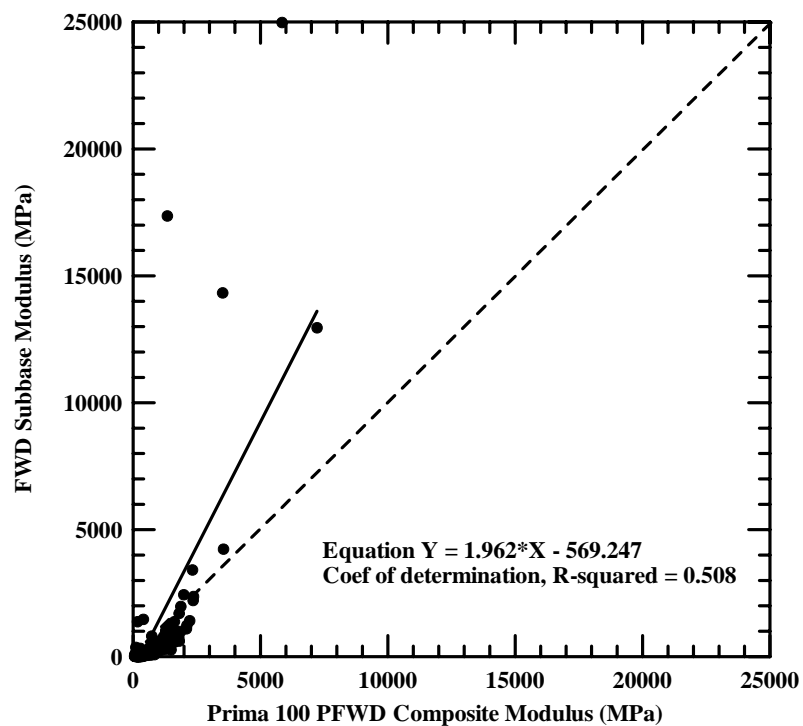


Figure 4.57 Comparison of FWD subbase moduli and PFWD composite moduli for asphalt thicknesses ≤ 127 mm (5 in.).

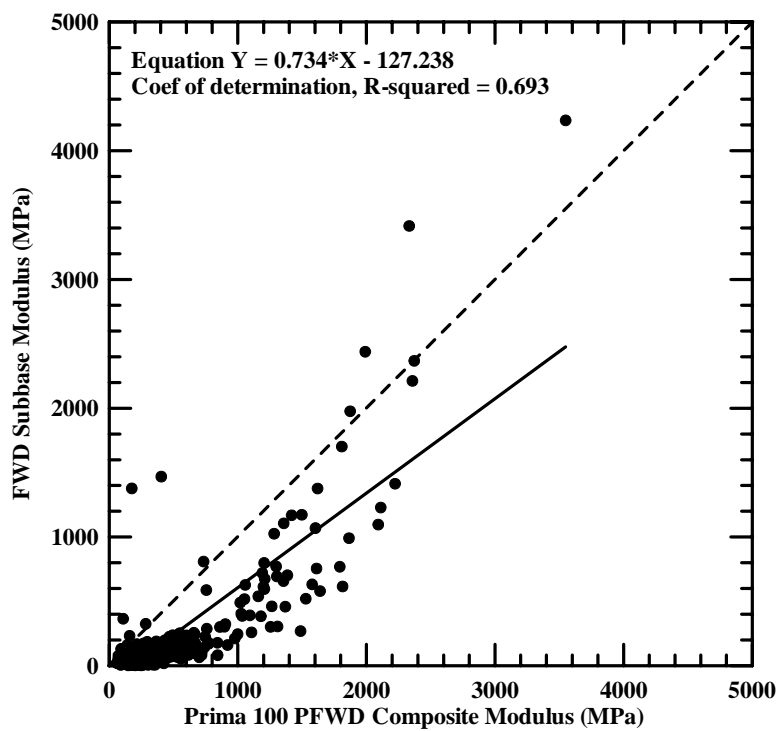


Figure 4.58 Comparison of FWD subbase moduli and PFWD composite moduli for asphalt thickness ≤ 127 mm (5 in.) and moduli ≤ 5000 MPa.

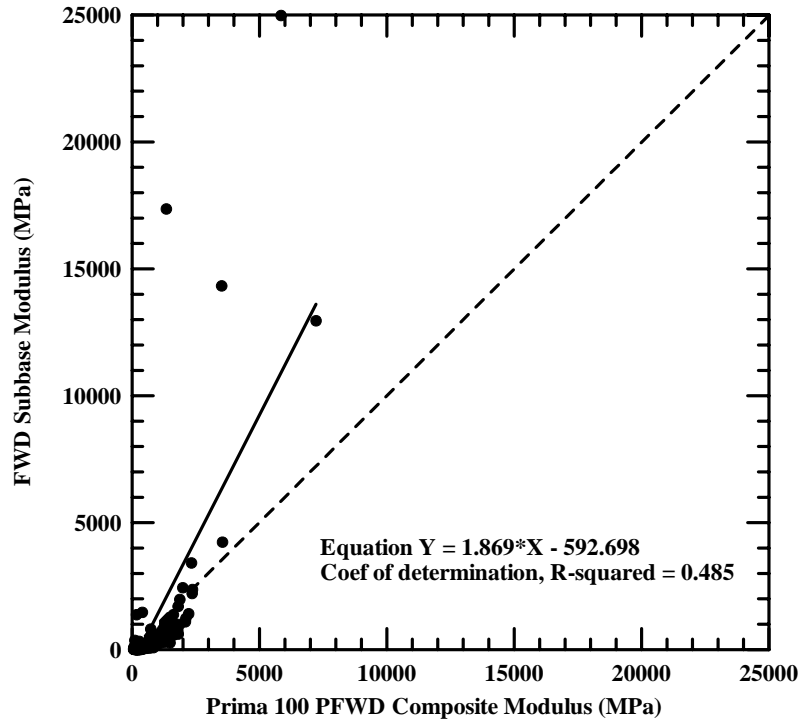


Figure 4.59 Comparison of FWD subbase moduli and PFWD composite moduli for all asphalt surfaced test sites.

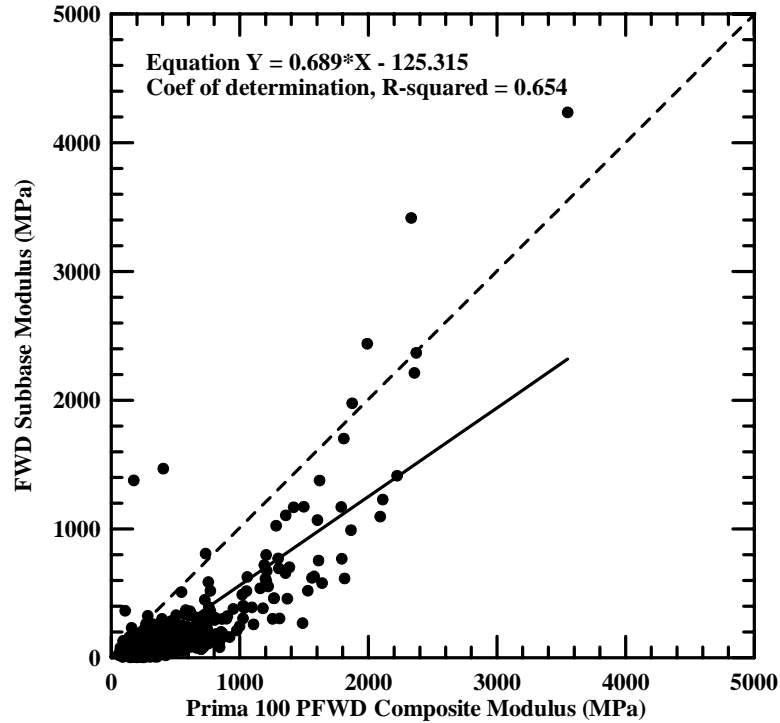


Figure 4.60 Comparison of FWD subbase moduli and PFWD composite moduli for all asphalt surfaced test sites and moduli ≤ 5000 MPa.

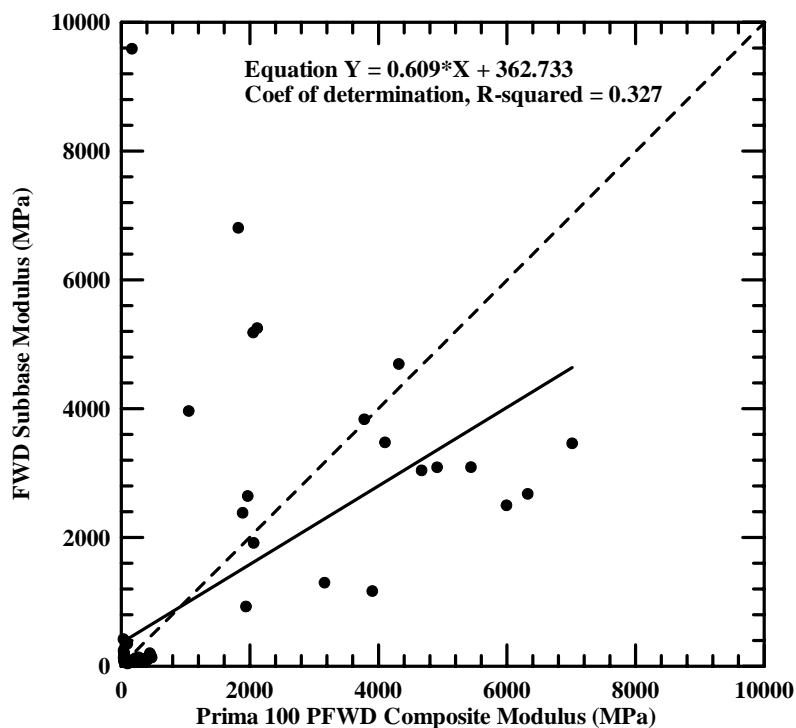


Figure 4.61 Comparison of FWD subbase moduli and PFWD composite moduli at Crosstown Road, Berlin, Vermont.

4.5.4 Impact Stiffness Modulus

Impact Stiffness Modulus (ISM) is defined as the ratio of the applied load to the deflection of the center sensor, or geophone, as seen by Equation 4.2.

$$ISM = \frac{P}{D_0} \quad \text{Eqn. 4.2}$$

where: ISM = Impact Stiffness Modulus
 P = Applied load, kN (kip)
 D₀ = Surface deflection at the center of the test load, μm (mils).

ISM values were determined for both the traditional and portable FWD. The advantage of ISM over composite modulus is that use of a modulus backcalculation program is avoided. The results for asphalt and gravel surfaced test sites are presented in the following sections.

Plots of FWD derived ISM are compared to corresponding PFWD values and are presented in Figures 4.62 through 4.68. The correlation tends to improve as pavement thickness decreases. To better illustrate this, separate plots were developed for sites with different asphalt thicknesses. These are shown in Figures 4.69 through 4.70, and Figure 4.68. All asphalt surfaced test sites are represented in Figure 4.71. This trend is similar to that exhibited by composite and subbase moduli. This discussion is provided in Section 4.5.2 and 4.5.3. Traditional and portable FWD derived ISM are compared for three gravel surfaced test sites in Figures 4.72 through 4.74. Regression analyses yielded correlation coefficients ranging from 0.638 (Lakeside Landing Road) to 0.914 (Crosstown Road). All gravel surfaced sites were combined and are shown in Figure 4.75. As a result, the PFWD and FWD derived ISM moduli appear to be equally effective indicators of section stiffness for thin asphalt surfaced and gravel surfaced sites.

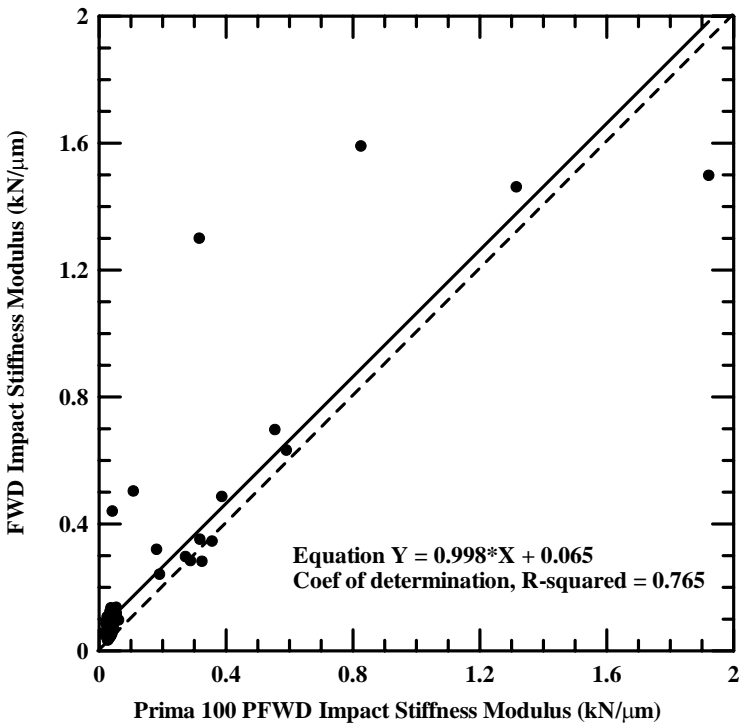


Figure 4.62 Comparison of FWD and PFWD ISM at Kennebec Road, Hampden/Dixmont, Maine.

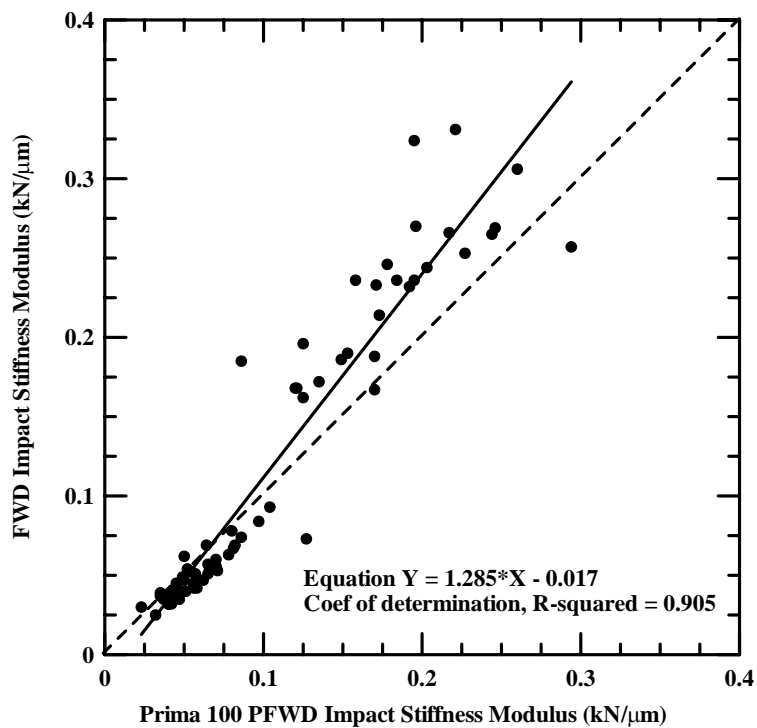


Figure 4.63 Comparison of FWD and PFWD ISM at Stinson Lake Road, Rumney, New Hampshire.

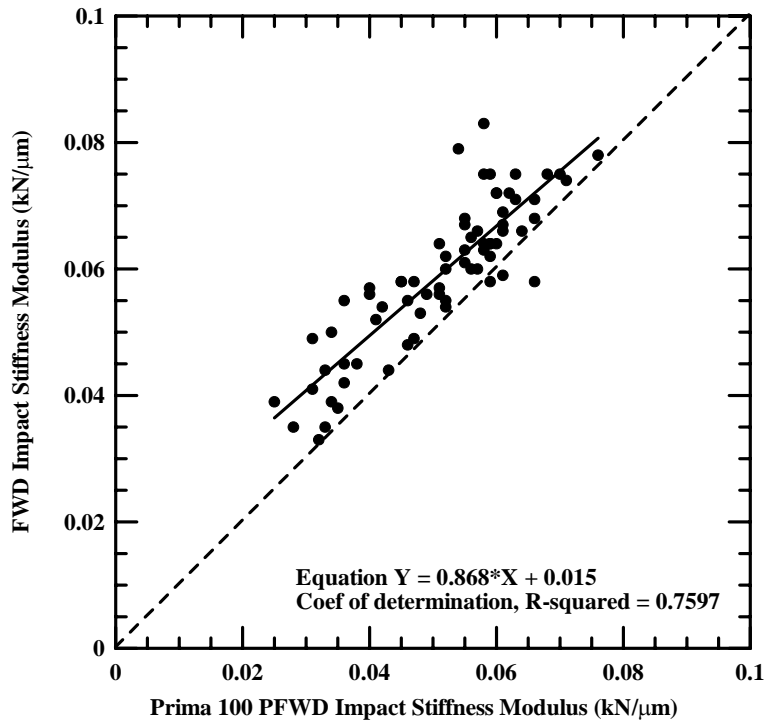


Figure 4.64 Comparison of FWD and PFWD ISM at Buffalo Road, Rumney, New Hampshire.

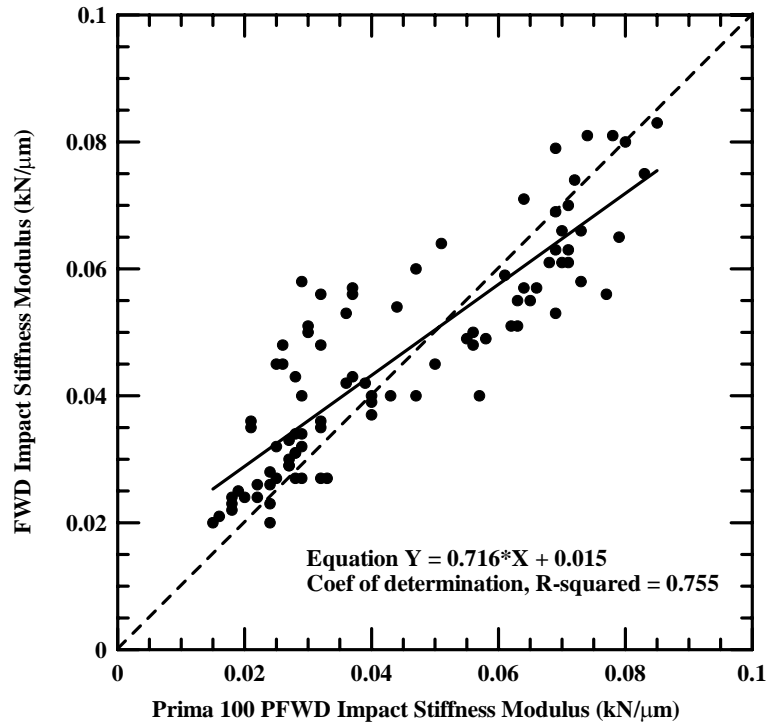


Figure 4.65 Comparison of FWD and PFWD ISM at Knapp Airport Parking Lot, Berlin, Vermont.

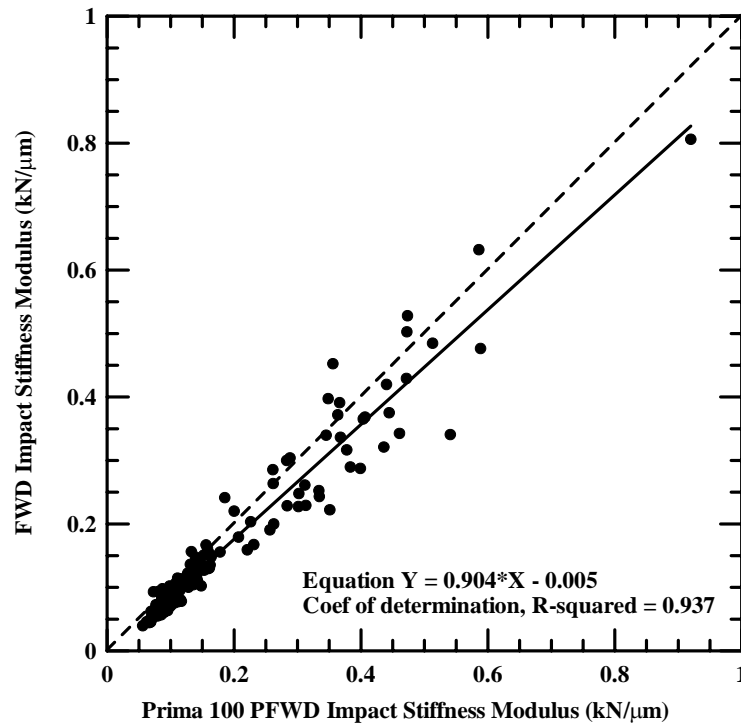


Figure 4.66 Comparison of FWD and PFWD ISM at Witter Farm Road, Orono, Maine.

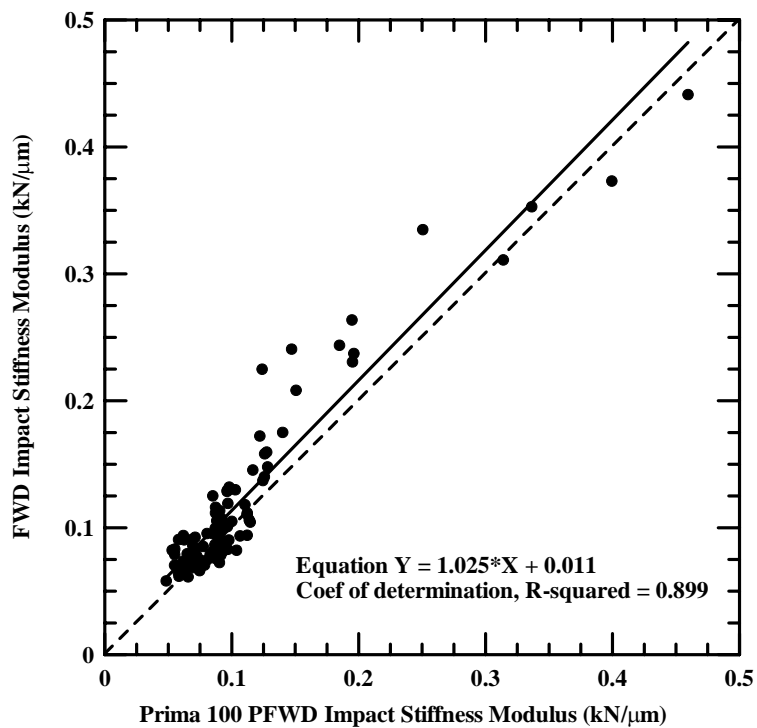


Figure 4.67 Comparison of FWD and PFWD ISM at Route 126, Monmouth/Litchfield, Maine.

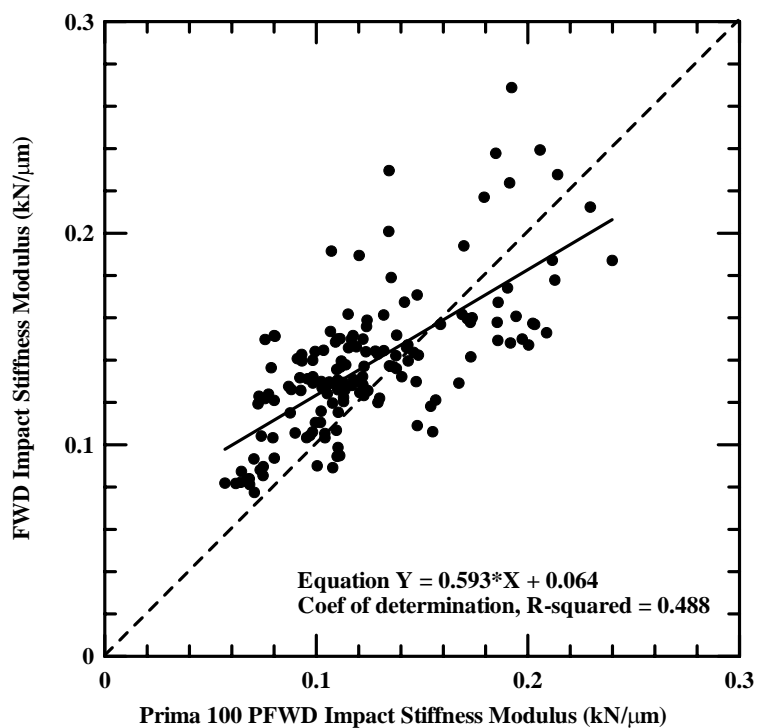


Figure 4.68 Comparison of FWD and PFWD ISM at Route 1A, Frankfort/Winterport, Maine.

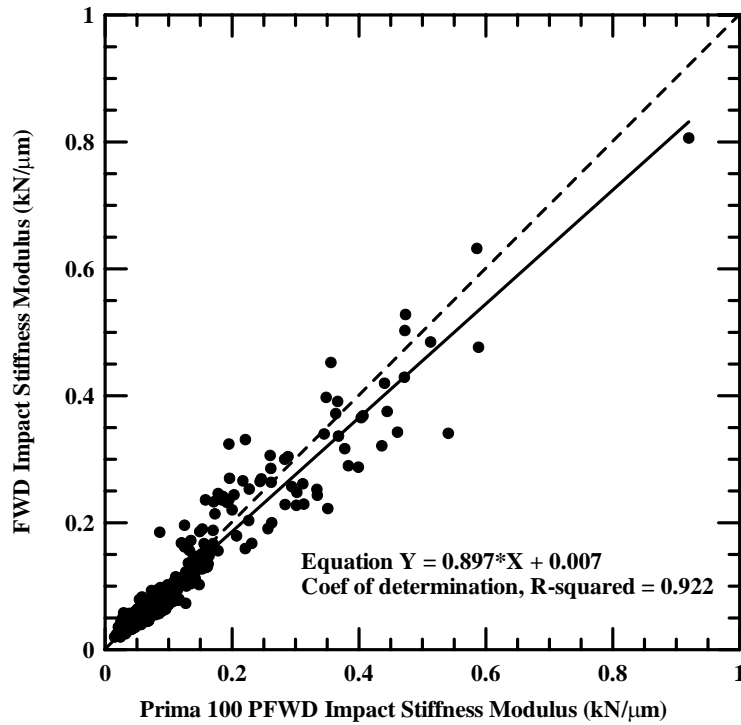


Figure 4.69 Comparison of FWD and PFWD ISM for test sites with asphalt thicknesses ≤ 127 mm (5 in.).

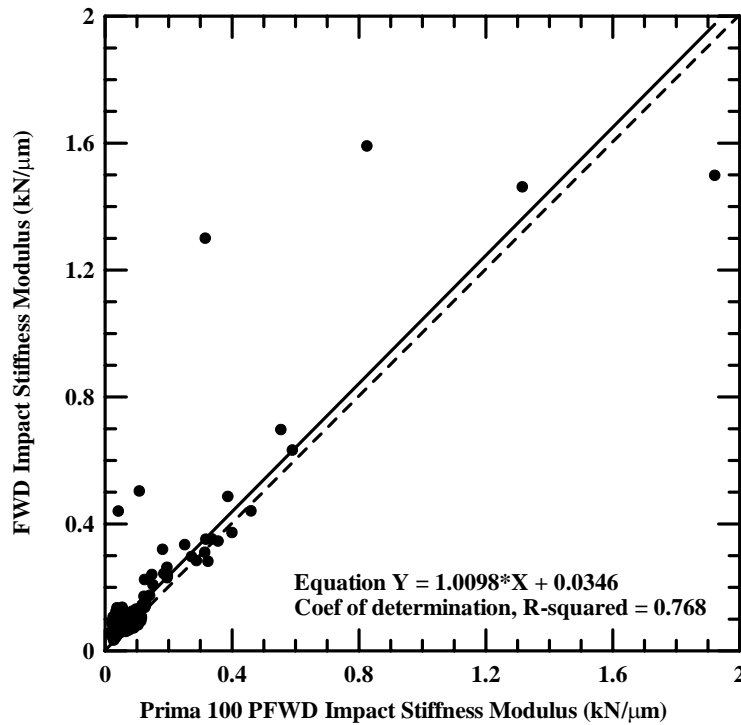


Figure 4.70 Comparison of FWD and PFWD ISM for test sites with asphalt thicknesses equal to 152 mm (6 in.).

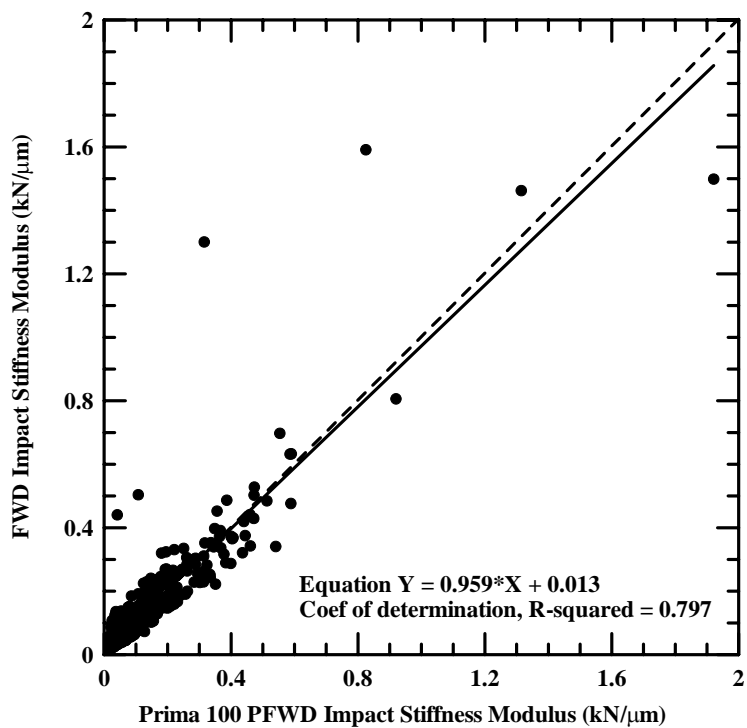


Figure 4.71 Comparison of FWD and PFWD ISM for all asphalt surfaced test sites.

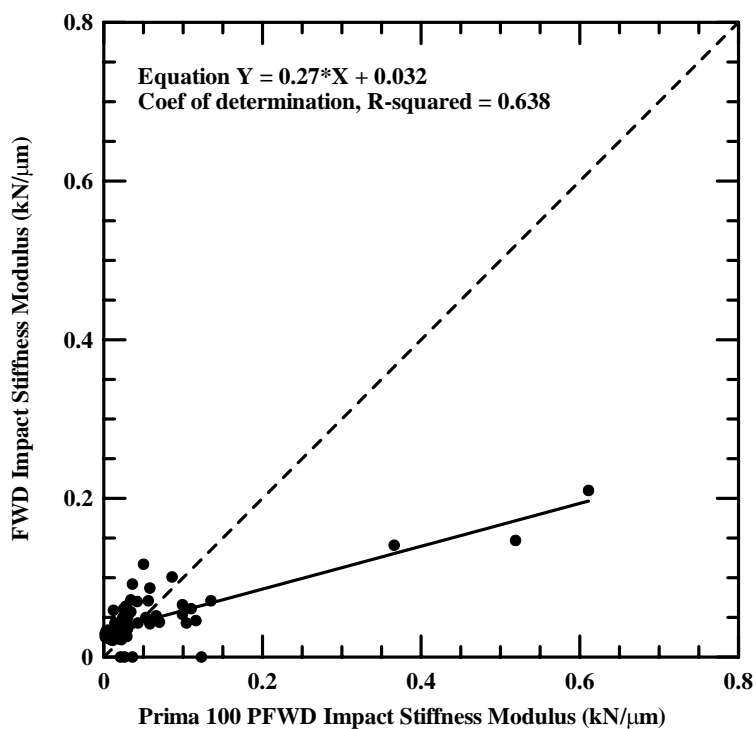


Figure 4.72 Comparison of FWD and PFWD ISM at Lakeside Landing Road, Glenburn, Maine.

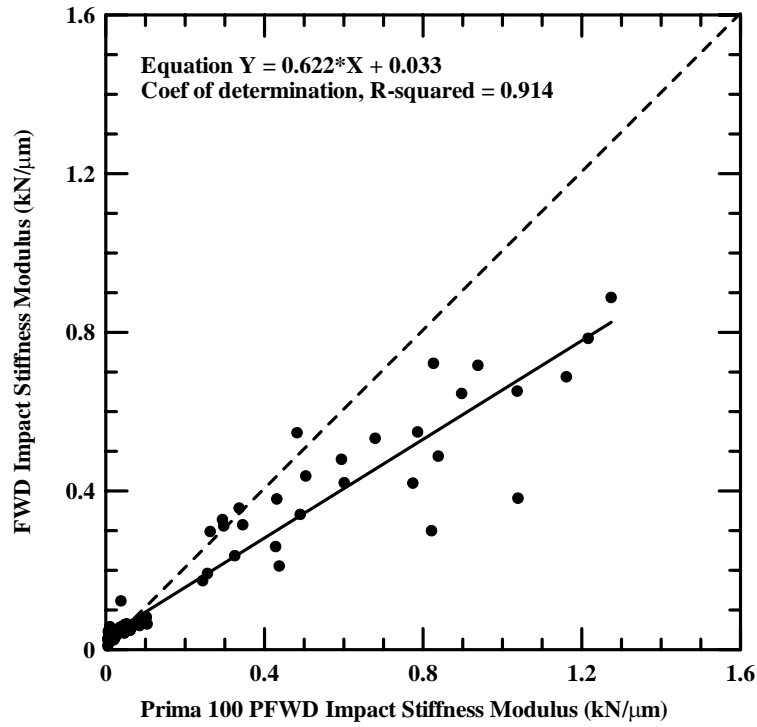


Figure 4.73 Comparison of FWD and PFWD ISM at Crosstown Road, Berlin, Vermont.

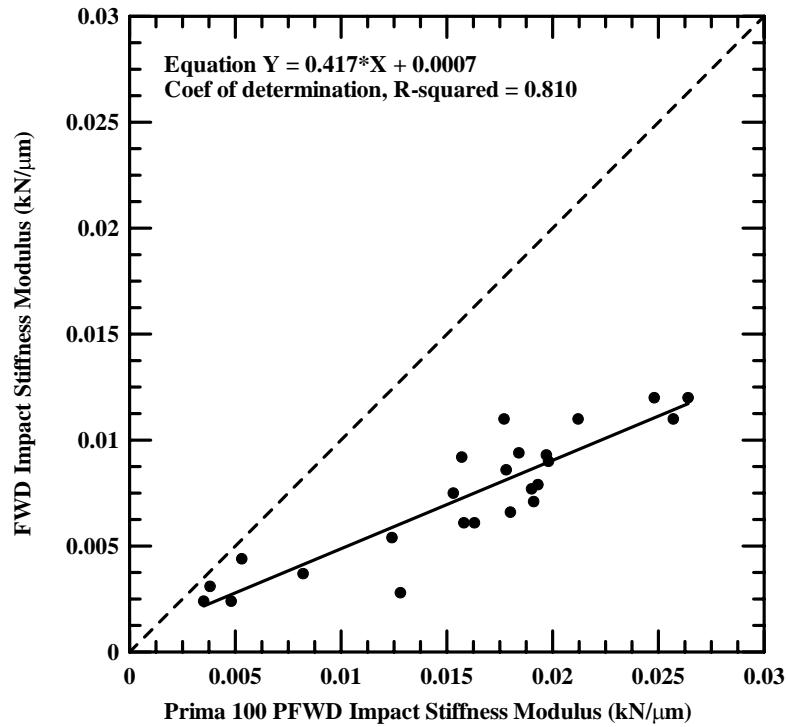


Figure 4.74 Comparison of FWD and PFWD ISM at USFS Parking Lot, Rumney, New Hampshire.

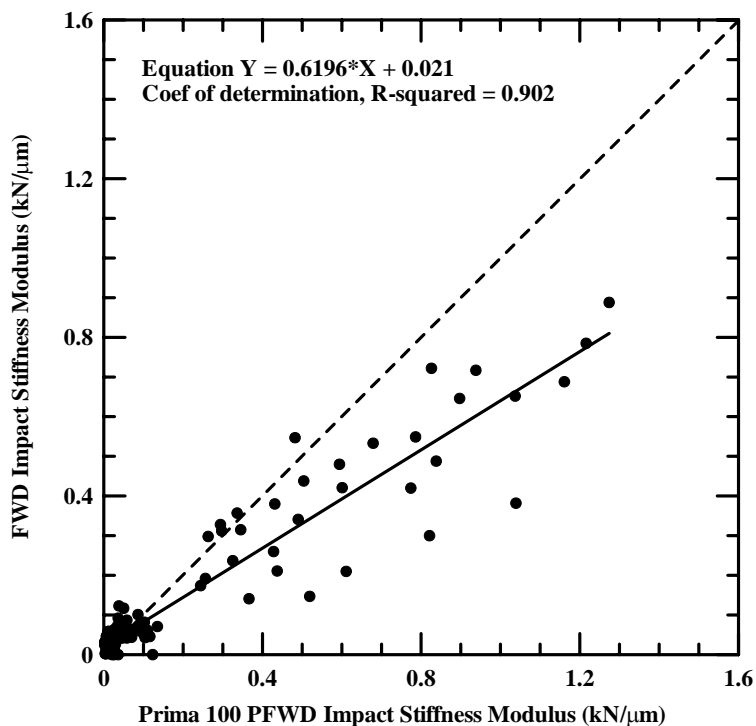


Figure 4.75 Comparison of FWD and PFWD ISM for all gravel surfaced test sites.

4.6 COMPARISON TO OTHER PORTABLE DEVICES

The traditional FWD was used as the basis for comparison for the Prima 100 PFWD, Loadman PFWD, Humboldt Soil Stiffness Gauge (SSG), and Clegg Impact Hammer. Loadman PFWD measurements were taken at Stinson Lake Road, Buffalo Road, and the USFS Parking Lot (2003 and 2004). SSG measurements were taken at the USFS Parking Lot during the spring of 2003. Clegg Impact Hammer measurements were taken at the USFS Parking Lot site during the spring of 2003 and 2004. A description of each of the portable devices is provided in Section 2.2.1. The Clegg Impact Hammer, Soil Stiffness Gauge, and the Prima 100 PFWD do not share a common variable with the FWD that can be compared. As a result, comparisons are only made between the Prima

100 and Loadman PFWDs. Comparisons between the devices and the FWD were developed and are presented separately in the following section.

Loadman and Prima 100 PFWD composite moduli are compared to FWD derived subbase moduli for two asphalt surfaced test sites in Rumney, New Hampshire. Best fit lines correlating the two devices with FWD subbase moduli are shown in Figure 4.76. In addition, Loadman composite moduli are plotted versus date and presented in Figures 4.5, 4.6, 4.21, 4.22, and 4.23. Correlations developed for asphalt surfaced test sites indicate that for a given FWD derived subbase modulus, the Loadman PFWD provides a composite modulus which is greater than the corresponding value provided by the Prima 100. The Prima 100 PFWD correlates better to FWD derived subbase moduli ($r^2 = 0.552$) than composite moduli obtained from the Loadman PFWD ($r^2 = 0.245$). The Loadman PFWD uses a smaller loading plate diameter and drop weight. As a result, higher moduli are obtained because only the upper most pavement section is influenced. Correlations developed for gravel surfaced test sites indicate that for a given Prima 100 PFWD composite modulus, the corresponding Loadman PFWD modulus is lower due to the shallow depth of influence.

Based on these results, it appears that the Prima 100 PFWD is a better tool to aid in tracking seasonal stiffness variations. In addition, the Prima 100 is more versatile than the Loadman as discussed in Section 2.2.2.1 and 2.2.2.2. Prima 100 PFWD input parameters allow the user to differentiate between asphalt, gravel, and other materials by selecting appropriate stress distribution factors and Poisson's ratio. However, this recommendation is based on results from only two asphalt surfaced test sites (Buffalo Road and Stinson Lake Road).

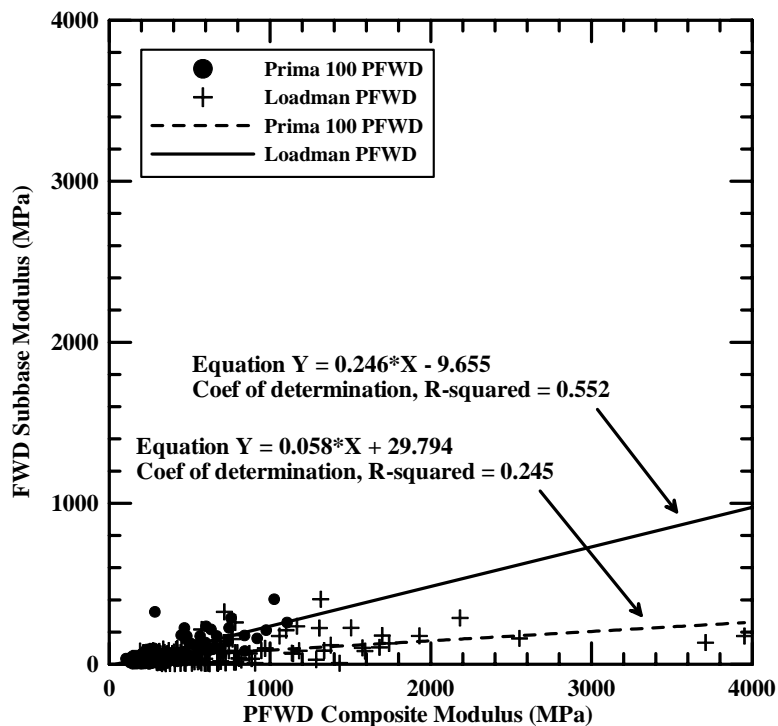


Figure 4.76 Comparison of FWD derived subbase moduli to Loadman and Prima 100 PFWD composite moduli on asphalt surfaced test sites.

4.7 EVALUATION OF FIELD TESTING TECHNIQUES

A number of different testing techniques were developed and implemented. The effect of drop weight, loading plate diameter, and drop height was investigated. In addition, multiple measurements were taken at each test location in order to examine the extent to which moduli change with subsequent drops. Lastly, additional geophones were used at each test site to investigate their usefulness. The influence of these variations on testing techniques are presented in the following sections.

4.7.1 Loading Plate Diameter and Drop Weight

The Keros Prima 100 PFWD was purchased in March 2003. At that time, the device came standard with 100 and 300 mm (4 and 12 in.) diameter loading plates and

one 10 kg (22 lb) drop weight. A 200 mm (8 in.) diameter loading plate and two 5 kg (11 lb) weights were also purchased. A preliminary study on an asphalt surfaced parking lot was undertaken to investigate the differences in moduli derived from using different combinations of drop weight and loading plate diameter. Measurements were taken at three different locations. The details of the findings are presented in Figure 4.77, and are discussed below.

In general, the 20 kg (44 lb) drop weight produced the lowest moduli. Moduli were independent of loading plate diameter. The 15 kg (33 lb) weight produced moduli that were greater than those obtained with the 20 kg (44 lb.) and also did not vary significantly with loading plate diameter. The highest moduli were obtained using the 10 kg (22 lb) drop weight. Moduli decreased with increasing loading plate diameter.

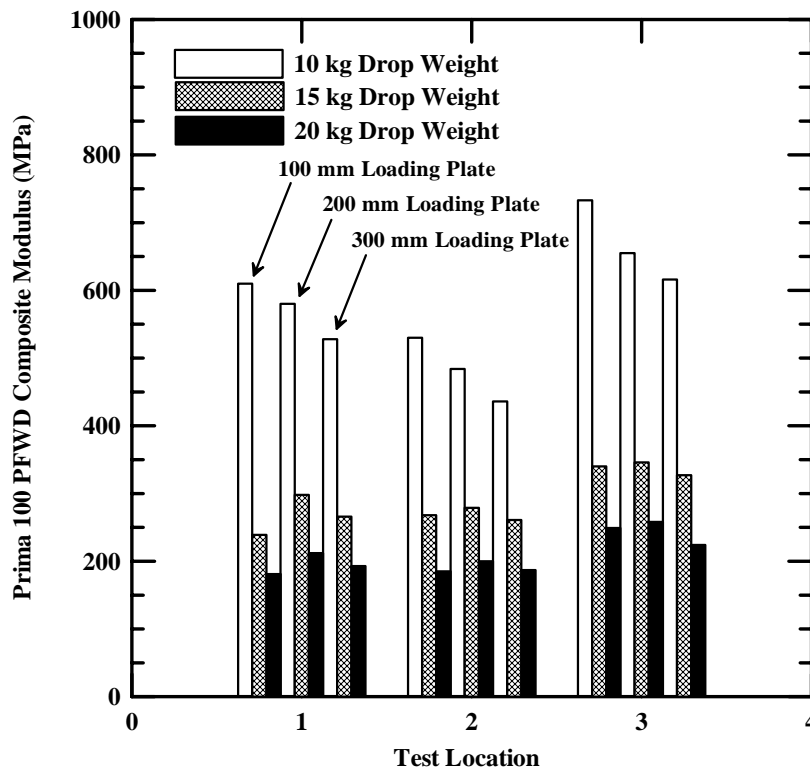


Figure 4.77 Effect of drop weight and loading plate diameter on Prima 100 PFWD composite moduli.

Reducing the drop weight to 10 kg (22 lb) results in a significantly higher modulus and as noted above, plate diameter has a larger effect. Small plate diameter and drop weight influence only the upper portions of the pavement section and thus the deflection responses are dominated by the stiffer pavement layer, producing a larger composite modulus. When plate diameter and drop weight are increased, depth of influence is increased and the stiffness of both the subbase and asphalt layers are reflected in the composite modulus, resulting in a lower value. During the spring thaw period, it is desirable to measure the stiffness of the subbase layer since it, not the asphalt layer, is more likely to undergo thaw weakening and recovery. As a result, it is recommended that the largest loading plate and drop weight be used in order to maximize the influence on the subbase layer.

4.7.2 Drop Height

Drop heights ranging from 10 to 850 mm (0.4 to 33.5 in.) may be used with the Prima 100 PFWD. Measurements were taken at three different drop heights at each test location throughout the monitoring period. Drop heights used were approximately equal to 850, 630, and 420 mm (33.5, 24.8, and 16.5 in.). Plots with best fit lines comparing moduli derived from different drop heights with FWD composite moduli are presented in Figures 4.78 through 4.80. In general, reduced drop heights produce moduli that are slightly less than moduli derived from using the full (850 mm) drop height. This trend is evident regardless of asphalt thickness, however, the differences tend to decrease with increasing asphalt thickness as illustrated in Table 4.8. Decreasing drop height reduces the depth of influence. When asphalt thickness increases and drop height is reduced simultaneously, measured moduli are heavily influenced by the stiffness of the asphalt

layer. For the purpose of monitoring seasonal stiffness variations, it is desirable to influence the greatest depth possible. As a result, it is recommended that the 850 mm (33.5 in.) drop height be used.

Table 4.8 Summary of the effects of reduced drop height on PFWD composite modulus for different asphalt thicknesses.

Test Site	Asphalt Thickness mm (in.)	FWD Composite Modulus (MPa)	Drop Height (mm)	Prima 100 PFWD Composite Modulus (MPa)	Percent Difference (%)
Witter Farm Road	127 (5)	2000	850	2498	24.9
			630	2444	22.2
			420	2271	13.6
Route 126	152 (6)	1000	850	960	4.0
			630	909	9.1
			420	889	11.1
Route 1A	178 (7)	3000	850	6430	114.3
			630	5651	88.4
			420	5663	88.8

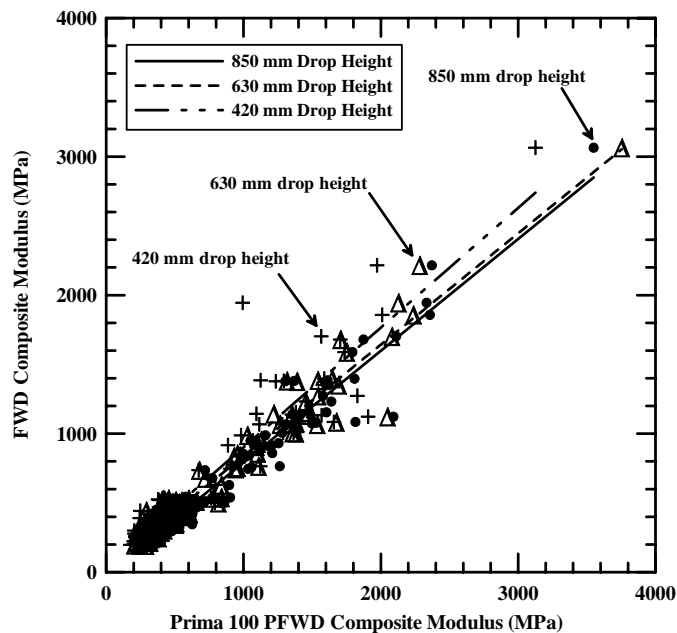


Figure 4.78 Effect of drop height on PFWD composite moduli at Witter Farm Road, Orono, Maine.

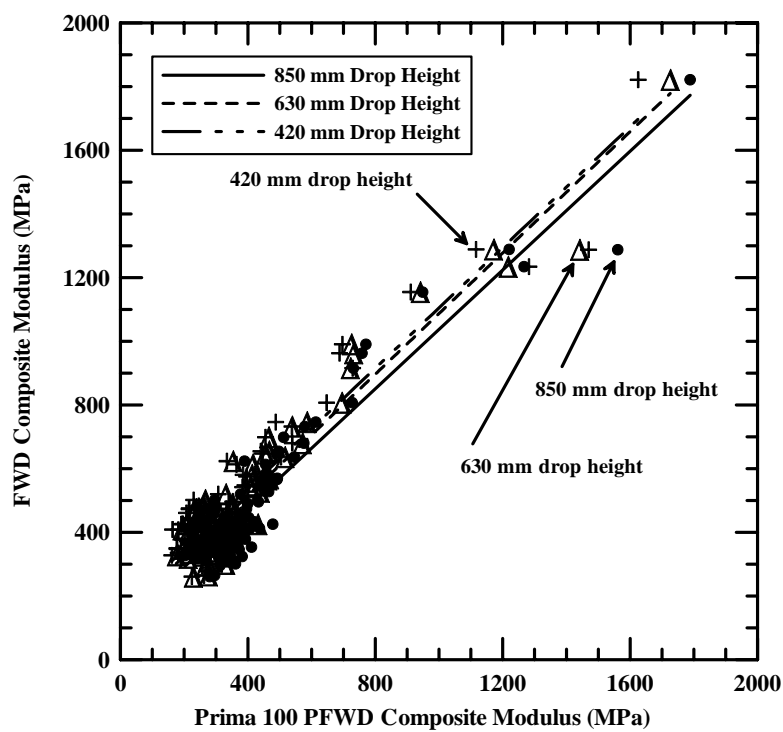


Figure 4.79 Effect of drop height on PFWD composite moduli at Route 126, Monmouth/Litchfield, Maine.

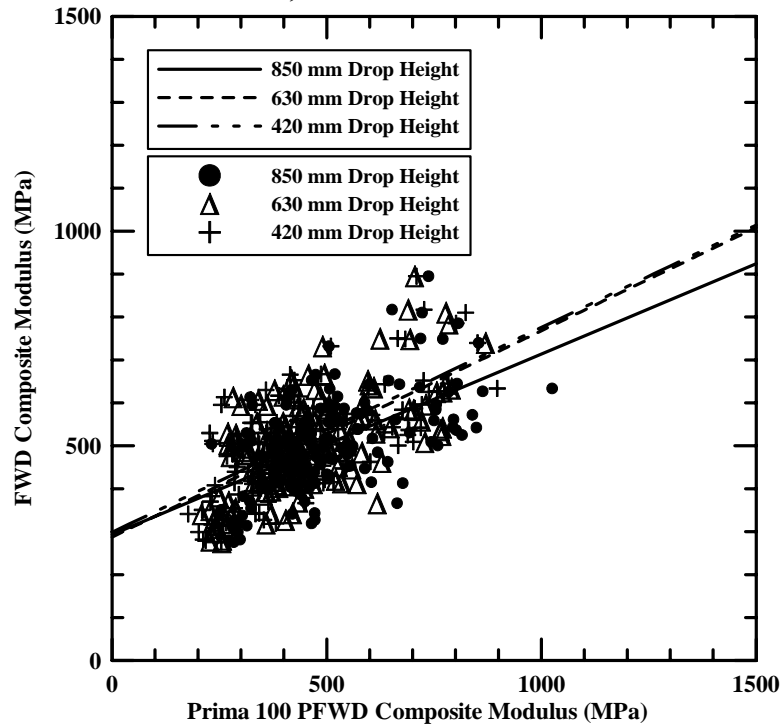


Figure 4.80 Effect of drop height on PFWD composite moduli at Route 1A, Frankfort/Winterport, Maine.

4.7.3 Moduli Derived from Additional Geophones

The Keros Prima 100 PFWD comes standard with one geophone. Two additional deflection sensors were purchased. Three deflection sensors were used at each site to observe differences in moduli derived from measurements taken from each of the geophones. Spacing of the sensors is as follows (as measured from the center of the loading plate): 0, 207, and 407 mm (0, 8, and 16 in.). Prima 100 PFWD software determines moduli from the measurements of just one geophone at a time by using the Boussinesq equations described in Section 2.2.2. Thus, when three geophones are used, three calculations for modulus are performed, yielding three estimates of composite modulus. In addition, unsuccessful attempts were made to use backcalculation software intended for a conventional FWD using all three geophone measurements in order to derive moduli for individual layers. Future research should be conducted to develop backcalculation software for the Prima 100 PFWD that uses all three sensors to estimate layer moduli. Results for asphalt and gravel surfaced roads are presented in Figures 4.81 through 4.83. Unless software can be developed to incorporate deflections from additional geophones into a more common backcalculation routine, additional geophones do not provide meaningful information. Based on the quality of the correlations between FWD derived moduli and PFWD moduli determined from the center geophone, it is recommended that only one geophone be used.

Table 4.9 Summary of the effects of reduced drop height on PFWD composite moduli for different asphalt thicknesses.

Test Site	Asphalt Thickness mm (in.)	FWD Composite Modulus (MPa)	Radial Offset (mm)	Prima 100 PFWD Composite Modulus (MPa)	Percent Difference (%)
Kennebec Road	127 (5)	10000	0	23057	131
			207	97586	8759
			407	119162	1092
Route 126	152 (6)	5000	0	5247	5
			207	27608	452
			407	24513	390
Route 1A	178 (7)	2000	0	4054	103
			207	17346	767
			407	20397	920

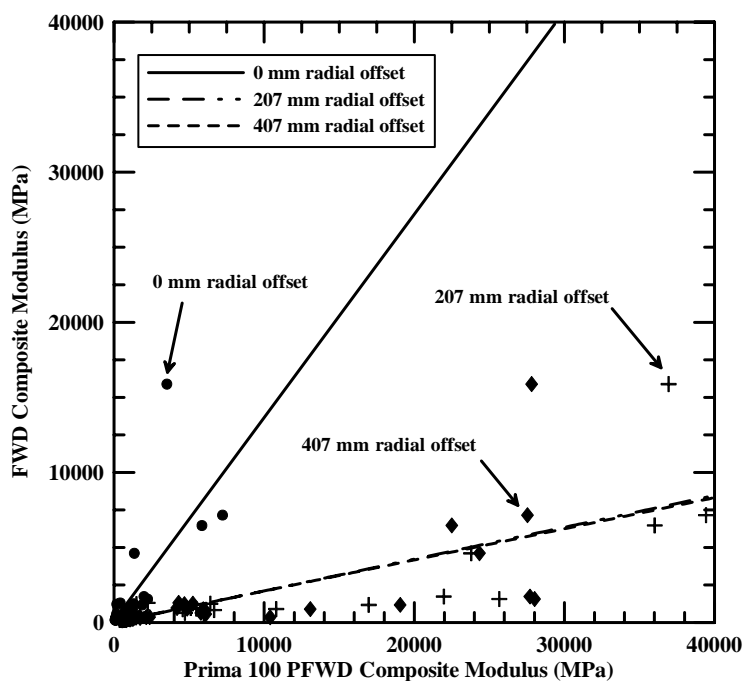


Figure 4.81 Comparison of FWD composite moduli to PFWD composite moduli derived from different geophones at Kennebec Road, Hampden/Dixmont, Maine.

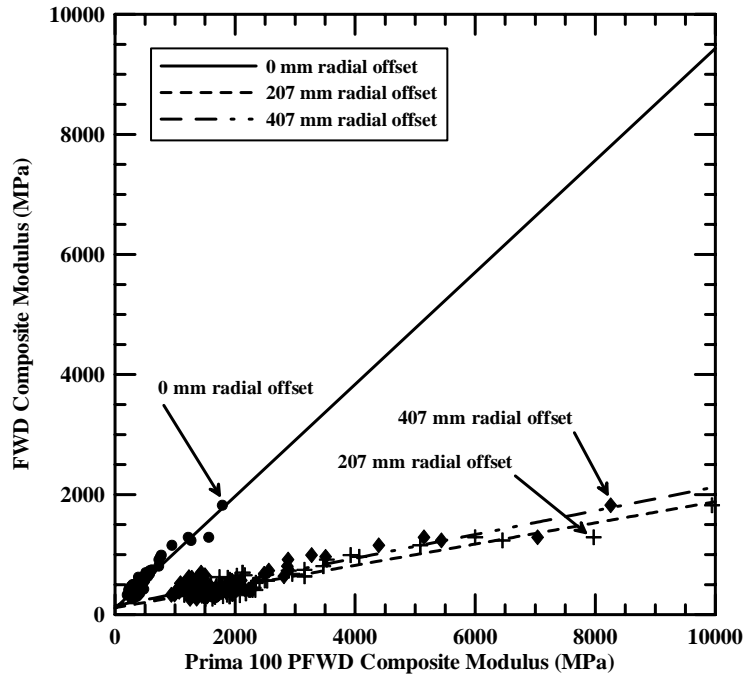


Figure 4.82 Comparison of FWD composite moduli to PFWD composite moduli derived from different geophones at Route 126, Monmouth/Litchfield, Maine.

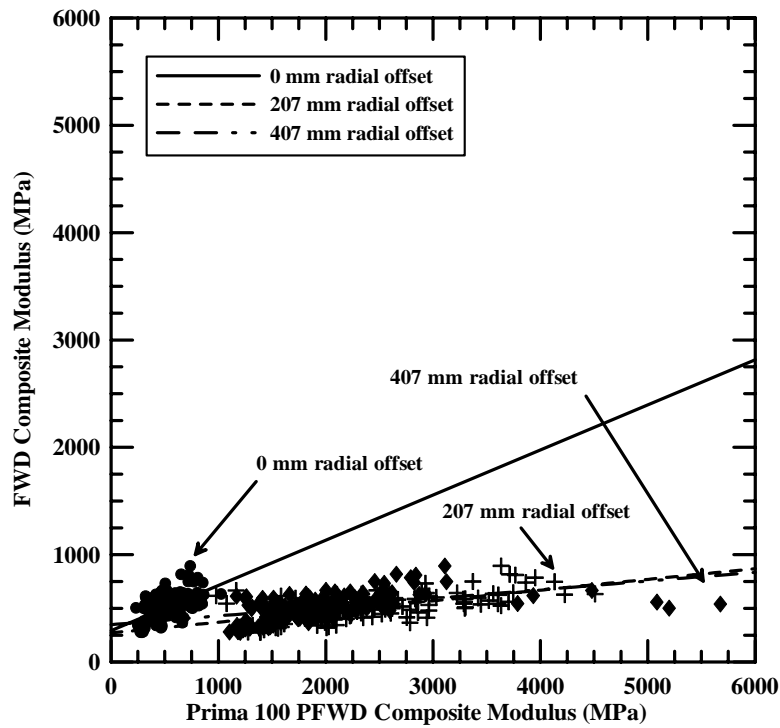


Figure 4.83 Comparison of FWD composite moduli to PFWD composite moduli derived from different geophones at Route 1A, Frankfort/Winterport, Maine.

4.7.4 Multiple Measurements at Each Test Location

Previous researches noted differences in moduli when taking multiple measurements at the same test location. Many researchers performed multiple measurements at each test location and suggested disregarding one or more of the initial readings, using the remaining measurements to determine a representative value. Six Prima 100 PFWD measurements were taken at each of three different drop heights, at each test location. In all cases, the first reading was neglected and the average of the remaining five was used for analysis and comparison. Observations by the researchers during field testing indicated that for the majority of points tested at all field sites; the first measurement was less than subsequent measurements. The difference between the first measurement and subsequent measurements is depicted in Figure 4.84 and Figure 4.85.

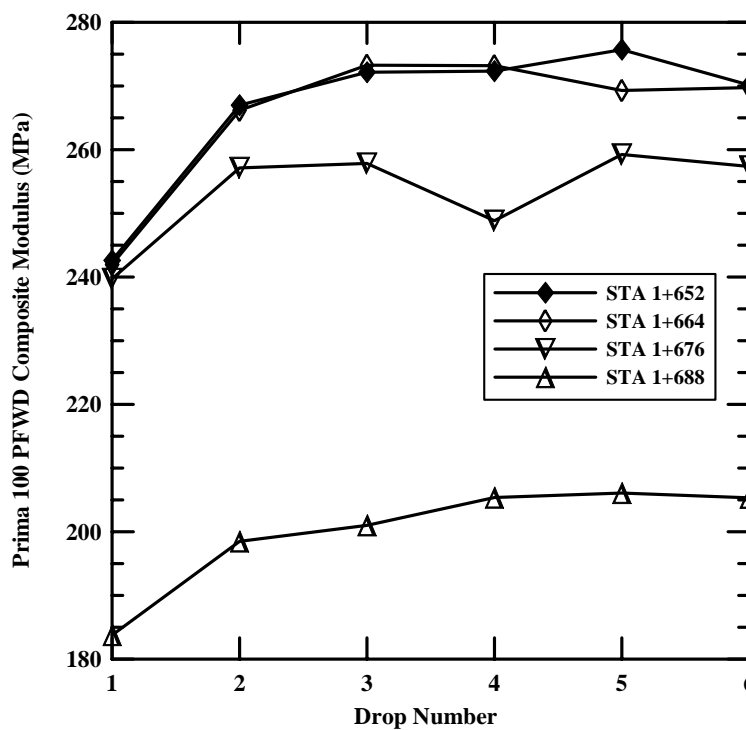


Figure 4.84 Effect of consecutive drops on composite modulus on May 12, 2004 at Route 126 (Section 3), Monmouth/Litchfield, Maine.

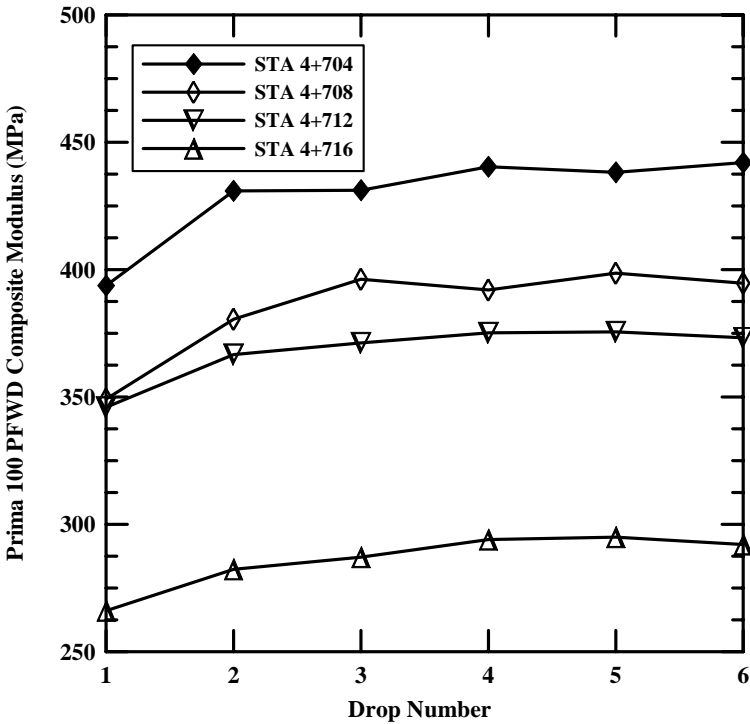


Figure 4.85 Effect of consecutive drops on composite modulus values on April 22, 2004 at Route 126 (Section 12), Monmouth/Litchfield, Maine.

In order to quantify this phenomenon, all measurements taken at Route 126 in the towns of Monmouth and Litchfield, Maine were analyzed. The first, second, and third measurements were compared to the average of the remaining measurements. These results are shown in Table 4.10. The observations confirm those made by other researchers discussed in Chapter 2. In any case, no matter the total number of drops selected for each test location and the material being tested, at least the first measurement should be ignored. The representative value should be determined from an average of the remainder of measurements taken at that test location.

Table 4.10 Comparison of the first, second, and third measurements with successive measurements at Route 126, Monmouth/Litchfield, Maine.

Average Value of First Measurement (MPa)	Average of Five Remaining Measurements (MPa)	Percent Difference (%)
388	428	9.4
Average Value of Second Measurement (MPa)	Average of Four Remaining Measurements (MPa)	Percent Difference (%)
426	430	0.95
Average Value of Third Measurement (MPa)	Average of Three Remaining Measurements (MPa)	Percent Difference (%)
428	429	0.35

4.8 RECOMMENDATIONS

There are few straight forward procedures to aid in determining the need for weight restrictions, the magnitude of the restriction, and when to place and remove the restriction from paved and unpaved, low volume roads. The basis of the methods for placing and removing load restrictions include observing the pavement structure for signs of distress, measuring surface deflections, and more recently, predicting thaw from air temperature data. For a load restriction policy to be implemented successfully it must be as simple as possible, yet include the most important factors common to the greatest number of roadway miles (Ovik, et al., 2000). In the following, we recommend procedures for using a PFWD to determine if a road should be posted for weight restriction and then a procedure to determine the duration of the restriction.

4.8.1 Factors that Affect Need for Seasonal Load Restrictions

As discussed by Rutherford, et al. (1985) many factors exist that should be considered when determining whether seasonal load restrictions are necessary at a particular location. These factors are listed below.

1. Pavements with surface deflections 45 to 50% higher during spring thaw than summer.
2. Pavements with frost susceptible subbase and subgrade material.
3. Pavement with subgrade soils classified as ML, MH, CL, and CH.
4. Roads which have historically exhibited deterioration during the spring thaw period.
5. Pavements in which distress has been observed (fatigue cracking and rutting).

The procedure that is recommended in the next section for use of the Prima 100 PFWD should be applied with due consideration of the factors listed above.

A procedure for using the PFWD to place and remove load restrictions is presented in the following section. The procedure is then applied to the field sites monitored as part of this study.

4.8.2 Field Testing Techniques

Field testing techniques for monitoring seasonal stiffness variation in paved and unpaved low volume roads using the Prima 100 PFWD have been developed. The recommendations are based on the experiences of the researchers in using the Prima 100 PFWD as discussed in previous sections and the techniques developed by previous researchers (Rutherford, et al., 1985; Van Deusen 1998; Ovik, et al., 2000). The

procedure relies on comparing composite moduli during the spring thaw to fully recovered values measured during the summer and fall. Thus, the underlying premise is that composite modulus is the primary factor controlling damage to the road section.

The researchers selected 80% of the fully recovered composite modulus as the trigger value for application and removal of load restrictions. The selection of 80% is arbitrary since the amount of damage that would occur at the reduced modulus depends on individual pavement sections, allowable vehicle weight, and traffic levels.

Assessment of these factors was beyond the scope of this study. Individual transportation agencies should examine these issues in light of the amount of damage that is acceptable to the road during the spring thaw period and the consequences to the regional economy that are created by weight restrictions.

The procedure recommended by the researchers is outlined in the following steps. It can be used to determine when to apply and remove load restrictions. In addition, it can be used as a screening procedure to identify roads that do not require posting.

1. For each road to be monitored, identify critical sections of the road that are most susceptible to spring thaw damage based on previous performance, soil type, access to ground water, or other factors. Within each critical section, select four test points. Test points should span the inside and outside wheelpaths in both travel lanes, if present. The location of the points should be marked so that the same locations can be tested on each test day.
2. Setup the Prima 100 PFWD with the 850 (33.5 in.) drop height, 20 kg (44 lb) drop weight, and 300 mm (12 in.) diameter loading plate.

3. Setup the Personal Digital Assistant (PDA) based recording software using the input parameters presented in Table 4.11.

Table 4.11 Prima 100 PFWD input parameters.

Setup Menu Item	Input Parameter	Asphalt Surfaced Test Sites	Gravel Surfaced Test Sites
Trigger	Pretrig time (ms)	10*	
	Pulsebase (%)	24*	
	Trig Level (kN)	0.90*	
View	Sample Time (ms)	60*	
Mechanical	Load Plate Radius (mm)	150	
	Number of sensors	1	
	D ₍₁₎ offset (cm)	0	
Formula	Poisson's Ratio	0.35**	0.35**
	Stress Distribution	2.0	2.67

* - default values

** - Huang (2004)

4. Establish moduli for each test point that are representative of the fully recovered period by taking readings at each test point during the summer and early fall. Readings should be taken on days that correspond to periods that are relatively dry. A reading at an individual test point is the average of drops 2 through 6. The results from drop 1 are discarded. It is recommended that readings be taken on four days spanning the summer and early fall. Average the four daily readings at each point to obtain the fully recovered composite modulus for that point. Finally, average the recovered composite modulus from each test point to obtain the recovered composite modulus for the section. Multiply this value by 80% to obtain the trigger value for load restriction application/removal.
5. Using the same test points and testing techniques that were used to establish the baseline values, take periodic readings at the start of the spring thaw. During the

critical thawing period, it may be necessary to take readings daily. Taking readings in the afternoon is preferred to avoid the influence of possible refreezing during the previous night. A reading at an individual test point is the average of drops 2 through 6. The results from drop 1 are discarded. Apply the load restriction when the average of the composite moduli at the test points in the section drops below 80% of the baseline (recovered) values.

6. Continue to take periodic readings, at least weekly. Once the average of the composite moduli at the test points in the section readings exceed 80% of the baseline (recovered) values for two consecutive sets of measurements the load restriction may be removed.
7. Sites where the moduli remain above 80% of the recovered value are potential candidates for roads that do not require posting.

4.8.3 Application of Procedure to Field Sites

Of the ten test sites monitored during the spring of 2004, four showed distinct minimum composite moduli during the thawing period before increasing into the recovery period. Asphalt surfaced test sites were Buffalo Road and Knapp Airport Parking Lot. Gravel surfaced sites were the USFS Parking Lot and Crosstown Road. Application of the criteria described in the previous section for placing and removing load restriction is applied to spring thaw test sites and is shown in Figures 4.86 through 4.89. The procedure was also used with available results from the FWD. A summary of the dates for placing and removing the restrictions are summarized in Table 4.11. In

general, the posting and removal dates determined by the PFWD and FWD agree within one week.

It should be noted that the recovered composite modulus used in the application of the procedure recommended in Section 4.8.2 were based on a single reading date in June rather than the average of four reading dates in late summer and early fall. Thus, the interpretation of the duration of the load restriction may have been somewhat different had the latter readings been available. Moreover, readings were taken weekly, whereas the composite modulus can experience a dramatic reduction over this period as illustrated in Figures 4.88 and 4.89. This shows the importance of taken readings more frequently during the thawing period.

Table 4.12 Summary of load restrictions for spring thaw field test sites.

Test Site	Restriction Posting Date		Date of Minimum Modulus		Restriction Removal Date		Date of Final Reading	
	PFWD	FWD	PFWD	FWD	PFWD	FWD	PFWD	FWD
Buffalo Road	3/25	3/18	4/1	3/25	4/15	4/8	6/9	6/9
USFS Parking Lot	4/1	NA	4/1	NA	5/14	NA	6/9	NA
Knapp Airport Parking Lot	NA	NA	3/26	4/2	5/14	NA	6/10	6/10
Crosstown Road	4/2	4/2	4/2	4/9	5/14	5/14	6/10	6/10

NA – not available – could not be determined from available data.

This research found that roads that have undergone full depth reconstruction with 125 mm (5 in.) or more of pavement supported by 600 mm (24 in.) of non-frost susceptible base (Witter Farm Road, Route 1A, and Route 126) did not experience a seasonal reduction in the composite resilient modulus, as shown in Figures 4.12 through 4.20, and thus do not require seasonal weight restrictions.

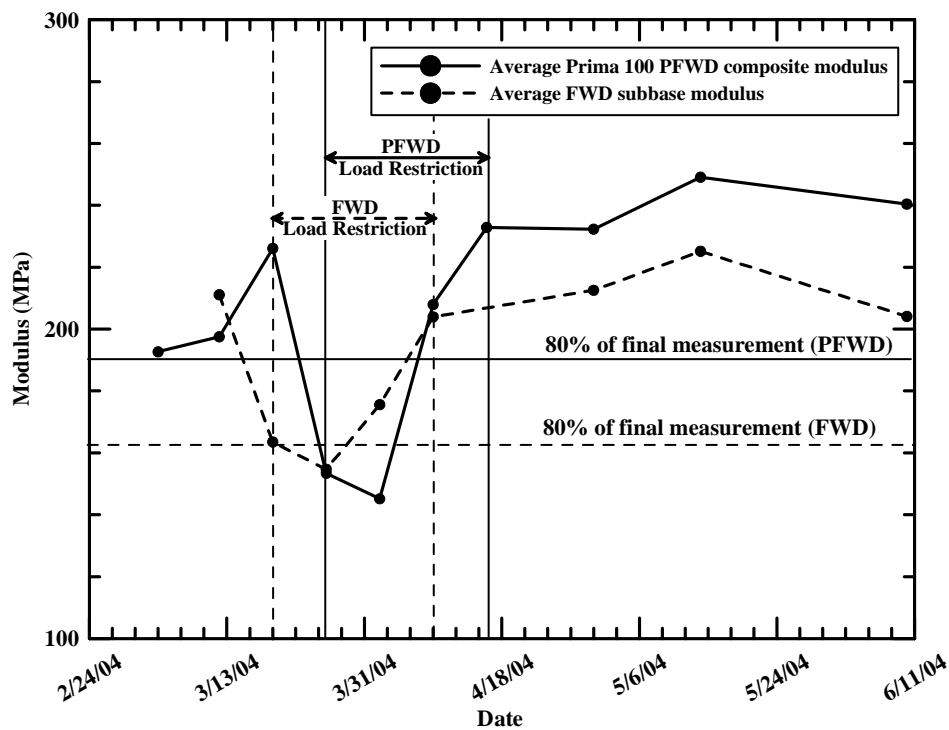


Figure 4.86 Buffalo Road, Rumney, New Hampshire.

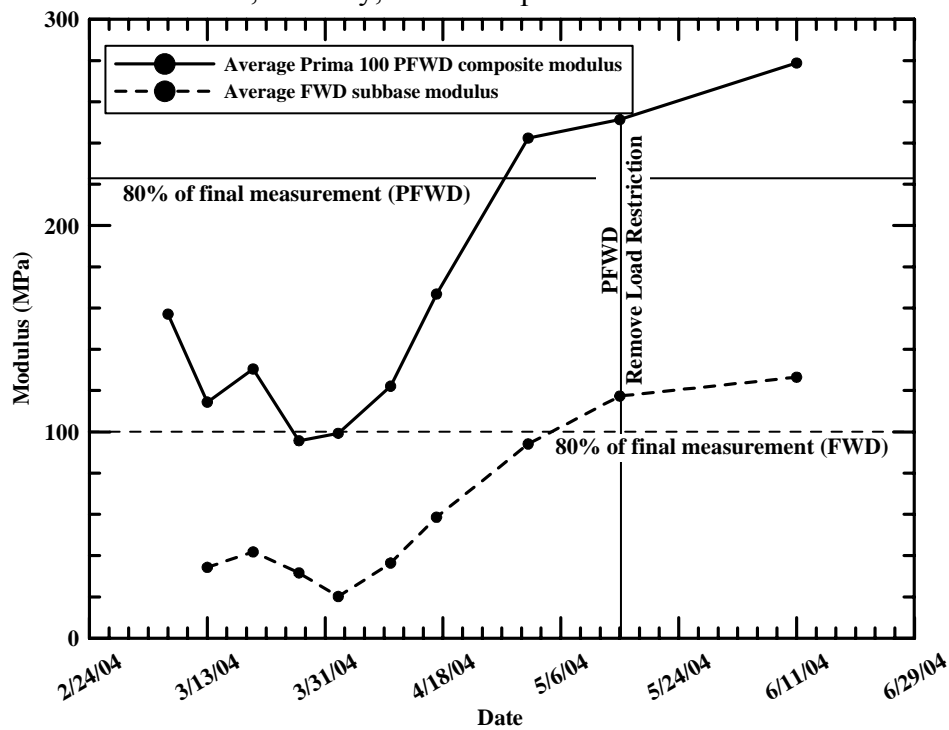


Figure 4.87 Knapp Airport Parking Lot, Berlin, Vermont.

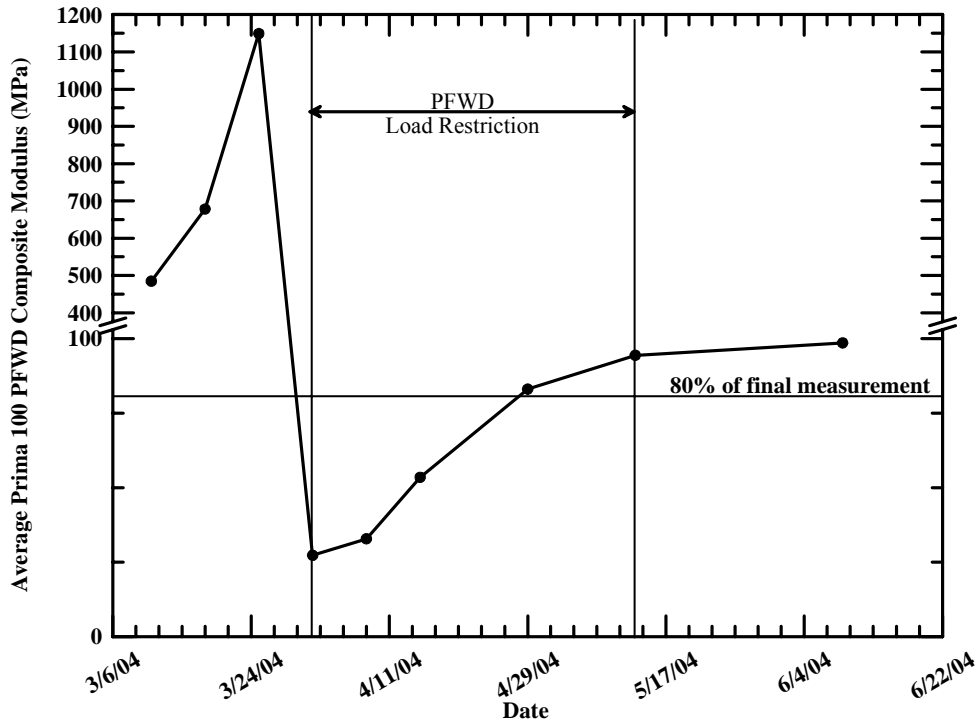


Figure 4.88 USFS Parking Lot, Rumney, New Hampshire.

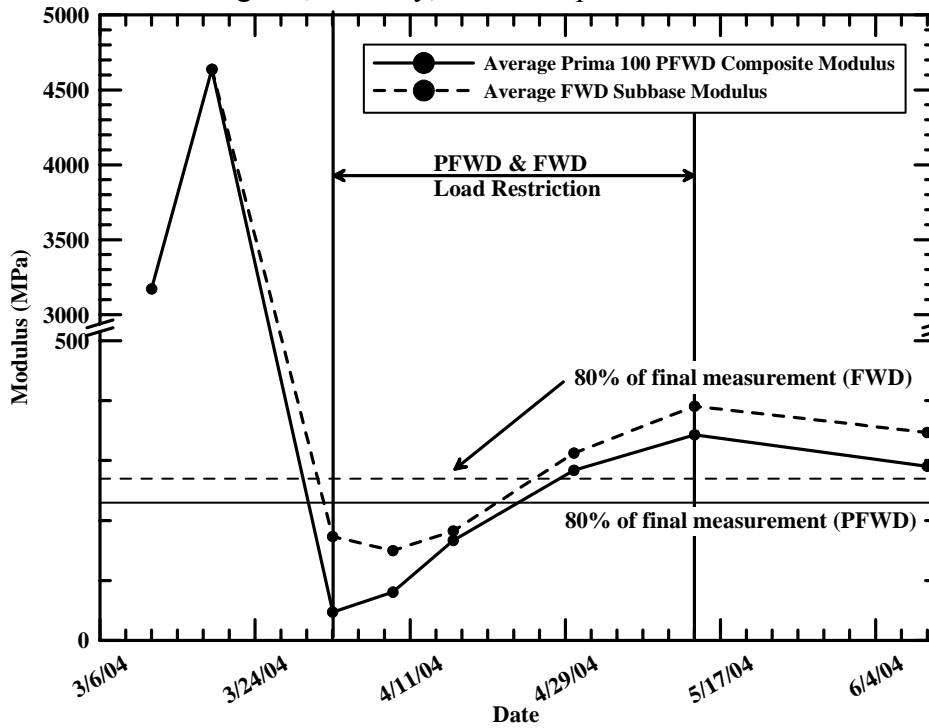


Figure 4.89 Crosstown Road, Berlin, Vermont.

4.9 SUMMARY

The results of monitoring seasonal stiffness variations in paved and unpaved, seasonally posted, low volume roads were presented and assessed in this chapter. For sites where the traditional FWD indicated a decrease in composite modulus during the spring thaw, the Prima 100 PFWD followed similar trends. Similarly, at sites where the FWD did not show a decrease in composite modulus, neither did the PFWD. Based on this result, the Prima 100 PFWD would be equally effective as a traditional FWD in determining when to place and remove load restrictions.

Prima 100 PFWD composite moduli were compared to composite moduli derived from the traditional FWD. Regression analyses comparing composite moduli from both devices yielded correlation coefficients for individual sites ranging from 0.336 (Route 1A) to 0.950 (Witter Farm Road). In general, PFWD composite moduli were slightly less than FWD composite moduli. Correlation coefficients tended to increase with decreasing pavement thickness. When combining all the results for paved roads, a strong correlation exists between Prima 100 PFWD and FWD derived composite. Ignoring errant FWD moduli greater than 4000 MPa (41,770 tsf), the regression coefficient for all the data combined was 0.809. Looking at subsets of the data confirmed that the regression coefficient increased as the pavement thickness decreased. This suggests that the PFWD could be used in lieu of an FWD for determination of composite modulus.

Regression analyses comparing composite and subbase moduli yielded correlation coefficients ranging from 0.163 (Route 1A) to 0.807 (Knapp Airport Parking Lot). Again, correlation coefficients tended to increase as pavement thickness decreased. The

PFWD had a reasonable correlation with FWD derived subbase moduli, suggesting that the Prima 100 composite moduli are at influenced in part by the subbase layer.

Impact Stiffness Modulus (ISM) is the ratio of applied load to the deflection measured by the center sensor (geophone). ISM values were determined for both the traditional and portable FWD. Regression analyses for paved test sites yielded correlation coefficients ranging from 0.488 (Route 1A) to 0.937 (Witter Farm Road). Correlations coefficients increased with decreasing asphalt thickness. Regression analyses for gravel test sites yielded correlation coefficients ranging from 0.638 (Lakeside Landing Road) to 0.914 (Crosstown Road). PFWD and FWD derived ISM appear to equally effective indicators of section stiffness for sites with asphalt pavements less than about 150 mm (6 in.) and gravel surfaced sites.

Loadman and Prima 100 PFWD derived composite moduli were compared to subbase moduli as determined from the traditional FWD for two asphalt surfaced test sites. This was done to determine which device would serve as a better tool for evaluating seasonal stiffness variations. The Prima 100 produced larger composite moduli than the Loadman and correlated better with the FWD derived moduli, producing an $r^2 = 0.552$. In contrast, the Loadman PFWD produced an $r^2 = 0.245$. It was recommended that the Prima 100 PFWD would serve as a better tool to aid in tracking seasonal stiffness variations.

Several testing techniques were used to observe their influence on composite moduli. The effect of drop weight, loading plate diameter, and drop height were investigated. Additionally, multiple measurements were taken at each test point with additional geophones. The lowest drop weight (10 kg) resulted in significantly higher

moduli, most likely because results for the lowest weight were primarily influenced by the stiffer pavement layer. Loading plate diameter had little effect. The largest drop weight and loading plate diameter are recommended for spring thaw monitoring.

Three different drop heights were used. Reduced drop heights produce moduli that are slightly less than moduli derived from using the full drop height. Increased asphalt thickness reduces the difference between moduli obtained from different drop heights. It is recommended that the full drop height be used.

Three different geophones were used for testing. The geophones were located at distances of 0, 207, and 407 mm (0, 8, and 16 in.) from the center of the drop plate. Deflection measurements from each geophone were used to make three separate calculations of modulus. The geophones located 207 and 407 mm (8 and 16 in.) from the center produced moduli that are unrealistically large. It is recommended that only the center geophone be used for testing. Future research should focus on developing backcalculation software for the Prima 100 that would enable measurements from all geophones to be simultaneously incorporated into a backcalculation routine.

Multiple PFWD measurements were taken at each test location to investigate how composite moduli change with successive drops. The first drop differed from the average of the remaining five measurements by nearly 10%. Whereas, the second drop differed from the average of the remaining four measurements by approximately 1%. It was recommended that the first measurement be neglected when determining the composite modulus for a particular test location.

Finally, recommendations were made on how the Prima 100 PFWD could be used to determine when spring load restrictions should be placed and removed, as well as,

roads where spring load restrictions were unnecessary. The core of the recommendations are that the load restrictions are placed and removed once the composite moduli measured with the PFWD reach 80% of the fully recovered baseline value measured during the summer and early fall.

CHAPTER 5

COMPACTION CONTROL

5.1 INTRODUCTION

This chapter presents the analysis and results of the field and laboratory evaluation of the Portable Falling Weight Deflectometer (PFWD) as an alternative to traditional compaction control devices. The objective of this portion of the research project was to establish a procedure for using the PFWD for compaction control. As part of this effort, the relationship between PFWD composite moduli and percent compaction for soil types representative of New England base and subbase aggregates was explored.

PFWD and Nuclear Moisture Density Meter (NDM) measurements were taken at five field test sites during the summer and fall of 2003. In addition, laboratory tests were completed on five different samples during the summer of 2004. The primary purpose of the laboratory tests was to provide complementary results to those collected in field tests. However, laboratory work was completed under more carefully controlled conditions. Target dry densities for laboratory work were 90%, 95%, and 100% of the maximum dry density (AASHTO T 180). The effect of water content was investigated at approximately 95% of the maximum dry density with target water contents equal to optimum and $\pm 3\%$ of the optimum water content (OWC). A more detailed description of laboratory testing procedures may be found in Section 3.5. Comparative side by side tests of PFWDs by multiple manufacturers were completed. Tests were done to investigate repeatability, accuracy, and susceptibility to operator technique.

This chapter is organized as follows. Water content and density measurements are compared and verified. This is followed by the effect of percent compaction and water content on modulus (stiffness) observed in both field and laboratory tests. Statistical relationships are discussed. Comparisons between portable devices are made and correlations were developed to compare performance. The effect of operator technique is discussed. Lastly, recommendations are made for utilizing the Prima 100 PFWD as a tool to monitor compaction control.

5.2 IN-PLACE WATER CONTENT AND DRY DENSITY

Laboratory tests were performed on five soil types representative of New England base and subbase aggregates. These materials include: one crushed material, one construction sand, three base/subbase aggregates. Classification and laboratory compaction (AASHTO T 180) results for laboratory samples are summarized in Table 5.1. Gradation and moisture density curves for each sample may be found in Appendixes A and B, respectively.

For the laboratory tests, each soil sample was compacted in the test box initially at a low density. Measurements were taken and samples were then compacted to a higher density and the measurements repeated. In total, 29 combinations of water content and density were tested in the laboratory. For each trial, nuclear density gage (NDM) measurements were made at five locations. NDM density measurements at the 203 mm (8 in.) depth are used in this report unless noted otherwise. The average in-place dry density, percent compaction, water content, and water content relative to optimum from each trial as determined by the NDM is summarized in Table 5.2. For most of the trials,

the actual percent compaction and water content relative to optimum deviated somewhat from the target values. Nonetheless, the range of values was sufficient to explore relationships with PFWD composite modulus.

Table 5.1 Summary of laboratory samples.

Material Description		Grain Size Characteristics				Moisture Density Characteristics ²	
Type	Name	AASHTO Classification	Percent Gravel ¹ (%)	Percent Sand ¹ (%)	Percent Fines ¹ (%)	$\gamma_{d(max)}$ Mg/m ³ (lb/ft ³)	W _{opt} (%)
Crushed Material	Conn. crushed gravel	A-1-a	66.3	28.5	5.2	2.31 (144)	7.4
Construction Sand	N.H. sand	A-1-b	24.6	72.6	2.8	2.06 (128)	10.6
Base/ Subbase Aggregate	N.H. gravel	A-1-b	45.0	52.1	2.9	2.05 (128)	9.2
	OJF gravel	A-1-b	34.2	61.3	4.5	2.00 (125)	11.2
	Wardwell gravel	A-1-a	51.9	42.1	6.0	2.10 (131)	5.1

¹ – based on ASTM D 422.

² – based on AASHTO T 180.

Water content values obtained from the NDM were compared to oven dried test results in order to verify the accuracy of the NDM measurements. The NDM results were taken to be the average of five readings, one at each test location, taken at a 203 mm (8 in.) depth. Oven dried water contents are compared to NDM water contents in Figure 5.1. In general, water contents determined from the NDM were greater than oven dried samples. Oven dried samples produce true moisture content by removing all water present. The NDM measures hydrogen present in the material, which typically is in the form of water. If the material contains naturally occurring hydrogen or bound hydrogen, the NDM will measure the moisture falsely high in many cases (Troxler, 2004). The comparison produced a reasonable correlation with $r^2 = 0.549$. As a result, water

contents determined from the NDM were used as the basis for analysis and comparison in the remainder of this chapter.

Table 5.2 Summary of laboratory measurements.

Material	Target Test	Average Dry Density Mg/m ³ (lb/ft ³)	Average Percent Compaction (%)	Average Water Content (%)	Average Water Content Relative to Optimum (%)
Connecticut crushed gravel	90%, w_{opt}	2.07 (129)	90	5.8	-1.6
	95%, w_{opt}	2.26 (141)	98	6.0	-1.4
	100%, w_{opt}	2.37 (148)	103	6.5	-0.9
	95%, +3% w_{opt}	2.32 (145)	100	5.5	-1.9
	95%, -3% w_{opt}	2.15 (134)	93	4.3	-3.1
New Hampshire sand	90%, w_{opt}	1.78 (111)	86	8.2	-2.4
	95%, w_{opt}	1.86 (116)	91	8.2	-2.4
		1.91 (119)	92	8.9	-1.7
		1.91 (119)	94	9.0	-1.6
	95%, +3% w_{opt}	1.94 (121)	94	8.8	-1.8
		1.87 (117)	91	11.7	+1.1
95%, -3% w_{opt}	1.92 (120)	94	8.0	-2.6	
New Hampshire gravel	90%, w_{opt}	1.97 (123)	96	11.6	+2.4
	95%, w_{opt}	1.95 (122)	95	10.9	+1.7
	100%, w_{opt}	2.02 (126)	98	7.8	-1.4
	95%, +3% w_{opt}	2.02 (126)	99	9.5	+0.3
	95%, -3% w_{opt}	1.89 (118)	92	7.7	-1.5
OJF gravel	90%, w_{opt}	2.02 (126)	98	11.6	+0.4
	95%, w_{opt}	1.94 (121)	97	10.9	-0.3
	100%, w_{opt}	2.02 (126)	101	10.6	-0.6
	95%, +3% w_{opt}	2.02 (126)	101	11.5	+0.3
	95%, -3% w_{opt}	1.89 (118)	94	7.7	-3.5
Wardwell gravel	90%, w_{opt}	1.94 (121)	92	6.0	+0.9
	95%, w_{opt}	2.05 (128)	98	6.2	+1.1
	100%, w_{opt}	2.13 (133)	101	6.7	+1.6
	95%, +3% w_{opt}	1.91 (119)	91	8.1	+3.0
		1.95 (122)	93	11.1	+6.0
		1.89 (118)	90	15.3	+10.2
95%, -3% w_{opt}	2.03 (127)	97	4.0	-1.1	

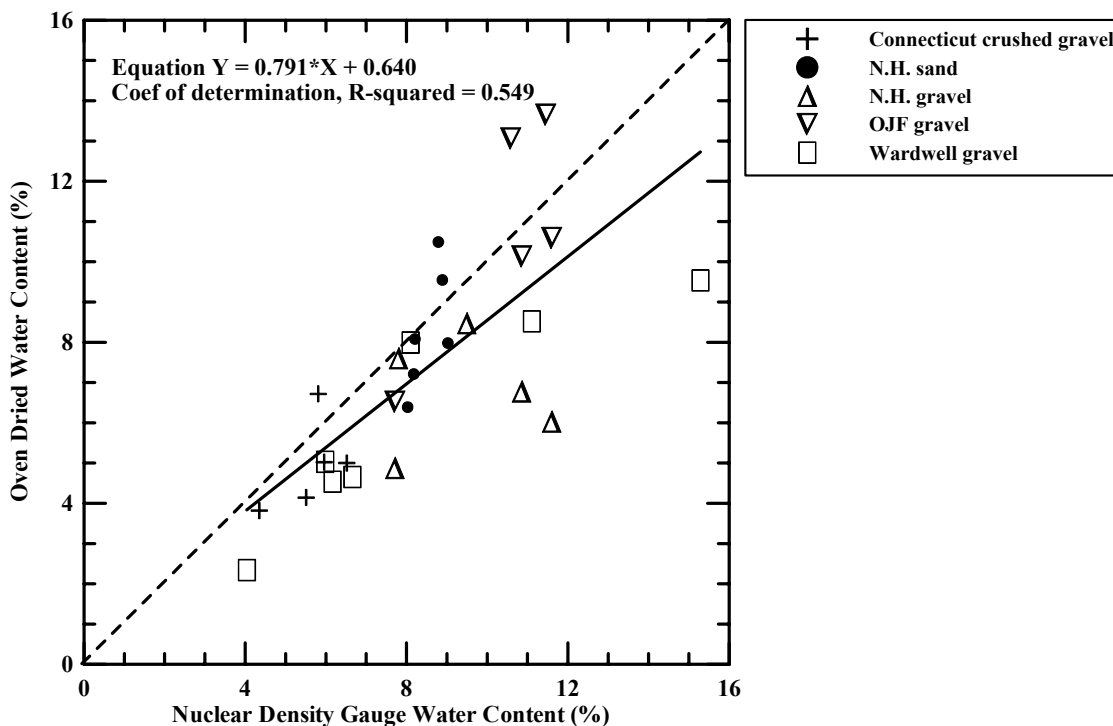


Figure 5.1 Comparison of oven dried and NDM water contents.

In addition, the percent compaction as determined from sand cone tests was compared to the percent compaction determined from the NDM. Like the water content results, the percent compaction results from the NDM were taken to be the average of five readings, one at each test location, taken at a 203 mm (8 in.) depth. The comparison is shown in Figure 5.2. When the data points from all the projects were included, there was essentially no correlation. However, it is difficult to perform accurate sand cone tests in crushed gravel. If the data from the Connecticut crushed gravel are ignored, there is a general trend of increasing percent compaction from the sand cone and NDM. The sand cone predicted percent compactions that were greater than the NDM, and many results were in the range of 100% to 123%. The upper end of the sand cone percent compactions are unreasonable. NDM measurements were also taken at depths of 0, 51, 102, and 152 mm (0, 2, 4, and 6 in.), all of which exhibited a similar comparison with the

sand cone results. Given the unreasonably high percent compactions resulting from some of the sand cone results, it was concluded that the NDM results were more reliable. In the balance of this chapter, the percent compaction determined by the NDM was used as the basis for comparison of the PFWD results.

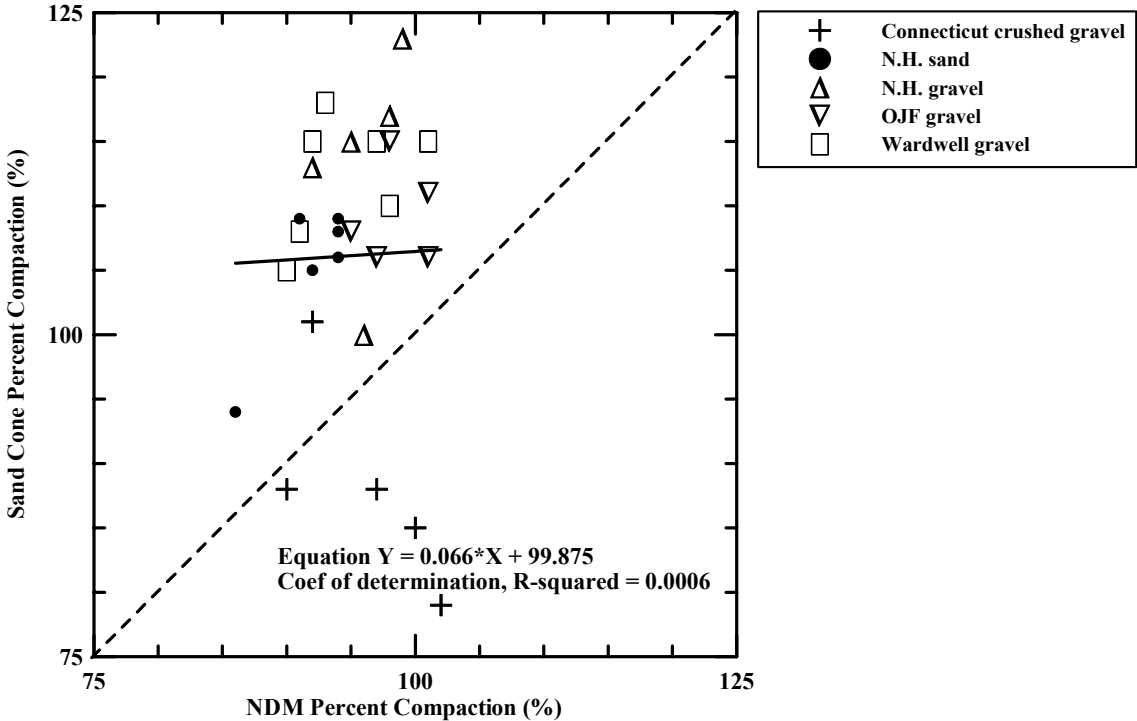


Figure 5.2 Comparison of percent compaction determined from sand cone and NDM tests.

Furthermore, measurements were made at field sites located in Maine, New Hampshire, and Connecticut. The field component included tests on two subgrades, one construction sand product, two aggregates, and one reclaimed stabilized base product. Classification and laboratory compaction results (AASHTO T 180) are summarized in Table 5.3. Gradation and moisture density curves for each sample may be found in Appendixes A and B, respectively. Overall, the water contents measured at the field sites were significantly lower than those in the laboratory tests.

Table 5.3 Summary of field samples.

Material Description		Grain Size Characteristics				Moisture Density Characteristics ²	
Type	Name	AASHTO Classification	Percent Gravel ¹ (%)	Percent Sand ¹ (%)	Percent Fines ¹ (%)	$\gamma_{d(max)}$ Mg/m ³ (lb/ft ³)	w_{opt} (%)
Subgrade	CPR	A-1-a	34.9	54.1	11.0	2.05 (128)	5.5
	I-84	A-1-b	28.5	57.4	14.1	NA	NA
Aggregate	I-84	A-1-a	66.3	28.5	5.2	2.31 (144)	7.4
	Route 25	A-1-b	36.8	59.4	3.8	1.92 (120)	12.3
	Route 26		52.0	46.0	2.0	1.99 (124)	12.0
Construction Sand	Route 25	A-1-b	36.8	60.4	2.8	2.17 (135)	11.4
Reclaimed Stabilized Base	CPR	NA	NA	NA	NA	NA	NA
	Route 201	NA	NA	NA	NA	NA	NA

NA – not available

¹ - based on ASTM D 422.² - based on AASHTO T 180.

5.3 FACTORS AFFECTING COMPOSITE MODULUS

The relationship of PFWD composite modulus as determined by the Prima 100 with percent compaction, water content, grain size distribution, and particle shape is explored in this section. Each is discussed separately below. In addition, multiple variable linear regression analysis is used to investigate the combined role of percent compaction and water content on composite modulus. Portable testing devices are compared and the effect of operator technique is discussed later in Section 5.4.

5.3.1 Effect of Percent Compaction on Composite Modulus

5.3.1.1 Laboratory Test Results

The Prima 100 PFWD composite modulus at each test location for each of the varying percent compaction and water content trials is shown as bar graphs in Figures 5.3 through 5.7. The water content relative to OWC and the percent compaction shown in the legend of these figures is the average of the values measured at the five test points for the trial. For a given test location, the bar graphs are ordered from low to high water content. The full dataset is shown in tabular form in Appendix C.

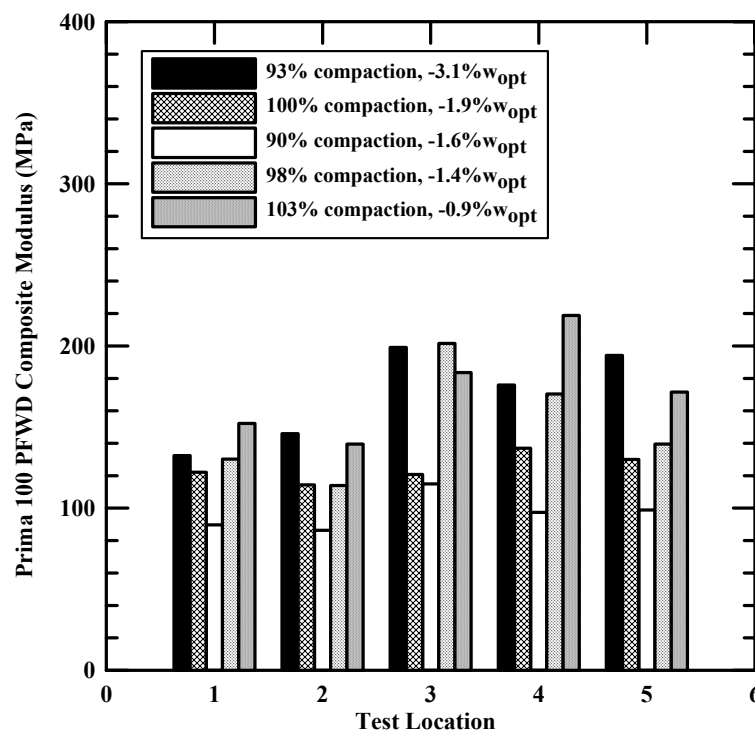


Figure 5.3 Effect of percent compaction on composite modulus, Connecticut crushed gravel.

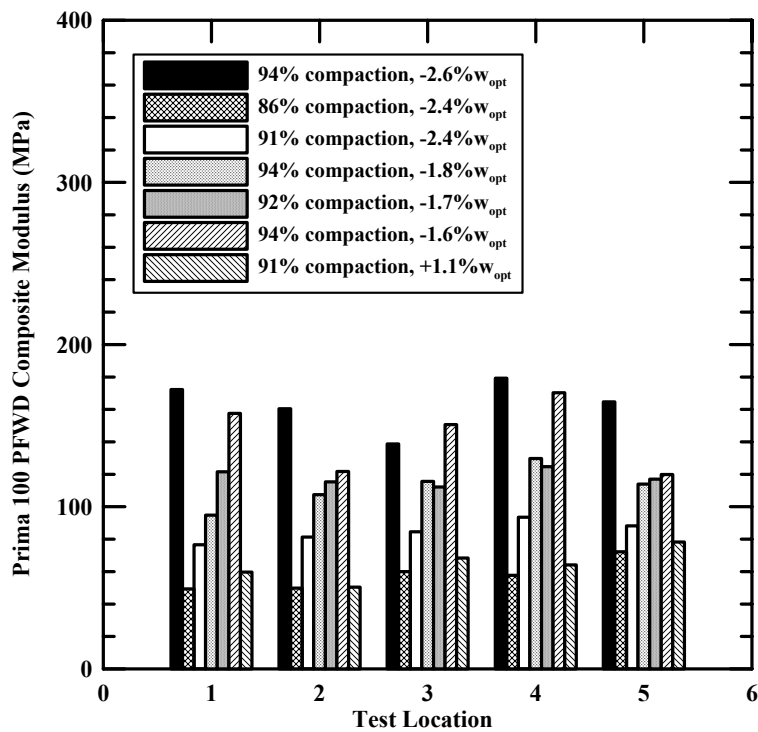


Figure 5.4 Effect of percent compaction on composite modulus, New Hampshire sand.

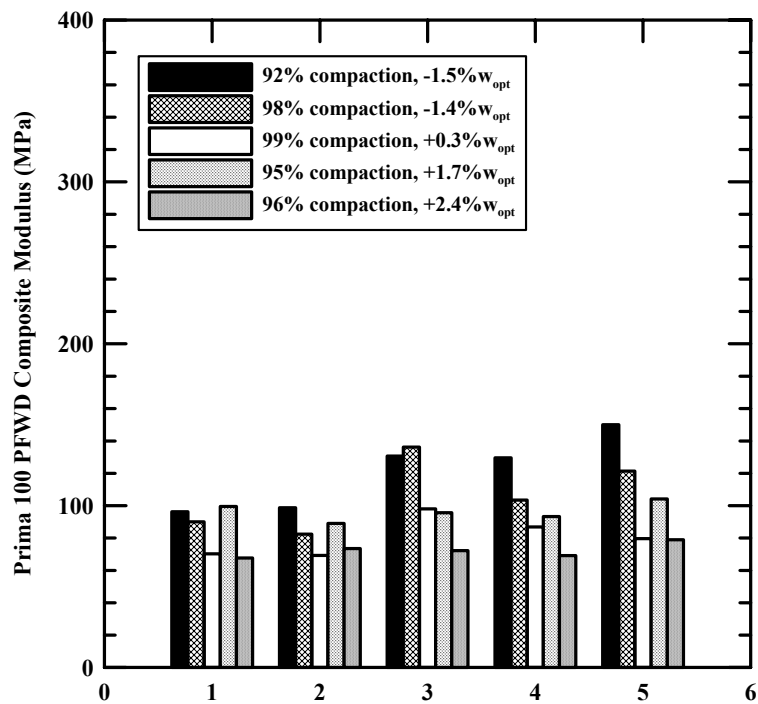


Figure 5.5 Effect of percent compaction on composite modulus, New Hampshire gravel.

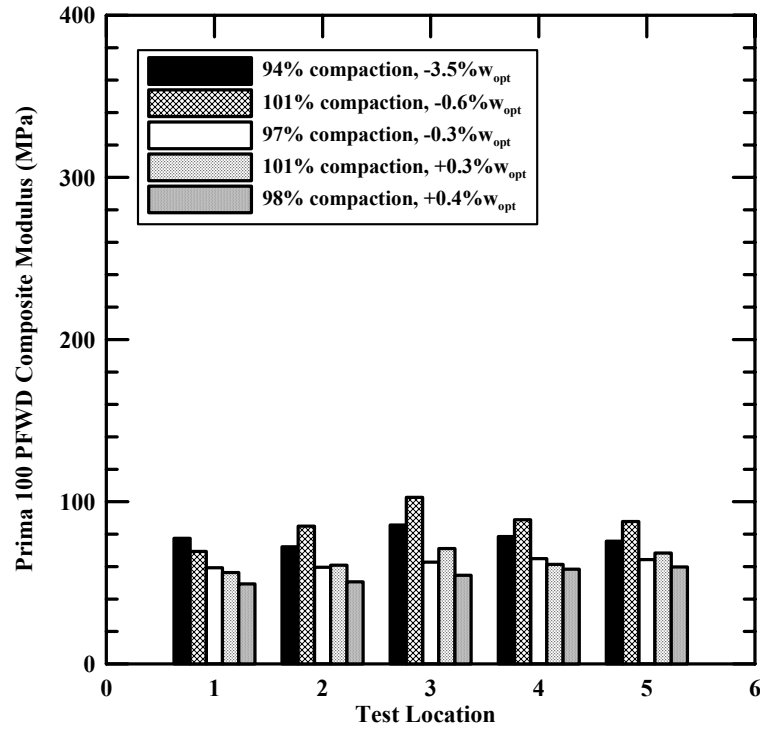


Figure 5.6 Effect of percent compaction on composite modulus, OJF gravel.

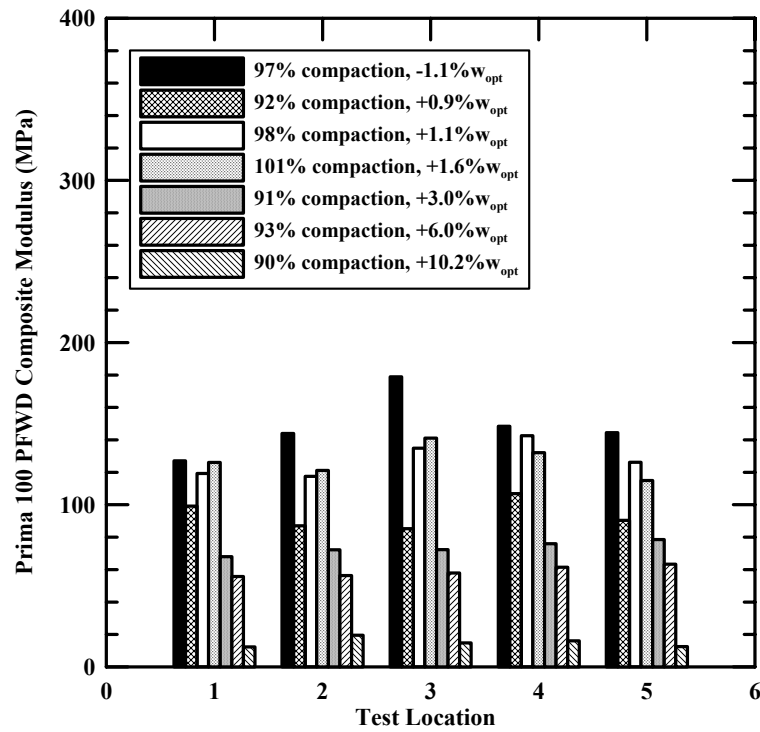


Figure 5.7 Effect of percent compaction on composite modulus, Wardwell gravel.

Plots of composite modulus versus percent compaction as measured at each test location were made. Single variable linear regression analyses (Neter, et al., 1982) were used to determine the best fit line for composite modulus as a function of percent compaction. The coefficient of simple determination (r^2) was used to measure the degree to which the variation of the dependent variable, in this case composite modulus, could be explained by a linear relation with an independent variable, in this case percent compaction (Walpole and Myers, 1978). For example, an r^2 of 0.9 would indicate that 90% of the variation in composite modulus was explained by a linear relation with percent compaction.

The plots of composite modulus versus percent compaction are shown in Figures 5.8 through 5.14. All data points regardless of water content are included. For four out of the five materials tested, there was a general trend of increasing composite modulus with increasing percent compaction. The r^2 for these four materials ranged from 0.027 to 0.531. In contrast, the New Hampshire gravel exhibited the opposite trend with decreasing composite modulus with increasing percent compaction and an r^2 of 0.147. Combining all laboratory samples produced an r^2 of 0.069. This is shown in Figure 5.13. However, when the two samples with the poorest correlation (New Hampshire gravel and OJF gravel), the correlation improves with $r^2 = 0.312$. The regression equations and r^2 are summarized in Table 5.4. With the exception of the New Hampshire sand, the regression coefficients were less than 0.5 indicating poor correlation. One reason for the poor correlation could be that water content has an important influence on composite modulus and this was not accounted for in Figures 5.8 through 5.14 or the regression results in Table 5.4.

Table 5.4 Summary of the correlations between percent compaction and composite modulus for laboratory samples.

Sample	Regression Equation	Coefficient of Simple Determination (r^2)
Connecticut crushed gravel	$y = 2.524x - 100.731$	0.122
New Hampshire sand	$y = 10.389x - 847.035$	0.531
New Hampshire gravel	$y = -2.725x + 357.106$	0.147
OJF gravel	$y = 0.663x + 3.899$	0.027
Wardwell gravel	$y = 6.096x - 484.889$	0.419
All Samples Combined	$y = 2.409x - 128.259$	0.069
All Samples Combined (w/o NHG and OJF)	$y = 5.437 - 400.906$	0.312

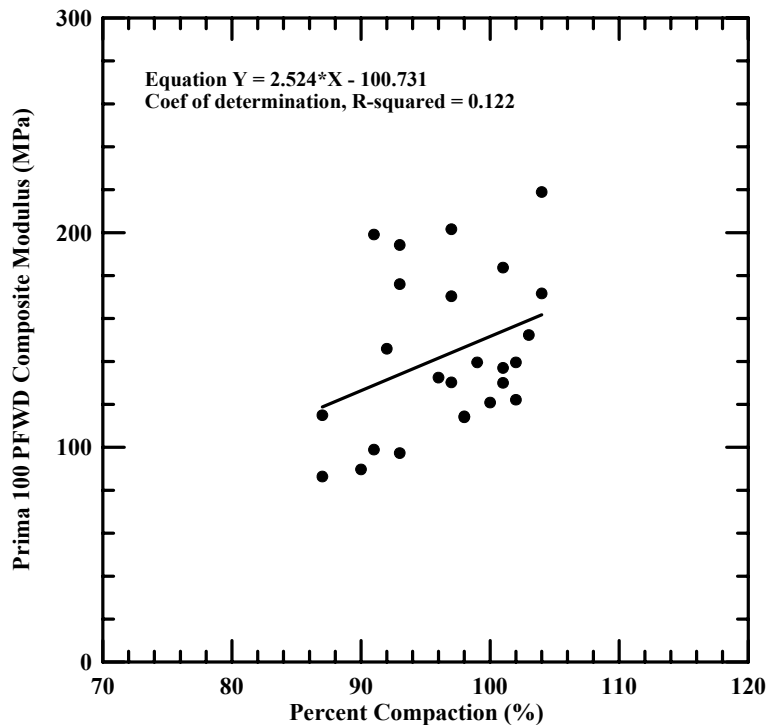


Figure 5.8 Comparison of percent compaction and composite modulus, Connecticut crushed gravel.

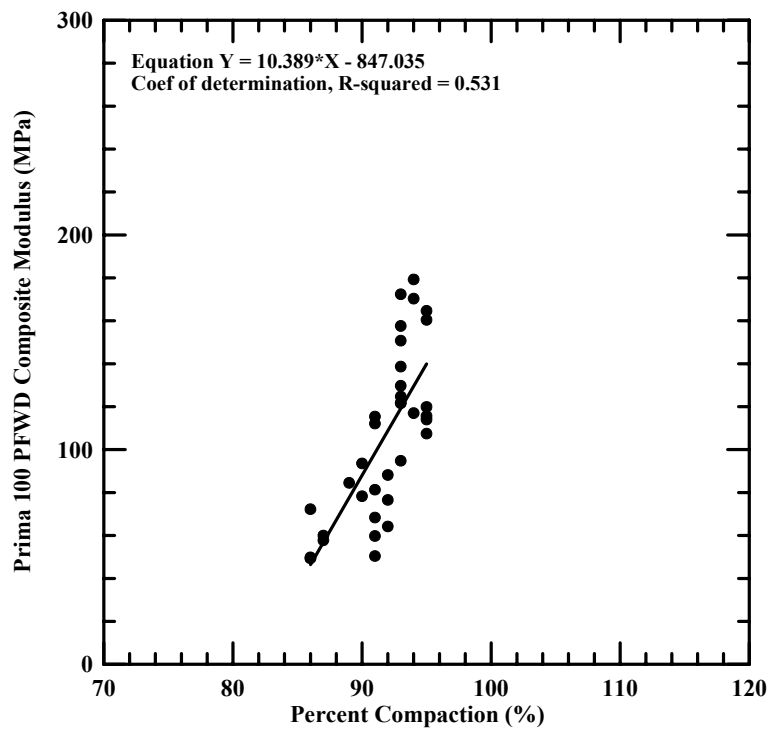


Figure 5.9 Comparison of percent compaction and composite modulus, New Hampshire sand.

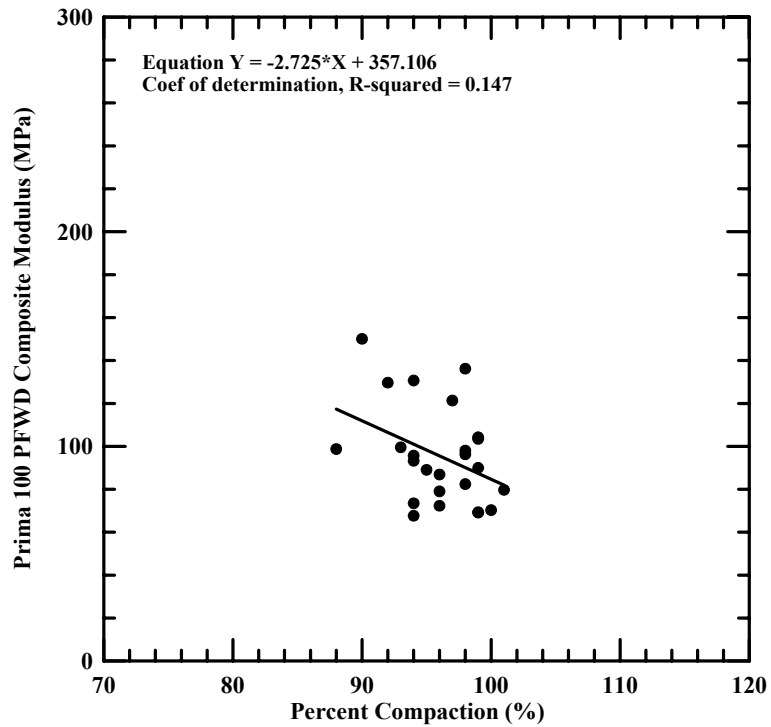


Figure 5.10 Comparison of percent compaction and composite modulus, New Hampshire gravel.

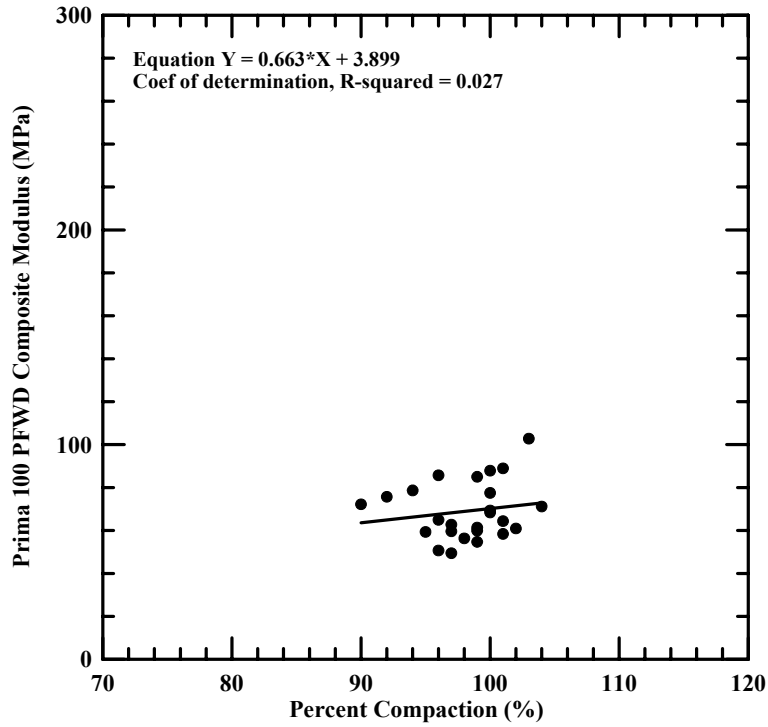


Figure 5.11 Comparison of percent compaction and composite modulus, OJF gravel.

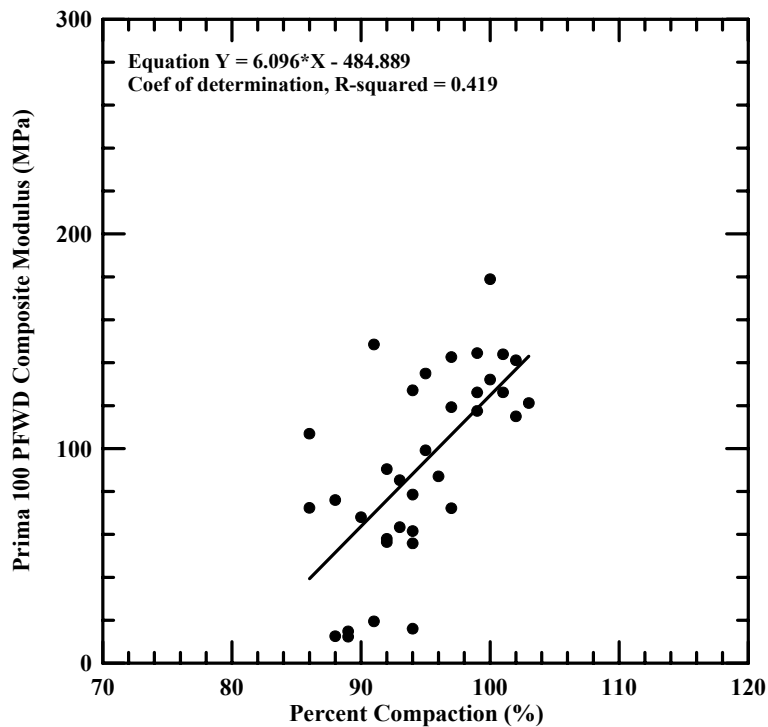


Figure 5.12 Comparison of percent compaction and composite modulus, Wardwell gravel.

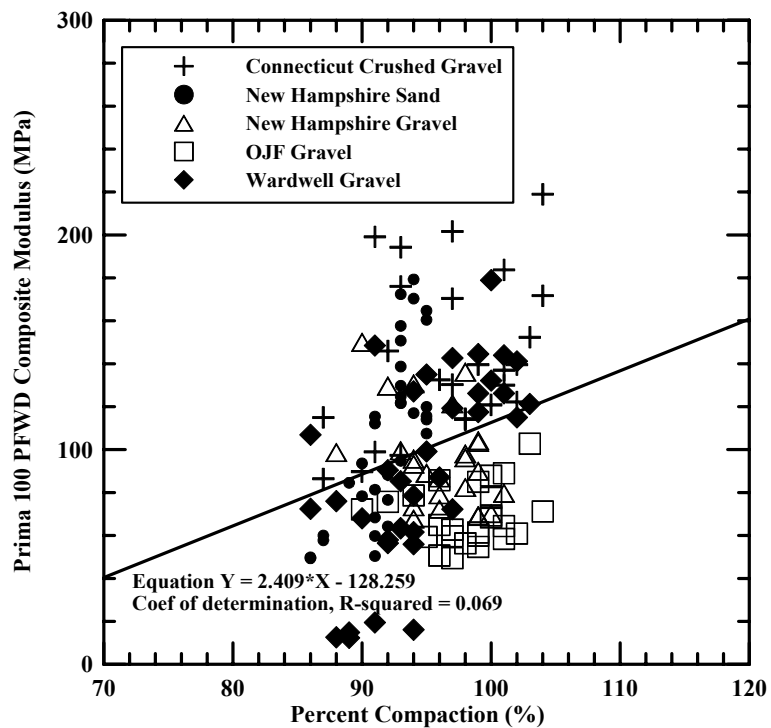


Figure 5.13 Comparison of percent compaction and composite modulus for all laboratory samples.

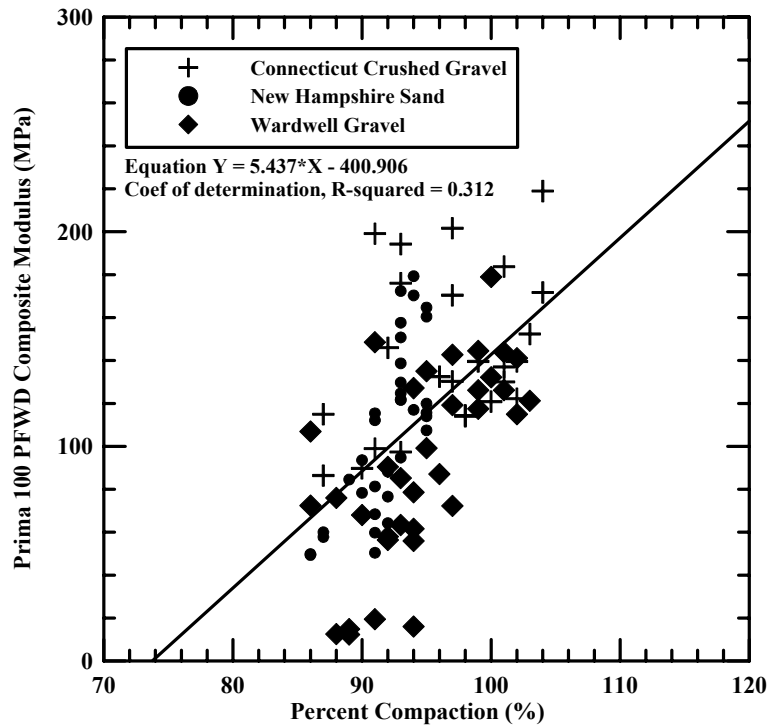


Figure 5.14 Comparison of percent compaction and composite modulus for three laboratory samples.

In an attempt to minimize the effect of water content, all laboratory data was divided into two groups: one for test points dry of the OWC, and one for test points wet of the OWC. Plots of composite modulus versus percent compaction for the two groups are shown in Figure 5.15 and 5.17. The correlation coefficients for the two groups are 0.045 and 0.211, respectively. Again, the two samples with the poorest correlation (New Hampshire gravel and OJF gravel) were removed. The correlation improves with r^2 of 0.350 and 0.455. These plots are shown in Figures 5.16 and 5.18. Thus, subdividing the data into those dry and wet of OWC did little to improve the correlation between composite modulus and percent compaction.

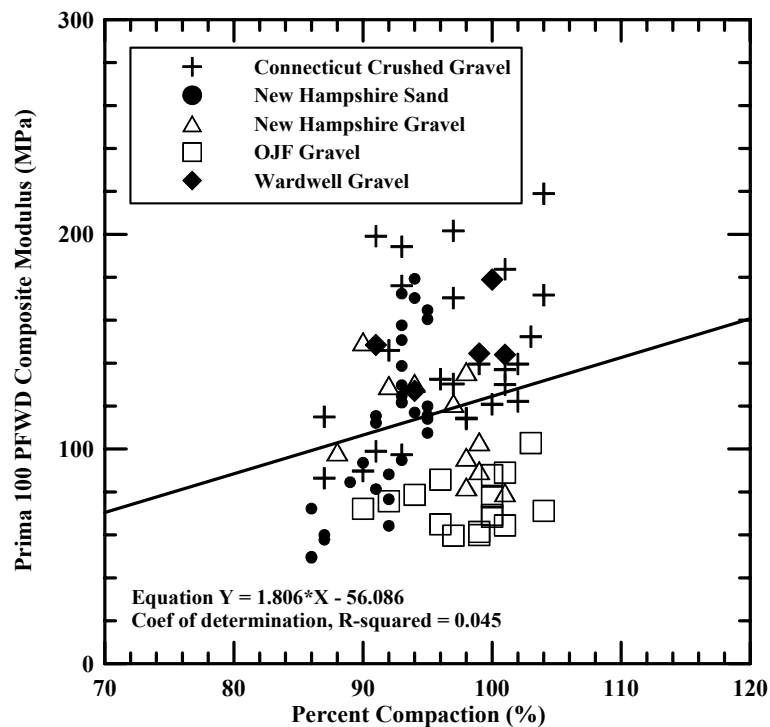


Figure 5.15 Comparison of percent compaction and composite modulus for laboratory tests with water contents dry of the OWC.

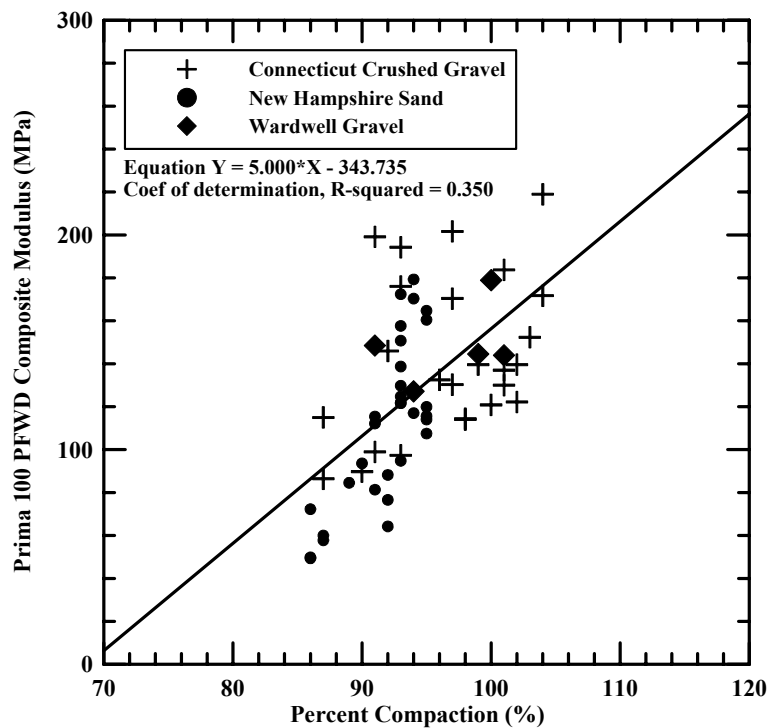


Figure 5.16 Comparison of percent compaction and composite modulus for selected laboratory samples with water contents dry of the OWC.

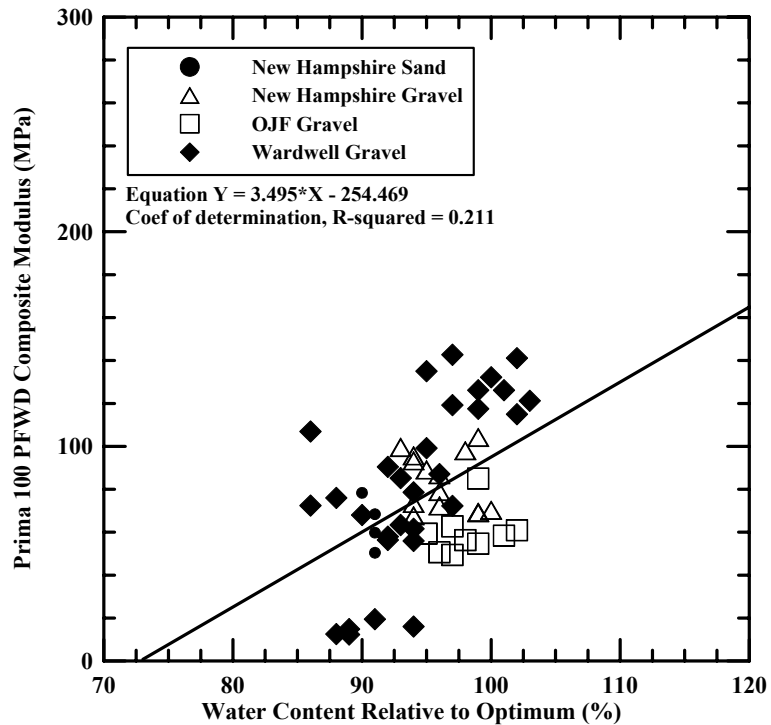


Figure 5.17 Comparison of percent compaction and composite modulus for laboratory tests with water contents wet of the OWC.

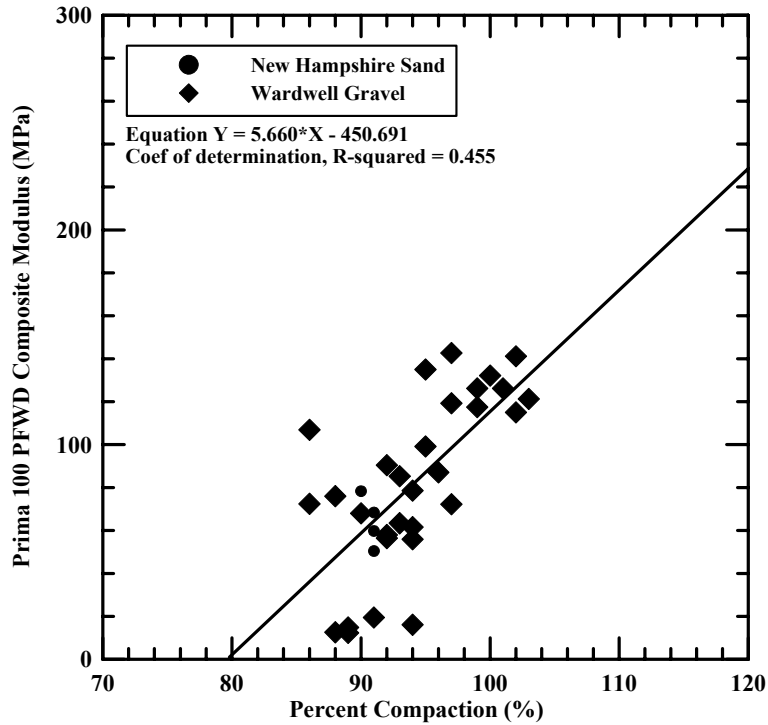


Figure 5.18 Comparison of percent compaction and composite modulus for selected laboratory samples with water contents wet of the OWC.

5.3.1.2 Field Test Results

The main objective of field site testing was to provide complementary measurements to those obtained under more carefully controlled conditions in the laboratory. The test sites had undergone varying degrees of compaction ranging from uncompacted base to base that had been well compacted with vibratory smooth drum rollers. Field testing techniques are described in Section 3.4.2. Compaction and soil property data is summarized in Section 5.2. Base aggregate tested at I-84 and Route 25 test sites were the same as those tested in the laboratory. Maximum dry density and optimum water content were unavailable for the I-84 subgrade soils, so the moduli from these tests were compared directly to dry density. NDM measurements at Route 26 and Route 201 test sections were taken prior to calibration. As a result, the NDM

measurements were deemed unreliable. Instead the change in composite modulus over time is considered.

Prima 100 PFWD composite moduli are compared to percent compaction as determined from the NDM for the Connecticut crushed gravel, New Hampshire sand, and New Hampshire gravel. This is shown in Figures 5.19 through 5.23. The aggregate was significantly dry of optimum (average of -4.4% for Connecticut crushed gravel, and -9.0% for both New Hampshire sand and gravel). Results from the field test sites indicate that as the degree of compaction increases, composite modulus also increases, mirroring the observations made in the laboratory. The r^2 and regression equations are summarized in Table 5.5. The r^2 for the Connecticut crushed gravel and New Hampshire sand were greater than 0.5 indicating a reasonable correlation. The low r^2 for the New Hampshire gravel may be due in part to the small range of percent compactions for these results. Results from these three sites were combined into a single plot as shown in Figure 5.24. This resulted in an r^2 of 0.818, indicating a reasonable degree of correlation. The regression equation and r^2 for the combined result is also shown in Table 5.5. The regression equation suggests that for aggregate compacted at water contents at least 4.4% drier than OWC, 100% of ASSHTO T180 compaction corresponds to a composite modulus of 154 MPa. Examining the results for select laboratory tests in Figure 5.14 shows that 100% of AASHTO T 180 corresponds to a composite modulus of 143 MPa, which is similar to the field result.

Table 5.5 Summary of the correlations between percent compaction and composite modulus for field samples.

Field Test Site	Material	Regression Equation	Coefficient of Simple Determination (r^2)
I-84	Crushed Gravel base	$y = 4.989x - 359.924$	0.647
	Subgrade*	$y = 0.953x - 33.463$	0.014
Route 25	Sand base	$y = 4.225x - 270.545$	0.544
	Gravel base	$y = 1.598x + 21.572$	0.008
CPR	Subgrade	$y = 8.193x - 548.367$	0.313
Three base materials combined	NA	$y = 5.75x - 420.736$	0.818

NA – not applicable

* - regression analysis results compare dry density and composite modulus

Reclaimed stabilized base products tested at the Route 201 and Commercial Paving & Recycling field sites were monitored on multiple dates to examine the increase in composite modulus over time. Results indicate an increase in composite modulus over time for all stations monitored. This is shown in Figures 5.25 and 5.26. The additional measurements were taken after completion of paving at both sites and both had been opened to vehicle traffic. Some of the increase at the Route 201 test site could simply be the result of increasing the pavement thickness since thicker pavement sections would likely produce greater composite moduli. This suggests that the PFWD could be used to monitor the time-dependent increases in composite modulus of asphalt stabilized base materials.

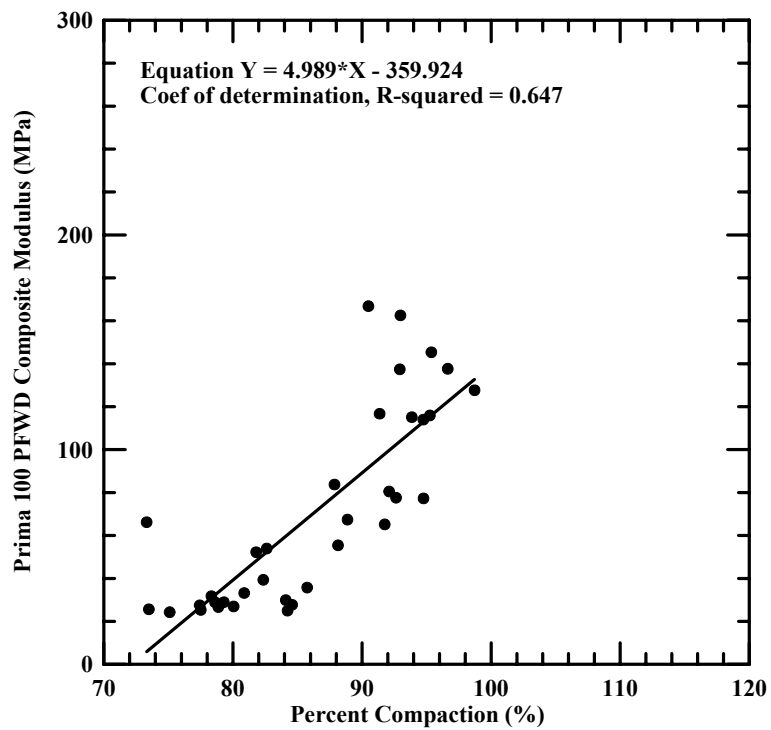


Figure 5.19 Comparison of percent compaction and composite modulus of crushed gravel tested at I-84, Southington, Connecticut.

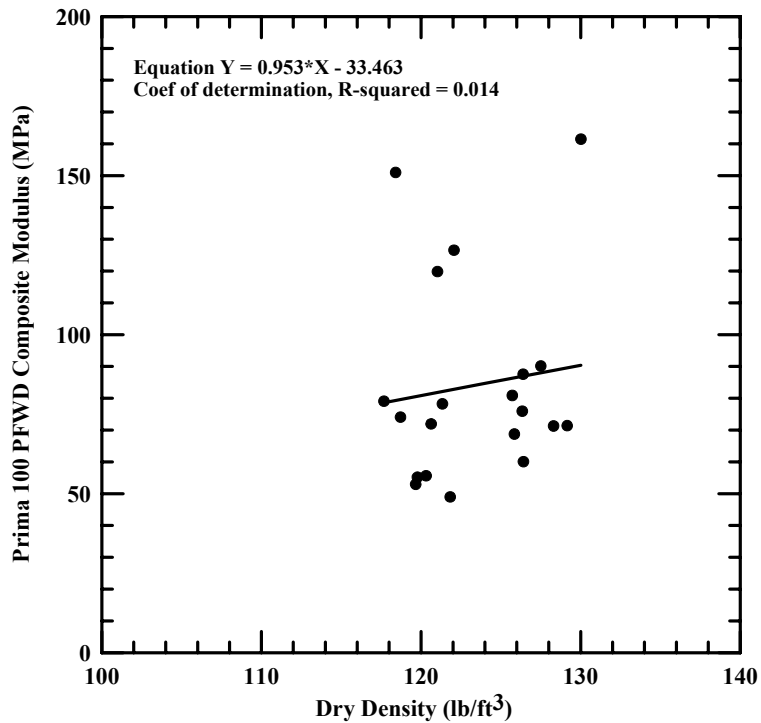


Figure 5.20 Comparison of dry density and composite modulus of subgrade tested at I-84, Southington, Connecticut.

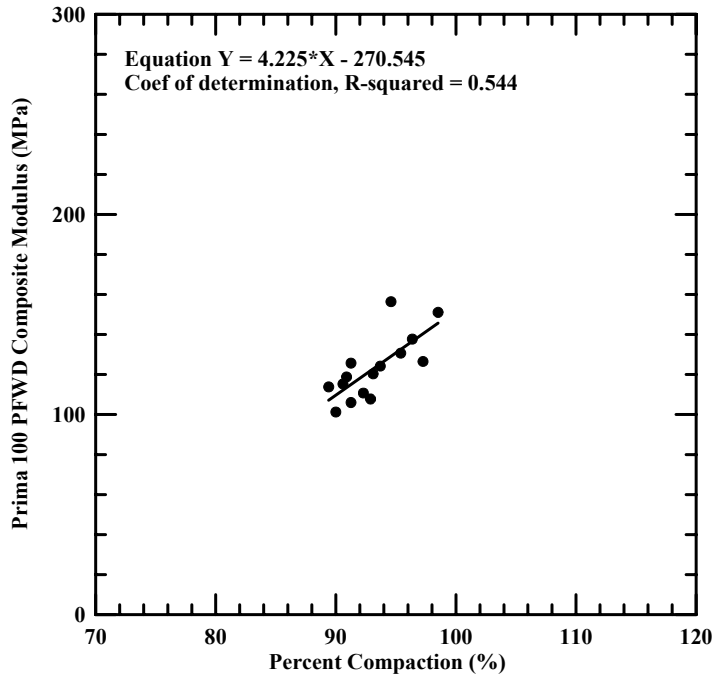


Figure 5.21 Comparison of percent compaction and composite modulus of construction sand tested at Route 25, Effingham/Freedom, New Hampshire.

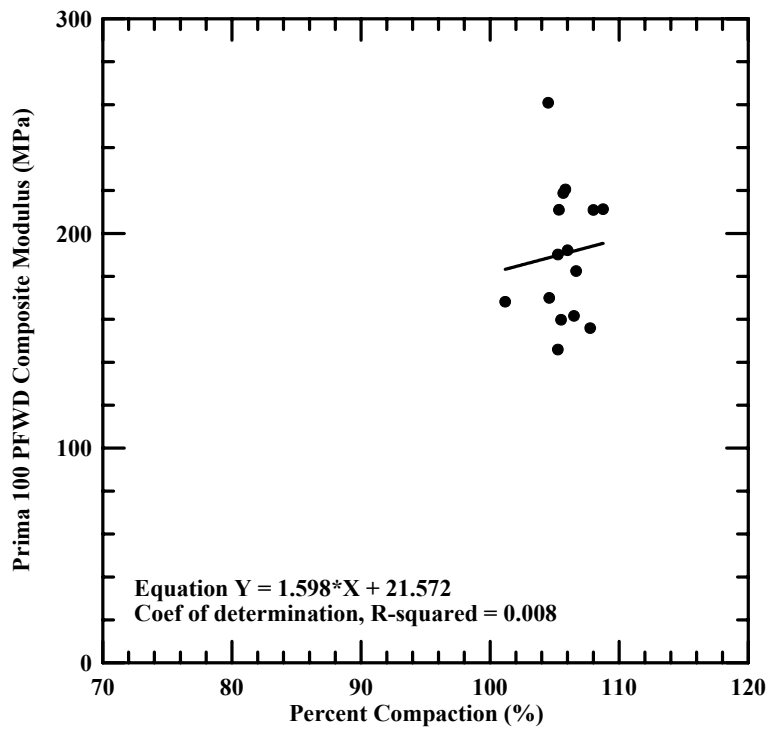


Figure 5.22 Comparison of percent compaction and composite modulus of gravel tested at Route 25, Effingham/Freedom, New Hampshire.

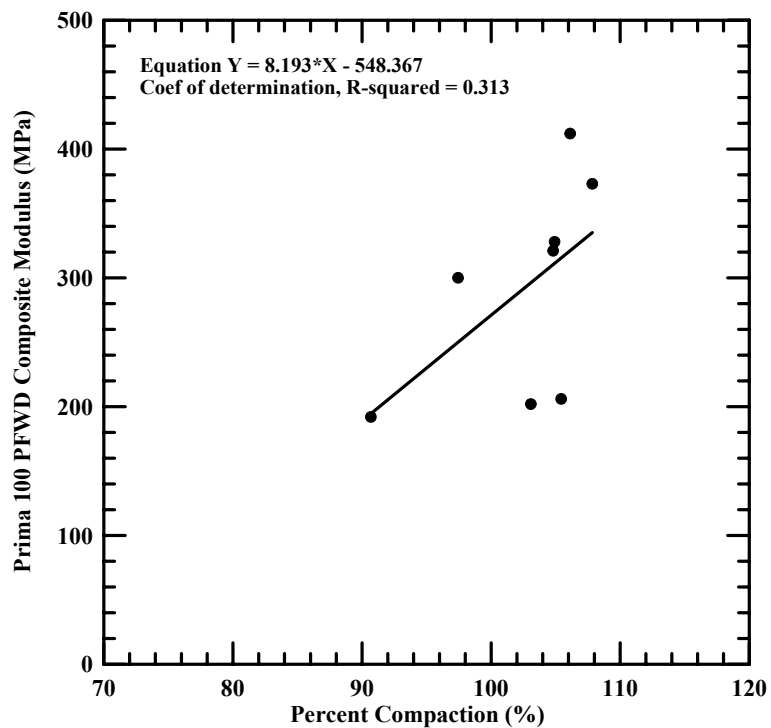


Figure 5.23 Comparison of percent compaction and composite modulus of subgrade tested at CPR, Scarborough, Maine.

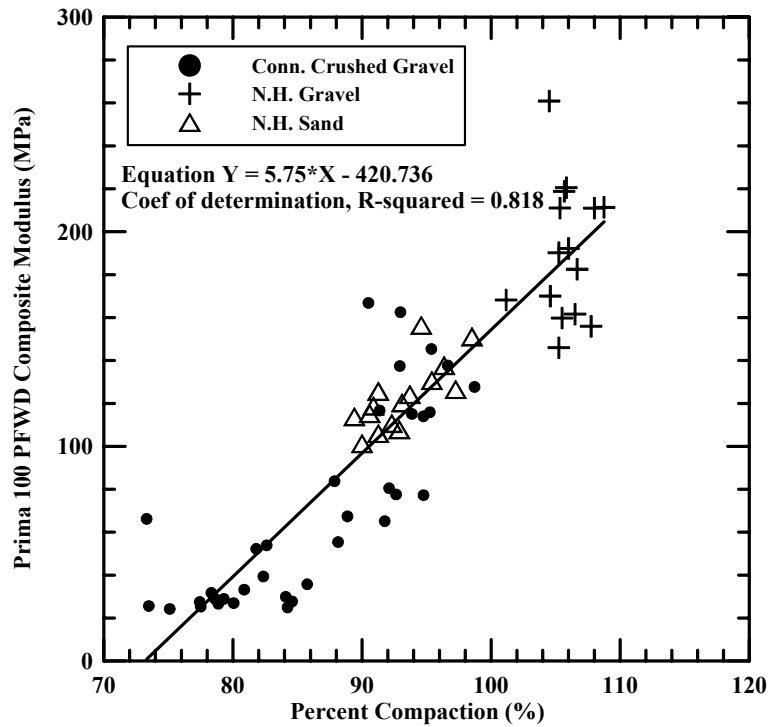


Figure 5.24 Comparison of percent compaction and composite modulus for materials tested at Route 25 and I-84 field test sites.

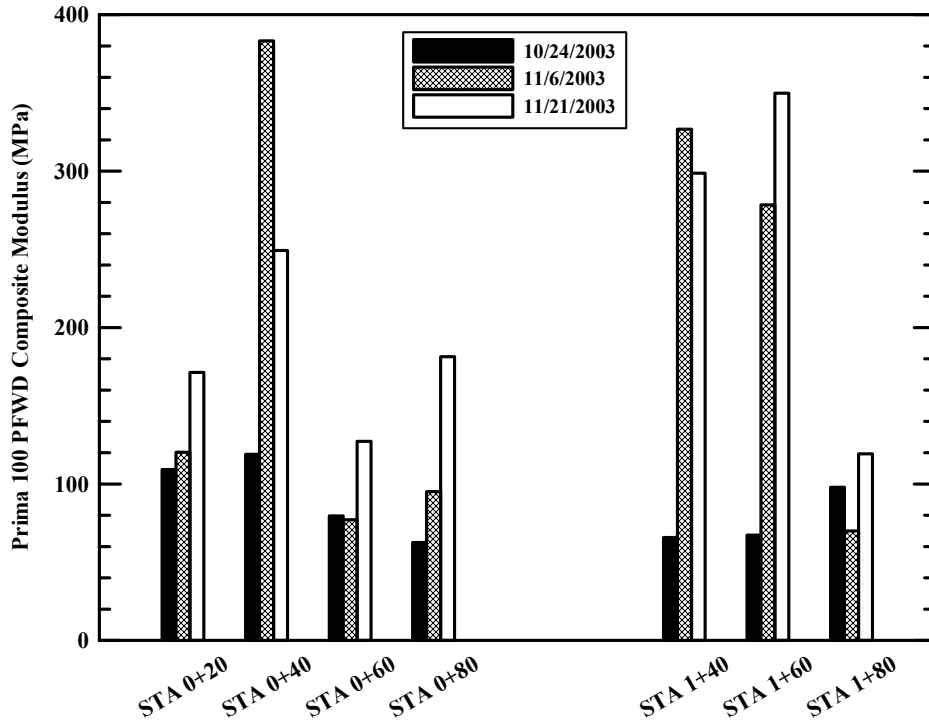


Figure 5.25 Change in moduli with time at CPR test site, Scarborough, Maine.

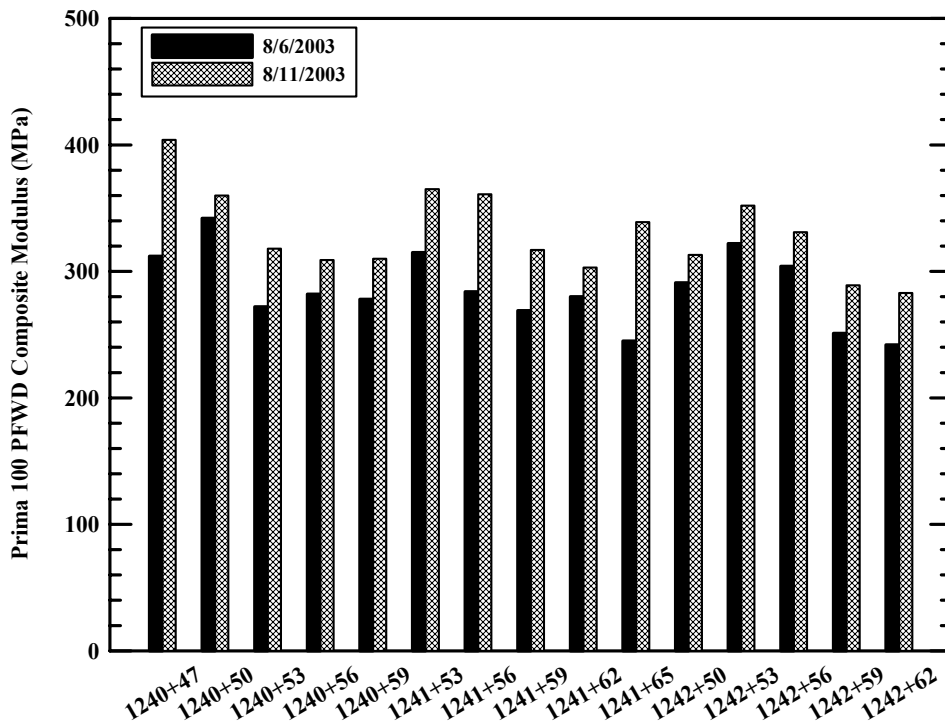


Figure 5.26 Change in moduli with time at Route 201 test site, The Forks, Maine.

5.3.2 Effect of Water Content on Composite Modulus

5.3.2.1 Laboratory Test Results

Examination of the bar graphs previously shown in Figures 5.3 through 5.7 shows that there is a general trend that the composite moduli tends to decrease as water content increases. This was examined for the individual data points in Figures 5.27 through 5.32. The equation for the best fit straight line and the associated r^2 is shown on these figures and summarized in Table 5.6. Correlation coefficients ranged from 0.003 (Connecticut crushed gravel) to 0.814 (Wardwell gravel). The generally low correlation coefficients are due in part to the role that percent compaction plays in the composite modulus, which is not accounted for in this analysis. The higher correlation coefficient for the Wardwell gravel may be due to the high water content of some of the samples as illustrated in Figures 5.33 and 5.34. Wet of optimum, increased water content would tend to produce lower densities, which also would contribute to a lower composite modulus and a stronger correlation.

Table 5.6 Summary of the correlations between water content and composite modulus for laboratory samples.

Sample	Regression Equation	Coefficient of Simple Determination (r^2)
Connecticut crushed gravel	$y = -2.309x + 139.147$	0.003
New Hampshire sand	$y = -10.005x + 90.036$	0.112
New Hampshire gravel	$y = -8.385x + 97.876$	0.407
OJF gravel	$y = -4.235x + 65.794$	0.297
Wardwell gravel	$y = -11.009x + 126.181$	0.814
All Samples Combined	$Y = -7.621x + 100.703$	0.285

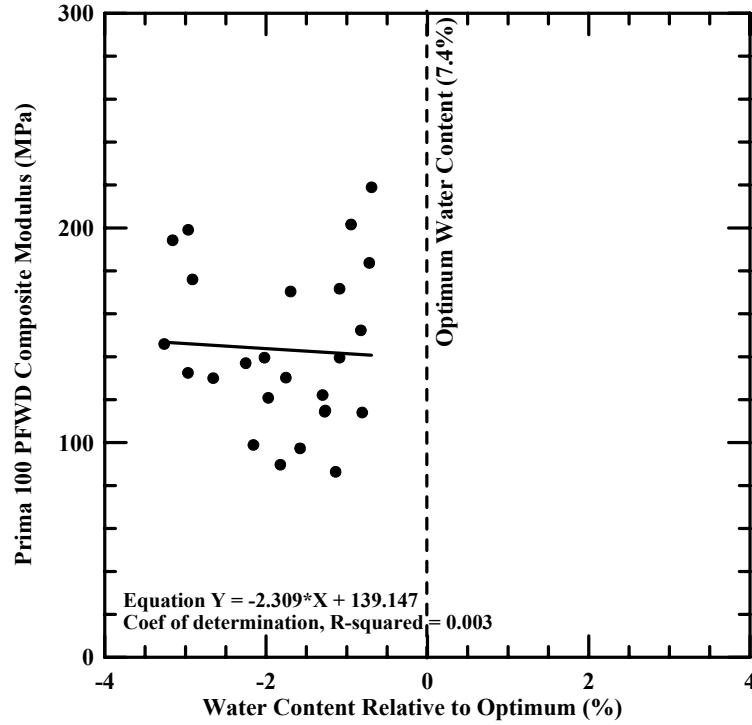


Figure 5.27 Comparison of water content and composite modulus, Connecticut crushed gravel.

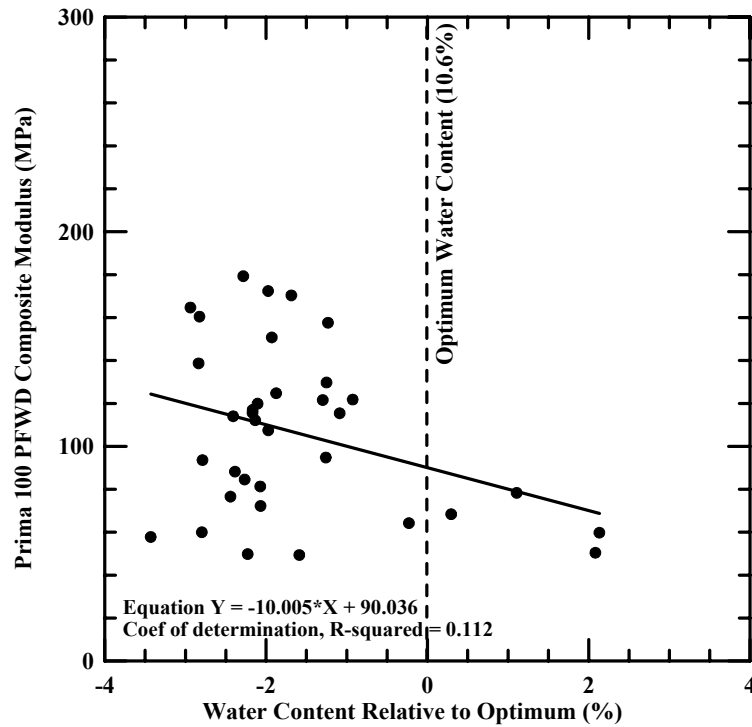


Figure 5.28 Comparison of water content and composite modulus, New Hampshire sand.

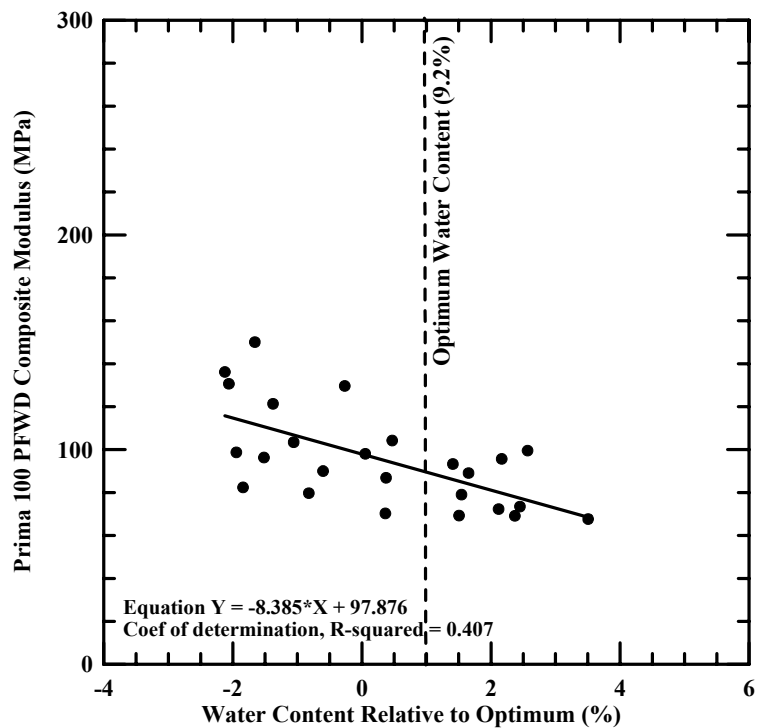


Figure 5.29 Comparison of water content and composite modulus, New Hampshire gravel.

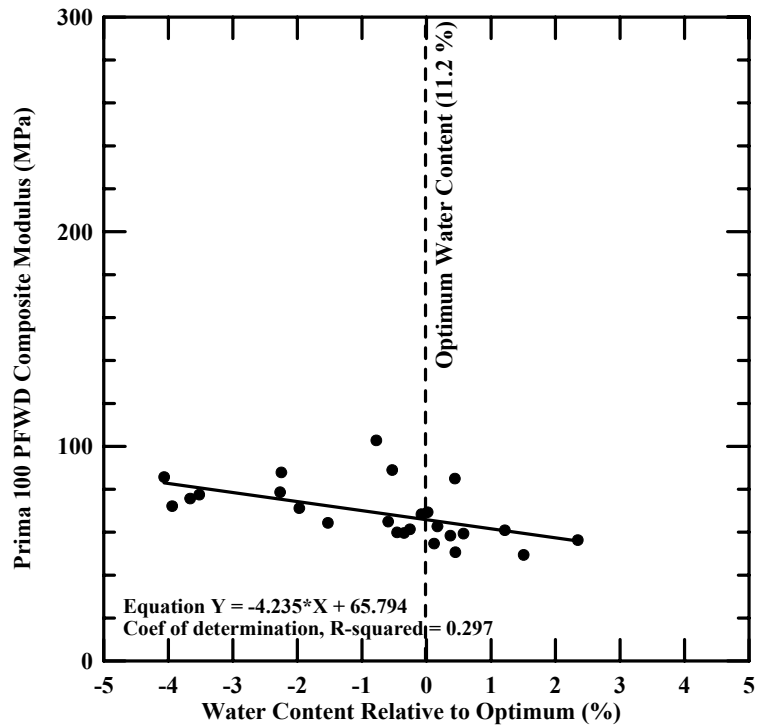


Figure 5.30 Comparison of water content and composite modulus, OJF gravel.

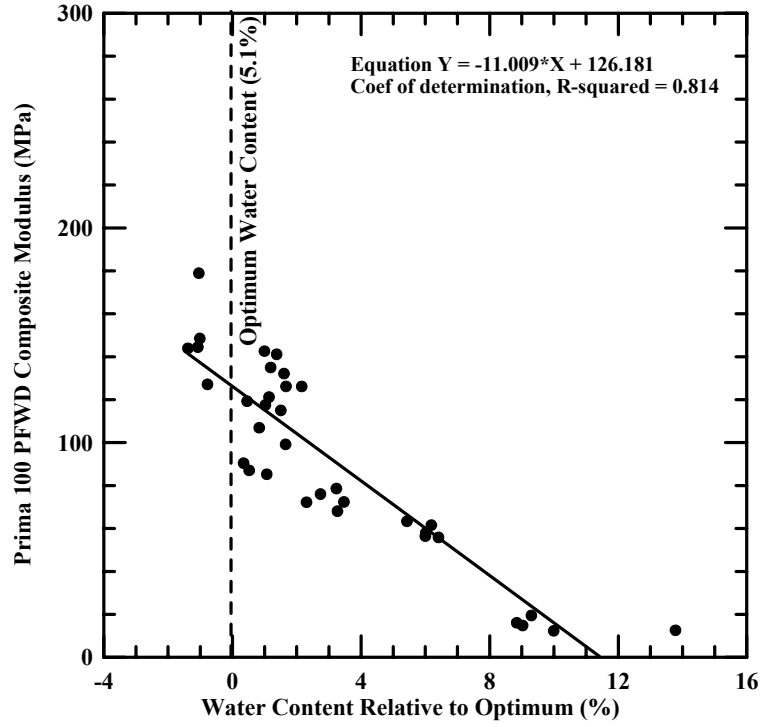


Figure 5.31 Comparison of water content and composite modulus, Wardwell gravel.

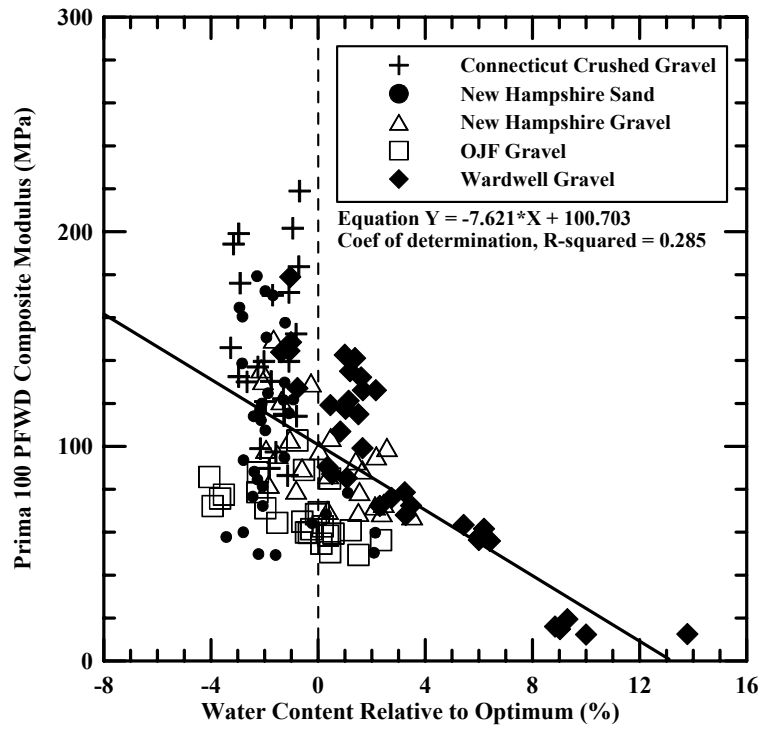


Figure 5.32 Comparison of water content and composite modulus for all laboratory samples.

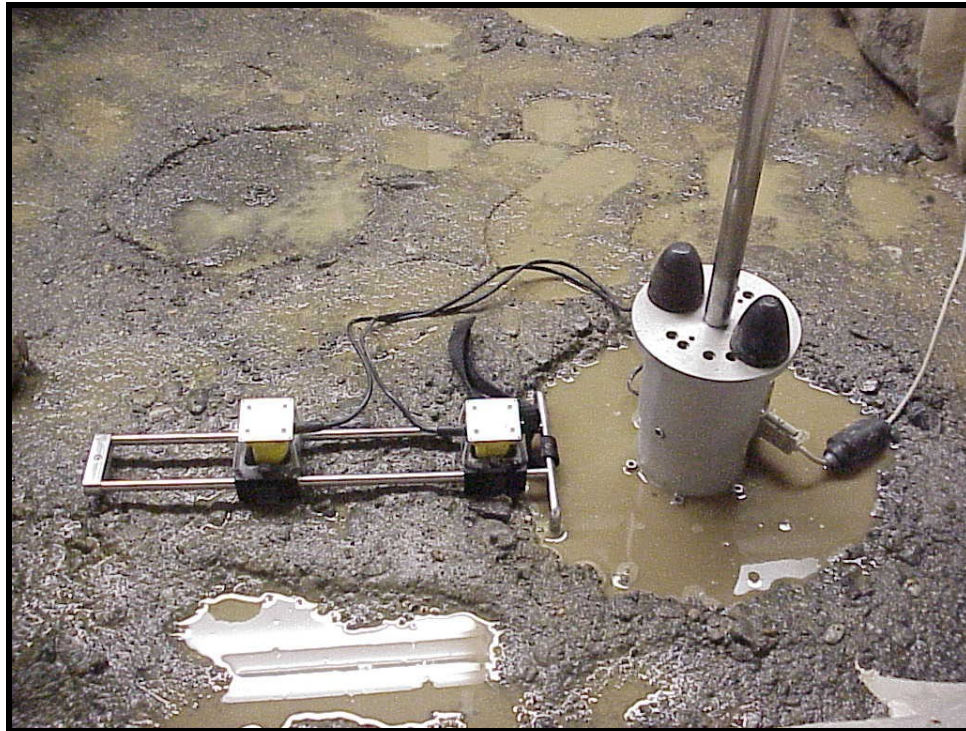


Figure 5.33 Prima 100 PFWD measurement on Wardwell gravel wet of optimum.



Figure 5.34 Prima 100 PFWD measurement on Wardwell gravel wet of optimum.

5.3.2.2 Field Test Results

Prima 100 PFWD composite moduli are compared to water content as determined from the NDM in Figures 5.35 through 5.40. Maximum dry density and optimum water content were unavailable for the I-84 subgrade soils, so the moduli from these tests were compared directly to water content. Regression analysis results for all field sites are shown in Table 5.7. With the exception of the subgrade material at the I-84 test site, all other materials exhibited trends indicating increasing modulus with increasing water content. This is contrary to expectations and opposite of what was seen in laboratory results. However, when the three base materials are combined, the trend is reversed, mirroring laboratory observations. This is shown in Figure 5.40. The coefficient of simple determination ranged from 0.008 (Route 25 gravel) to 0.521 (Route 25 sand). One possible explanation for the low coefficients is that the water contents of base materials at field sites were all dry of the OWC and, at individual sites, spanned a narrow range.

Table 5.7 Summary of the correlations between water content and composite modulus for field samples.

Field Test Site	Material	Regression Equation	Coefficient of Simple Determination (r^2)
I-84	Crushed Gravel base	$y = 30.580x + 218.660$	0.226
	Subgrade*	$y = -19.525x + 203.639$	0.412
Route 25	Sand base	$y = 15.179x + 250.263$	0.521
	Gravel base	$y = 2.133x + 208.394$	0.008
CPR	Subgrade	$y = 55.604x + 244.918$	0.402
Three base materials combined	NA	$y = -16.85x + 1.135$	0.288

NA – not applicable.

* - correlated with density and water content.

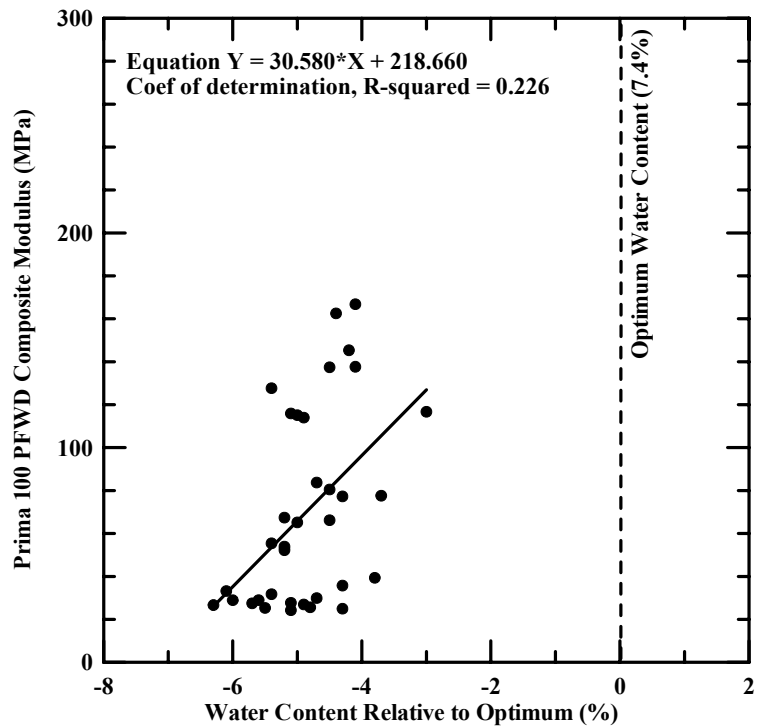


Figure 5.35 Comparison of water content and composite modulus of crushed gravel tested at I-84, Southington, Connecticut.

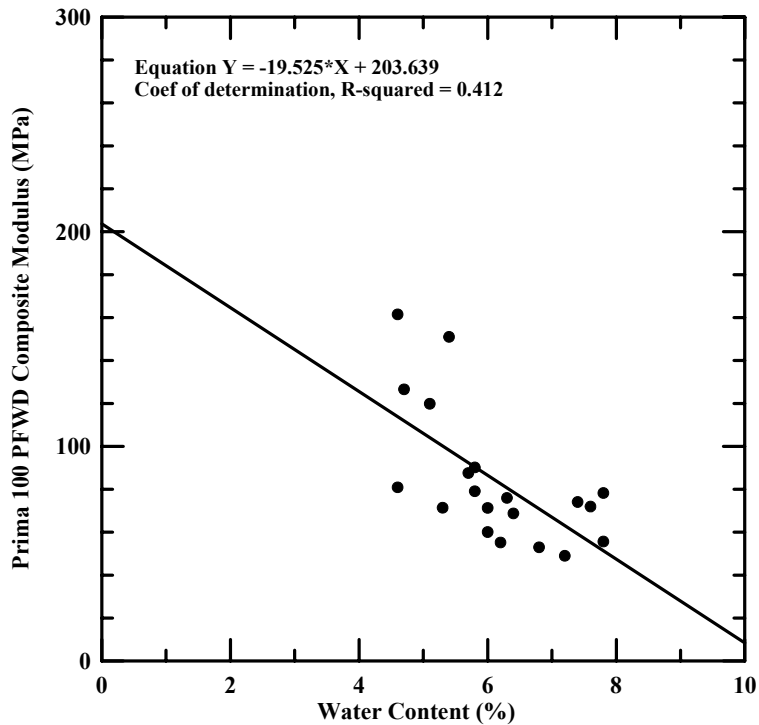


Figure 5.36 Comparison of water content and composite modulus of subgrade tested at I-84, Southington, Connecticut.

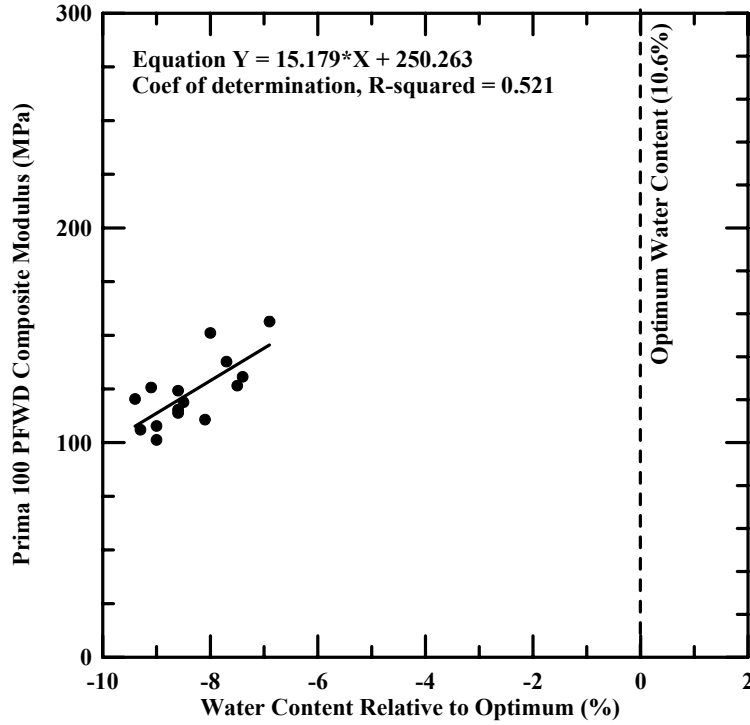


Figure 5.37 Comparison of water content and composite modulus of sand tested at Route 25, Effingham/Freedom, New Hampshire.

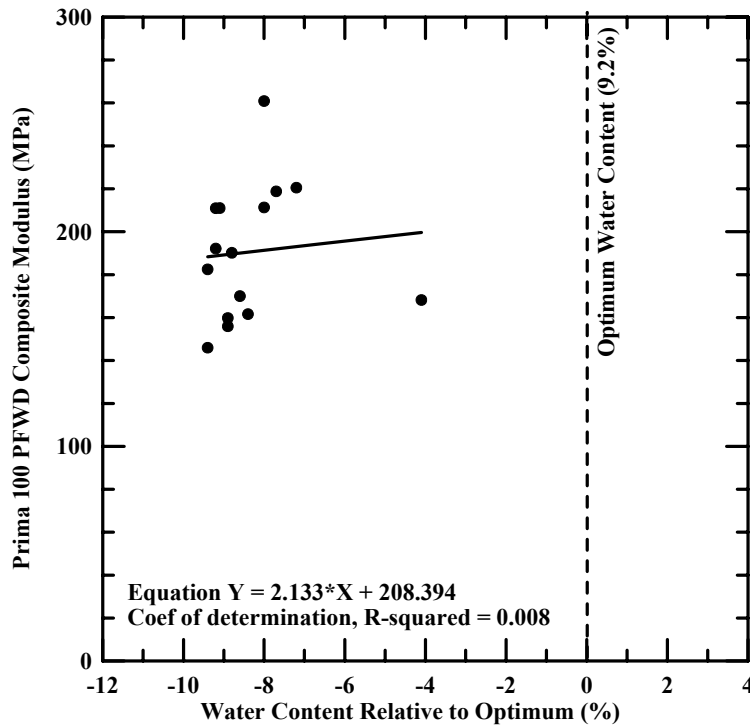


Figure 5.38 Comparison of water content and composite modulus of gravel tested at Route 25, Effingham/Freedom, New Hampshire.

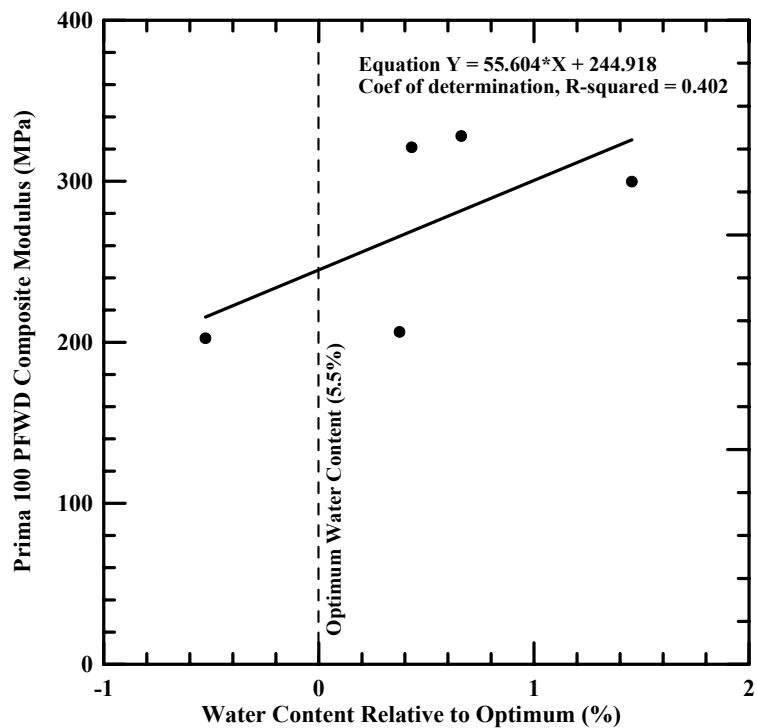


Figure 5.39 Comparison of water content and composite modulus of subgrade tested at CPR, Scarborough, Maine.

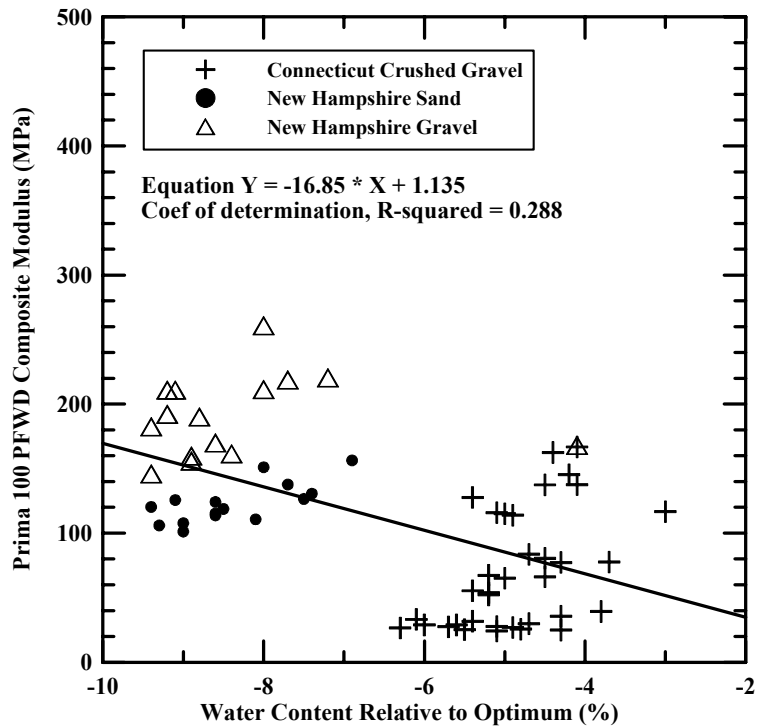


Figure 5.40 Comparison of water content and composite modulus for all field test sites.

5.3.3 Multivariate Linear Regression

Multivariable linear regression analysis (Neter, et al., 1982) was used to determine the best fit line for composite modulus as a function of percent compaction and water content. All data points regardless of water content are included. The coefficient of multiple determination (R^2) was used to measure the degree to which the variation of the dependent variable, in this case composite modulus, could be explained by a linear relation with two independent variables, in this case percent compaction and water content (Walpole and Myers, 1978). For example, an R^2 of 0.9 would indicate that 90% of the variation in composite modulus was explained by a linear relation with percent compaction and water content.

Coefficient of multiple determination as well as the regression equations are provided for laboratory and field results in Tables 5.8 and 5.9, respectively. The R^2 for the laboratory materials ranged from 0.141 (Connecticut crushed gravel) to 0.867 (Wardwell gravel). Combining all laboratory samples produced an R^2 of 0.326. However, when the two samples with the poorest correlation between composite modulus and percent compaction (New Hampshire Gravel and OJF Gravel) are removed from the analysis, the correlation improves with $R^2 = 0.624$. These R^2 are significantly higher than when only percent compaction is considered ($R^2 = 0.069$ for all samples and $R^2 = 0.312$ when NH gravel and OJF gravel are removed as, shown in Table 5.4), illustrating the importance of considering water content in the empirical equation to predict composite modulus. The R^2 for the field materials ranged from 0.001 (Route 25 gravel) to 0.679 (I-84 crushed gravel). Combining the field results for the three sites where base materials were tested produced an R^2 of 0.823 indicating a reasonably strong correlation between

Table 5.8 Summary of multivariate linear regression analyses on laboratory samples.

Sample	Regression Equation	Coefficient of Multiple Determination (R^2) for composite modulus as a function of percent compaction and water content relative to optimum
Connecticut crushed gravel	$M_c = -118.22 + 2.596(PC) - 5.946(RWC)$	0.141
New Hampshire sand	$M_c = -832.27 + 10.083(PC) - 8.153(RWC)$	0.609
New Hampshire gravel	$M_c = 300.4 - 2.113(PC) - 7.341(RWC)$	0.457
OJF gravel	$M_c = -99.275 + 1.672(PC) - 5.247(RWC)$	0.451
Wardwell gravel	$M_c = -133.14 + 2.682(PC) - 9.268(RWC)$	0.867
All Samples Combined	$M_c = -77.989 + 1.878(PC) - 7.296(RWC)$	0.326
Combined (CT, NHS, and Wardwell)	$M_c = -332.91 + 4.720(PC) - 7.658(RWC)$	0.624

M_c = composite modulus; PC = percent compaction; RWC = relative water content.

Table 5.9 Summary of multivariate linear regression analyses on field tests on granular base.

Type	Field Test Site	Material	Regression Equation	Coefficient of Multiple Determination (R^2) for composite modulus as a function of percent compaction and water content relative to optimum
Base	I-84	Crushed Gravel	$M_c = -294.49 + 4.728(PC) + 8.833(RWC)$	0.679
	Route 25	Sand	$M_c = -87.276 + 2.828(PC) + 6.331(RWC)$	0.602
		Gravel	$M_c = 652.69 - 4.249(PC) + 1.504(RWC)$	0.001
	Combined	---	$M_c = -411.26 + 5.454(PC) - 2.757(RWC)$	0.823
Sub-grade	I-84	Subgrade*	$M_c = -1167.8 + 8.798(PC) + 27.086(WC)$	0.497
	CPR	Subgrade	$M_c = 174.53 + 1.038(PC) - 6.947(RWC)$	0.044

* - based on dry density and water content.

M_c = composite modulus; PC = percent compaction; RWC = relative water content.; WC = water content
Note: Range of water contents for the base course results are 3 to 9.5% dry of optimum water content so the regression equations should be used with caution for higher water contents.

variables. This was only slightly higher than when considering percent compaction alone, but as noted previously the field sites were all dry of optimum and the range of water contents was small. The influence of water content may have been higher if a greater range of water contents was tested at the field sites.

The relationship between the combined regression equations based on the laboratory and field results was explored by plotting the predicted composite modulus versus percent compaction for water contents of 4% dry of OWC, at OWC, and 4% wet of OWC as shown in Figures 5.41 through 5.43. It is seen that there is reasonable agreement between the composite moduli predicted by the three regression equations. Moreover the slopes for the lab (select) and field equations are very similar.

The relative importance of percent compaction and water content on the predicted composite modulus was examined using the regression equation based on the combined lab results for Connecticut crushed gravel, New Hampshire sand, and Wardwell gravel. This equation was selected since it has a higher correlation coefficient than the equation based on all the lab results and it is based on data with a much larger range of water contents than at the field sites. The comparison is shown in graphical form in Figure 5.44. It is seen that a change in percent compaction from 90 to 100% would increase the composite modulus by about 50 MPa whereas increasing the water content from 4% dry of optimum to 4% wet of optimum would decrease the composite modulus by about 60 MPa. Thus, percent compaction and water content relative to optimum have a similar significance on the predicted composite modulus.

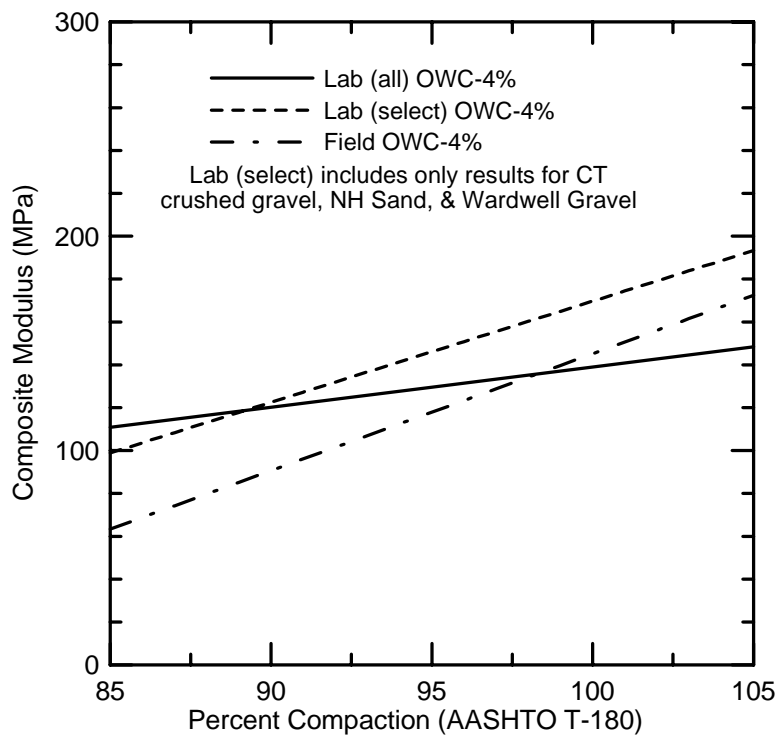


Figure 5.41 Composite modulus predicted by regression equations at 4% dry of optimum.

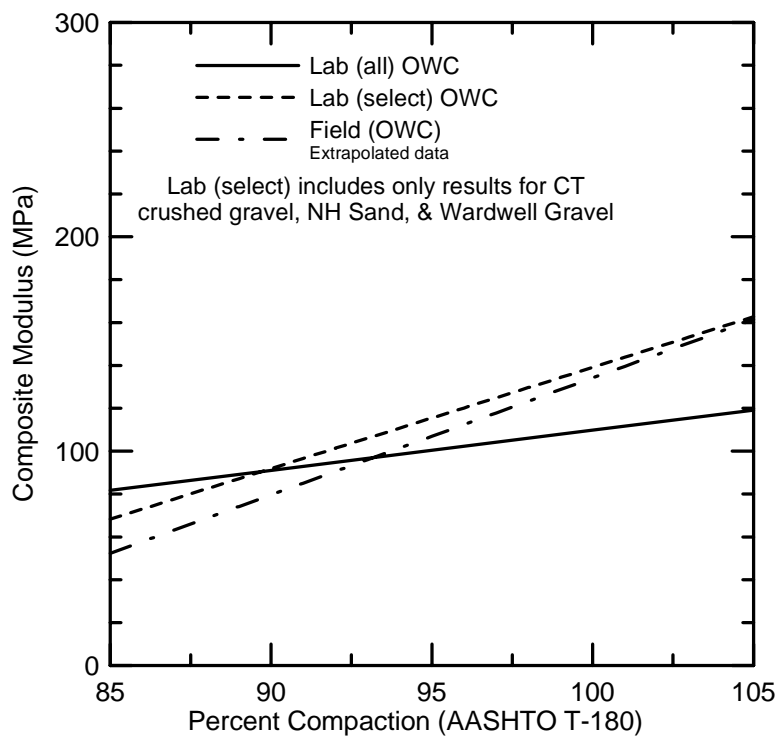


Figure 5.42 Composite modulus predicted by regression equations at optimum.

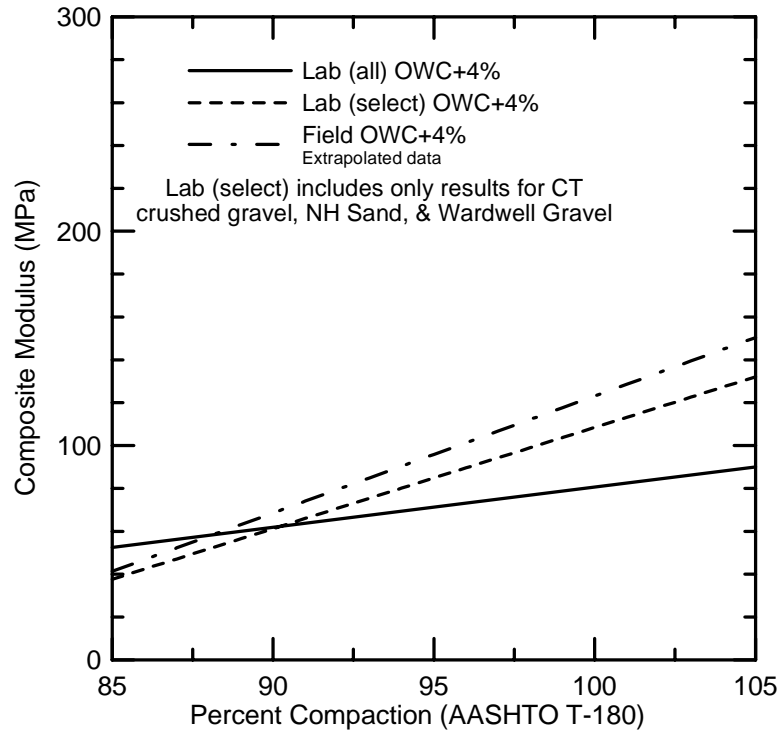


Figure 5.43 Composite modulus predicted by regression equations at 4% wet of optimum.

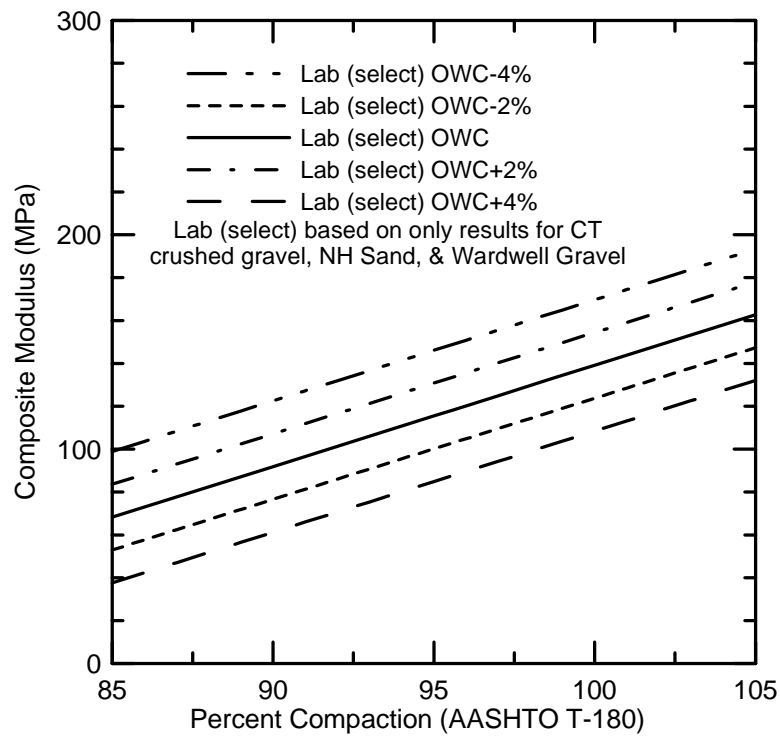


Figure 5.44 Effect of percent compaction and water content on predicted composite modulus based on laboratory results for Connecticut crushed gravel, New Hampshire sand, and Wardwell gravel.

5.3.4 Additional Factors Influencing Composite Modulus

The stiffness characteristics of compacted cohesionless materials are not only influenced by percent compaction and water content, but also by mineralogical composition, size and gradation of the individual particles, and shape of the individual particles (Langfelder and Nivargikar, 1967). Aggregate characteristics for laboratory samples are provided in Table 5.10.

Laboratory results were separated by sample, degree of compaction, and water content relative to optimum. Trials with relative water contents outside the range of $\pm 3\%$ of optimum were removed. The remaining results were separated into three groups based on percent compaction. The low degree of compaction refers to those trials which the percent compaction was less than or equal to 92%. Moderate degree of compaction refers to those trials for which the percent compaction was between 93% and 97%. Finally, high degree of compaction refers to those trials for which the percent compaction was greater than or equal to 98%. Average composite moduli for these categories, as determined from the Prima 100 PFWD, are presented in Table 5.10.

Table 5.10 Comparison of average composite moduli associated with varying degrees of compaction.

Sample	Coefficient of Uniformity (C_u)	Percent Fines (%)	Prima 100 PFWD Composite Modulus (MPa)		
			Low Degree of Compaction ($E \leq 92\% \gamma_{dmax}$)	Moderate Degree of Compaction ($93\% \leq E \leq 97\% \gamma_{dmax}$)	High Degree of Compaction ($E \geq 98\% \gamma_{dmax}$)
Connecticut crushed gravel	18	5.2	114	162	145
New Hampshire sand	5	2.8	75	137	NA
New Hampshire gravel	20	2.9	126	94	91
OJF gravel	10	4.5	NA	61	71
Wardwell gravel	47	6.0	105	108	135

NA – percent compaction was not achieved for given range.

In general terms, for the low degree of compaction, larger composite moduli are associated with higher coefficient of uniformity (C_u). This trend is also evident for moderate and high degrees of compaction with the exception of New Hampshire sand which produced the second largest composite moduli. High values of C_u indicate that a material is well graded. Fine grained particles present in the well graded materials fill the voids between larger particles allowing for a more compact soil fabric and a higher modulus.

The shape of the soil particles may have some effect on the composite modulus. Samples with subangular and angular particles appeared to produce somewhat larger composite moduli than those samples with rounded and subrounded particles. A visual description of particle shapes is provided in Figure 5.45. The most distinct difference is seen when comparing New Hampshire sand (Figure 5.46) and Connecticut crushed gravel (Figure 5.47). The Connecticut crushed gravel sample tended to have higher composite moduli as shown in Table 5.10. The combination of subangular and angular shaped particles and a higher C_u appears to produce higher composite moduli.

5.4 COMPARISON OF PORTABLE DEVICES

The repeatability of results from two different Prima 100 PFWDs as well as a comparison between results from the Prima 100 PFWD and Clegg Impact Hammer (CIH) are examined in this section. A description of the portable devices is provided in Section 2.2.1. A comparison of results from two Prima 100 PFWDs is presented first followed by a comparison between the two different PFWD devices. The effect of operator technique is discussed last.

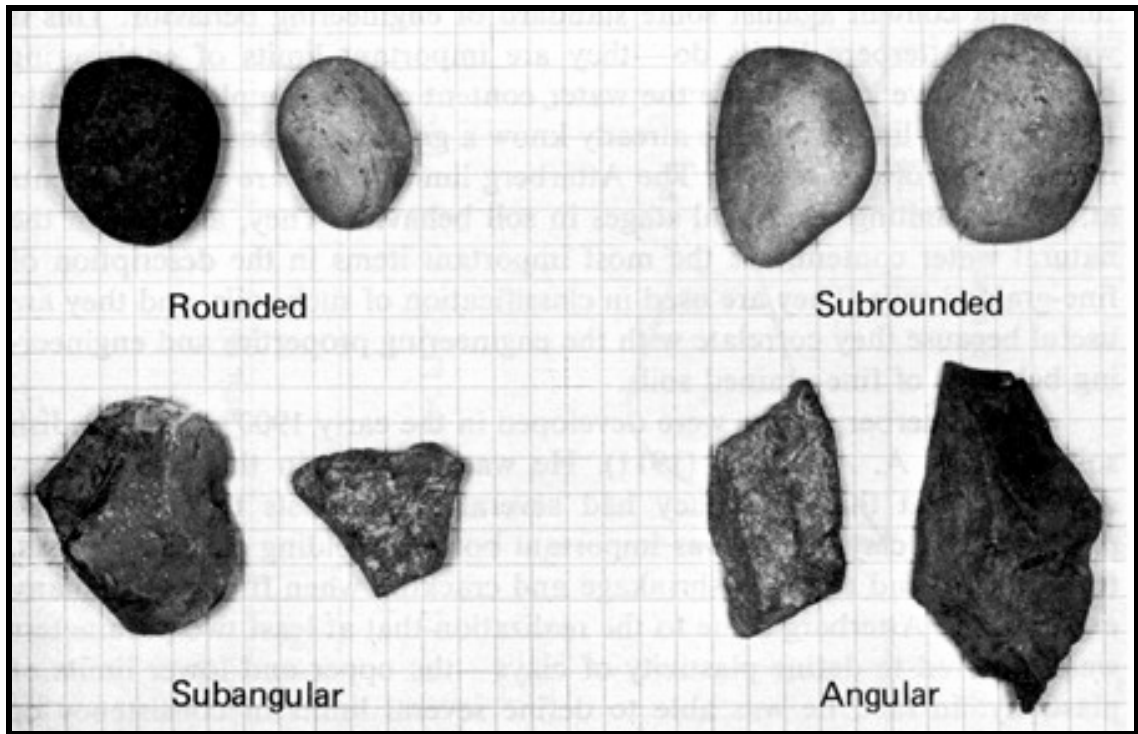


Figure 5.45 Typical shapes of coarse grained bulky particles (Holtz and Kovacs, 1981).



Figure 5.46 Poorly graded New Hampshire sand.



Figure 5.47 Well graded Connecticut crushed gravel.

5.4.1 Prima 100 PFWD Comparison

The results from two Prima 100 PFWDs were compared on gravel samples obtained from Owen J. Folsom & Sons, and Robert Wardwell & Sons Inc. One Prima 100 PFWD was purchased by the UMaine in the spring of 2003 and the other was purchased by the United States Forest Service (USFS) in late fall 2003. During laboratory tests, USFS PFWD measurements were performed first, followed by the UMaine PFWD. Both Prima 100s are shown in Figure 5.48. At each test point, 18 drops (six drops at three different heights) were completed with each device. Additional testing details can be found in Section 3.5.2.3. Composite moduli derived from both devices are plotted versus drop number. This is shown in Figures 5.49 and 5.50.

USFS Prima 100 composite moduli are less than UMaine Prima 100 composite moduli for each drop height. In general, the first drop at each drop height was less than the remaining drops for the same height. This is true for both devices. Prior to the first drop, nonuniform contact exists between the loading plate and the gravel surface. Once the first drop occurs, the surface is compacted and more uniform contact between the surfaces develops. The test point becomes more compact with successive drops. UMaine Prima 100 composite moduli are greater, at least in part, due to the amount of additional compaction the test point has undergone due to testing with the prior testing with the USFS Prima 100.

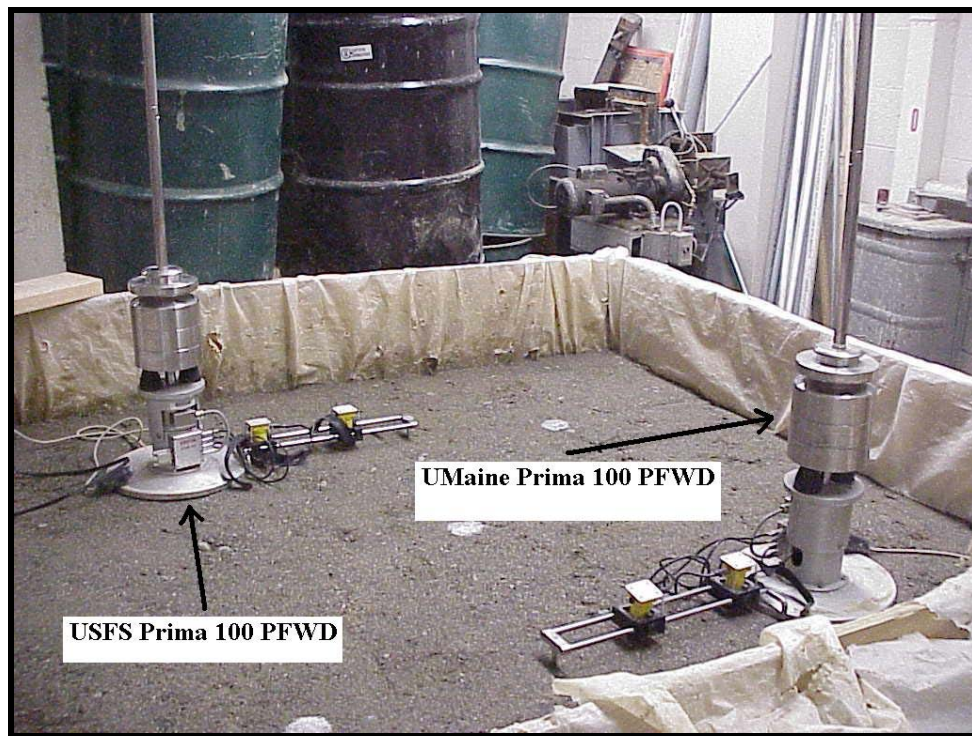


Figure 5.48 Testing with USFS and UMaine Prima 100 PFWDs.

A plot of the composite modulus determined from the USFS PFWD versus the modulus from the UMaine PFWD at the 850 mm (33.5 in.) drop height is shown in Figure 5.51.

The plot confirms that the UMaine Prima 100 produced slightly higher moduli than the USFS Prima 100. A regression analysis yielded a correlation coefficient of 0.954. This shows that two different Prima 100 units give results that correlate very well with each other, even though the modulus values are slightly different. To determine the percent difference between the two units, the regression equation shown in Figure 5.51 was used to compute the USFS moduli corresponding to three different UMaine moduli. The results are shown in Table 5.11. This shows that the UMaine modulus is 18 to 20 percent larger than the USFS modulus. As noted previously, this could be due in part to the higher compaction for the tests with the UMaine device. Alternately, the UMaine device could be biased to give results that are slightly higher than the USFS device.

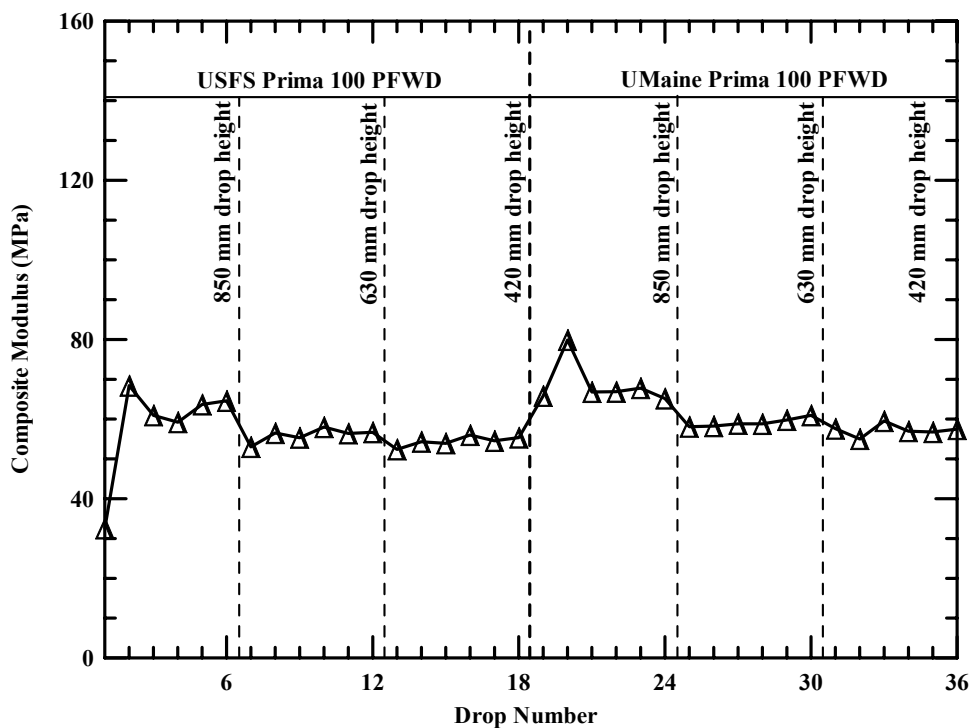


Figure 5.49 Change in composite modulus with subsequent drops for two PFWDs at the same test point for OJF gravel at 100% compaction and optimum water content (TP #1).

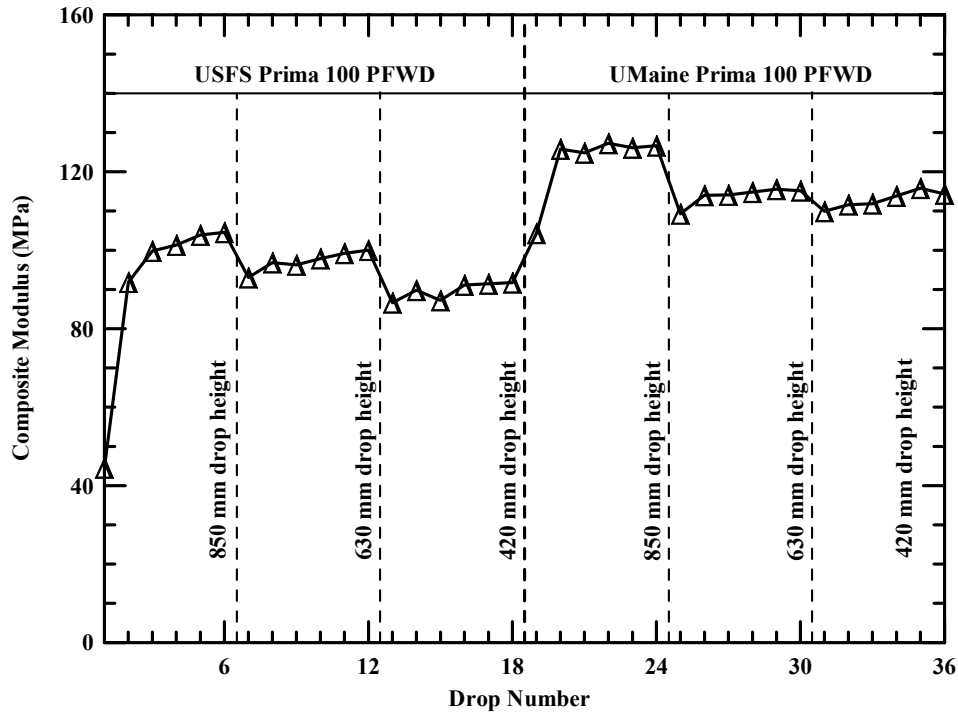


Figure 5.50 Change in composite modulus with subsequent drops for two PFWDs at the same test point for Wardwell gravel at 100% compaction and optimum water content (TP #1).

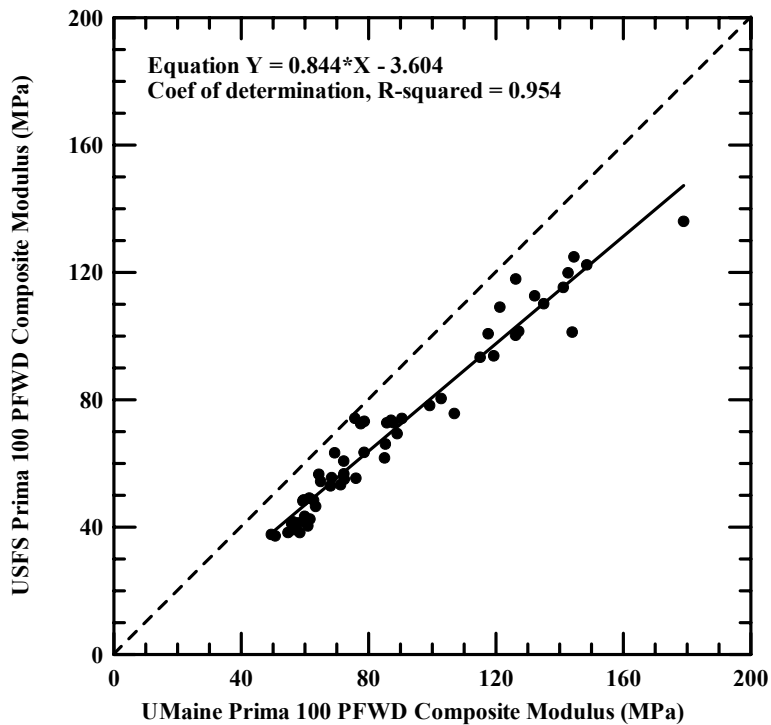


Figure 5.51 Comparison of USFS and UMaine Prima 100 PFWD composite moduli.

Table 5.11 Comparison of composite moduli from USFS and UMaine Prima 100 PFWDs.

USFS Prima 100 PFWD Composite Modulus (MPa)	UMaine Prima 100 PFWD Composite Modulus (MPa)	Percent Difference (%)
64	80	20
98	120	18
131	160	18

5.4.2 Clegg Impact Hammer

The Clegg Impact Hammer (CIH) was used on all laboratory samples. CIH measurements were taken last, after both the USFS and UMaine PFWDs. Six measurements were taken at each location. Additional information pertaining to testing techniques is provided in Section 3.5.2.3. Composite moduli derived from each device are plotted against drop number. Results are shown in Figure 5.52.

Prima 100 composite moduli are greater than composite moduli from CIH measurements. In general, the first drop with the CIH produced moduli that were less than those from subsequent measurements. Moreover, the CIH moduli tended to increase with each subsequent drop. It appeared that a shallow bearing capacity failure occurred upon impact of the falling mass, displacing material down and to the side of the contact surface. This is shown in Figure 5.53. This could be an explanation of why the CIH modulus increased with each subsequent drop. Moreover, the additional vertical displacement induced by bearing capacity failure could contribute to a lower CIH moduli. A plot of Prima 100 PFWD moduli versus CIH moduli is shown in Figure 5.54. A regression analysis yielded a correlation coefficient of 0.483, significantly greater than that obtained during spring thaw monitoring during the spring of 2003 at the USFS Parking Lot. The coefficient of simple determination (r^2) was 0.230.

Table 5.12 Comparison of Prima 100 PFWD composite moduli and CIH moduli.

Prima 100 PFWD Composite Modulus (MPa)	Clegg Impact Hammer Modulus (MPa)	Percent Difference (%)
75	8	89
150	26	83
225	43	81

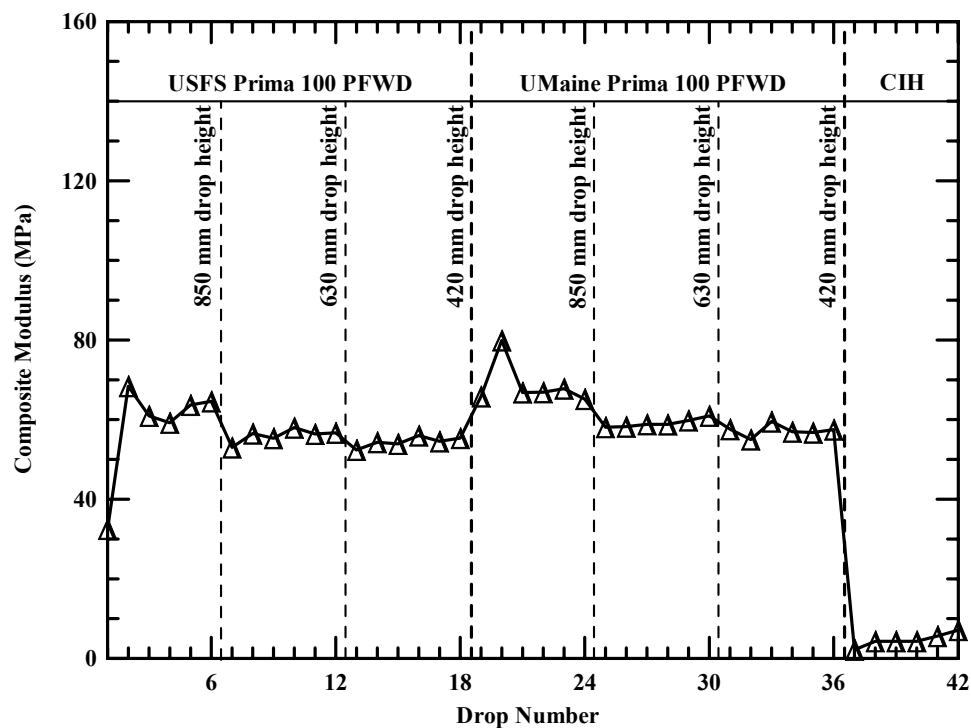


Figure 5.52 Change in composite modulus with subsequent drops for different devices at the same test point for OJF gravel at 100% compaction and optimum water content (TP #1).



Figure 5.53 Clegg Impact Hammer measurement on New Hampshire sand.

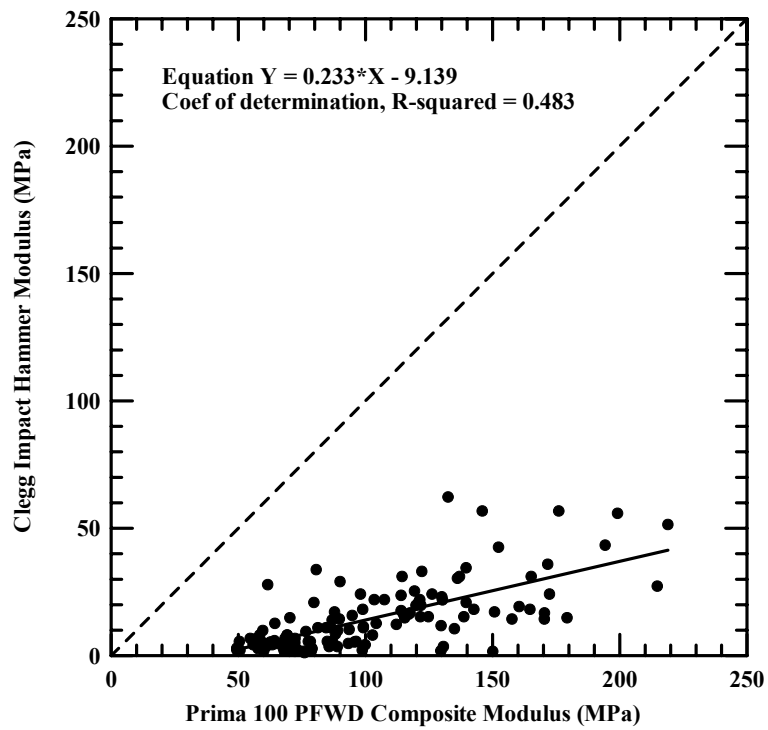


Figure 5.54 Comparison of Clegg Impact Hammer and UMaine Prima 100 PFWD composite moduli.

5.4.3 Effect of Operator Technique

The effect of operator technique was investigated by comparing the results obtained by five different operators, two of which were Maine Department of Transportation technicians. The remaining three operators were made up of undergraduate and graduate research assistants. One of the operators is shown in Figure 5.55. Each user trial was completed on Wardwell gravel sample which was several percentages above optimum water content. Initial instructions were given by the principal investigators to each of the operators prior to use. Each operator completed six measurements at each of the five test locations. The results are compared to determine to what extent individuals operators could produce similar results. This is shown in Table 5.13. Average composite moduli for each user decreased as the testing progressed. In other words, average composite moduli for operator #2 was less than operator #1, operator #3 less than operator #2, and so on. One possible explanation for this is that since the trials were performed on a sample wet of optimum, successive measurements by multiple operators locally increased pore water pressure at each of the test locations. As pore water pressure is increased, modulus (stiffness) is reduced. Minimal elapsed time between users did not allow for dissipation of pore water pressure. Based on visual observation of the operators, none appeared to have difficulties in using the device. Their technique differed only slightly from that used by the primary investigators. As a result, it appears that only minimal training would be required in order to produce acceptable results.



Figure 5.55 MaineDOT representative (operator #2) performing laboratory PFWD measurements.

Table 5.13 Comparison of Prima 100 PFWD composite moduli determined by different users.

Test Point	Operator #1	Operator #2	Operator #3	Operator #4	Operator #5	Average & (Standard Deviation)
1	30	23	26	31	25	27.0 (3.3)
2	34	33	33	35	25	34.6 (1.6)
3	29	31	22	12	13	21.4 (8.9)
4	22	28	13	14	12	17.6 (6.9)
5	29	27	27	22	19	24.8 (4.0)
Average	28.8	28.4	24.2	22.8	18.8	25.1
Std. Dev.	4.3	3.9	7.4	10.1	6.3	4.9

5.5 RECOMMENDATIONS

Despite the importance of modulus, some aspects of pavement construction and management are still based on measurement of other parameters that are not directly

connected with long-term performance or, even less desirable, on empirical based judgments. One critical area that does not currently make use of modulus is evaluating the adequacy of subgrade and base compaction during construction.

Based on the results of this research the tentative procedure given below is recommended for using the Prima 100 PFWD to monitor compaction of granular base courses. The procedure is based on the observation that there is a rough equivalency between percent compaction and composite modulus for granular base at optimum water content. Correction factors are recommended to correct the composite modulus measured at the field water content to the equivalent value at optimum water content. The regression equation for the combined results for Connecticut crushed gravel, New Hampshire sand, and Wardwell gravel (Table 5.8) was used to derive the recommendations. This equation was used since it had a higher correlation coefficient than the regression that included all five laboratory samples combined and it had a larger range of water contents than the field samples.

The target composite modulus at optimum water content should be chosen based on Table 5.14 that gives a rough equivalency with percent compaction based on AASTHO T-180. Composite moduli measured in the field should be corrected to the equivalent composite modulus at optimum water content by adding the factors given in Table 5.15. Thus, it is necessary to determine the field water content relative to OWC to apply this procedure. Possibilities for measuring the water content include oven drying, pan drying, Speedy Moisture Meter[®], time domain reflectometry, or nuclear density meter in backscatter mode. The researchers caution that the values given in Tables 5.14

and 5.15 are based on a limited dataset. It is recommended that these equivalences be confirmed for additional materials used by individual state DOTs.

Table 5.14 Tentative equivalences between percent compaction and composite modulus at optimum water content for base and subbase course aggregate.

Percent Compaction based on AASTHO T-180 (%)	Equivalent Prima 100 PFWD Composite Modulus (MPa) at Optimum Water Content
90	92
95	115
98	130
100	139

Table 5.15 Factor to correct composite modulus measured at field water content to equivalent value at optimum water content.

Water Content Relative to Optimum		Correction Factor to be Added to Composite Modulus (MPa) Measured at Field Water Content
Dry of OWC	-4%	-31
	-3%	-23
	-2%	-15
	-1%	-8
At OWC		0
Wet of OWC	+1%	8
	+2%	15
	+3%	23
	+4%	31

Subgrade soils were tested in the field as part of this project. However, the range of water contents was small. Thus, there is insufficient data to draw conclusions on equivalent composite moduli and the very important effect of water content at the time of testing for subgrade soils.

Field testing techniques for monitoring compaction of aggregates using the Prima 100 PFWD have been developed. These recommendations are based on the experiences of the researchers in using the Prima 100 PFWD as discussed in previous sections. The procedure is similar to that used for testing for thaw weakening discussed in Chapter 4. The Prima 100 PFWD should be setup with the 850 (33.5 in.) drop height, 20 kg (44 lb) drop weight, and 300 mm (12 in.) diameter loading. The Personal Digital Assistant (PDA) based recording software should be setup using the input parameters presented in Table 5.16. Six measurements should be taken at each test location. The first measurement should be discarded and the average of the remaining five should be used as the modulus at that test location. In addition, three locations should be tested within a 3 m (10 ft) diameter area, the average of which will provide a representative value for that particular station.

Table 5.16 Prima 100 PFWD input parameters.

Setup Menu Item	Input Parameter	Value
Trigger	Pretrig time (ms)	10*
	Pulsebase (%)	24*
	Trig Level (kN)	0.90*
View	Sample Time (ms)	60*
Mechanical	Load Plate Radius (mm)	150
	Number of sensors	1
	D ₍₁₎ offset (cm)	0
Formula	Poisson's Ratio	0.35**
	Stress Distribution	2.67
* - default values.		
** - Huang (2004)		

Further research is recommended to validate and refine this procedure for a wider range of soil types. This should be based on measurements obtained at field test sites. Manual water content and sand cone tests should be performed to check the measurements obtained with the NDM. Samples should be obtained for gradation, maximum dry density, and optimum water content determination.

5.6 SUMMARY

This chapter presents the analysis and results of the field and laboratory evaluation of the PFWD as an alternative to traditional compaction control devices. As part of this effort, the relationship between PFWD composite moduli, percent compaction, and water content relative to optimum for soil types representative of New England base and subbase aggregates was explored. PFWD and NDM measurements were taken at five field test sites during the summer and fall of 2003. In addition, laboratory tests were completed on five different samples during the summer of 2004.

For the laboratory tests, each soil sample was compacted in lifts in the 1.8 m x 1.8 m x 0.9 m (6 ft x 6 ft x 3 ft) deep test box initially at a low density. Measurements were taken, then the sample was removed, reconditioned to the desired water content, and recompactd to a higher density and the measurements repeated. Tests were performed percent compactions ranging from 86 to 103 percent and water contents ranging from 3.5 percent dry to 10.2 percent wet of optimum. In total, 29 combinations of water content and density were tested in the laboratory.

The relationship between composite modulus and percent compaction was explored. For four out of the five materials tested, there was a general trend of increasing

composite modulus with increasing percent compaction. New Hampshire gravel exhibited the opposite trend. With the exception of the New Hampshire Sand, the regression coefficients were less than 0.5 indicating poor correlation. Combining all the results yielded a correlation coefficient of 0.045, indicating no correlation. However, including only the results for Connecticut crushed gravel, New Hampshire sand, and Wardwell gravel resulted in a correlation coefficient of 0.35, which still indicates a poor correlation. Regression coefficients were slightly higher when separate correlations were developed for samples dry and wet of optimum, however the r^2 were still less than 0.5. Results from the field test sites also indicate that as the degree of compaction increases, composite modulus increases. In general, correlation coefficients were greater for field test results compared to laboratory test results. Combining the results for the three base materials tested in the field, resulted in a correlation coefficient of 0.818, which is a relatively strong correlation. However, the significance of this correlation is diminished by the fact the water content at all the field sites was dry of optimum. The Prima 100 PFWD also proved adequate in measuring time dependent increases in composite modulus for asphalt stabilized base products tested on Route 201 in The Forks, Maine, and at Commercial Recycling Systems in Scarborough, Maine.

Laboratory results also show that there is a general trend that the composite moduli tends to decrease as water content increases. Correlation coefficients ranged from 0.003 (Connecticut Crushed Gravel) to 0.814 (Wardwell Gravel). The low correlation coefficients for several of the samples are due in part to the role that percent compaction plays in the composite modulus, which is not accounted for when only water content is considered. Combining at the laboratory results yielded a correlation coefficient of 0.285

which indicates poor correlation. For measurements taken at field sites the correlation coefficient ranged from 0.008 (Route 25 Gravel) to 0.521 (Route 25 Sand). However, water contents measured at field sites were generally drier than -3% of the OWC and in some instances were as low as -9% of the OWC, which are significantly different from water contents obtained during laboratory tests.

It is known that stiffness characteristics of compacted cohesionless materials are not only influenced by percent compaction and water content, but also by mineralogical composition, size and gradation of the individual particles, and shape of the individual particles (Langfelder and Nivargikar, 1967). The effect of these factors on composite moduli was difficult to quantify and future research in this area is recommended.

Multivariable linear regression analyses (Neter, et al., 1982) were used to determine the best fit line for composite modulus as a function of percent compaction and water content. The R^2 for the laboratory materials ranged from 0.141 (Connecticut crushed gravel) to 0.867 (Wardwell gravel). Combining all laboratory samples produced an R^2 of 0.326. However, including only laboratory results for Connecticut crushed gravel, New Hampshire sand, and Wardwell gravel increased the R^2 to 0.624. This indicates that 62% of the variation in composite modulus is explained by the percent compaction and water content relative to optimum. The R^2 for the field materials ranged from 0.001 (Route 25 gravel) to 0.679 (I-84 crushed gravel). Combining the three field sites where granular base was tested yielded an R^2 of 0.823, which indicates a reasonably strong correlation of composite modulus with percent compaction and water content, independent of the type of material tested. However, the water contents for the field sites were all dry of optimum which may limit the significance of this result. The multi-

variable linear regressions based on the three laboratory samples indicated above and field results yielded predicted composite modulus at 95% percent compaction that were agreed within 20% which is reasonable agreement.

The results from two Prima 100 PFWDs were compared on gravel samples obtained from Owen J. Folsom & Sons and Robert Wardwell & Sons Inc. The UMaine Prima 100 produced slightly higher moduli than the USFS Prima 100. The USFS PFWD was used first, completing six measurements at three different drop heights, at each of the five test locations before the process was repeated with the UMaine PFWD. The differences in moduli could, in part, be due to additional compaction test points underwent as a result of using the USFS PFWD first. A regression analysis yielded a correlation coefficient of 0.954. This shows that two different Prima 100 units give results that correlate well with each other, even though the modulus values are slightly different.

The Prima 100 PFWD and Clegg Impact Hammer (CIH) were used on all laboratory samples. Prima 100 composite moduli were greater than composite moduli derived from CIH measurements. The occurrence of a shallow bearing capacity failure caused by the impact of the CIH could help to explain the large differences between moduli from the devices. Additionally, the first drop with the CIH produced moduli that were less than those derived from subsequent measurements. Finally, the CIH moduli tended to increase with each subsequent drop.

The effect of operator technique was investigated by comparing the results obtained by five different operators on one trial of Wardwell gravel (90% compaction, +10% w_{opt}). Average composite moduli for each user decreased as testing progressed

which could partially be caused by the presence of excess water in the material at the time of testing, as minimal time was allotted for dissipation of pore water pressure between tests.

Recommendations were made for utilizing the Prima 100 PFWD as a tool to monitor compaction. Tentative equivalences between percent compaction and composite modulus for base course aggregates at optimum water content were provided. The recommendations were based on a multi-variable linear regression on laboratory results for Connecticut crushed gravel, New Hampshire sand, and Wardwell gravel. In addition, correction factors to correct composite moduli measured at the field water content to the equivalent value at optimum were proposed. Additional study on a wider range of base course aggregates and water contents is recommended.

CHAPTER 6

SUMMARY, CONCLUSIONS, AND RECOMMENDATIONS

6.1 SUMMARY

Vehicles can cause significant damage to roads that are weakened during the spring thaw. To minimize damage, many road maintenance agencies impose load restrictions on selected roads during damage susceptible periods. Although, the maximum allowable load and the duration of the reduced load period vary widely among agencies, they try to strike a balance between minimizing the disruption to the local economy caused by the load restrictions and minimizing road damage.

The decrease in the stiffness of the pavement system during the spring thaw is a key factor leading to pavement damage. The term stiffness is often used interchangeably with elastic modulus, resilient modulus, or in some cases, simply modulus. Stiffness can be monitored during spring thaw and through recovery using a Falling Weight Deflectometer (FWD). However, FWD purchase, operation, and maintenance is expensive. Moreover, even if a state owns a FWD, it can only cover so many roads within a given time frame. As a result, determining when the road has thawed to the point where a load restriction is needed and when the road has recovered sufficient strength to remove the restriction is often left to personal experience and subjective judgment.

Irrespective of the seasonal changes in modulus, the overall stiffness of compacted base and subgrade layers has a significant effect on pavement life. The current practice during construction is to achieve a high modulus by reaching a specified percent compaction. However, current techniques for monitoring compaction exhibit numerous shortcomings.

Prior to the 1980's, the sandcone was widely used to measure density and provide quality control for construction. However, the sandcone test is labor intensive and time consuming. In practice, it has been replaced by the nuclear moisture density gauge, or densimeter. Although considerably faster than the sandcone, the densimeter's radioactive source constrains use and handling. Because of the problems, compaction conformance is sometimes left to subjective judgment. This may compromise the integrity of the finished project resulting in reduced service life and increased maintenance costs. Moreover, none of the methods measure stiffness directly.

The objective of the study were to address the concerns discussed above. Specific objectives are listed below.

1. Evaluate the portable falling weight deflectometer (PFWD) as a means of optimizing timing for load restriction placement and removal on secondary roads in New England.
2. Develop guidelines for PFWD use on pavement structures typical of New England low volume roads.
3. Evaluate the effectiveness of the PFWD as a means for monitoring compaction, density, or bearing capacity at construction sites. This includes developing correlations between PFWD results and percent compaction for a range of soils.
4. Develop guidelines, including acceptance and testing protocols, determined via testing and subsequent conventional and statistical analyses.

5. Compare the results from different PFWD's and several alternative devices for measuring the degree of compaction of highway subgrade soils and base/subbase coarse aggregates.

6.1.1 Literature Review

Portable falling weight deflectometers (PFWD) have been developed by several manufacturers to measure the in situ stiffness of construction layers including subgrades, base courses, and pavements. For paved roads, moduli or deflection results determined by PFWDs were compared by several investigators to values determined by FWDs and Benkelman Beams. The Loadman PFWD was used for most of these studies. In general, the comparisons showed marginal correlation coefficients (r^2) less than 0.5, however one study obtained an r^2 of 0.86 for a correlation between moduli determined by the FWD and PFWD. The PFWD generally produced higher modulus values than the FWD, possibly due to the smaller depth of influence. Several investigators reported that the zone of influence for the PFWD lies primarily between one and two loading plate diameters. Large aggregate particles beneath the loading plate of the portable devices also affect the results, as the particles increase the resulting modulus values. Some investigators imply that the PFWD is better suited to roads with thin pavements.

For unbound layers, PFWD results were compared to results from FWD, plate bearing test, Clegg Hammer, surface stiffness gage, and Benkelman Beam. PFWD from several manufacturers were tested including Handy, Loadman, Prima 100, and German Dynamic Plate Tester. In general, each device could detect changes in soil stiffness. Several studies found good correlation between moduli from PFWD and FWD with r^2 between 0.31 and 0.99 with most values greater than 0.5. The Clegg Hammer generally correlated poorly

with results from other devices. reasonably with other devices when testing on unbound layers. A limited number of studies examined correlations between PFWD moduli and percent compaction. Correlations were generally poor.

The PFWD has the potential to track seasonal stiffness variations in paved and unpaved low volume roads. Pavement modulus is a key parameter in determining damage-susceptibility of pavements. Pavements in areas with seasonal freezing and thawing often undergo frost heave and thaw weakening in addition to load-induced pavement distress. To minimize damage, many road maintenance agencies impose load restrictions during damage-susceptible periods. This can be monitored during spring thaw and through recovery using a traditional FWD to assist in determining when to place and remove the restrictions. However, the initial investment in purchasing a FWD, as well as high operation and maintenance costs limits its use. As a result, determining when the road has thawed and recovered sufficient strength to remove the restriction is left to personal experience and subjective judgment.

Limited studies have been conducted to evaluate the PFWD as a tool for tracking seasonal stiffness variations. Correlation coefficients relating the PFWD and the Benkelman Beam were generally high. For thin pavement sections, the PFWD did adequately follow the seasonal stiffness variations.

An increasing number of studies have been conducted to develop quantitative techniques that may be used to better determine when load restrictions should be placed and removed. A majority of state and local agencies use subjective techniques, such as observation, to both place and remove load restrictions. Fewer departments were using quantitative methods to place load restrictions, however, an even smaller number use the

same methods to remove load restrictions. Additionally, some simply keep restrictions in place for a specific length of time. Studies conducted in Washington and Minnesota have attempted to use air temperature to determine when to place and remove the restrictions, and appear to have worked adequately for the conditions in their respective states. Additional work done in Washington has suggested that using deflection data to aid in load restriction placement and removal can be done and recommends that during the spring thaw, once the deflections reach 40 to 50% of their fully recovered values, weight restrictions should be placed and removed.

6.1.2 Field & Laboratory Test Protocol

The performance of seven paved and three gravel surfaced roads were monitored during the spring of 2004. Test sites were located in Maine, New Hampshire, and Vermont. Two additional sites in Northern Maine were used for testing on one day as part of an ongoing MaineDOT research project. The test sites varied in asphalt thickness, subbase thickness and type, and subgrade type.

Instrumentation was used to quantify the condition of the test sections on days when measurements were made. Thermocouples, thermistors, and frost tubes were used at selected sites to monitor the advance and retreat of freezing conditions during late winter and spring months. Vibrating wire and standpipe piezometers were installed at selected sites to monitor pore water pressures in the subbase, and at some sites, subgrade layers. Time Domain Reflectometry (TDR) probes were used to monitor water content through the spring thaw and recovery periods at some sites. Instrumentation was used to examine the extent to which the road had thawed and provided the context for interpretation of PFWD and FWD results.

Manual instrumentation readings were taken approximately weekly through the spring thaw and recovery periods. At selected sites, instrumentation was read automatically by data acquisition systems and was downloaded approximately weekly.

Prima 100 PFWD and traditional FWD measurements were taken at a minimum of eight locations at each test site. Measurements were taken approximately weekly during the spring thaw period. In addition, Loadman PFWD measurements were taken at spring thaw test sites in Rumney, New Hampshire. Clegg Impact Hammer and Humboldt Soil Stiffness Gauge measurements were taken at the United States Forest Service (USFS) Parking Lot during the spring of 2003 and 2004. With the Prima 100 PFWD, six measurements were taken at each of three different drop heights, at each test location. The drop heights were approximately 850, 630, and 420 mm (34, 25, and 17 in.). Deflection sensors were used with spacing as follows (as measured from the center of the loading plate): 0, 207, and 407 mm (0, 8, and 16 in.). The PFWD measurements were taken utilizing a 20 kg (44 lb) drop weight and a 300 mm (11.8 in.) loading plate. In all cases, the first reading was neglected and the average of the remaining five was used for analysis and comparison. In addition, five Loadman PFWD, four Clegg Impact Hammer, and one Soil Stiffness Gauge measurement was taken at each test location. The MaineDOT provided a FWD for seasonally posted roads in Maine. The United States Army Corps of Engineers Cold Regions Research and Engineering Laboratory (CRREL) provided a FWD for test sites in Rumney, New Hampshire. The Vermont Agency of Transportation (VAOT) provided a FWD for seasonally posted low volume roads in Vermont. MaineDOT provided backcalculation of FWD data from field test sites in Maine using DARWin. The researchers completed

backcalculation procedures for FWD data obtained from New Hampshire and Vermont field test sites using Evercalc.

Five field test sites in Maine, New Hampshire, and Connecticut were used to evaluate the effectiveness of the PFWD as a tool to monitor compaction. Different material types were tested at each field site. Tests were performed at a minimum of 12 locations, utilizing both the Prima 100 PFWD and Nuclear Moisture Density Gauge (NDM) (AASHTO T 238). With the PFWD, six measurements were taken at each test location utilizing the 20 kg drop weight, 300 mm diameter loading plate, and 850 mm drop height. Only the deflection sensor integral to the loading plate was used. The Connecticut Department of Transportation and the New Hampshire Department of Transportation provided a NDM for field test sites in their respective states. NDM measurements were taken at depths of 203, 152, 102, 51, and 0 mm (8, 6, 4, 2, and 0 in.) at each test location. Samples were taken at each site for sieve analysis, maximum dry density, and optimum water content determination. Tests were performed in accordance with AASHTO test procedures.

The primary purpose of the laboratory component of this project was to determine a relationship between PFWD results and percent compaction under controlled conditions. The large-scale laboratory study to correlate PFWD results to percent compaction was constructed in the geotechnical research laboratory at the University of Maine. The tests were conducted in a 1.8 m x 1.8 m x 0.9 m (6 ft x 6 ft x 3 ft) deep test container. The bottom 203 mm (8 in.) of material met MaineDOT Type D aggregate specifications. This material was kept in place throughout all laboratory tests. Five different material types were used to fill the remaining height of the test box. Material was added to the container in approximately 152 mm (6 in.) lifts. Each lift was compacted using a hand tamper and

electric jackhammer with a modified flat plate attachment. Each aggregate was compacted in the container to approximately 90, 95, and 100% of the maximum dry density (AASHTO T 180). The effect of water content was determined at 95% of the maximum dry density. Measurements were taken at optimum water content as well as $\pm 3\%$ of the optimum water content. Once all the material was compacted in the test container, several portable testing devices were used. Prima 100 PFWD, Clegg Impact Hammer, NDM, and Dynamic Cone Penetrometer (DCP) tests were performed at multiple locations. Prima 100 PFWD and Clegg Impact Hammer measurements were taken in the same manner as was done for the spring thaw portion of the research. In addition, one sand cone test was completed, and two water content samples were taken for each trial for comparison to NDM measurements.

6.1.3 Spring Thaw Monitoring

6.1.3.1 Instrumentation Measurements

Subsurface temperatures were measured at each field site during the end of the freezing season, throughout the thawing period, and into the recovery period. Measurements taken at asphalt surfaced test sites indicated freezing temperatures penetrated to their maximum depths between February 17 and March 24, 2004. Maximum depths ranged from a low of 866 mm (34 in.) at Stinson Lake Road to a high of 1930 mm (76 in.) at Route 1A (Section D-2). Complete thaw occurred at all test sites between mid-March and mid-April. Measurements taken at gravel surfaced test sites indicated freezing temperatures penetrated to their maximum depths between March 1 and April 21, 2004. Maximum depths ranged from a minimum of 1128 mm (44 in.) at the USFS Parking Lot to a maximum of 2134 mm

(84 in.) at Crosstown Road. Complete thaw had occurred at all sites between early April and mid May.

Pore water pressures were measured in the subbase layer at each field site during the thawing and into the recovery period. At some sites, pore water pressures were also measured in the subgrade layer. The highest water levels observed in standpipe piezometers roughly correspond to the date of complete thaw for that particular site. This is true for both asphalt and gravel surfaced test sections. TDR moisture sensors used at the USFS Parking Lot and Stinson Lake Road also indicate an increase in moisture content at or near the date of complete thaw. The relationship between manual vibrating wire piezometer measurements and thawing at the Route 126 and Route 1A sites is unclear.

At the Route 126, Sections 3 and 8, vibrating wire piezometer readings were monitored hourly by a datalogger. At the initiation of thawing, subgrade porewater pressures in these sections were negative. Once thawing commenced, the subgrade porewater pressure increased reaching a maximum head of 1.2 m (4 ft) about a month after complete thawing. In the subbase at Section 3, the head was near zero from the initiation of thawing through the end of monitoring in mid-June. In Section 8, the subbase pore water pressure was about -0.6 m (-2 ft) from the initiation of thawing through the end of monitoring.

Overall, the piezometer results indicate that at most sites higher porewater pressures in the subgrade and subbase soils were associated with the thawing period. This is a factor that could contribute to reduction of pavement stiffness during the spring thaw.

6.1.3.2 Seasonal Stiffness Variations

For each test site, Prima 100 PFWD composite modulus, and where it is available, FWD asphalt, subbase, subgrade, and composite modulus and Loadman PFWD composite modulus values were plotted versus date. In general, for asphalt surfaced test sites, the moduli are high when the pavement section is frozen and during the early part of the period when section is partially thawed. At some field sites there are significant differences in moduli from nearby test locations and from one week to the next. This variability is more apparent in gravel surfaced test sites compared to asphalt surfaced test sites. For both asphalt and gravel surfaced test sites, composite moduli generally decreased as thawing progressed. It was anticipated that a distinct minimum would occur before increasing through the recovery period. However, this was only evident at the Buffalo Road, USFS Parking Lot, Knapp Airport Parking Lot, Crosstown Road, and to a lesser extent Stinson Lake Road. At the remaining sites, the composite modulus that was reached during the spring thaw was about the same as, or in some, cases greater than the values measured during the summer. FWD derived layer moduli confirm these observations. In general, portable and traditional FWD moduli follow similar trends for both asphalt and gravel surfaced test sites through the monitoring period. Thus, the PFWD and FWD would be equally as effective in monitoring stiffness change during the spring thaw.

6.1.3.3 Comparison of Portable and Traditional FWD Moduli

The degree of correlation between composite moduli backcalculated using FWD and Prima 100 PFWD results were investigated. This was done for five sites in Maine where the composite moduli from the FWD were available. Regression analyses yielded correlation

coefficients ranging from 0.336 (Route 1A) to 0.950 (Witter Farm Road). In general, correlation coefficients tended to increase as pavement thickness decreased. The data from three test sites with asphalt thicknesses less than or equal to 127 mm (5 in.) were combined and produced the best correlation with $r^2 = 0.873$. Two test sites with an asphalt thickness of 152 mm (6 in.) followed with $r^2 = 0.559$. However, when excluding unreasonably high moduli greater than 4000 MPa, the correlation improves with $r^2 = 0.802$. Route 1A was the single test site with a 180 mm (7 in.) asphalt thickness and produced the poorest correlation with $r^2 = 0.336$. A regression analysis combining all asphalt surfaced test sites produced a correlation coefficient of 0.531. Again, when moduli greater than 4000 MPa are excluded, the correlation improved with $r^2 = 0.809$. The average FWD and PFWD composite moduli were lower for the 178 mm (7 in.) asphalt thickness than the 127 mm (5 in.) thickness. This is contrary to expectations, since thicker pavements would be expected to yield higher composite moduli.

Subbase moduli were derived from backcalculating traditional FWD data using Evercalc. For each site, subbase moduli were plotted against composite moduli as measured with the Prima 100 PFWD to determine if a correlation existed between the two measured variables. Regression analyses yielded correlation coefficients ranging from 0.163 (Route 1A) to 0.807 (Knapp Airport Parking Lot). In general, correlation coefficients tended to increase as pavement thickness decreased. Five test sites with an asphalt thicknesses equal to 127 mm (5 in.) had an $r^2 = 0.508$. However, when excluding moduli greater than 5000 MPa, the correlation improves with $r^2 = 0.693$. One test site (Route 126) with a 150 mm (6 in.) asphalt thickness produced the best correlation with $r^2 = 0.698$. Route 1A served as the single test site with a 180 mm (7 in.) asphalt thickness produced the poorest correlation with

$r^2 = 0.363$. Regression analysis was completed for all the data combined, this yielded a correlation coefficient of 0.485, however, when excluding all moduli greater than 5000 MPa (Figure 4.59), the correlation improved with $r^2 = 0.654$. These results suggest that the PFWD composite modulus is influenced by the stiffness of the subbase.

6.1.3.4 Impact Stiffness Modulus

The Impact Stiffness Modulus (ISM) is the ratio of the applied force (kN) to the deflection (μm) measured from the center sensor. Correlations between portable and traditional FWD derived ISM tend to increase as pavement thickness decreases. This trend is similar to that exhibited by composite and subbase moduli. Traditional and portable FWD derived ISM are compared for three gravel surfaced test sites. Regression analyses yielded correlation coefficients ranging from 0.638 (Lakeside Landing Road) to 0.914 (Crosstown Road).

6.1.3.5 Comparison to Other Portable Devices

Loadman and Prima 100 PFWD composite moduli are compared to FWD derived subbase moduli for two asphalt surfaced test sites in Rumney, New Hampshire. Correlations developed indicate that for a given FWD derived subbase modulus, the Loadman PFWD provides a composite modulus that is less than the corresponding value provided by the Prima 100. The Prima 100 PFWD correlates better to FWD derived subbase moduli ($r^2 = 0.552$) than composite moduli obtained from the Loadman PFWD ($r^2 = 0.245$).

6.1.3.6 Evaluation of Field Testing Techniques

6.1.3.6.1 Loading Plate Diameter and Drop Weight

Operation of the Prima 100 PFWD with drop weights of 10, 15, and 20 kg (22, 33, and 44 lb), and plate diameters of 100, 200, and 300 mm (4, 8, and 12 in.) were investigated. In general, the 20 kg (44 lb) drop weight produced the lowest moduli and moduli that were independent of loading plate diameter. The 15 kg (33 lb) weight produced moduli that were greater than those obtained with the 20 kg (44 lb) and also did not vary significantly with loading plate diameter. The highest moduli were obtained using the 10 kg (22 lb) drop weight. At this weight, moduli decreased with increasing loading plate diameter. A possible explanation for this behavior is that a small plate diameter and drop weight influence only the upper portions of the pavement section and thus the deflection responses are dominated by the stiffer pavement layer, producing a larger composite modulus. When plate diameter and drop weight are increased, depth of influence is increased and the stiffness of both the subbase and asphalt layers are reflected in the composite modulus, resulting in a lower value.

6.1.3.6.2 Drop Height

Measurements were taken at three different drop heights at each test location throughout the monitoring period. Drop heights used were approximately equal to 850, 630, and 420 mm (33.5, 24.8, and 16.5 in.). In general, reduced drop heights produce moduli that are slightly less than moduli derived from using the full (850 mm) drop height. This trend is evident regardless of asphalt thickness; however, the differences tend to decrease with increasing asphalt thickness. Decreasing drop height reduces the depth of influence. When

asphalt thickness increases and drop height is reduced simultaneously, measured moduli are heavily influenced by the stiffness of the asphalt layer.

6.1.3.6.3 Moduli Derived From Additional Geophones

Three deflection sensors were used at each site to observe differences in moduli derived from measurements taken from each of the geophones. Spacing of the sensors (as measured from the center of the loading plate) is: 0, 207, and 407 mm (0, 8, and 16 in.). The current Prima 100 software uses only the deflections of a single geophone to backcalculate the modulus. The user selects which geophone will be used. Moduli derived from measurements from the outer two geophones are significantly greater than the composite moduli determined from the center geophone. Unless software can be developed to incorporate the deflections from all three geophones simultaneously into a backcalculation routine, the additional geophones provide little useful additional information.

6.1.3.6.4 Effect of Number of Drops on Composite Modulus

Six Prima 100 PFWD measurements were taken at each of three different drop heights, at each test location. For the majority of points tested at the field sites; the first measurement was less than subsequent measurements. This was consistent with observations made by other researchers as discussed in the Literature Review. On the average, first drop was less than the average of the remaining five drops by nearly 10%. However, the second drop was only 1% less than the average of the remaining four drops. This shows that the results of the first drop should always be neglected. It is recommended that the results from drops two through six be averaged to obtain results that are representative of a test location.

6.1.3.6.5 Recommendations

Field testing techniques for monitoring seasonal stiffness variation in paved and unpaved low volume roads using the Prima 100 PFWD were developed. The core of the recommendations is that load restrictions are placed once the composite moduli measured with the PFWD drops below 80% of the fully recovered baseline value measured during the summer and early fall. The load restriction is then removed when the moduli recover to 80% of the baseline value. The selection of 80% is arbitrary since the amount of damage that would occur at the reduced modulus depends on individual pavement sections, allowable vehicle weight, and traffic levels. Assessment of these factors was beyond the scope of this study. Baseline value measurements and measurements during the spring thaw should be made at the same locations. During the early portion of thawing period, it may be necessary to take daily readings to monitor the sometimes rapid decrease in composite modulus. It is recommended that the 300 mm (12 in.) loading plate, maximum drop height, and maximum drop weight be used for testing.

6.1.4 Compaction Control

6.1.4.1 Laboratory Measurement Verification

As a check on the accuracy of the Nuclear Density Meter (NDM) used in the laboratory tests, oven-dried water content and sand cone tests were also performed. Two water content and one sand cone test were completed for each trial. Water contents determined from both methods compared reasonably. A regression analysis yielded a correlation coefficient of 0.55. As a result, using water contents determined from NDM

measurements was justified and were used for analysis and comparison. There was essentially no correlation between the percent compaction NDM and sand cone. Moreover, the sand cone predicted percent compactions that were greater than the NDM and many results were in the range of 100% to 123%. Given the unreasonably high percent compactions resulting from some of the sand cone results, it was concluded that the sand cone results were unreliable and NDM derived values were used for comparison.

6.1.4.2 Field and Laboratory Test Results

Laboratory tests were performed on five soil types representative of New England base and subbase aggregates. These materials include: one crushed material, one construction sand, and three base/subbase aggregates. The field component included tests on two subgrades, one construction sand product, two aggregates, and one reclaimed stabilized base product.

For the laboratory tests, the composite moduli generally increased as percent compaction increased. This was true for all samples with the exception of the New Hampshire Gravel which exhibited the opposite trend. With the exception of the New Hampshire Sand, the regression coefficients were less than 0.5 indicating poor correlation. Combining all the results yielded a correlation coefficient of 0.045, indicating no correlation. However, including only the results for Connecticut crushed gravel, New Hampshire sand, and Wardwell gravel resulted in a higher correlation coefficient of 0.35, but still indicating a poor correlation. Regression coefficients were slightly higher when separate correlations were developed for samples dry and wet of optimum, however the r^2 were still less than 0.5. Results from the field test sites also indicate that as the degree of compaction increases,

composite modulus increases. In general, correlation coefficients were greater for field test results compared to laboratory test results. Combining the results for the three base materials tested in the field, resulted in a correlation coefficient of 0.818, which is a relatively strong correlation. However, the significance of this correlation is diminished by the fact the water content at all the field sites was dry of optimum. The Prima 100 PFWD also proved adequate in measuring time dependent increases in composite modulus for asphalt stabilized base products tested on Route 201 in The Forks, Maine, and at Commercial Recycling Systems in Scarborough, Maine.

Laboratory results also show that there is a general trend that the composite moduli tends to decrease as water content increases. Correlation coefficients ranged from 0.003 (Connecticut Crushed Gravel) to 0.814 (Wardwell Gravel). The low correlation coefficients for several of the samples are due in part to the role that percent compaction plays in the composite modulus, which is not accounted for when only water content is considered. Combining at the laboratory results yielded a correlation coefficient of 0.285 which indicates poor correlation. For measurements taken at field sites the correlation coefficient ranged from 0.008 (Route 25 Gravel) to 0.521 (Route 25 Sand). However, water contents measured at field sites were generally drier than -3% of the OWC and in some instances were as low as -9% of the OWC, which are significantly different from water contents obtained during laboratory tests.

Multivariable linear regression analyses (Neter, et al., 1982) were used to determine the best fit line for composite modulus as a function of percent compaction and water content. The R^2 for the laboratory materials ranged from 0.141 (Connecticut crushed gravel) to 0.867 (Wardwell gravel). Combining all laboratory samples produced an R^2 of 0.326.

However, including only laboratory results for Connecticut crushed gravel, New Hampshire sand, and Wardwell gravel increased the R^2 to 0.624. This indicates that 62% of the variation in composite modulus is explained by the percent compaction and water content relative to optimum. The R^2 for the field materials ranged from 0.001 (Route 25 gravel) to 0.679 (I-84 crushed gravel). Combining the three field sites where granular base was tested yielded an R^2 of 0.823, which indicates a reasonably strong correlation of composite modulus with percent compaction and water content, independent of the type of material tested.

However, the water contents for the field sites were all dry of optimum which may limit the significance of this result. The multi-variable linear regressions based on the three laboratory samples indicated above and field results yielded predicted composite modulus at 95% percent compaction that agreed within 20% which is reasonable agreement.

The results from two Prima 100 PFWDs were compared on gravel samples obtained from Owen J. Folsom & Sons and Robert Wardwell & Sons Inc. The UMaine Prima 100 produced slightly higher moduli than the USFS Prima 100. The USFS PFWD was used first, completing six measurements at three different drop heights, at each of the five test locations before the process was repeated with the UMaine PFWD. The differences in moduli could, in part, be due to additional compaction test points underwent as a result of using the USFS PFWD first. A regression analysis yielded a correlation coefficient of 0.954. This shows that two different Prima 100 units give results that correlate well with each other, even though the modulus values are slightly different.

The Prima 100 PFWD and Clegg Impact Hammer (CIH) were used on all laboratory samples. Prima 100 composite moduli were greater than composite moduli derived from CIH measurements. The occurrence of a shallow bearing capacity failure caused by the

impact of the CIH could help to explain the large differences between moduli from the devices. Additionally, the first drop with the CIH produced moduli that were less than those derived from subsequent measurements. Finally, the CIH moduli tended to increase with each subsequent drop.

The effect of operator technique was investigated by comparing the results obtained by five different operators on one trial of Wardwell gravel (90% compaction, +10% w_{opt}). Average composite moduli for each user decreased as testing progressed which could partially be caused by the presence of excess water in the material at the time of testing, as minimal time was allotted for dissipation of pore water pressure between tests.

Recommendations were made for utilizing the Prima 100 PFWD as a tool to monitor compaction. Tentative equivalences between percent compaction and composite modulus for base course aggregates at optimum water content were provided. The recommendations were based on a multi-variable linear regression on laboratory results for Connecticut crushed gravel, New Hampshire sand, and Wardwell gravel. In addition, correction factors to correct composite moduli measured at the field water content to the equivalent value at optimum were proposed. Additional study on a wider range of base course aggregates and water contents is recommended.

6.2 CONCLUSIONS

The conclusions listed below are based on the work presented in this report and the experience of the researchers in using the Prima 100 PFWD.

6.2.1 Spring Thaw Monitoring

1. Prima 100 PFWD composite moduli follow similar trends to composite moduli and subbase moduli as determined from FWD measurements on both asphalt and gravel surfaced roads.
2. A strong correlation exists between portable and traditional FWD composite moduli. The correlation increases with decreasing asphalt thickness.
3. A reasonable correlation exists between Prima 100 PFWD composite moduli and subbase moduli determined from FWD measurements on both asphalt and gravel surfaced roads. The correlation increases with decreasing pavement thickness.
4. Loadman PFWD provides a composite modulus which is greater than the corresponding value provided by the Prima 100. The Prima 100 PFWD correlates better than the Loadman PFWD to FWD subbase moduli.
5. The PFWD can be used as a tool to evaluate whether specific roadways experience strength loss during the spring thaw and thus warrant load restrictions. For roads where load restrictions are placed, the PFWD can be used as an aid in determining when restrictions should be placed and removed.

6.2.2 Field Testing Techniques

1. Composite moduli increase with decreasing drop weight.
2. Composite moduli are independent of loading plate diameter when using 15 and 20 kg drop weight.

3. Reduced drop heights produce moduli that are slightly less than moduli derived from using the full (850 mm) drop height.
4. Moduli derived from measurements from the outer two geophones are significantly greater than composite moduli determined from the center geophone.
5. The composite moduli determined from the first drop was generally less than those derived from subsequent drops and should be ignored when computing the composite modulus for a test location.

6.2.3 Compaction Control

1. Field and laboratory test results indicate that as percent compaction increases, composite modulus increases. The correlation between the two was poor, however, it was better for field tests compared to laboratory tests.
2. Field and laboratory test results indicate that as water content increases, composite modulus decreases. With the exception of one sample, the correlation between the two variables was poor. The correlation was better for field results compared to laboratory results.
3. A reasonable correlation exists between the PFWD composite modulus and the combination of percent compaction and water content relative to optimum. These results were used as the basis for a technique to use the PFWD as a tool for field compaction control.
4. Two Prima 100 PFWDs produced nearly identical results.

5. Moduli determined from the Clegg Impact Hammer were significantly less than those determined by the Prima 100. A marginal correlation exists between the two devices.
6. Composite moduli did not appear to be affected by operator technique.

6.3 RECOMMENDATIONS FOR FURTHER RESEARCH

1. Additional spring thaw measurements should be made in order to verify the adequacy of using 80% of the fully recovered composite modulus as a basis for placing and removing spring load restrictions. Moreover, the influence of pavement structure, allowable load, and traffic level on the adequacy of using 80% as the basis of placing and removing load restrictions should be examined.
2. Software should be developed for the Prima 100 PFWD to incorporate deflections from three geophones into a single backcalculation routine for determination of the composite modulus.
3. Additional studies should be undertaken to better define the relationship between composite modulus, percent compaction, and water content for a wide range of base course aggregates, subgrade soils, and compaction water contents. These tests should be based on field test results.
4. In situ measurements should be taken with the Prima 100 PFWD and compared with laboratory determined resilient moduli.

REFERENCES

- AASHTO T180, “Standard Method of Test for Moisture-Density Relations of Soils Using a 10 lb. (4.54 kg) Rammer and an 18 in. (457 mm) Drop,” Standard Specifications for Transportation Materials and Methods of Sampling and Testing, Part II, Tests, American Association of State Highway and Transportation Officials, Washington D.C.
- AASHTO T191, “Standard Method of Test for Density of Soil In-Place by the Sand-Cone Method,” Standard Specifications for Transportation Materials and Methods of Sampling and Testing, Part II, Tests, American Association of State Highway and Transportation Officials, Washington D.C.
- AASHTO T238, “Standard Method of Test for Density of Soil and Soil-Aggregate in Place by Nuclear Methods (Shallow Depth),” Standard Specifications for Transportation Materials and Methods of Sampling and Testing, Part II, Tests, American Association of State Highway and Transportation Officials, Washington D.C.
- AASHTO T239, “Standard Method of Test for Moisture Content of Soil and Soil-Aggregate in Place by Nuclear Methods (Shallow Depth),” Standard Specifications for Transportation Materials and Methods of Sampling and Testing, Part II, Tests, American Association of State Highway and Transportation Officials, Washington D.C.
- AASHTO T265, “Standard Method of Test for Laboratory determination of Moisture Content of Soils,” Standard Specifications for Transportation Materials and Methods of Sampling and Testing, Part II, Tests, American Association of State Highway and Transportation Officials, Washington D.C.
- AASHTO T311, “Standard Method of Test for Grain Size Analysis of Granular Soil Materials,” Standard Specifications for Transportation Materials and Methods of Sampling and Testing, Part II, Tests, American Association of State Highway and Transportation Officials, Washington D.C.
- Baumgardner, R.H. (1993). “Overview of permeable bases,” *Materials: performance and Prevention of Deficiencies and Failure*, New York, FHWA-SA-94-045, pp. 275-287.
- Bouchedid, M., and Humphrey, D.N. (2004). “Permeability of base material for Maine roads,” report prepared for Maine Department of Transportation by Department of Civil and Environmental Engineering, University of Maine, Orono, Maine.
- Brown, Warren (February 2003), Personal communication.

- Canadian Strategic Highway Research Program, (2000). "Seasonal Load Restrictions in Canada and Around the World," Technical Brief No. 21, September, 8pp.
- Christensen, Ole R. (March 2003), Personal communication.
- Davies, Tom (1997). "Assessing the suitability of the 'Loadman' single point falling weight deflectometer to tracking the change in strength in thin asphalt surfaced roads through spring thaw in Saskatchewan," UNB International Symposium on Thin Pavements, Surface Treatments, and Unbound Roads, New Brunswick, Canada.
- Dynatest International, (2004). http://www.dynatest.com/hardware/fwd_hwd.htm
- Federal Highway Administration (1994). "Pavement Deflection Analysis: Participant Workbook," Report No. FHWA-HI-94-021, NHI Course No. 13127, U.S. Department of Transportation, February 1994.
- Fetten, C.P., and Humphrey, D.N. (1998). "Instrumentation and Performance of Geosynthetics Beneath Flexible Pavements in Winterport and Frankfort, Maine," A Study for the Maine Department of Transportation, by The Department of Civil and Environmental Engineering, University of Maine, Orono, Maine, pp. 137.
- Fleming, P.R., and Rogers, C.D.F., (1995). "Assessment of Pavement Foundations during Construction," Transport, Proceedings of the I.C.E., vol. 111, No. 2, pp. 105-115.
- Fleming, P.R., Frost, M.W., and Rogers, C.D.F. (2000). "A comparison of devices for measuring stiffness in-situ," Unbound Aggregates in Road Construction, Proceedings of the Fifth International Symposium on Unbound Aggregates in Roads/UNBAR 5, Nottingham, United Kingdom, 21-23 June 2000, A.A. Balkema, Rotterdam, Netherlands, pp. 239-246.
- Fleming, P.R., Lambert, J.P., and Frost, M.W. (2002). "In-situ assessment of stiffness modulus for highway foundations during construction," Proceedings of the Ninth International Conference on Asphalt Pavements, Copenhagen 2002, Conference Proceedings in PDF Format, Vol. 1, CD-ROM.
- Groenendijk, J., Van Haasteren, C.R., and van Niekerk, A.A. (2000). "Comparison of stiffness moduli of secondary road base materials under laboratory and in-situ conditions," Unbound Aggregates in Road Construction, Proceedings of the Fifth International Symposium on Unbound Aggregates in Roads/UNBAR 5, Nottingham, United Kingdom, 21-23 June 2000, A.A. Balkema, Rotterdam, Netherlands, pp. 201-208.
- Gros, Christophe (1993). "Use of a Portable Falling Weight Deflectometer; 'Loadman'," Publications of Road and Transport Laboratory 20, University of Oulu, Finland.

- Helstrom, C.L., and Humphrey, D.N. (2005). "Performance and Effectiveness of a Thin Pavement Section Using Geogrids and Drainage Geocomposite In A Cold Region," A Study for the New England Transportation Consortium, by The Department of Civil and Environmental Engineering, University of Maine, Orono, Maine, pp. 194.
- Holtz, Robert D. and Kovacs, William D. (1981). An Introduction To Geotechnical Engineering, N.M. Newmark and W.J. Hall, Prentice Hall, Englewood Cliffs, New Jersey.
- Honkanen, Pentti (1997). "Loadman: Comparison of Test Results Obtained Using Loadman with Those Obtained Using a Falling Weight Deflectometer and Plate Bearing Test," Finnish National Road Administration, District Surveys and Studies, Turku 1991.
- Huang, Yang H. (2004). Pavement Analysis and Design, Second Edition, Pearson Education, Inc., Pearson Prentice Hall, Upper Saddle River, New Jersey.
- Janoo, Vincent, and Cortez, Edel, (2002). "Pavement Evaluation in Cold Regions," Proceedings of the Eleventh International Conference on Cold Regions Engineering. Anchorage, Alaska, 20-22 May 2002, ASCE.
- Kamiura, M., Sekine, E., Abe, N., and Maruyama, T. (2000). "Stiffness evaluation of the subgrade and granular aggregates using the portable FWD," Unbound Aggregates in Road Construction, Proceedings of the Fifth International Symposium on Unbound Aggregates in Roads/UNBAR 5, Nottingham, United Kingdom, 21-23 June 2000, A.A. Balkema, Rotterdam, Netherlands, pp. 239-246.
- Kestler, M.A., Knight, T., and Krat, A.S. (2000). "Thaw Weakening and Load Restriction Practices on Low Volume Roads," ERDC/CRREL TR-00-6, Technical Report.
- Langfelder, L.J., and Nivargikar, V.R. (1967). "Some factors influencing shear strength and compressibility of compacted soils," Highway Research Board, No. 177, National Research Council, pp. 4-21.
- Lawrence, B.K, Chen, L.H., and Humphrey, D.N. (2000). "Use of Tire Chip/Soil Mixtures to Limit Frost Heave and Pavement Damage of Paved Roads," A Study for the New England Transportation Consortium, by The Department of Civil and Environmental Engineering, University of Maine, Orono, Maine, pp. 316.
- Lenke, L.R., McKeen, R.G., and Grush, M.P. (2003). "Laboratory Evaluation of GeoGauge for Compaction Control," Transportation Research Record 1849, Washington, D.C.

- Livneh, Moshe (1997). "A portable FWD for determining in-situ asphalt layers moduli," Mechanical Tests for Bituminous Materials, Proceedings of the Fifth International Rilem Symposium MTBM, Lyon, France, 14-16 May 1997.
- Livneh, Moshe (1997). "Single-Measurement Estimation of In Situ Asphalt-Layer Moduli with Portable Falling Weight Deflectometer," Transportation Research Record 1570, Washington, D.C.
- Livneh, M., Livneh, N.A., and Elhadad, E. (1997). "Determining a Pavement Modulus from Portable FWD Testing," Geotechnical Testing Journal, GTJODJ, Vol. 20, No. 4, December 1997, pp. 373-383.
- Lukanen, E., Stubstad, R., and Briggs, R. (2000). "Temperature Predictions and Adjustment Factors for Asphalt Pavement," Report No. FHWA-RD-98-085, FHWA, U.S. Department of Transportation.
- Nazzal, M. (2003). "Field Evaluation of in-situ test technology for Q_c/Q_A during construction of pavement layers and embankments," M.S. Thesis, The Department of Civil and Environmental Engineering, Louisiana State University, Baton Rouge, Louisiana, pp. 112.
- Neter, J., Wasserman, W., and Whitmore, G.A. (1982). Applied Statistics, Second Edition, Allyn and Bacon, Inc., Boston, Massachusetts.
- Newcomb, D.E., and Birgisson, B. (1999). "Measuring In Situ Mechanical properties of Pavement Subgrade Soils," NCHRP synthesis 278, Transportation Research Board, National Research Council, Washington, D.C., 1999.
- Ovik, J.M., Siekmeier, J.A., and Van Deusen, D.A. (2000). "Improved Spring Load Restriction Guidelines Using Mechanistic Analysis," Minnesota Department of Transportation, Report No. MN/RC-2000-18, 87 pp.
- Pidwerbesky, B. (1997). "Predicting rutting in unbound granular basecourses from Loadman and other *in situ* non-destructive tests," Road and Transport Research, Volume 6 No. 3, September.
- Pidwerbesky, B. (1997). "Evaluation of non-destructive in situ tests for unbound granular pavements," IPENZ Transactions, Vol. 24, No. 1/CE, 1997.
- Rutherford, M.S., Mahoney, J.P., Hicks, R.G., and Rwebingira, T. (1985). "Guidelines for Spring Highway Use Restrictions," Report No. FHWA-RD-86-501, Washington State Department of Transportation, Seattle, WA, 1985.

- Siekmeier, J.A., Young, D., and Beberg, D., (2000). "Comparison of the Dynamic Cone Penetrometer with Other Tests During Subgrade and Granular Base Characterization in Minnesota," Nondestructive Testing of Pavements and Backcalculation of Moduli, Third Volume, ASTM STP 1375, S.D. Tayabji and E.O. Lukanen, Eds., American Society for Testing and Materials, West Conshohocken, PA, 2000.
- Thom, N.H., and Fleming, P.R. (2002). "Experimental and Theoretical Comparison of Dynamic Plate Testing Methods," Bearing Capacity of Roads, Railways and Airfields, Proceedings of the Sixth International Conference on the Bearing Capacity of Roads and Airfields, Lisbon, Portugal, 24-26 June 2002, Correia, A.G., Vol.1, pp. 731-740.
- Thompson, Marshall and Garcia, Gabriel (2003). "Subgrade strength/stiffness evaluation" Draft White Paper 1, Department of Civil Engineering, University of Illinois Urbana-Champaign.
- Van Deusen, Dave (1998). "Improved Spring Load Restriction Guidelines Using Mechanistic Analysis," Proceedings of the Ninth International Conference on Cold Regions Engineering. Duluth, Minnesota, 27-30 September 1998, ASCE.
- Van Gorp, C., Groenendijk, J., and Beuving, E. (2000). "Experience with various types of foundation tests," Unbound Aggregates in Road Construction, Proceedings of the Fifth International Symposium on Unbound Aggregates in Roads/UNBAR 5, Nottingham, United Kingdom, 21-23 June 2000, A.A. Balkema, Rotterdam, Netherlands, pp. 239-246.
- Walpole, R.E., and Myers, R.H. (1978), Probability and Statistics for Engineers and Scientists, MacMillan Publishing, New York, 580 pp.
- Washington State Department of Transportation (1999). "WSDOT Pavement Guide," Volume 3, Seattle, Washington.
- Whaley, Andrew M. (1994). "Non-Destructive Pavement Testing Equipment: Loadman, Falling Weight Deflectometer, Benkelman Beam, Clegg Hammer," Department of Civil Engineering, University of Canterbury, Christchurch, New Zealand, 19 pp.

(BLANK PAGE)

**APPENDIX A -
GRAIN SIZE DISTRIBUTION CURVES**

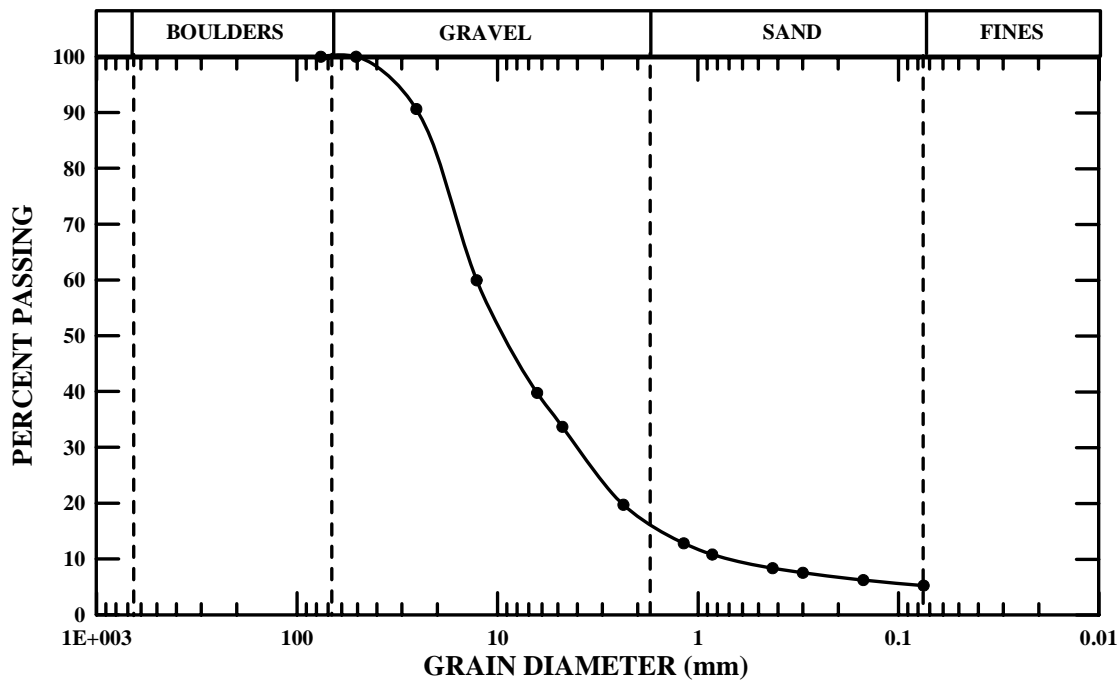


Figure A.1 Grain size distribution of Connecticut crushed gravel.

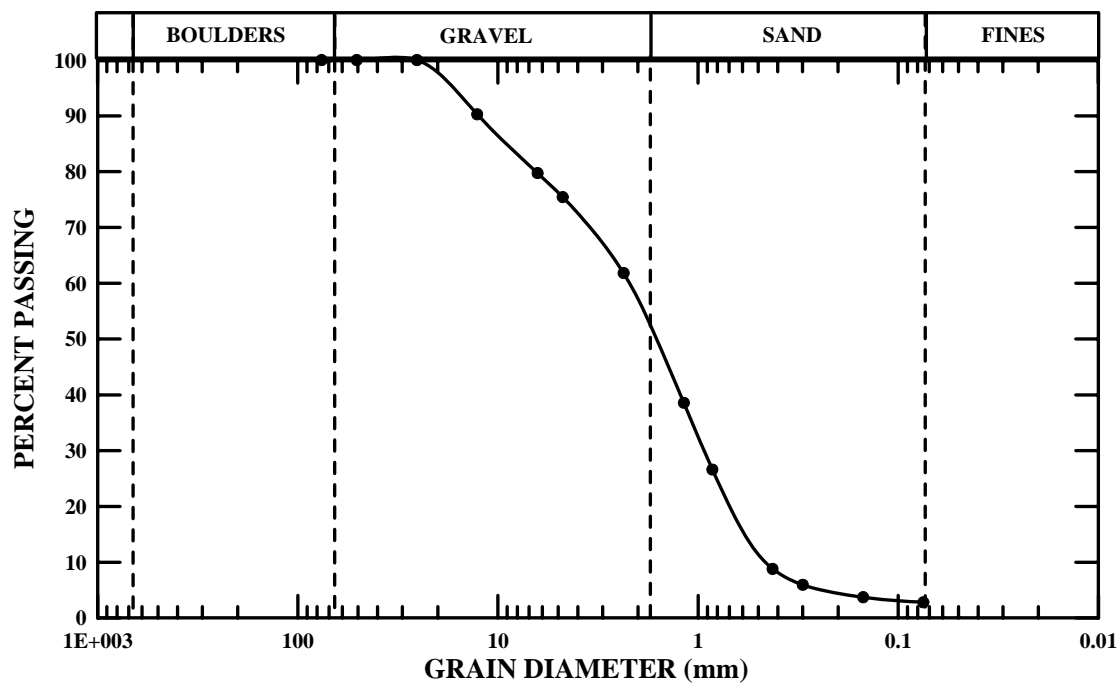


Figure A.2 Grain size distribution of New Hampshire sand.

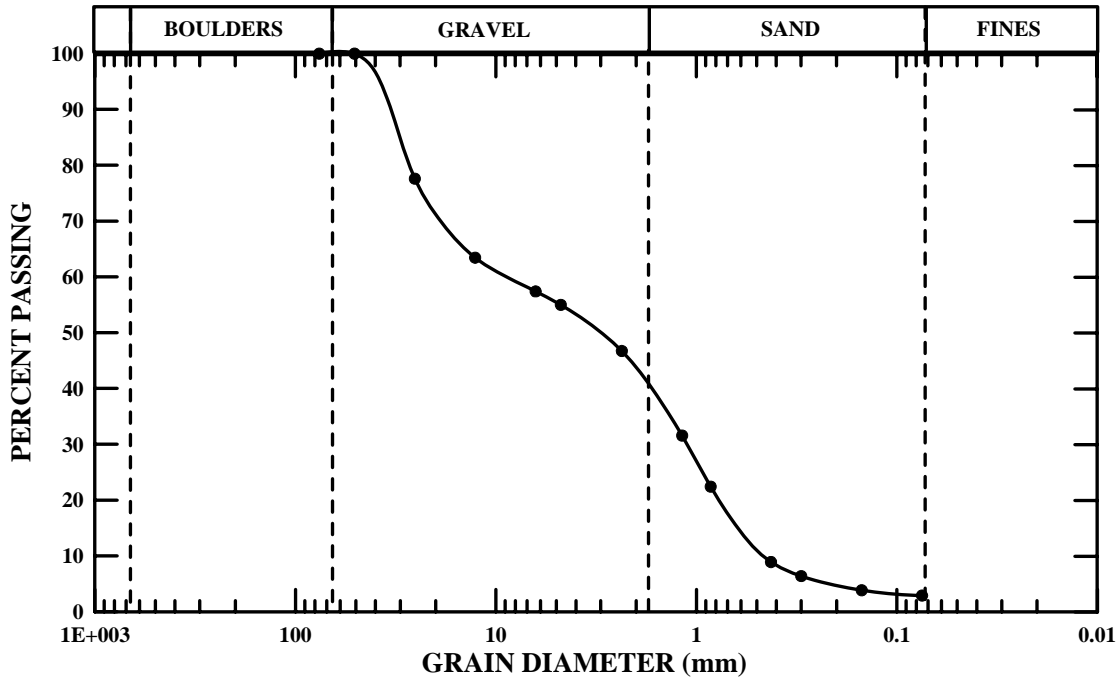


Figure A.3 Grain size distribution of New Hampshire gravel.

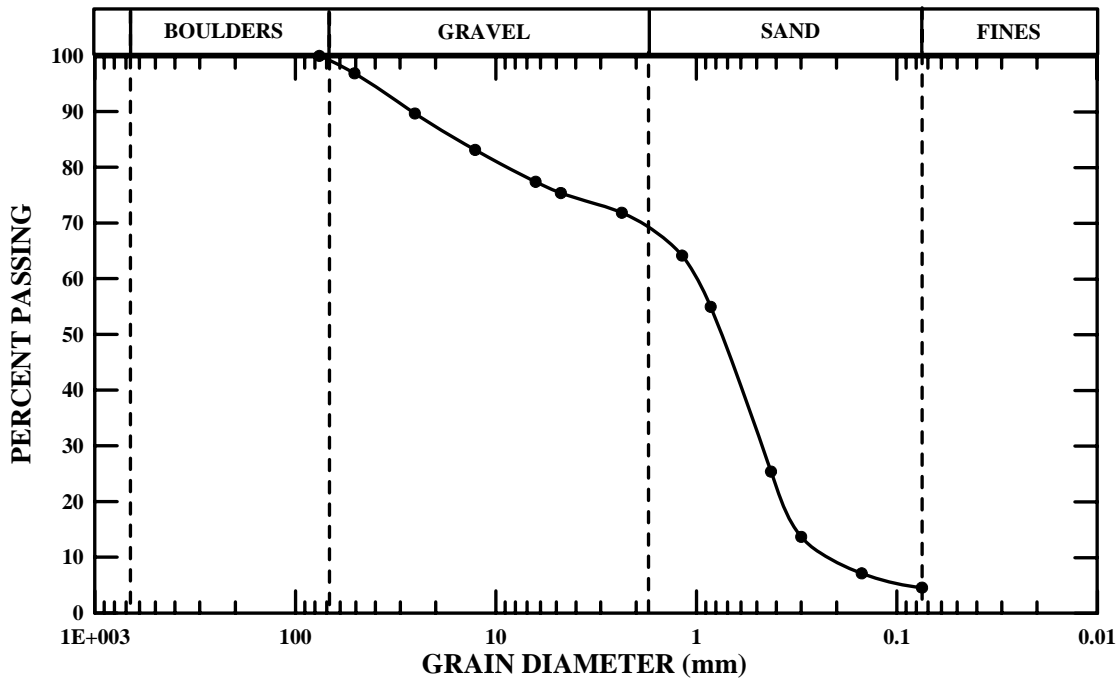


Figure A.4 Grain size distribution of bottom 1 ft of OJF gravel.

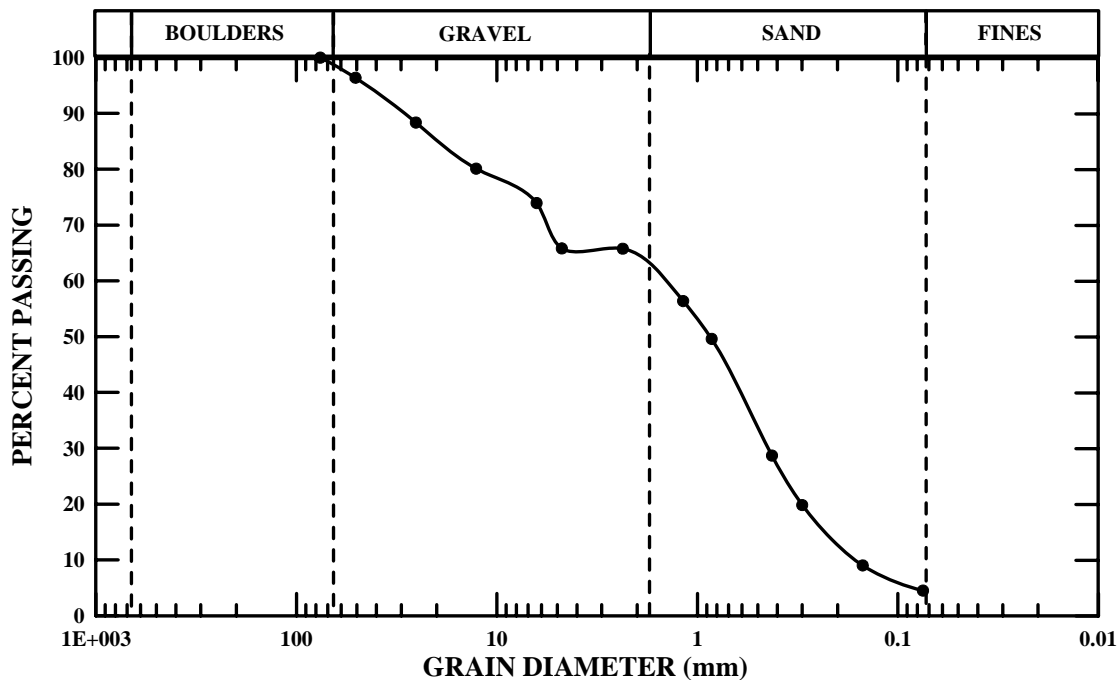


Figure A.5 Grain size distribution of Owen J. Folsom gravel.

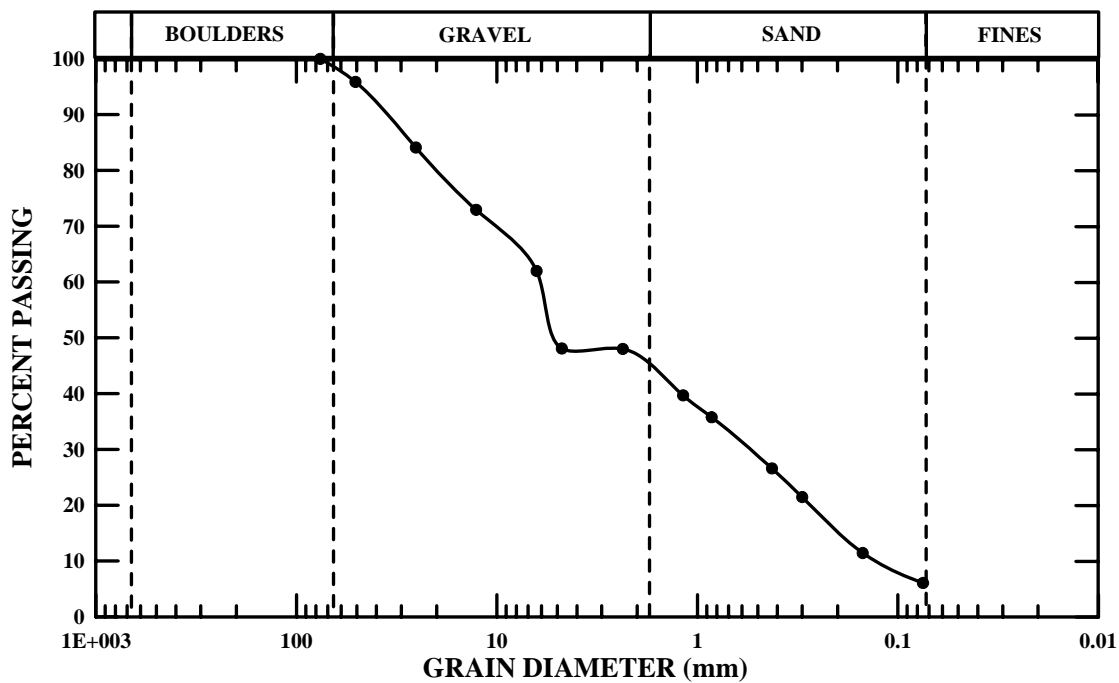


Figure A.6 Grain size distribution of Wardwell gravel.

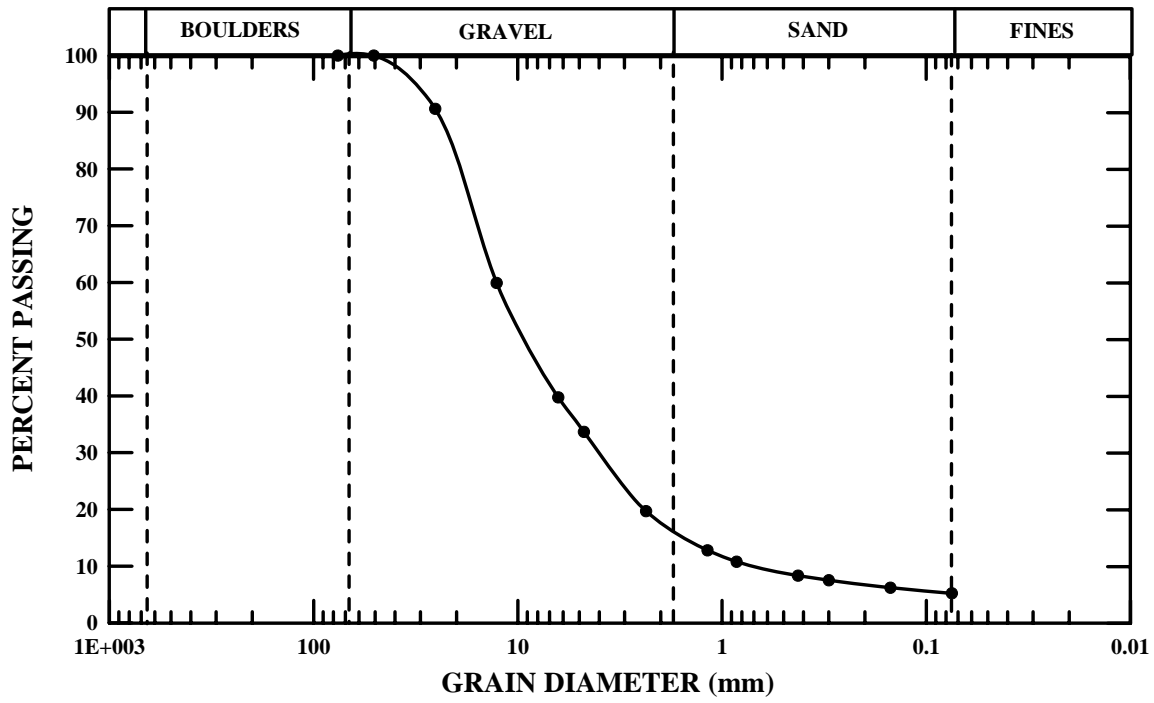


Figure A.7 Grain size distribution of crushed gravel tested at I-84, Southington, Connecticut.

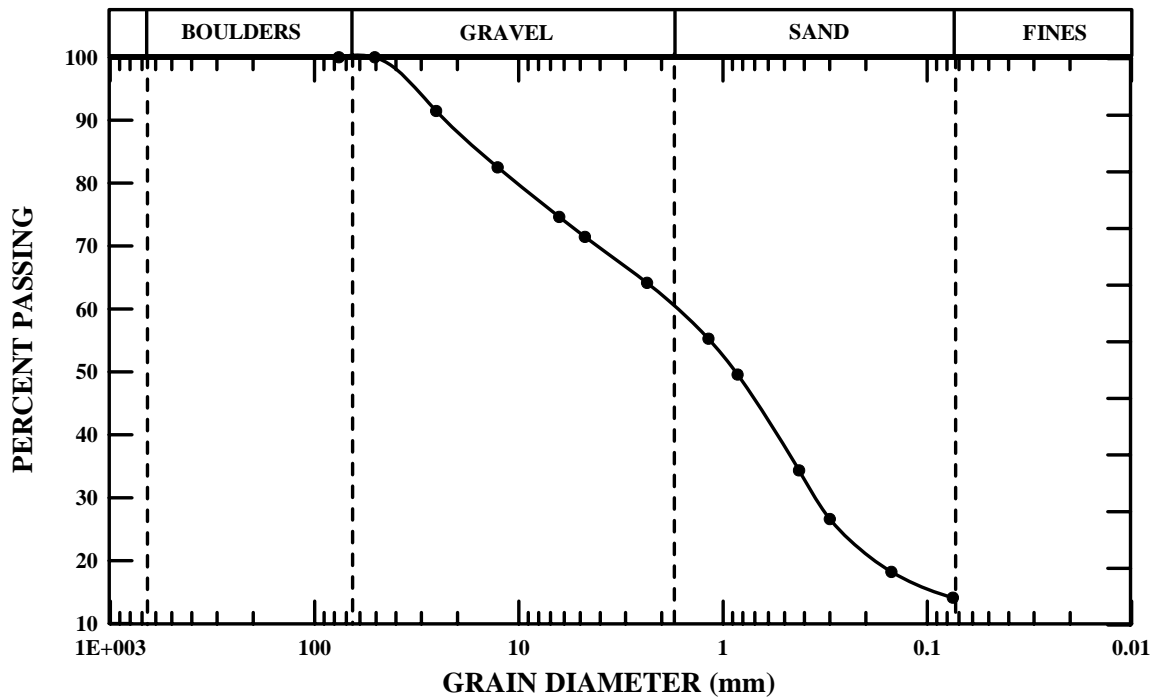


Figure A.8 Grain size distribution of existing subgrade material tested at I-84, Southington, Connecticut.

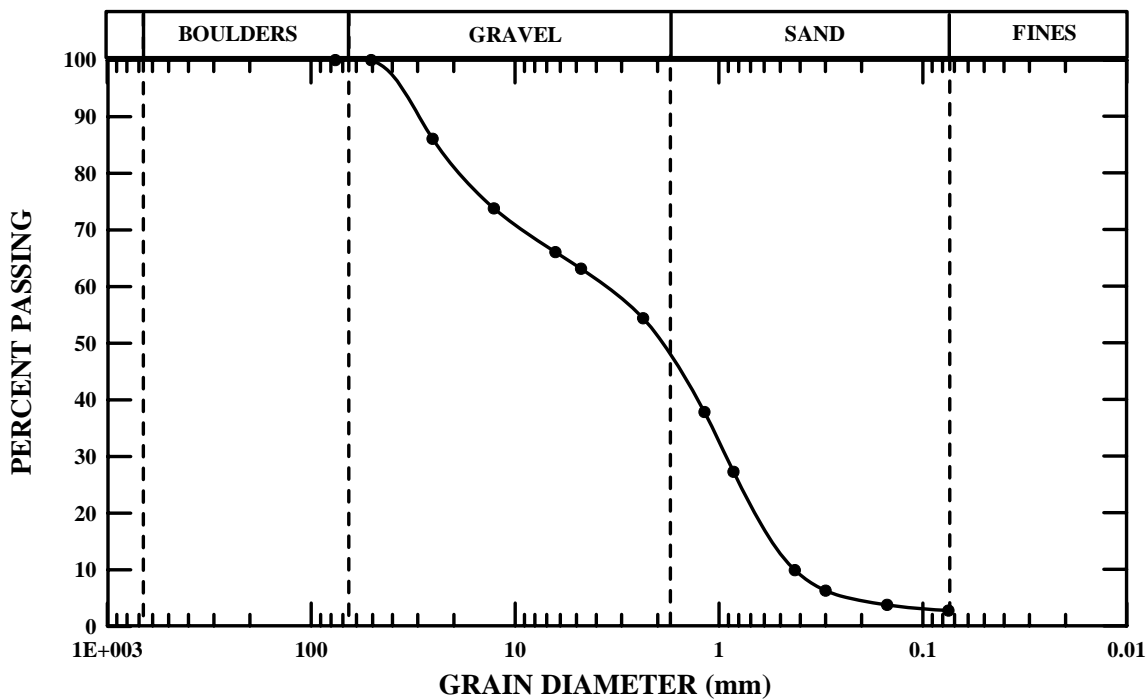


Figure A.9 Grain size distribution of construction sand tested at Route 25, Effingham/Freedom, New Hampshire.

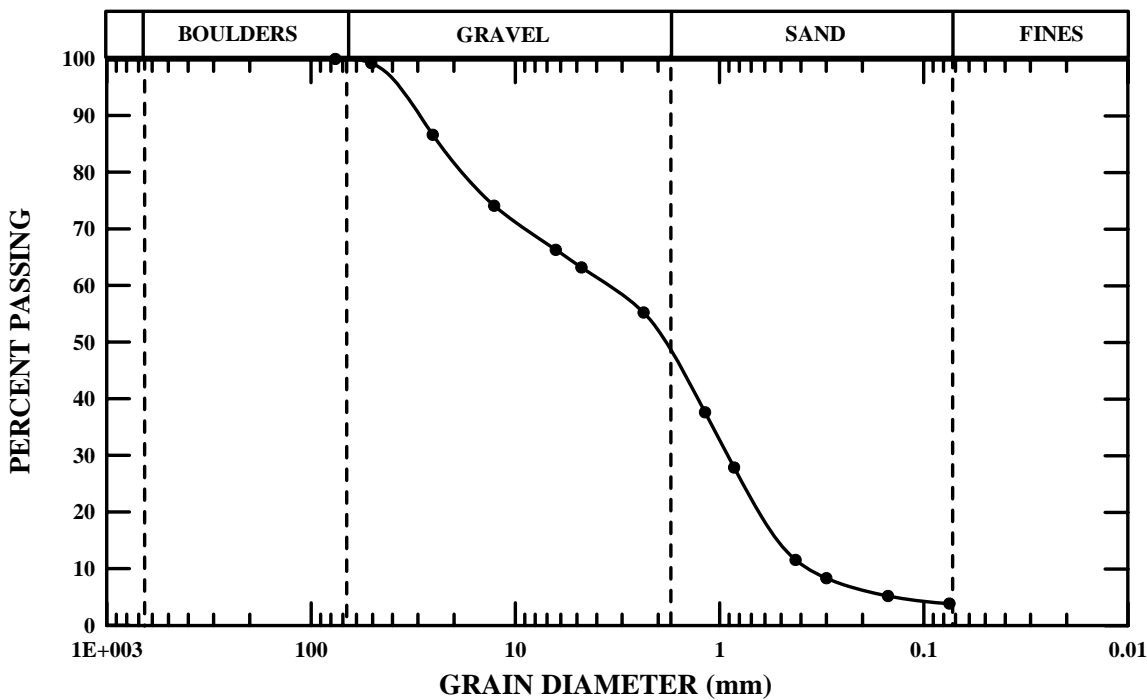


Figure A.10 Grain size distribution of gravel tested at Route 25, Effingham/Freedom, New Hampshire.

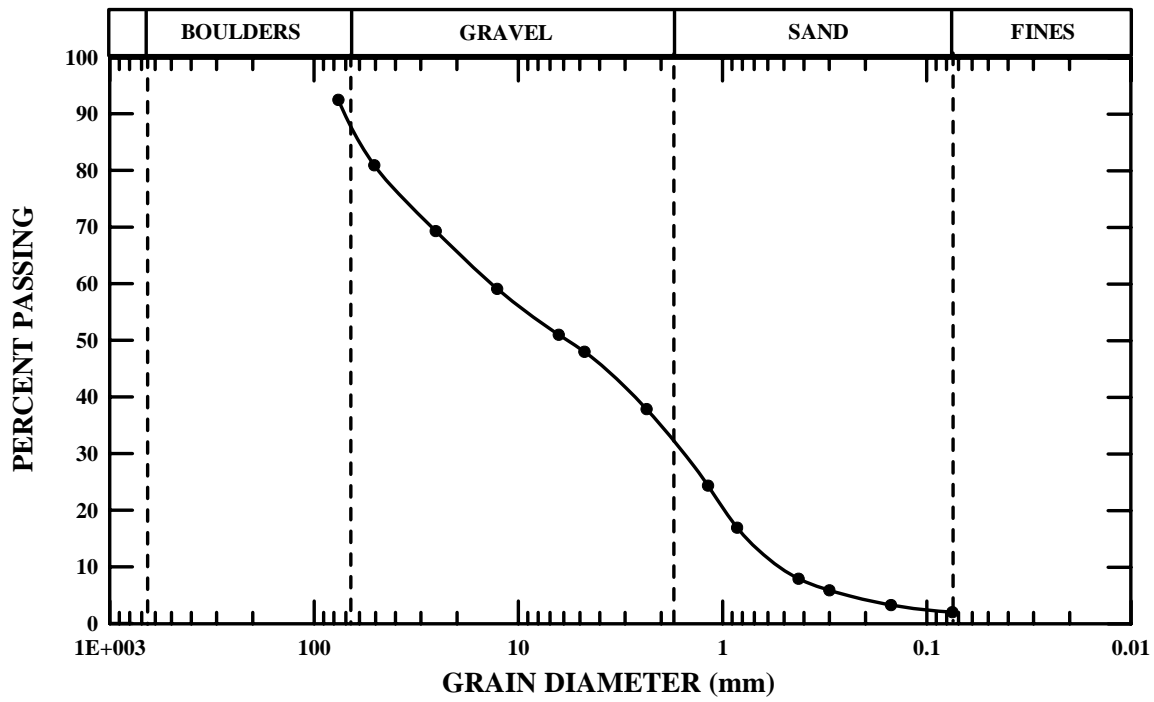


Figure A.11 Grain size distribution of MaineDOT Type D gravel tested at Route 26, New Gloucester, Maine.

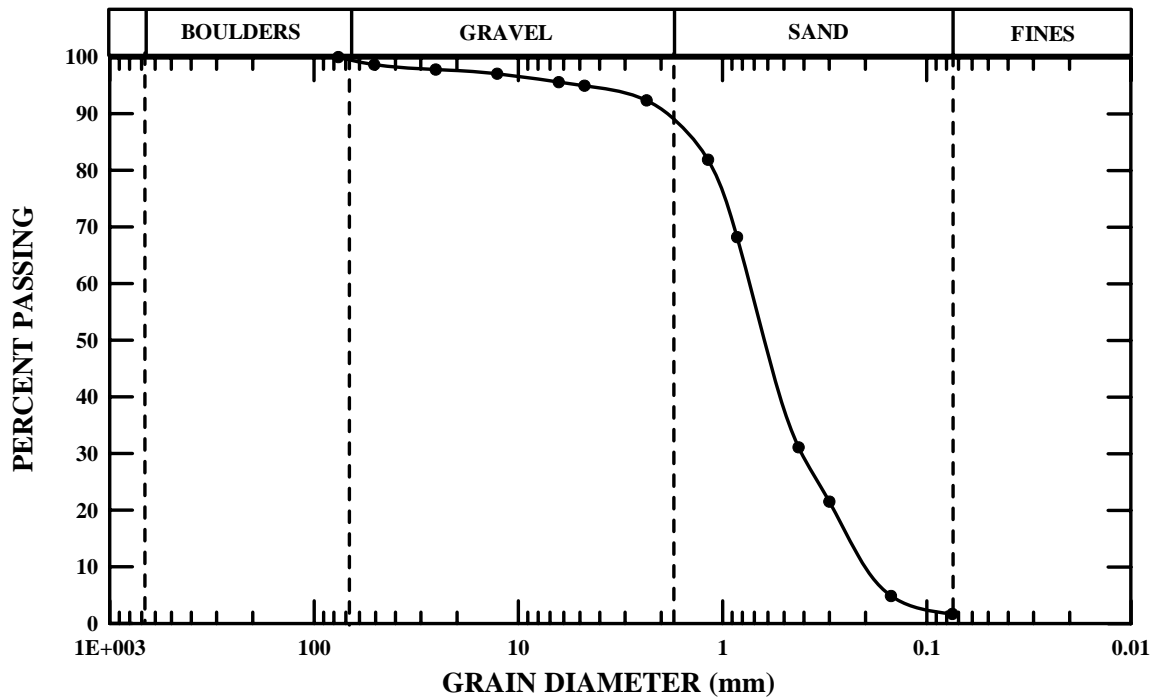


Figure A.12 Grain size distribution of MaineDOT Type E gravel tested at Route 26, New Gloucester, Maine.

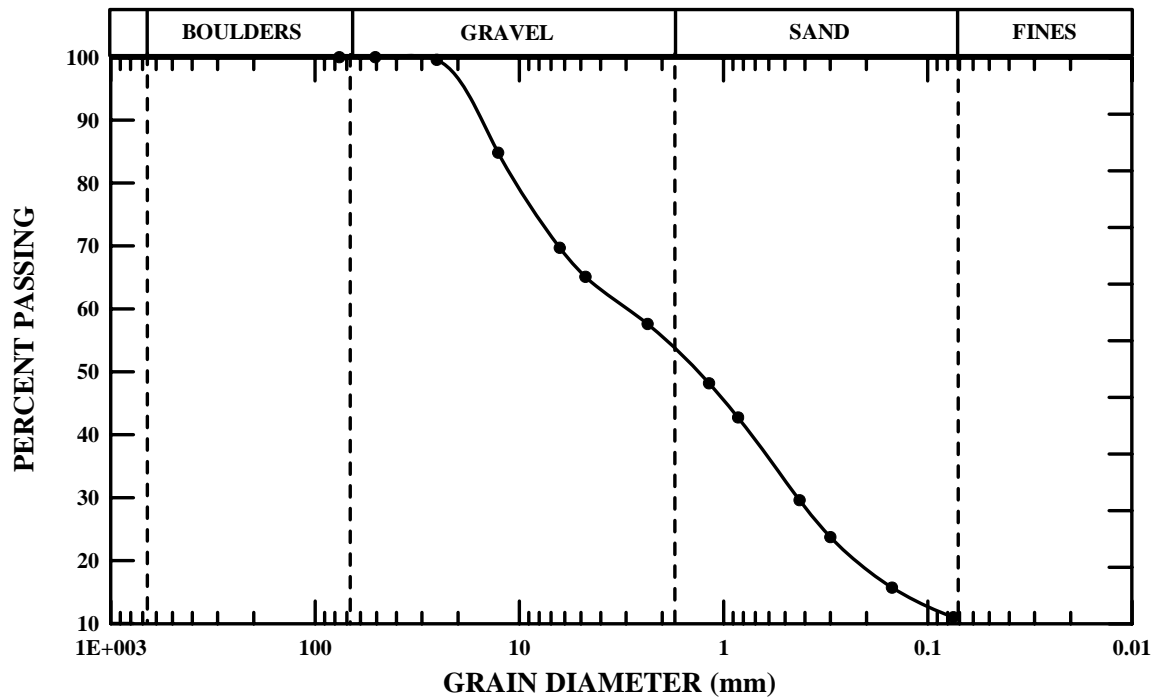


Figure A.13 Grain size distribution of existing subgrade tested at CPR, Scarborough, Maine.

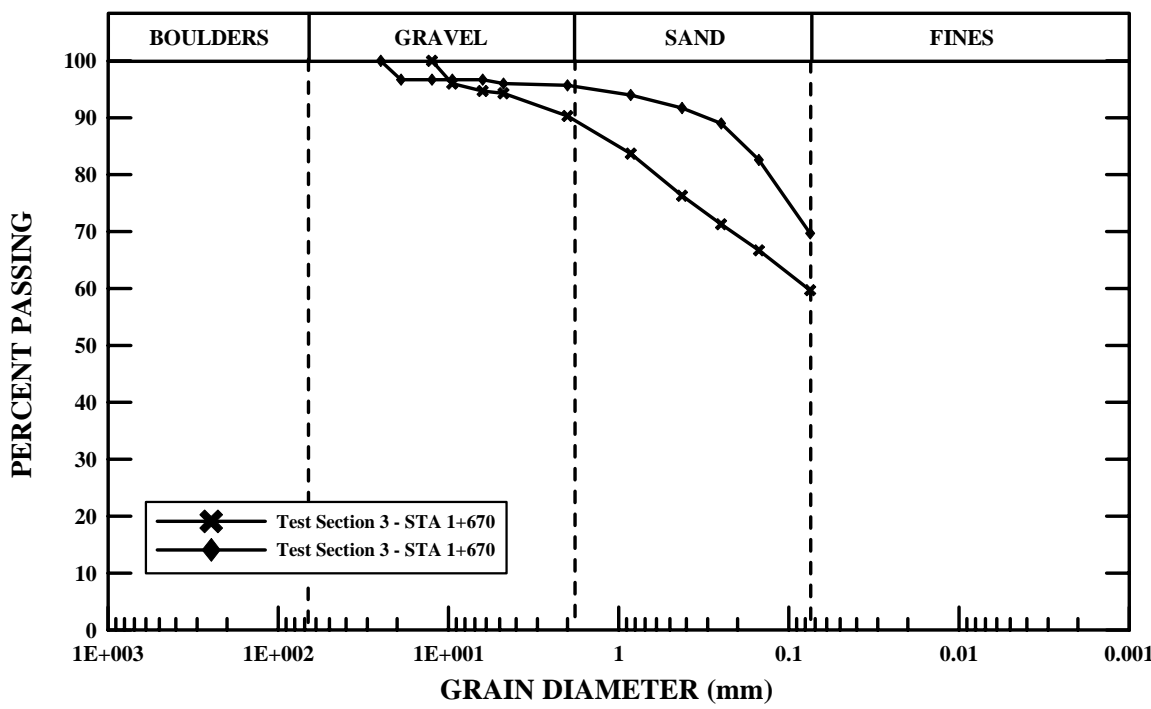


Figure A.14 Grain size distribution of existing subgrade material at Route 126 (Section 3), Monmouth/Litchfield, Maine.

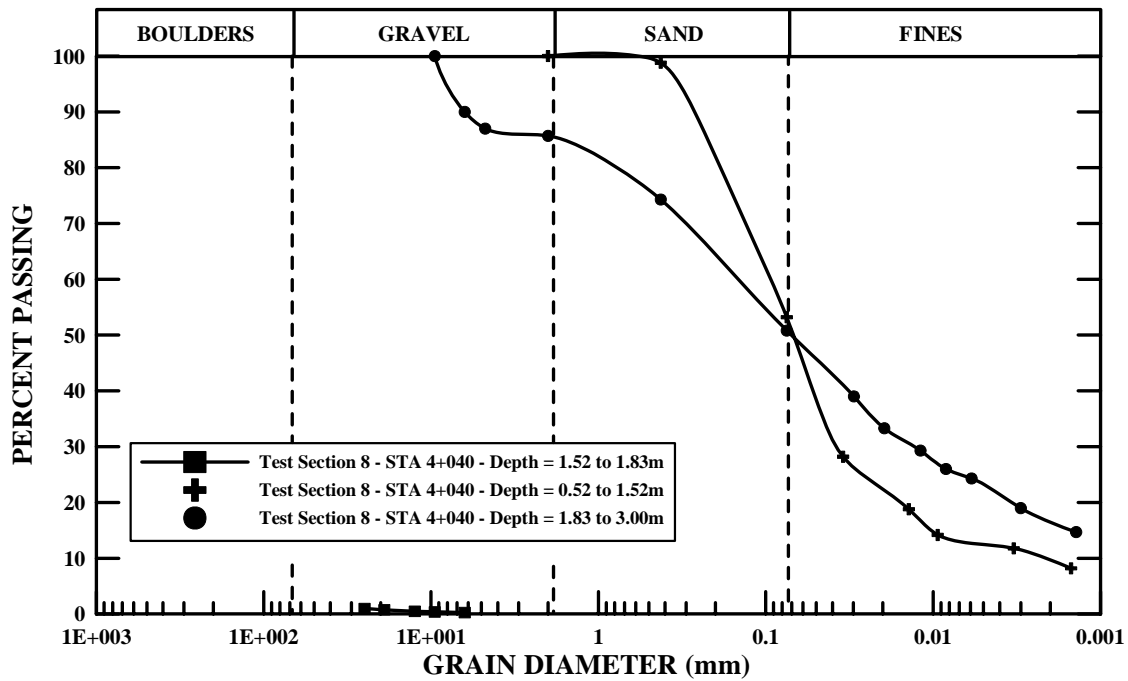


Figure A.15 Grain size distribution of existing subgrade material at Route 126 (Section 8), Monmouth/Litchfield, Maine.

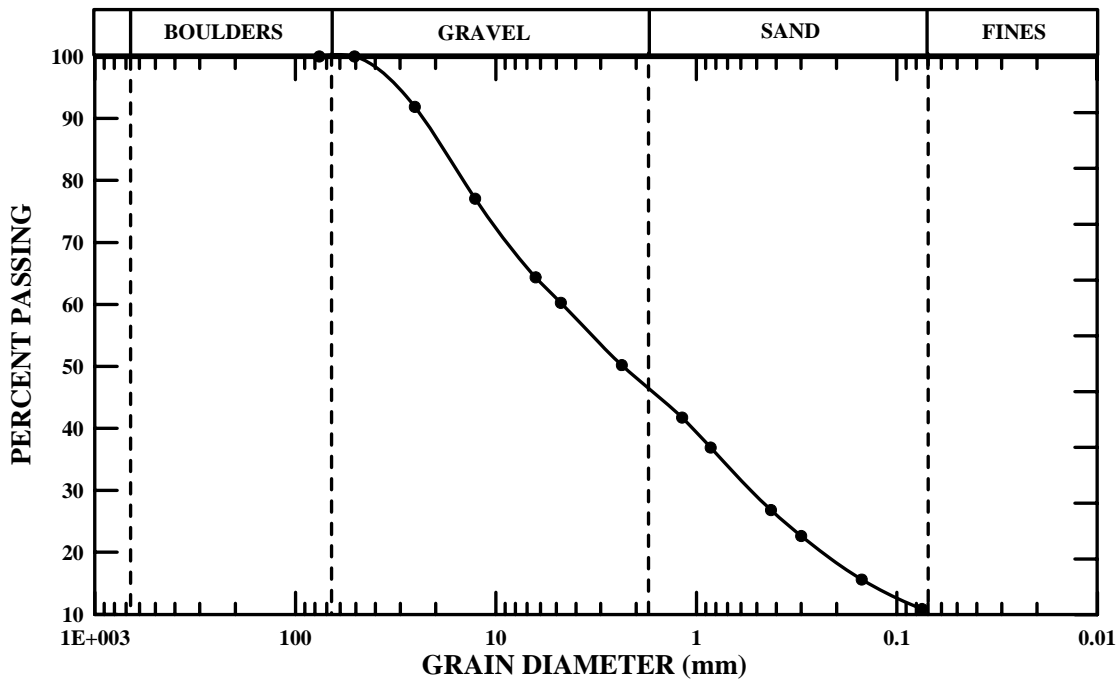


Figure A.16 Grain size distribution of existing subbase material at Stinson Lake Road, Rumney, New Hampshire.

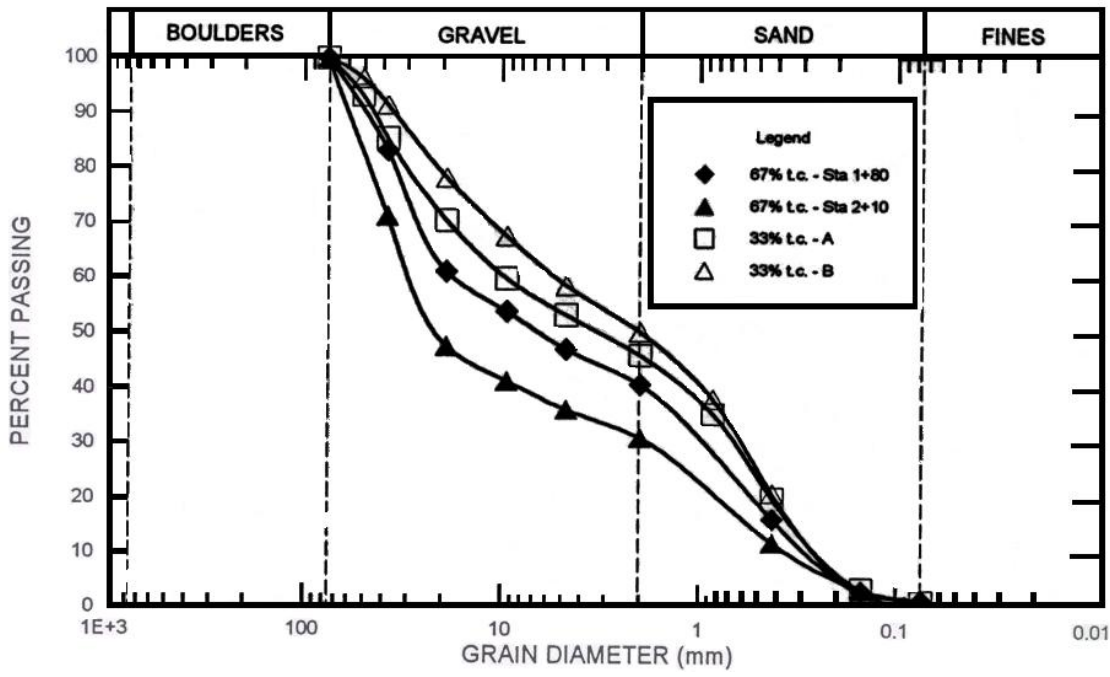


Figure A.17 Grain size distribution of tire chip / soil mixtures at Witter Farm Road, Orono, Maine (Lawrence, et al., 2000).

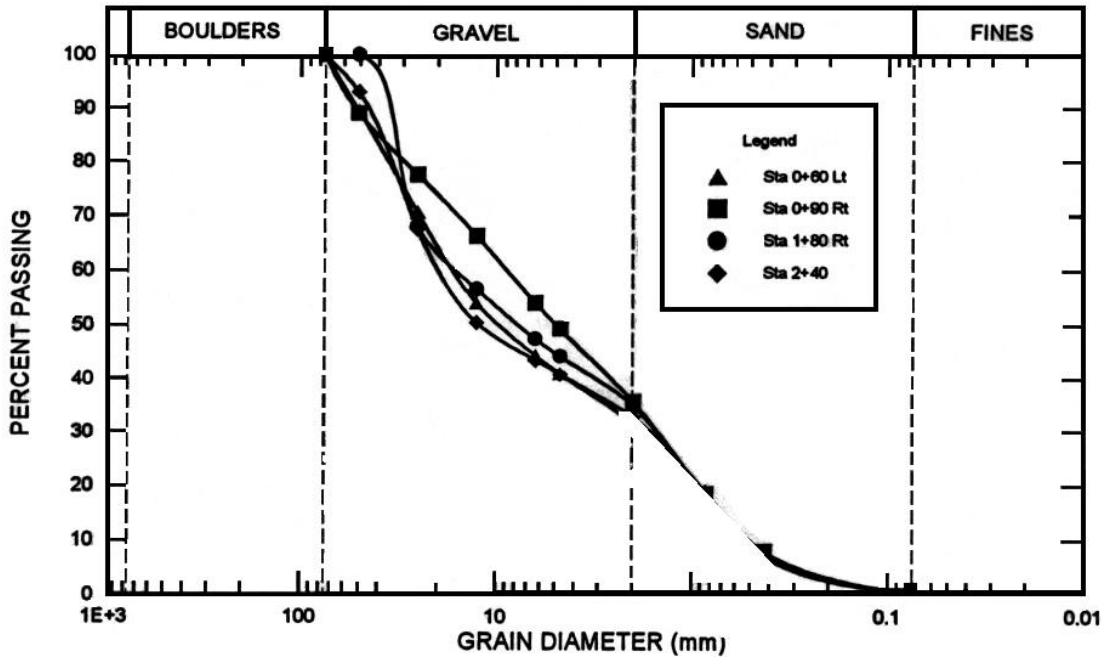


Figure A.18 Grain size distribution of MaineDOT Type D subbase used at Witter Farm Road, Orono, Maine (Lawrence, et al., 2000).

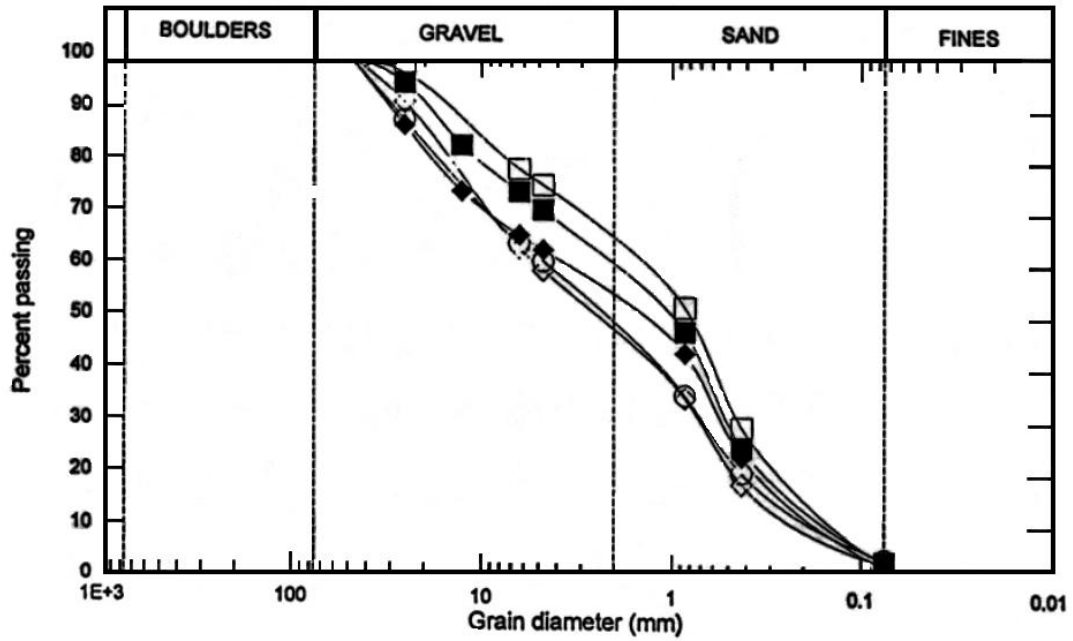


Figure A.19 Grain size distribution of MaineDOT Type D subbase used at Witter Farm Road, Orono, Maine (Lawrence, et al., 2000).

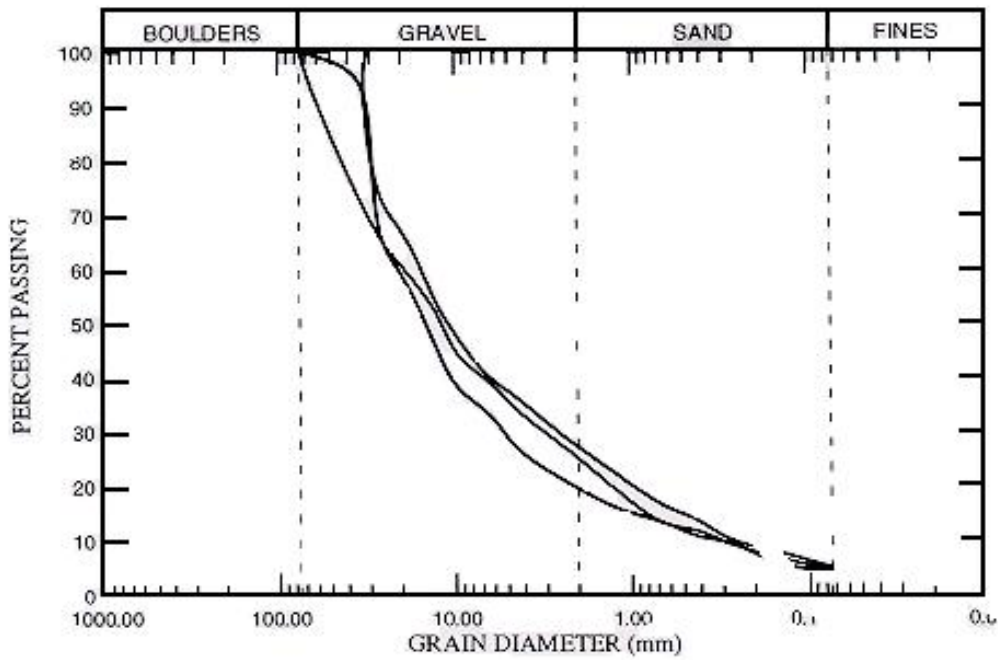


Figure A.20 Grain size distribution of subbase material at Route 1A, Frankfort/Winterport, Maine (Fetten and Humphrey, 1998).

**APPENDIX B -
MOISTURE DENSITY CURVES**

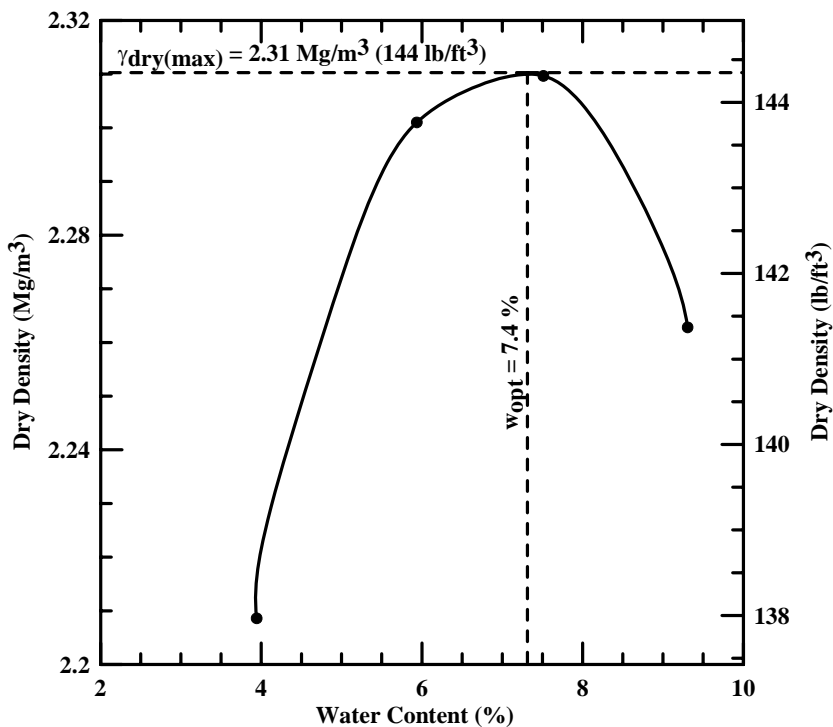


Figure B.1 Connecticut crushed gravel moisture density curve.

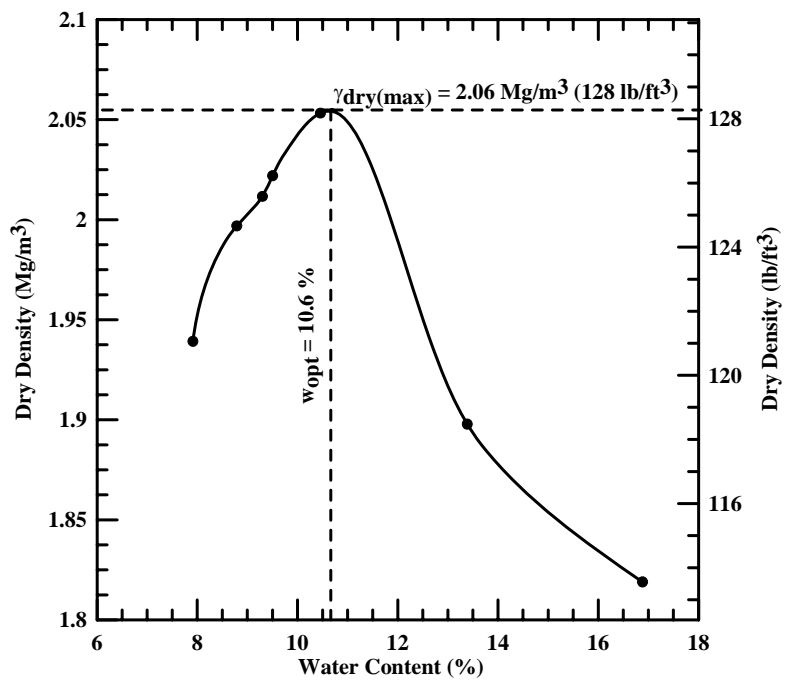


Figure B.2 New Hampshire sand moisture density curve

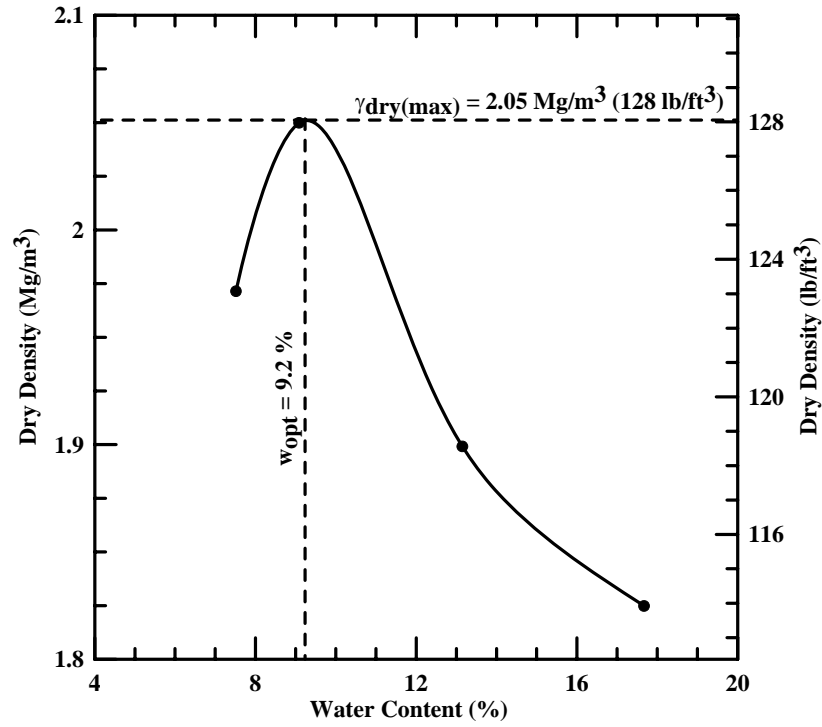


Figure B.3 New Hampshire gravel moisture density curve.

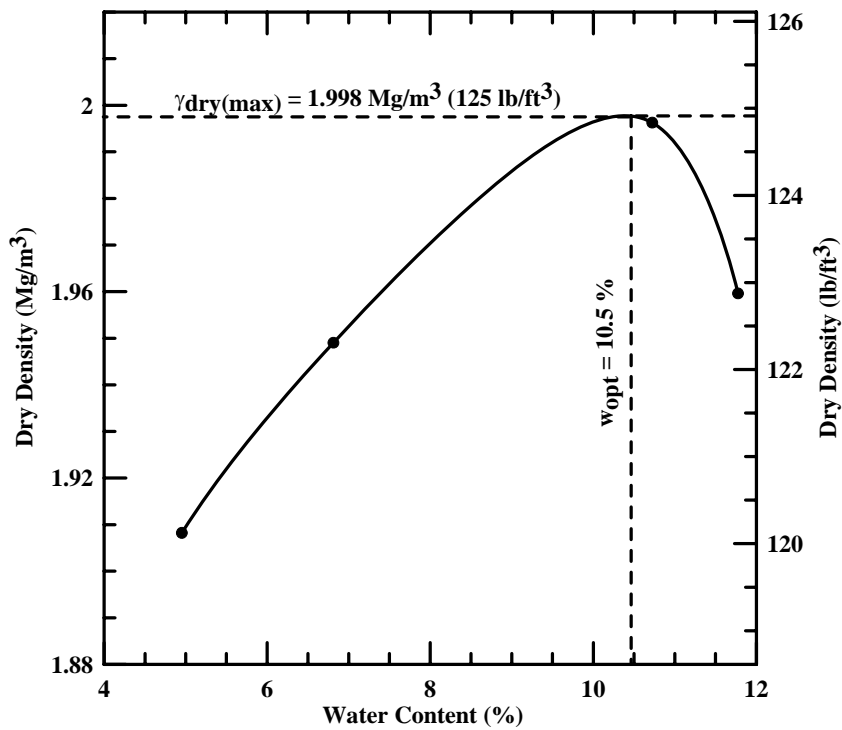


Figure B.4 Owen J. Folsom #1 moisture density curve.

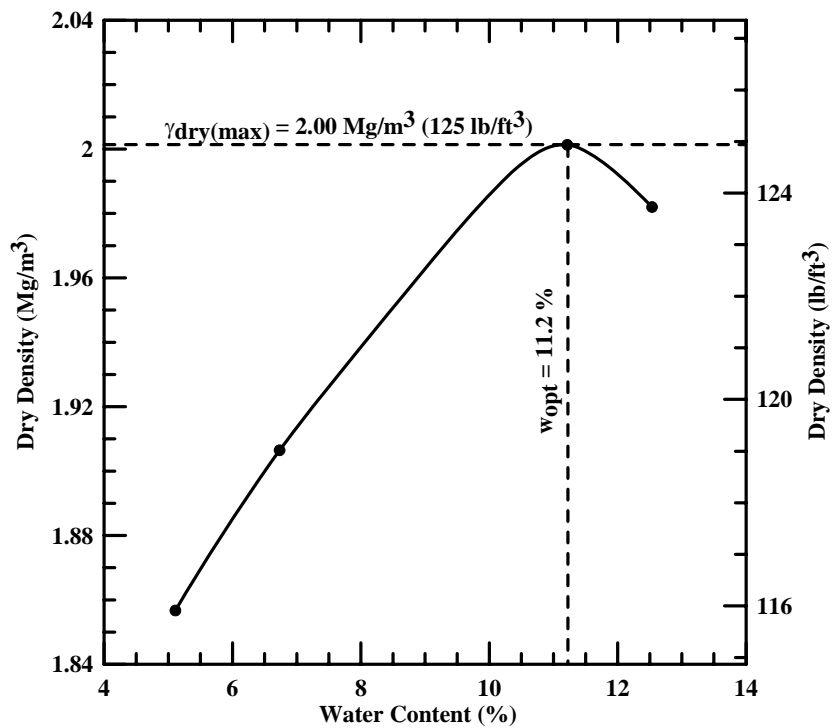


Figure B.5 Owen J. Folsom #2 moisture density curve.

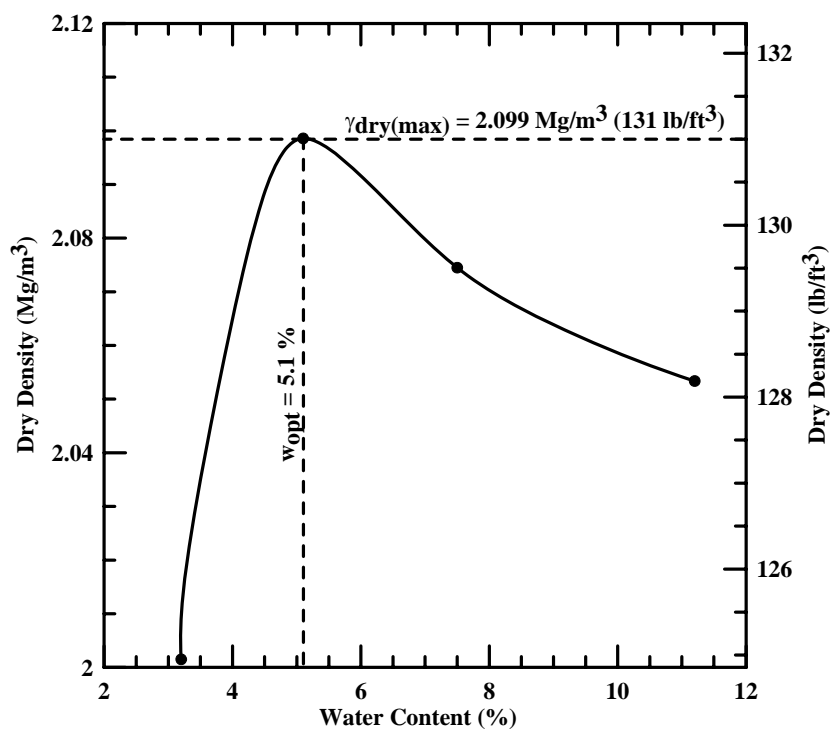


Figure B.6 Wardwell gravel moisture density curve.

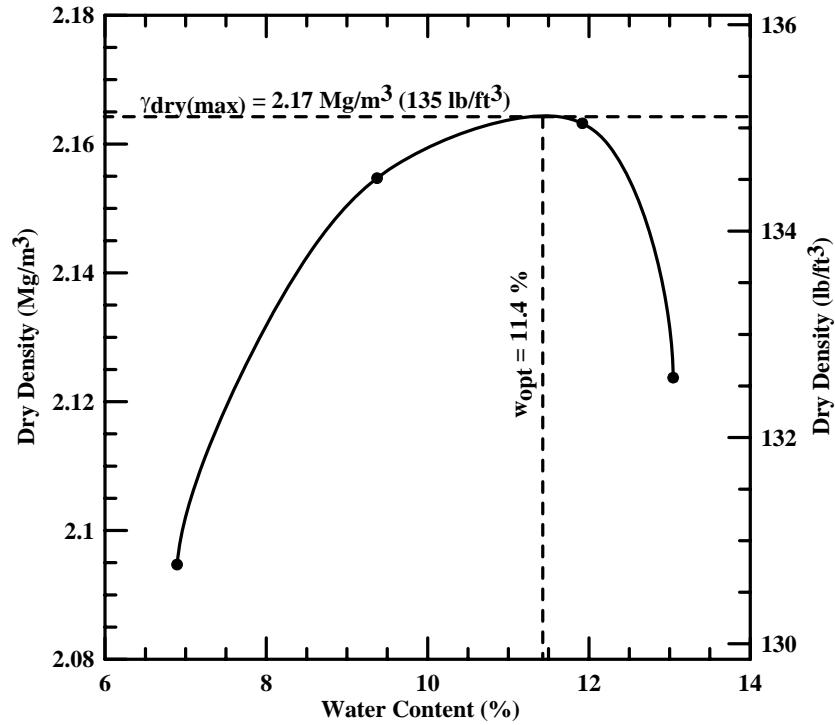


Figure B.7 Moisture density curve of sand tested at Route 25, Effingham/Freedom, New Hampshire.

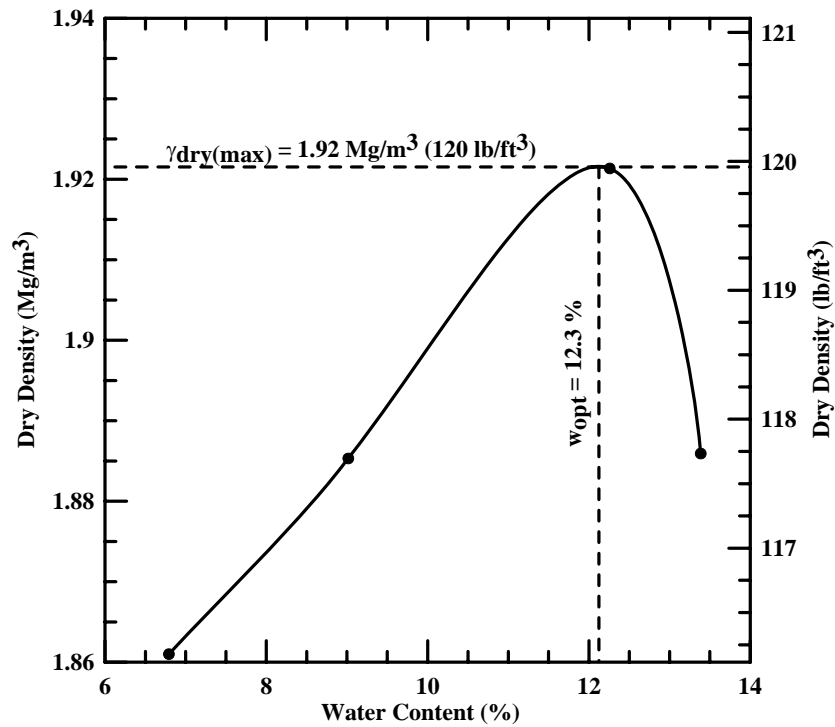


Figure B.8 Moisture density curve of gravel tested at Route 25, Effingham/Freedom, New Hampshire.

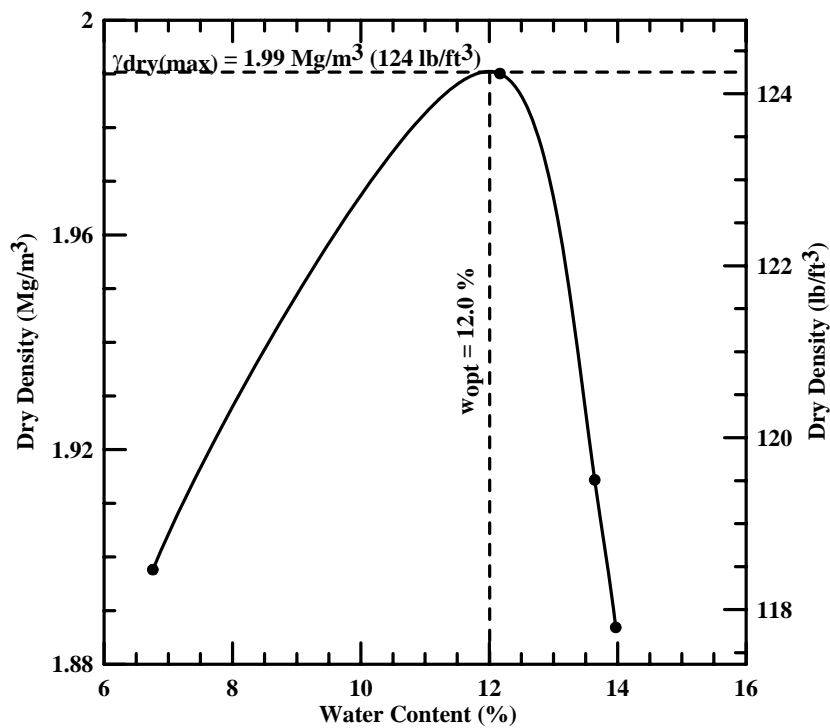


Figure B.9 Moisture density curve of MaineDOT Type D at Route 26, New Gloucester, Maine.

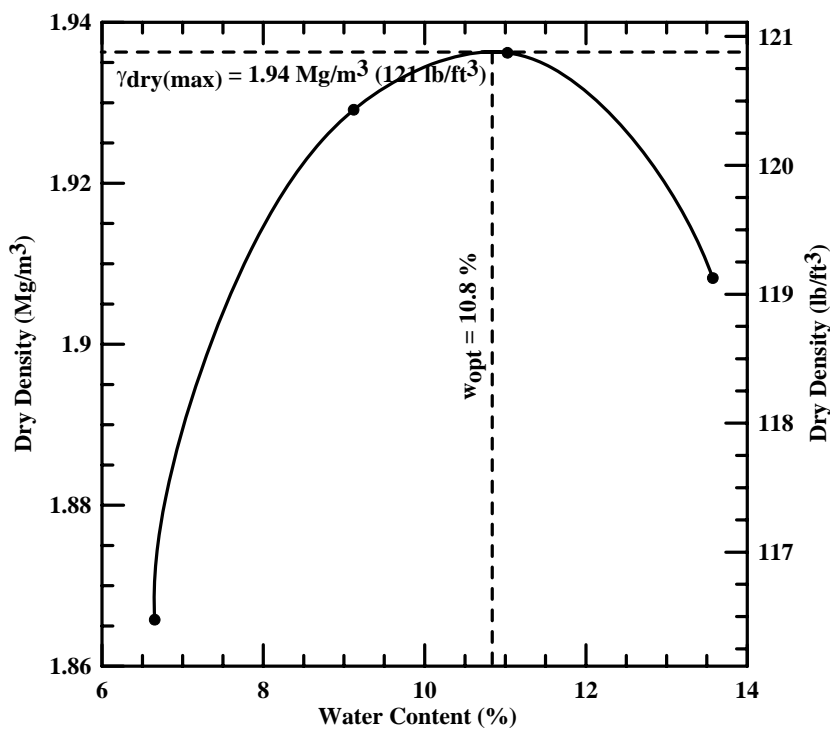


Figure B.10 Moisture density curve of MaineDOT Type E at Route 26, New Gloucester, Maine.

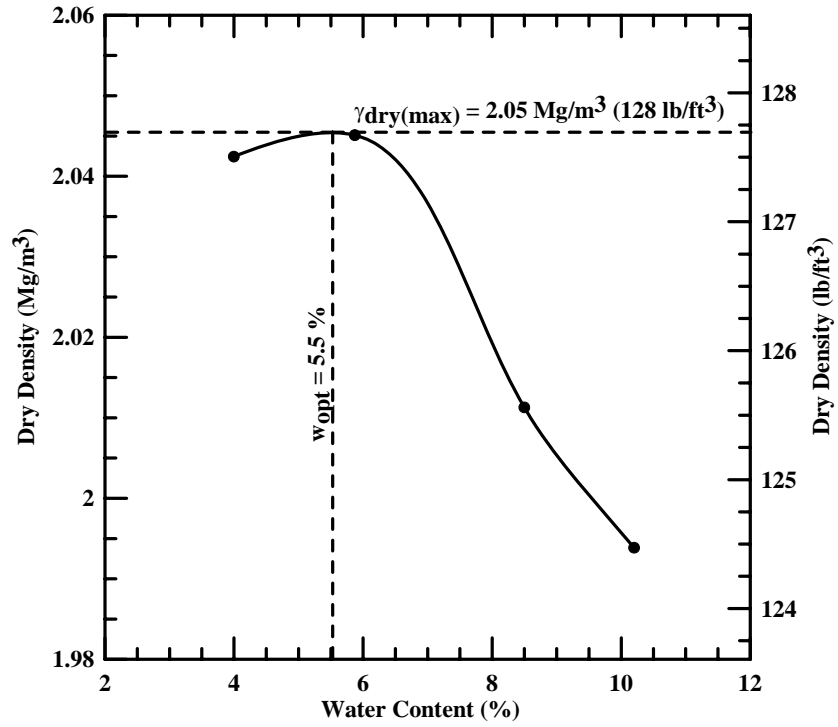


Figure B.11 Moisture density curve of existing subgrade material at CPR, Scarborough, Maine.

APPENDIX C -
COMPACTION CONTROL RAW LABORATORY DATA

Table C.1 Summary of Connecticut crushed gravel raw laboratory data.

Target Test	Test Point	Dry Density Mg/m³ (lb/ft³)	Percent Compaction (%)	Water Content (%)	Water Content Relative to Optimum (%)	PFWD Composite Modulus (MPa)
90%, W _{opt}	1	2.07 (129)	90	5.6	-1.8	90
	2	2.00 (125)	87	6.3	-1.1	86
	3	2.00 (125)	87	6.1	-1.3	115
	4	2.13 (133)	93	5.8	-1.6	97
	5	2.10 (131)	91	5.2	-2.2	99
95%, W _{opt}	1	2.24 (140)	97	5.6	-1.8	130
	2	2.26 (141)	98	6.6	-0.8	114
	3	2.24 (140)	97	6.5	-0.9	202
	4	2.23 (139)	97	5.7	-1.7	170
	5	2.27 (142)	99	5.4	-2.0	140
100%, W _{opt}	1	2.37 (148)	103	6.6	-0.8	152
	2	2.35 (147)	102	6.3	-1.1	140
	3	2.34 (146)	101	6.7	-0.7	184
	4	2.39 (149)	104	6.7	-0.7	219
	5	2.40 (150)	104	6.3	-1.1	172
95%, +3% W _{opt}	1	2.35 (147)	102	6.1	-1.3	122
	2	2.26 (141)	98	6.1	-1.3	114
	3	2.31 (144)	100	5.4	-2.0	121
	4	2.34 (146)	101	5.1	-2.3	137
	5	2.32 (145)	101	4.7	-2.7	130
95%, -3% W _{opt}	1	2.21 (138)	96	4.4	-3.0	132
	2	2.11 (132)	92	4.1	-3.3	146
	3	2.10 (131)	91	4.4	-3.0	199
	4	2.15 (134)	93	4.5	-2.9	176
	5	2.15 (134)	93	4.2	-3.2	194

Table C.2 Summary of New Hampshire sand raw laboratory data.

Target Test	Test Point	Dry Density Mg/m ³ (lb/ft ³)	Percent Compaction (%)	Water Content (%)	Water Content Relative to Optimum (%)	PFWD Composite Modulus (MPa)
90%, W _{opt}	1	1.76 (110)	86	9.0	-1.6	49
	2	1.78 (111)	86	8.4	-2.2	50
	3	1.79 (112)	87	7.8	-2.8	60
	4	1.79 (112)	87	7.2	-3.4	58
	5	1.76 (110)	86	8.5	-2.1	72
95%, W _{opt}	1	1.89 (118)	92	8.2	-2.4	77
	2	1.87 (117)	91	8.5	-2.1	81
	3	1.83 (114)	89	8.3	-2.3	85
	4	1.86 (116)	90	7.8	-2.8	94
	5	1.89 (118)	92	8.2	-2.4	88
	1	1.91 (119)	93	9.3	-1.3	122
	2	1.87 (117)	91	9.5	-1.1	115
	3	1.86 (116)	91	8.5	-2.1	112
	4	1.91 (119)	93	8.7	-1.9	125
	5	1.94 (121)	94	8.4	-2.2	117
	1	1.91 (119)	93	9.4	-1.2	158
	2	1.87 (117)	93	9.7	-0.9	122
	3	1.86 (116)	93	8.7	-1.9	151
	4	1.91 (119)	94	8.9	-1.7	170
	5	1.94 (121)	95	8.5	-2.1	120
95%, +3% W _{opt}	1	1.91 (119)	93	9.3	-1.3	95
	2	1.94 (121)	95	8.6	-2.0	107
	3	1.94 (121)	95	8.4	-2.2	116
	4	1.91 (119)	93	9.3	-1.3	130
	5	1.95 (122)	95	8.2	-2.4	114
	1	1.87 (117)	91	12.7	+2.1	60
	2	1.86 (116)	91	12.7	+2.1	50
	3	1.87 (117)	91	10.9	+0.3	68
	4	1.89 (118)	92	10.4	-0.2	64
	5	1.84 (115)	90	11.7	+1.1	78
95%, - 3% W _{opt}	1	1.91 (119)	93	8.6	-2.0	172
	2	1.94 (121)	95	7.8	-2.8	160
	3	1.92 (120)	93	7.8	-2.8	139
	4	1.92 (120)	94	8.3	-2.3	179
	5	1.94 (121)	95	7.7	-2.9	165

Table C.3 Summary of New Hampshire gravel raw laboratory data.

Target Test	Test Point	Dry Density Mg/m ³ (lb/ft ³)	Percent Compaction (%)	Water Content (%)	Water Content Relative to Optimum (%)	PFWD Composite Modulus (MPa)
90%, W _{opt}	1	1.94 (121)	94	12.7	+3.5	68
	2	1.92 (120)	94	11.6	+2.4	73
	3	1.97 (123)	96	11.3	+2.1	72
	4	2.02 (126)	99	11.6	+2.4	69
	5	1.97 (124)	96	10.7	+1.5	79
95%, W _{opt}	1	1.92 (120)	93	11.8	+2.6	100
	2	1.94 (121)	95	10.9	+1.7	89
	3	1.94 (121)	94	11.4	+2.2	96
	4	1.92 (120)	94	10.6	+1.4	93
	5	2.02 (126)	99	9.7	+0.5	104
100%, W _{opt}	1	2.03 (127)	99	8.6	-0.6	90
	2	2.00 (125)	98	7.4	-1.8	82
	3	2.00 (125)	98	7.1	-2.1	136
	4	2.02 (126)	99	8.1	-1.1	103
	5	1.97 (124)	97	7.8	-1.4	121
95%, +3% W _{opt}	1	2.05 (128)	100	9.6	+0.4	70
	2	2.03 (127)	99	10.7	+1.5	69
	3	2.00 (125)	98	9.3	+0.1	98
	4	1.97 (123)	96	9.6	+0.4	87
	5	2.07 (129)	101	8.4	-0.8	80
95%, -3% W _{opt}	1	2.02 (126)	98	7.7	-1.5	96
	2	1.79 (112)	88	7.3	-1.9	99
	3	1.92 (120)	94	7.1	-2.1	131
	4	1.89 (118)	92	8.9	-0.3	130
	5	1.84 (115)	90	7.5	-1.7	150

Table C.4 Summary of Owen J. Folsom gravel raw laboratory data.

Target Test	Test Point	Dry Density Mg/m ³ (lb/ft ³)	Percent Compaction (%)	Water Content (%)	Water Content Relative to Optimum (%)	PFWD Composite Modulus (MPa)
90%, W _{opt}	1	1.94 (121)	97	12.7	+1.5	49
	2	1.92 (120)	96	11.6	+0.4	51
	3	1.97 (123)	99	11.3	+0.1	55
	4	2.02 (126)	101	11.6	+0.4	58
	5	1.99 (124)	99	10.7	-0.5	60
95%, W _{opt}	1	1.91 (119)	95	11.8	+0.6	59
	2	1.94 (121)	97	10.9	-0.3	60
	3	1.94 (121)	97	11.4	+0.2	63
	4	1.92 (120)	96	10.6	-0.6	65
	5	2.02 (126)	101	9.7	-1.5	64
100%, W _{opt}	1	2.02 (126)	100	11.2	0.0	69
	2	1.97 (123)	99	11.6	+0.4	85
	3	2.05 (128)	103	10.4	-0.8	103
	4	2.02 (126)	101	10.7	-0.5	89
	5	2.00 (125)	100	9.0	-2.2	88
95%, +3% W _{opt}	1	1.95 (122)	98	13.5	+2.3	56
	2	2.03 (127)	102	12.4	+1.2	61
	3	2.08 (130)	104	9.2	-2.0	71
	4	1.99 (124)	99	10.9	-0.3	61
	5	2.00 (125)	100	11.1	-0.1	68
95%, -3% W _{opt}	1	2.02 (126)	100	7.7	-3.5	77
	2	1.79 (112)	90	7.3	-3.9	72
	3	1.92 (120)	96	7.1	-4.1	86
	4	1.89 (118)	94	8.9	-2.3	79
	5	1.84 (115)	92	7.5	-3.7	76

Table C.5 Summary of Wardwell gravel raw laboratory data.

Target Test	Test Point	Dry Density Mg/m ³ (lb/ft ³)	Percent Compaction (%)	Water Content (%)	Water Content Relative to Optimum (%)	PFWD Composite Modulus (MPa)
90%, W _{opt}	1	1.97 (124)	95	6.8	+1.7	99
	2	2.02 (126)	96	5.6	+0.5	87
	3	1.95 (122)	93	6.2	+1.1	85
	4	1.81 (113)	86	5.9	+0.8	107
	5	1.92 (120)	92	5.4	+0.3	90
95%, W _{opt}	1	2.05 (128)	97	5.6	+0.5	119
	2	2.08 (130)	99	6.1	+1.0	118
	3	2.00 (125)	95	6.3	+1.2	135
	4	2.03 (127)	97	6.1	+1.0	143
	5	2.13 (133)	101	6.8	+1.7	126
100%, W _{opt}	1	2.07 (129)	99	7.3	+2.2	126
	2	2.16 (135)	103	6.2	+1.1	121
	3	2.15 (134)	102	6.5	+1.4	141
	4	2.11 (132)	100	6.7	+1.6	132
	5	2.15 (134)	102	6.6	+1.5	115
95%, +3% W _{opt}	1	1.89 (118)	90	8.4	+3.3	68
	2	2.03 (127)	97	7.4	+2.3	72
	3	1.81 (113)	86	8.6	+3.5	72
	4	1.84 (115)	88	7.8	+2.7	76
	5	1.94 (124)	94	8.3	+3.2	79
	1	1.97 (123)	94	11.5	+6.4	56
	2	1.92 (120)	92	11.1	+6.0	56
	3	1.94 (121)	92	11.1	+6.0	58
	4	1.97 (123)	94	11.3	+6.2	62
	5	1.94 (121)	93	10.5	+5.4	63
	1	1.87 (117)	89	15.1	+10.0	12
	2	1.91 (119)	91	14.4	+9.3	19
	3	1.87 (117)	89	14.1	+9.0	15
	4	1.94 (124)	94	13.9	+8.8	16
	5	1.86 (116)	88	18.9	+13.8	13
95%, - 3% W _{opt}	1	1.97 (123)	94	4.3	-0.8	127
	2	2.11 (132)	101	3.7	-1.4	144
	3	2.10 (131)	100	4.1	-1.0	179
	4	1.91 (119)	91	4.1	-1.0	148
	5	2.07 (129)	99	4.0	-1.1	144